

P189

MICROSPACECRAFT AND EARTH OBSERVATION: ELECTRICAL FIELD (ELF) MEASUREMENT PROJECT



UTAH STATE UNIVERSITY
1989 - 1990

(NASA-CR-186321) MICROSPACECRAFT AND EARTH
OBSERVATION: ELECTRICAL FIELD (ELF)
MEASUREMENT PROJECT (Utah State Univ.)
189 p

CSCL 04A

N70-26430

Unclas
0295015

65/46

FOREWORD

This final report describes the final design for the "Electrical Field (ELF) Measurement Project." This project consists of a constellation of microspacecraft orbiting the earth to measure the earth's electrical field. The satellites were designed entirely by a team of Utah State University students. The project has been complete under the sponsorship of NASA/OAST through the Universities Space Research Association (USRA).

We at Utah State University are very pleased with the results of this design effort. We are proud of the product, and we are excited about the achievement of all our learning objectives. The systems design process is one that cannot be taught, it must be experienced. The opportunity to use our maturing engineering and scientific skills in producing the ELF satellite final design has been both challenging and rewarding. We are proud of the skills we have developed in identifying system requirements, spreading them into subsystems specifications, communicating with each other in all kinds of technical environments, conducting parametric and trade-off studies, learning to compromise for the good of the system, and selecting the actual hardware to be used on the satellite.

Elements of this design project have migrated into other forums. In mid-May 1990, class members presented the final design to the monthly meeting of the Utah Section of the American Institute for Aeronautics and Astronautics (AIAA). Also, in mid-February 1990, Dr. Frank Redd and Miss Tanya Olsen presented a paper at the AIAA American Engineering Conference and Show in Los Angeles. A revision of that paper will be presented at other conferences in the Fall. McDonnell Douglas has given Utah State University a contract to complete the design of the ELF satellite for interfacing with a secondary payload on the Delta II.

We wish to acknowledge the support of NASA/OAST and USRA without which this experience could never happen. We would like to thank Dr. Jan Sojka of Utah State University's Center for Atmospheric and Space Sciences for giving us this project to work on as well as for all his invaluable help in the actual design. We would also like to thank Mr. Gilbert Moore for his invaluable expertise in progressing the design as well as critiquing and polishing our presentation.

Frank J. Redd, PhD
Professor, ME

Tanya A. Olsen
Teaching Assistant

CLASS PARTICIPANTS

Tanya Olsen	System Engineering
Scot Elkington	Electrical Field Sensing Package
Scott Parker	Electrical Field Sensing Package
Grover Smith	Electrical Field Sensing Package
Andrew Shumway	Mission Description/Deployment
Craig Christensen	Launch Vehicle Interface/Deployment
Mehrdad Parsa	Launch Vehicle Interface/Deployment
Layne Larsen	Attitude Control and Determination
Ranae Martinez	Attitude Control and Determination
George Powell	Attitude Control and Determination
Dan Baker	Data Processing
Steven Morris	Power and Communication
Randy West	Power and Communication
Jeff Gessaman	Structure and Configuration
Scott Jamison	Structure and Configuration
Michael Daines	Thermal Control
Kevin Thomas	Thermal Control
Brian Williams	Thermal Control

MICROSPACECRAFT AND EARTH OBSERVATION THE ELECTRICAL FIELD (ELF) MEASUREMENT PROJECT

ABSTRACT

Past attempts to map the earth's electrical field have been severely limited by the lack of simultaneous global measurements. Previous measurements have been made by sounding rocket and satellite borne sensors, but these measurements have covered only singular points in the field. These satellite observations are augmented by ground radar (incoherent scatter) plasma drift measurements; however, only six ground-based installations are producing such local electrical field maps. The expansion of this ground-based radar network to meet a global objective is politically and financially impossible. Global electrical field maps constructed by forcing mathematically formulated models to fit this limited set of data points are not only inaccurate, but the degree of inaccuracy is impossible to evaluate.

The Utah State University space system design project for 1989-1990 focuses on the design of a global electrical field sensing system to be deployed in a constellation of microspacecraft. The design includes the selection of the sensor and the design of the spacecraft, the sensor support subsystems, the launch vehicle interface structure, on board data storage and communications subsystems, and associated ground receiving stations. Optimization of satellite orbits and spacecraft attitude are critical to the overall mapping of the electrical field and, thus, are also included in the project.

The spacecraft design incorporates a deployable sensor array (5 m booms) into a spinning oblate platform. Data is taken every 0.1 seconds by the electrical field sensors and stored on-board. An omni-directional antenna communicates with a ground station twice per day to down-link the stored data. Wrap-around solar cells cover the exterior of the spacecraft to generate power. Nine Pegasus launches may be used to deploy fifty such satellites to orbits with inclinations greater than 45°. Piggyback deployment from other launch vehicles such as the DELTA II is also examined.

TABLE OF CONTENTS

1.0 INTRODUCTION

- 1.1 DESIGN CONSIDERATIONS
- 1.2 DESIGN EVOLUTION
 - 1.2.1 Gravity Gradient Satellite
 - 1.2.2 Dual Spinner Satellite
 - 1.2.3 Simple Spinner Satellite
- 1.3 ELECTRICAL FIELD SENSING SYSTEM
- 1.4 MISSION DESCRIPTION
- 1.5 ELF CONSTELLATION DEPLOYMENT
- 1.6 ATTITUDE CONTROL AND DETERMINATION SYSTEM
- 1.7 DATA PROCESSING SYSTEM
- 1.8 COMMUNICATION SYSTEM
- 1.9 POWER SYSTEM
- 1.10 ELF SATELLITE STRUCTURE AND CONFIGURATION
- 1.11 THERMAL CONTROL SYSTEM
- 1.12 CONCLUSIONS

2.0 ELECTRICAL FIELD SENSING SYSTEM

- 2.1 INTRODUCTION
- 2.2 DOUBLE CONDUCTING PROBE TECHNIQUE
- 2.3 INSTRUMENT DESIGN
- 2.4 ERRORS

3.0 MISSION

- 3.1 MISSION GOALS
- 3.2 SATELLITE LAUNCH
- 3.3 CLUSTER SEPARATION THROUGH RELATIVE NODAL REGRESSION
- 3.4 INCLINATION VERSUS ALTITUDE DEPLOYMENT METHODS
- 3.5 LAUNCH CONFIGURATION
- 3.6 CONSTELLATION OVER TIME

4.0 DEPLOYMENT

- 4.1 LAUNCH VEHICLE SELECTIONS
- 4.2 PEGASUS LAUNCH
 - 4.2.1 Individual Satellite Deployment Capability
 - 4.2.2 Pegasus Bus System
 - 4.2.2.1 Interface
 - 4.2.2.2 Satellite mounting
 - 4.2.2.3 Pegasus modifications
 - 4.2.2.4 Future considerations of the bus system
 - 4.2.3 Orbital Maneuvering and Requirements
 - 4.2.3.1 Inclination maneuvering
 - 4.2.3.2 Altitude maneuvering
 - 4.2.3.3 Release from bus
 - 4.2.4 Mass Requirements of System
- 4.3 DELTA II LAUNCH
 - 4.3.1 Launch Vehicle Interface
 - 4.3.2 Orbital Maneuvering

5.0 ATTITUDE CONTROL AND DETERMINATION SYSTEM

- 5.1 DESIGN REQUIREMENTS
- 5.2 DESIGN EVOLUTION
- 5.3 ATTITUDE CONTROL OPERATIONS
- 5.4 SATELLITE MOTION
 - 5.4.1 Equations of Motion
 - 5.4.2 Stability Analysis
- 5.5 ATTITUDE DETERMINATION
 - 5.5.1 Finding the Stars
 - 5.5.2 Finding the Sun
 - 5.5.3 Finding the Earth
 - 5.5.4 Finding the Earth's Magnetic Field
 - 5.5.5 Using Gyroscopes and Accelerometers
 - 5.5.6 Sensors Used
 - 5.5.7 Totals
 - 5.5.8 Position of Sensors
- 5.6 CLOSED LOOP CONTROL SYSTEM
- 5.7 PROPULSION SYSTEM
 - 5.7.1 Tank and Nozzle Design
 - 5.7.2 Propellant Expenditures
- 5.8 CONCLUSION

6.0 DATA PROCESSING SYSTEM

- 6.1 SYSTEM REQUIREMENTS**
- 6.2 SYSTEM COMPONENTS**
 - 6.2.1 Processor
 - 6.2.2 Processor Memory
 - 6.2.3 Data Storage
 - 6.2.3.1 Options for data storage memory
 - 6.2.3.2 Expansion of data storage memory
 - 6.2.4 Communication System Interface
 - 6.2.5 Programmable Timer
 - 6.2.6 Watchdog Timer
 - 6.2.7 Programmable Interrupt Controller
- 6.3 RAW DATA STORAGE**
- 6.4 HAZARDS TO THE SYSTEM**
 - 6.4.1 Van Allen Radiation Belts
 - 6.4.2 Ionizing Radiation
- 6.5 RADIATION DAMAGE PREVENTION**

7.0 COMMUNICATION SYSTEM

- 7.1 REQUIREMENTS**
- 7.2 ANTENNAE**
 - 7.2.1 ELF Satellite Antenna
 - 7.2.2 Ground Station Antenna
 - 7.2.3 Off-the-Shelf Technology
- 7.3 ELF DATA LINK**
 - 7.3.1 RF Downlink
 - 7.3.2 Transmission
 - 7.3.3 RF Uplink

8.0 POWER SYSTEM

- 8.1 SOLAR CELLS**
- 8.2 BATTERIES**
- 8.3 SINGLE POINT FAILURES**

9.0 ELF STRUCTURE AND CONFIGURATION

9.1 TOP LEVEL REQUIREMENTS

9.2 DESIGN PHASES

9.2.1 Gravity Gradient

9.2.2 Dual-Spin Satellite

9.2.3 Simple Spinner

9.3 MATERIALS

9.4 SENSOR BOOMS

9.5 SUBSYSTEM PLACEMENT

9.6 CONCLUSIONS

10.0 THERMAL CONTROL

1.0 INTRODUCTION

Past attempts to map the earth's electrical field have been severely limited by the lack of simultaneous global measurements. Previous measurements have been made by sounding rocket and satellite borne sensors, but these measurements have covered only singular points in the field. These satellite observations are augmented by ground radar (incoherent scatter) plasma drift measurements; however, only six ground-based installations are producing such local electrical field maps. The expansion of this ground-based radar network to meet a global objective is politically and financially impossible. Global electrical field maps constructed by forcing mathematically formulated models to fit this limited set of data points are not only inaccurate, but the degree of inaccuracy is impossible to evaluate (1). Therefore, we see a need for an inexpensive, extensive, long-lasting global electrical field measurement system (ELF).

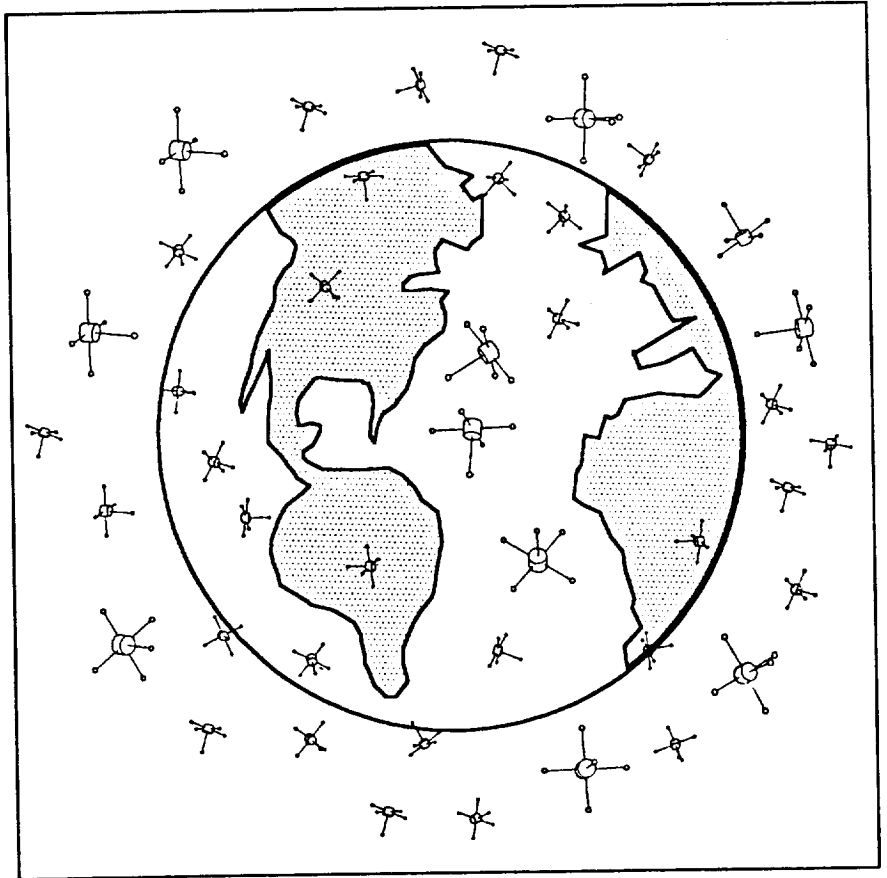


Figure 1-1 Artist's conception of the ELF constellation surrounding the earth.

1.1 Design Considerations

The primary performance driver for this mission is the need to measure the attitude of each spacecraft very accurately. In addition, it is necessary to know the electrical charge generated by the satellite as it crosses the magnetic field lines ($\mathbf{E} = \mathbf{V} \times \mathbf{B}$). This value must be factored out of the measurements. It will not be necessary to control the attitude of the satellite precisely, but the attitude will have to be known to within $\pm 1^\circ$ to

achieve the desired accuracy. Also, the payload sensing booms must rotate in order to balance photoelectric effects and aid in the measurement of the $\mathbf{V} \times \mathbf{B}$ bias.

In order to achieve the desired global coverage, a constellation of about 50 satellites in at least 18 different orbits will be used as shown by the artist's conception in figure 1-1. To reduce the cost of each satellite, off-the-shelf, proven technology will be used wherever possible. We set a limit of 25 kg and \$500,000 per satellite. We expect the program cost, including the deployment of the entire constellation, to be less than \$100 million. The minimum projected mission life is 5 years.

1.2 Design Evolution

Several designs were considered for the ELF satellite:

- 1) gravity gradient satellite;
- 2) dual spinner satellite; and
- 3) simple spinner satellite.

1.2.1 Gravity Gradient Satellite The first design considered was a gravity gradient satellite. This is a satellite in which, because of its mass distribution, one face of the satellite constantly points at the earth. Because this is a very stable configuration, there is no need for an active attitude control system. This design was discarded due to the electrical field sensor requirement that it must spin.

1.2.2 Dual Spinner Satellite Second, a dual spinner satellite such as those used for communication purposes was considered. This was in order to satisfy the sensor requirement of spinning as well as to have a face of the satellite constantly earth-pointing for ease of communication. We abandoned this design due to the unnecessary complications caused by having to interface between the rapidly spinning and slowly spinning platforms of the satellite.

1.2.3 Simple Spinner Satellite Last, a simple spinner satellite was considered. With this design, the complexities of interfacing between two platforms spinning at different rates do not exist, yet the sensor requirements are still satisfied. The rest of this document describes this final design configuration.

1.3 Electrical Field Sensing System

The electrical field sensing system will consist of 3 orthogonal sets of insulated booms with conductive spheres attached to the ends as shown by figure 1-2. The electrical potential across each pair of conductive spheres will be measured to get the 3-dimensional electrical field measurement at a point. The boom system must be rotating in order to mitigate the photoelectric charge build-up caused by exposure to the sun. To achieve the desired accuracy, the spheres must be separated by at least 1 meter and be rotating at no more than 10 radians per second. Since the rotation causes a sinusoidal variation in the output, potential readings must be taken at least every 0.1 seconds to get the desired resolution.

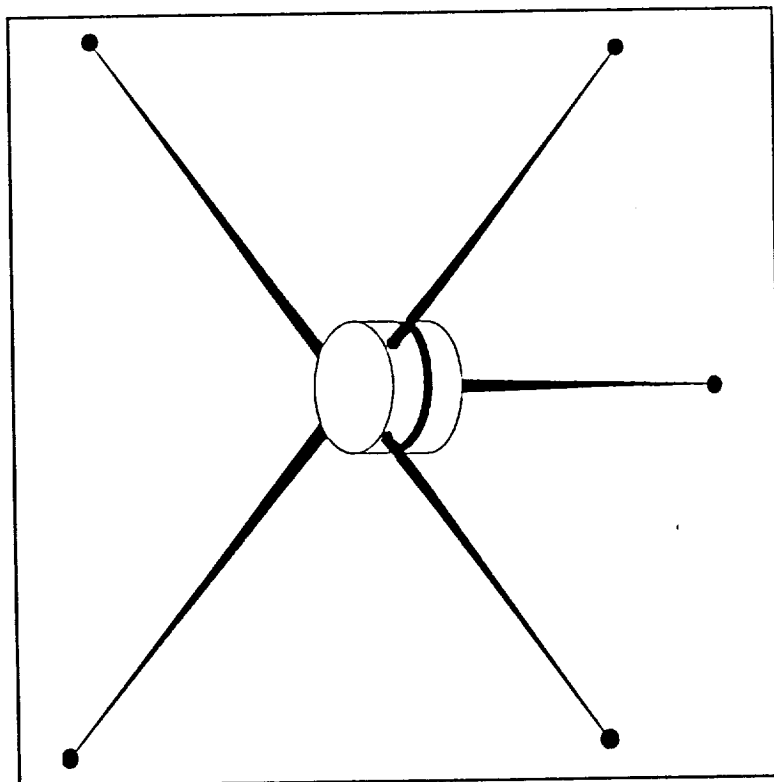


Figure 1-2 Close-up exterior view of an ELF satellite.

1.4 Mission Description

The most dynamic electrical field activity around the earth occurs near the poles in the 50° to 70° latitude regions. It is in this region that phenomena such as the aurora are observed most frequently. Little activity of interest occurs in the equatorial regions. Therefore, the ELF satellites will be placed in orbits with inclinations between 45° and 90°. This placement gives good coverage of the poles as well as some coverage of the equatorial regions.

The ELF satellites will be placed at altitudes between 500 and 1000 km. In this range, the earth's electrical field does not change dramatically with a change in altitude. Also, 500 km is high enough to give the lowest satellite a minimum mission life of 5 years

before the orbit decays, and 1000 km is low enough to escape the radiation from the Van Allen belts.

1.5 ELF Constellation Deployment

Two different deployment scenarios are being considered. The first considers using Orbital Sciences Corporation's Pegasus as a dedicated launch vehicle. The second option looks at piggyback opportunities on McDonnell Douglas's Delta II launch vehicle.

If the Pegasus is used, 6 satellites at a time will be launched. When the proper orbit is reached, one of the 6 satellites will be ejected from the Pegasus upper stage. The rest of the cluster will remain attached to the stage. This concept is shown in figure 1-3. The stage will then be maneuvered to a slightly different altitude (about 75 km higher) or a slightly different inclination (about 2.5° difference) where another ELF satellite will be ejected. This sequence will be repeated until all 6 satellites have been ejected. Launching the satellites in clusters like this reduces the required number of launches. By slightly changing either the altitude or inclination of each satellite in the cluster, the satellites will be dispersed even further by orbital perturbations caused by the earth's oblateness. This will result in the required global coverage.

The Delta II has the room for 4 ELF satellites to piggyback on it. The major problem with using this launch vehicle is that the satellites will go to wherever the primary payload dictates. Few polar launches are planned for the 1990's; most launches will be to inclinations below about 35° . Therefore, some sort of on-board propulsion for each ELF satellite will be required to get it into the proper type of orbit and altitude. However, there does not appear to be enough room for such a propulsion system. A possible alternative might be to use a tether deployment system. The details and requirements for this type of launch are still being investigated.

Upon insertion into orbit, a radio signal will be sent to the satellites to activate them. A programmed routine on-board the spacecraft will cause the sensor booms to deploy and the attitude control jets to fire, spinning the satellite.

1.6 Attitude Control and Determination System

The satellite is modelled as a spinning oblate platform which spins at 10 rpm. The orientation or attitude of each satellite will not be controlled, but the spin rate will be controlled to 10 ± 2 rpm. An on-board cold gas propellant system will be used to spin-

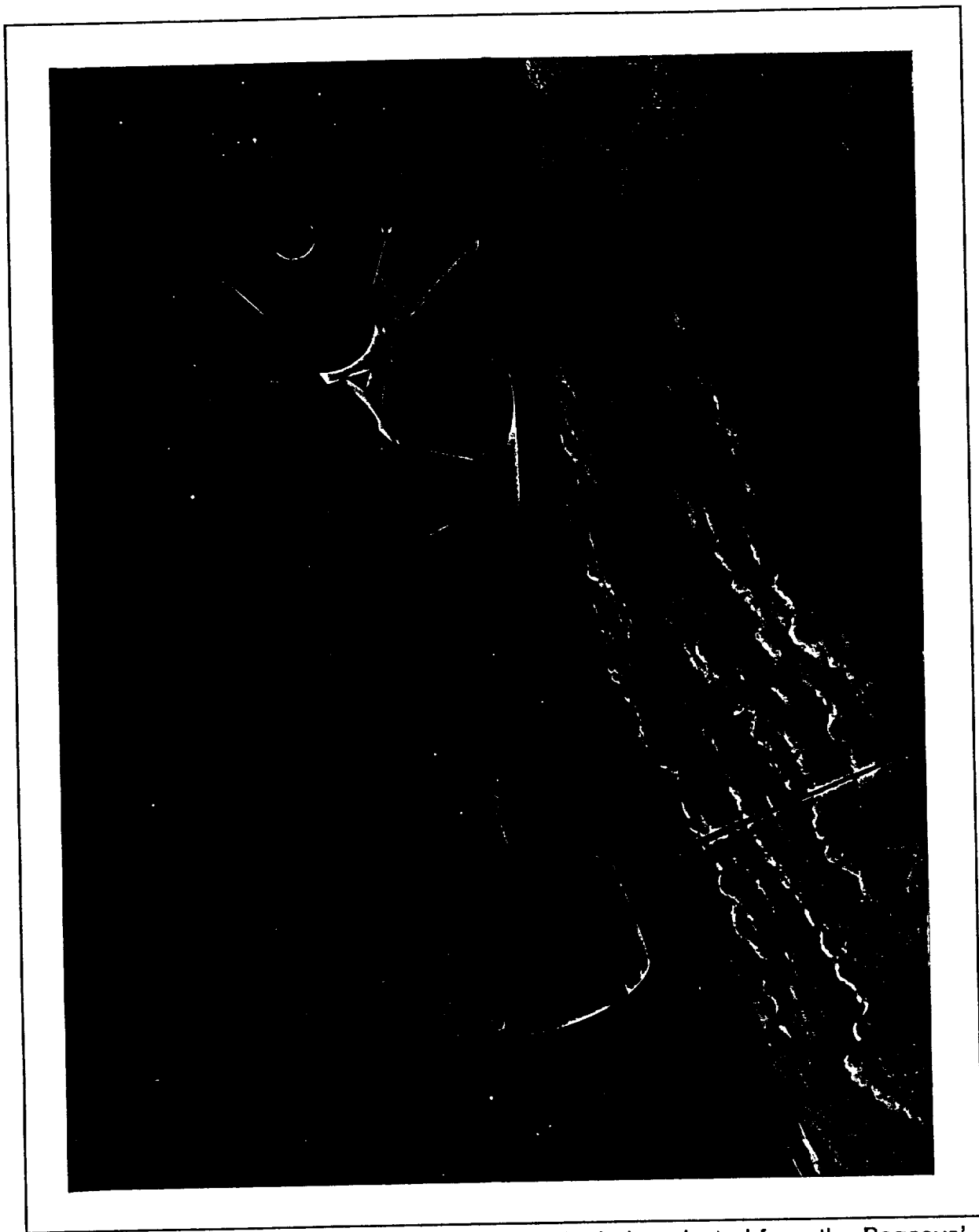


Figure 1-3 Artist's conception of an ELF satellite being ejected from the Pegasus' upper stage.

up the satellite initially as well as make any necessary spin rate adjustments.

Two 2-axis magnetometers, 2 sun sensors, and 1 horizon crossing sensor are used to determine the attitude of each ELF satellite. By using different combinations of these 5 sensors, the attitude of the satellite can be determined at all times during the orbit. Some of the data will be redundant, but this redundancy can be used to enhance the accuracy of the readings. These readings will lie within the $\pm 1^\circ$ error in attitude knowledge margin.

1.7 Data Processing System

The data processing system is sized to store up to 24 hours worth of data. These data include the electrical field potential as well as the attitude readings. This system will also handle housekeeping functions on-board the satellite.

1.8 Communication System

Because the attitude of each ELF satellite will not be controlled and each satellite can maintain a different orientation, a virtually omni-directional antenna is needed on-board for communication. A stripline wraparound antenna meets this requirement. Frequencies in the S-band will be used for receiving instructions and transmitting the collected data to a ground station. Data will be transmitted twice per day to one ground station. The ground station will use a 4.3 m parabolic dish with tracking capabilities. The actual location of this ground station is yet to be determined. Each satellite will take a maximum of 82 seconds to transmit the stored data. It is expected that each satellite will pass within range of the ground station at least twice per day.

1.9 Power System

The each satellite's power will come from solar cells wrapped around the exterior of the spacecraft. Since the satellites will not generally be placed in sun synchronous orbits, they will have to function in the dark as well. Therefore, the solar cells will be backed up with batteries. The minimum power generation will be 12.77 W which will be sufficient to cover the power requirements of all systems.

1.10 ELF Satellite Structure and Configuration

The cylindrical primary structure is 45 cm in diameter and 35 cm high. It will be composed of 0.16 to 0.32 cm thick aluminum 6061-T6. The primary support plate will be made of 1.25 cm thick aluminum honeycomb. Most subsystem components will be mounted on this plate as shown by figure 1-4. Individual component covers will provide radiation shielding as required.

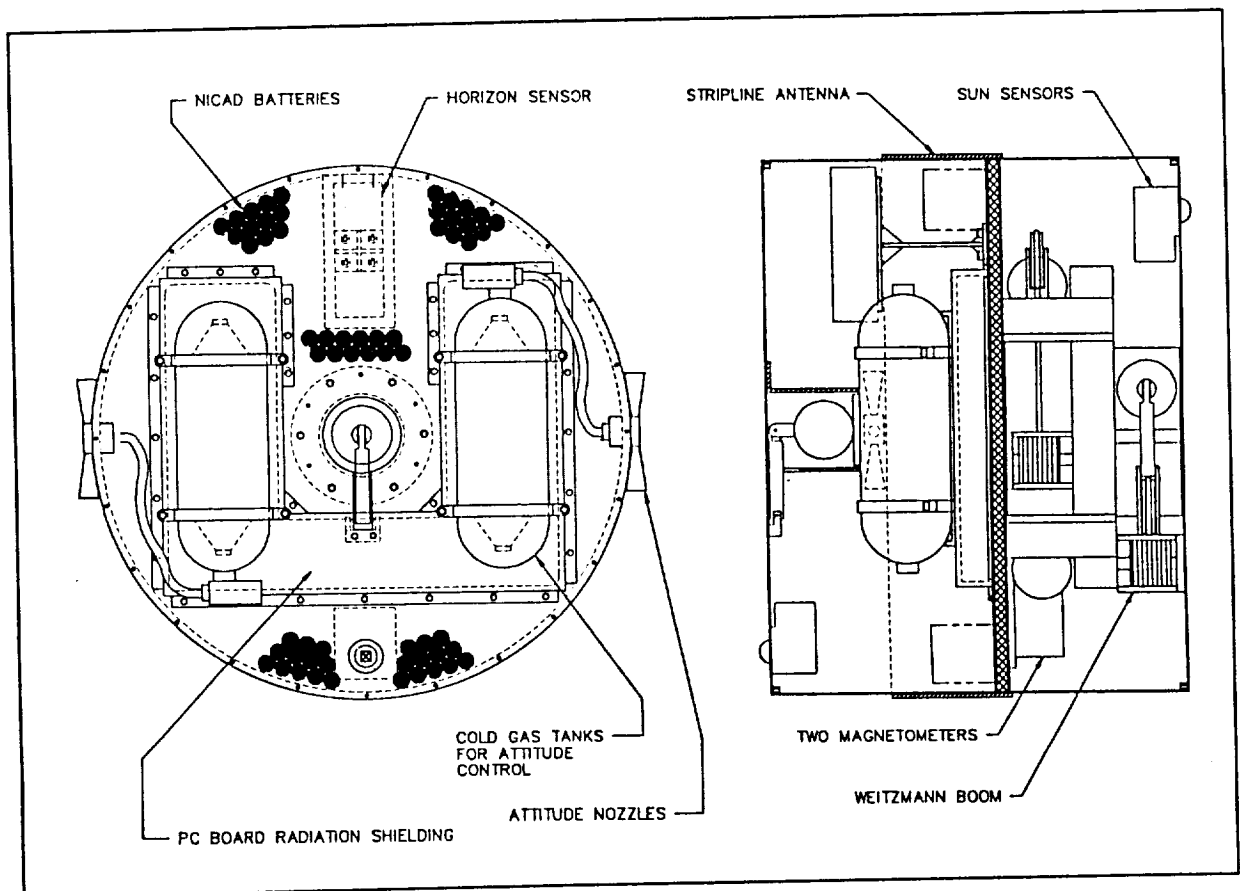


Figure 1-4 Internal layout of the subsystem components.

1.11 Thermal Control System

The extreme temperatures were determined for the ELF satellites by considering the worst cases of the hottest and coldest orbits. The hottest orbit is one in which one flat face of the satellite constantly faces the sun. If an ELF satellite winds up with this orientation, all on-board components will stay within their temperature ranges. The

coldest orbit considered was one in which the flat faces of the satellite never see the sun. The temperature ranges for this case went below the component limits. In order to compensate for this, 3 one W heaters will be used to bring the components into their required operating temperature. These heaters are equipped with their own temperature regulating switches.

1.12 Conclusions

Each satellite has a mass of 19.1 kg and will cost less than \$250,000 for the actual hardware. Including deployment costs, the program will cost about \$70 million for 8 Pegasus launches and 48 satellites. Labor costs have not yet been computed.

We expect to be able to deploy about 50 satellites. Because we are deploying a constellation of 50 satellites there is inherent redundancy in this system. The most catastrophic event that could happen is to have the launch vehicle explode. But even this will not affect the system drastically since at the most 6 satellites will be lost. We expect to lose not more than 10% of the satellites to launch vehicle malfunction, ELF subsystem failure, or space debris impact.

REFERENCES

1. Sojka, J.J.: 2-DEF A two dimensional electric field mission. Center for Atmospheric and Space Sciences, Utah State University, Logan, Utah. CASS Report #89-5-2, November, 1989.
2. French, J.R.: Very small spacecraft for planetary exploration missions. Lightsat Conference, 1988.
3. Jones, R.M.: Think small-in large numbers. Aerospace America pp. 14-17, October, 1989.
4. Jones, R.M.: Coffee-can-sized spacecraft. Aerospace America pp. 36-38, October, 1988.
5. Barakat, W.A., et al: Microspacecraft and Science. Global Technology Initiative, General Research Corporation, December 1988.

2.0 ELECTRICAL FIELD SENSING SYSTEM

The ELF experiment consists of five spherical conducting probes arranged along three orthogonal axes. Common mode potential readings from each probe are taken at selectable rates throughout the orbit. On board data manipulation is limited to allow maximum freedom in data interpretation. Errors in the information collected by ELF are expected to be within experimentally acceptable limits.

2.1 Introduction

The ELF project focuses on the mapping of ambient d.c. electric fields in the ionosphere using a constellation of small, single-experiment spacecraft. Knowing the temporal and spatial characteristics of these fields is vital in the development of magnetospheric models and the understanding of auroral electrodynamics (1). The purpose of this paper is to describe the method of measurement selected for the ELF satellites and the instrumentation by which these measurements will be made.

The regions of interest to electrodynamicists lie above 50° latitude at altitudes from 600 to 1000 km. Typical electric field intensities in these areas are expected to range from 2 mV/m across the polar cap to 150 mV/m in the auroral regions (2). The ELF experiment will be capable of providing the global, three dimensional data necessary to determine the nature of these fields.

Minimizing cost by using proven, off-the-shelf technology was a top level requirement driving the design of the electric field instrument on the ELF satellites. One method considered in the design of this system included particle velocity measurements using a retarding potential analyzer in conjunction with an ion drift meter. Data obtained from these instruments would yield electric field information, as well as plasma density and temperature (12, 13, 17). Another technique considered was the use of two spatially separated conducting elements, allowing a direct measurement of the potential difference between these elements (3). Due to the ease with which data may be interpreted and the simplicity of the design, the latter method was selected for use on the ELF satellites.

2.2 Double Conducting Probe Technique

The symmetric double probe technique has proven to be a reliable method of measuring ionospheric d.c. electric fields (3, 5, 9, 10). The theory of such a system has been detailed by Fahleson (4); points relevant to this paper will follow.

The electrical field \underline{E}' detected by a sensor moving with velocity \underline{v} about the earth will be given by

$$\underline{E}' = \underline{E} + (\underline{V} \times \underline{B})$$

where \underline{E} is the ambient electrical field and $\underline{V} \times \underline{B}$ is the electrical field component induced by the motion of the sensor through the earth's magnetic field. Two conducting probes suspended in a rarified plasma and separated by a distance d will register this field as a difference of potential between the probes. On the satellites, this potential difference is related to the electric field \underline{E}' by

$$\begin{aligned} V_A - V_B &= (V_A - V_S) - (V_B - V_S) \\ &= (\underline{E} + \underline{V} \times \underline{B}) \cdot \underline{d} \end{aligned}$$

where V_S corresponds to the ground (spacecraft) potential. The above equation shows that any error in the measured potential or any uncertainty in spacecraft attitude will produce some uncertainty in the final value of \underline{E} . This will be discussed further in section 2.4.

The operation of such a system is heavily dependant on the local electron temperature and density (9). High electron temperatures or low plasma densities may drive uncertainties in the data over acceptable limits. In regions of interest to us, average electron temperatures of 2100 K are expected with maximum temperatures of 8000 K during auroral events. Ion densities may change by several orders of magnitude. Table 2-1 details the range of conditions expected to be encountered by ELF (2).

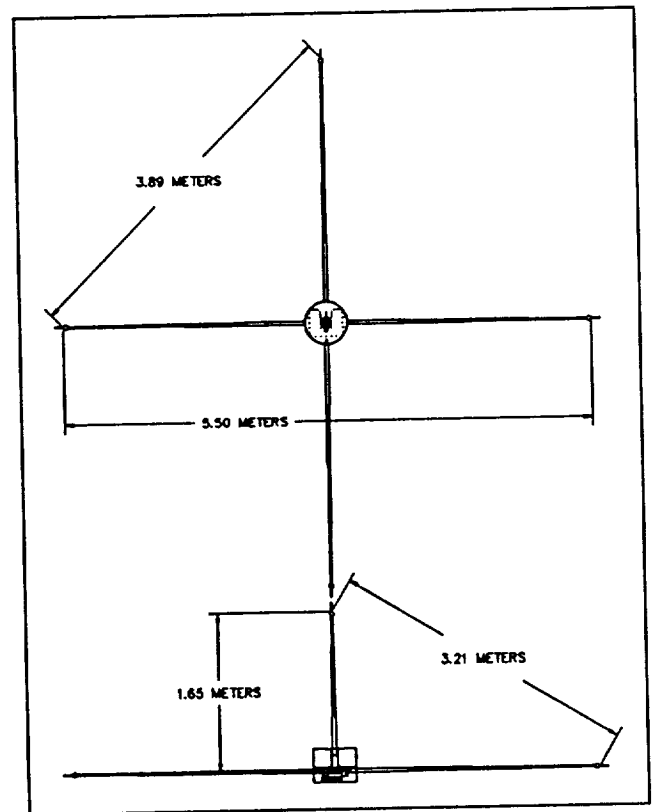


Figure 2-1 ELF sensor configuration.

Table 2-1 ELF Satellite Environment

Electron density (cm^{-3})	mean	maximum	minimum
Polar cap (winter)	2×10^4	10^5	2×10^3
Polar cap (summer)	6×10^4	2×10^5	6×10^3
Dayside aurora	2×10^5	5×10^5	3×10^4
Trough	2×10^4	10^5	10^3
Electron temperature (K)			
Polar cap	1800	3000	1000
Dayside aurora	2500	8000	2000
Trough	2000	4000	1500
Ion temperature (K)			
Polar cap	1800	2500	800
Dayside aurora	2500	4000	1500
Trough	1800	3000	800
Electric field (mV/m)			
Polar cap	10	50	2
Dayside aurora	40	150	5
Trough	10	50	5

2.3 Instrument Design

The ELF satellite sensor configuration is shown in figure 2-1. The conducting portion of each boom consists of a gold plated aluminum sphere with a 5 cm radius. Four of the spheres lie in the same plane and are supported by the 2.75 m Weitzmann Quadrupole Stacer boom system. The fifth sensor lies 1.65 m from the spacecraft body and is supported by a Weitzmann Monopole Stacer boom. All booms are composed of insulated beryllium copper. Stubs added to the end of the booms will minimize the photoelectric current and work function differences that could bias the system. Chapter

9 gives a more complete description of the boom composition.

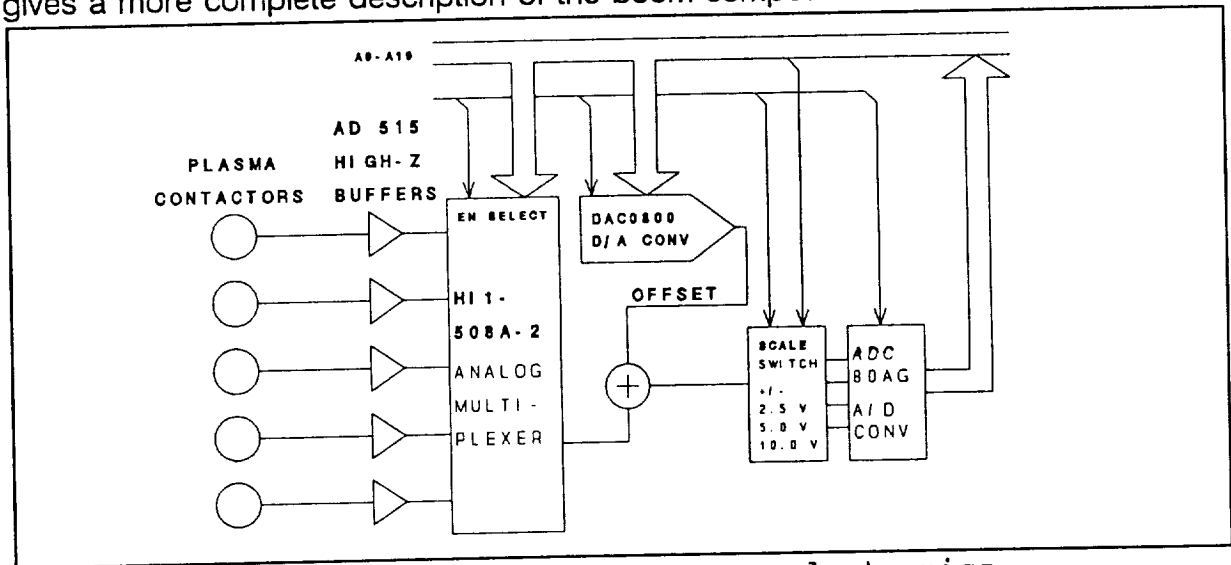


Figure 2-2 Block diagram of the sensor electronics.

Figure 2-2 shows a block diagram of the sensor electronics. Probe voltages impressed across the high impedance (1.2×10^9 ohm) amplifiers are selected by the 8-1 analog multiplexer. The rate at which these signals are selected is variable and may be programmed to maximize data gathering efficiency. For instance, in some region of particular interest the sample rate could be increased to maximize temporal resolution, and subsequently decreased to conserve memory. The 12 bit digital/analog converter will produce a pre-programmed voltage, which, when compared with the signal from the multiplexer, will allow voltage biases to be removed. The dynamic range of this instrument is also variable and may be switched between ± 2.5 V, ± 5 V, and ± 10 V. Thus, the 12 bit analog/digital converter will allow an amplitudinal resolution of 0.6 mV/m, 1.2 mV/m, or 2.4 mV/m from the 2.75 m booms, and a resolution of 1 mV/m, 2mV/m, or 4 mV/m from the 1.65 m boom. Table 2-2 lists some specific characteristics of the components used in this portion of the design. Total power used by this system is seen to be about 1 watt.

Data recorded by this sensor will be stored as common mode voltages from each probe. As opposed to differential voltages, data in this form will to allow individual researchers some flexibility when resolving the electric field: each axis of the field may possibly be obtained from any arbitrary combination of probe voltages. This ability will also provide redundancy in the information from which the ambient electric field can be obtained.

Table 2-2 Electronics

Item	Part number	Power
5 $1.2 \times 10^9 \Omega$ amplifiers	Burr-Brown AD515	.18 watts
8-1 analog multiplexer	Burr-Brown HI1-508A-2	.012 watts
12 bit D/A converter	Burr-Brown ADC574	.27 watts
Range switch	--	.11 watts
12 bit A/D converter	Burr-Brown ADC80AG	.37 Watts

Spinning the spacecraft allows easy evaluation of any voltage biases inherent in the system (5), and provides some information about the probe location with respect to the spacecraft. A rotating spacecraft also eliminates the possibility of one boom remaining in the spacecraft wake or shadow for an extended period. For these reasons, it was required that the ELF satellites be given an angular velocity of 1.05 rad/s about the 1.65 m boom. Further discussion of this rotation may be found in chapter 5.

2.4 Errors

Errors in the electrical field measurements taken by the ELF satellites may arise from many effects; contact potential differences caused by variations in the work function associated with each probe can cause voltage errors as large as several hundred millivolts (5). Care must be taken in the construction and deployment of the probes to minimize the geometric differences and contamination effects that lead to this problem. Contact potentials and other biasing effects, if relatively constant throughout the orbit, may be evaluated using measurements taken in regions where \underline{E} is expected to be near zero.

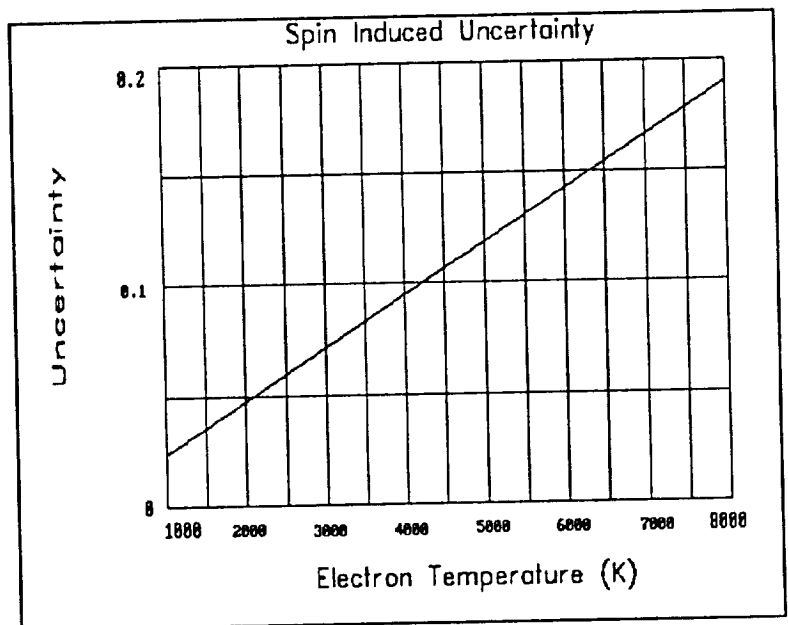


Figure 2-3 Variation of spin-induced uncertainty with electron temperature.

Errors in attitude evaluation will cause a corresponding error in the determination of the $\underline{V \times B}$ electrical field component in satellite's frame of reference. This component will be evaluated using data collected by the magnetometer and other attitude sensing instruments, as described in chapter 5. Appendix A1 lists a simple program that calculates the effect of attitude errors on the calculated value of $\underline{V \times B}$. Using this program, it has been found that every degree of uncertainty in attitude determination or knowledge of boom orientation can cause an uncertainty of up to 1 percent in $\underline{V \times B}$.

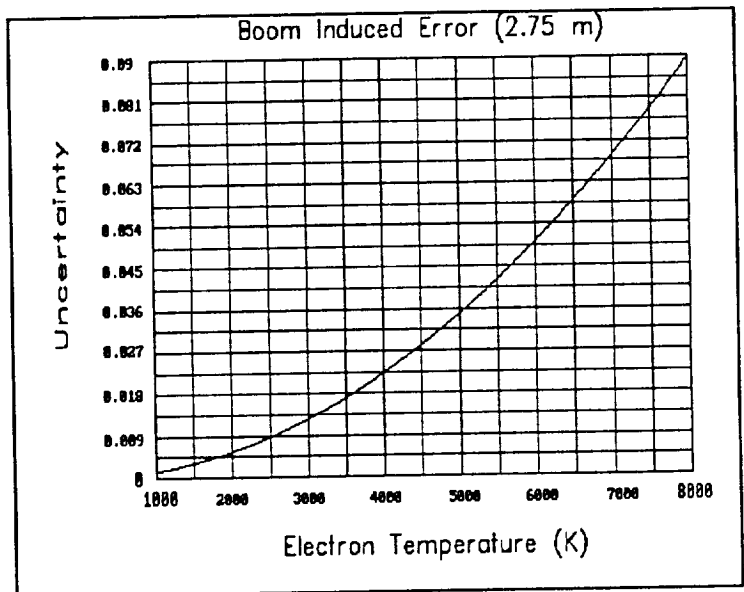


Figure 2-4 Variation of the boom induced uncertainty with electron temperature for the 1.5 m boom.

Another source of error in the potentials recorded by the ELF satellites are caused by inhomogeneities in the temperature and density of the plasma through which the sensors

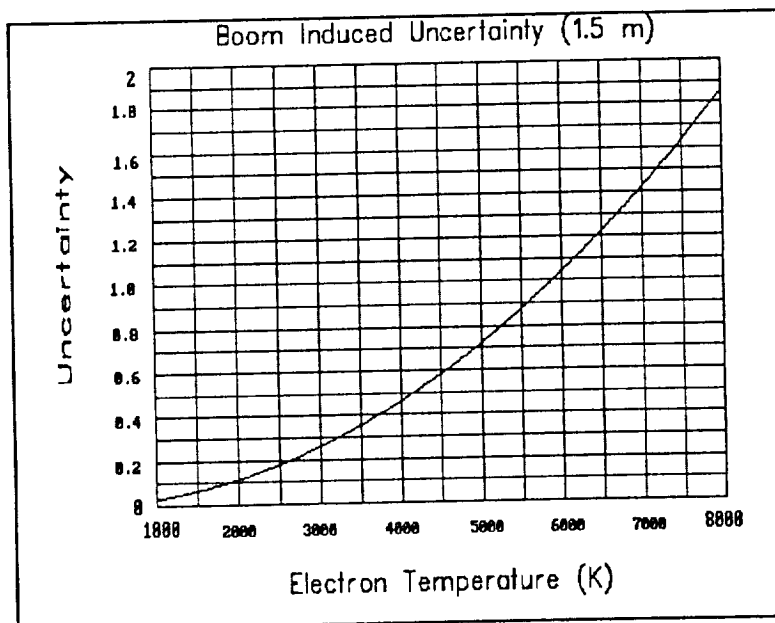


Figure 2-5 Variation in the boom induced uncertainty with electron temperature for the 2.75 m boom.

are moving. Differences in probe velocities caused by the rotation of the satellite will contribute to this error. Figure 2-3 shows how this uncertainty varies with the electron temperature. The equation from which this graph was generated (4) and the values of other parameters used in this equation are given in appendix A2. All values were selected to represent a worst case scenario; errors of these magnitudes will rarely be encountered by the satellites.

The booms supporting the

conducting probes can cause some differences in plasma density and temperature by screening particles from the conducting portion of the probe. Thermal noise from the input amplifiers will cause additional uncertainty in the measurement. Figures 2-4 and 2-5 show the approximate error due to both effects. The equation governing this error (4) and other parameters used are again given in appendix A2.

The total error in the electric field measurement will be the sum of the above errors and any errors arising from other effects. This error is expected to be about 10% - 20%, depending on the accuracy with which individual errors can be interpreted. Table 2-3 shows the total uncertainty due to particle screening and spacecraft rotation expected for average conditions found in the regions of interest.

Table 2-3 Spin-induced and boom-induced uncertainty

Region	Mean Uncertainty
Polar cap	.96%
Aurora-dayside	1.1%
Trough	.36%

Photoelectric current differences caused by unequal shading or plasma inhomogeneities caused by the spacecraft wake or high energy particle fluxes may occasionally upset potential readings. However, due to the form in which these potential readings are stored (ie. common mode voltages), data points recognized as having been recorded during one of these events may often be discarded with no loss of continuity in the electric field constructed for that orbit.

REFERENCES

1. Sojka, J. J.: 2-DEF A two dimensional electric field mission. Paper presented to Utah State University Advanced Design Program, Logan, Utah, 1989. (Available from Center for Atmospheric and Space Sciences, Utah State University, Logan, Utah.)
2. Sojka, J. J., Private communication, 1990.
3. Mozer, F. S.: Analyses of techniques for measuring d.c. and a.c. electric fields in the magnetosphere. *Space Sci Rev* 14:272-313, 1973.
4. Fahlson, U. V.: Theory of electric field measurements conducted in the magnetosphere with electric probes. *Space Sci Rev* 7:238-262, 1967.
5. Fahlson, U. V., Kelly, M. C., Mozer F. S.: Investigation of the operation of a d.c. electric field detector. *Planet. Space Sci* 18:1551-1556, 1970.
6. Burke, W. J., Hardy, D. A., Rich, F. J., Kelly, M. C., Smiddy, M., Shuman, B., Sagalyn, R.C., Vancour, R. P., Widman, P. J. L., Lai, S. T.: Electrodynamic structure of late evening sector of the auroral zone. *J Geophys Res* 85:1179-1193, 1980.
7. Maynard, N. C., Bielecki, E. A., Burdick, H. F.: Instrumentation for vector electric field measurements from DE-B. *Space Sci Instrument* 5:523-534, 1981.
8. Heppner, J. P., Bielecki, E. A., Aggson, T. L., Maynard N. C.: Instrumentation for d.c. and low frequency electric field measurements on ISEE-A. *IEEE Trans Geosci Electronics* GE16:253-257, 1978.
9. Cauffman, D. P., Gurnett, D. A.: High latitude convection electric fields. *Space Sci Rev* 13:369-410, 1972.
10. Heppner, J. P., Maynard, N. C., Aggson, T. L.: Early results from ISEE-1 electric field measurements. *Space Sci Rev* 22:777-789, 1978.
11. Mozer, F. S., Cattell, C. A., Temerin, M., Torbert, R. B., Von Glinski, S., Woldorff, M., Wygant, J.: The d.c. and a.c. electric field, plasma density, plasma temperature, and field aligned current experiments on the S3-3 satellite. *J Geophys Res* 84:5875-5883, 1979.

12. Knudson, W. C.: Evaluation and demonstration of the use of retarding potential analyzers for measuring several ionospheric quantities. J Geophys Res 71:4669-4668, 1966.
13. Heelis, R. A., Private communication, 1990.
14. Hanson, W. B., Heelis, R. A., Power, R. A., Lippincott, C. R., Zuccaro, D. R., Holt, B. J., Harmon, L. H., Sanatani, S.: The retarding potential analyzer for Dynamics Explorer-B. Space Sci Instrument 5:503-510, 1981.
15. Raitt, W. J., Private communication, 1990.
16. Baker, K. D., Private communication, 1990.
17. Hanson, W. B., Zuccaro, D. R., Lippincott, C. R., Sanatani, S.: The retarding potential analyzer on atmosphere explorer. J Geophys Res 78:333-339, 1973.
18. Mc Clure, J. P., Troy, B. E. Jr.: Equatorial ion temperature: a comparison of conflicting incoherent scatter and Ogo 4 retarding potential analyzer values. J Geophys Res 76:4534-4540, 1971.
19. Heelis, R. A., Hanson, W. B., Lippincott, C. R., Zuccaro, D. R., Harmon, L. H., Holt, B. J., Doherty, J. E., Power, R. A.: The ion drift meter for Dynamics Explorer-B. Space Sci Instrument 5:511-521, 1981.
20. Rodriguez, P., Private communication, 1990.

3.0 MISSION

3.1 Mission Goals

The goals of the mission design are to deploy about 50 satellites that will disperse around the earth to give good global coverage. The satellite orbits should emphasize the polar regions, especially between 50° to 70° latitude. The cost of launching the 50 satellites should be minimized. The satellites should have a minimum life time of 7 years. The deployment procedure should be simple.

3.2 Satellite Launch

It is possible to buy a large class launcher to send all 50 satellites into the same orbit. However, in order to achieve a good global electrical field measurement, the satellites need to form a mesh of different orbits covering the earth. Achieving this mesh of orbits from a single launch orbit is very costly.

The following discussion centers on the use of the Pegasus vehicle to provide 8 launches with 6 satellites in each launch. Pegasus will insert the payloads into 550 km altitude orbits for a minimum 7 year orbit lifetime.

3.3 Cluster Separation through Relative Nodal Regression

Upon initial launch of the eight Pegasus vehicles, the 48 satellite orbits will appear as seen in figure 3-1. These eight orbits are shown ranging between 55° and 90° . The satellites are still in clusters of six. Each cluster of satellites now needs to be separated into six individual orbits. This is done by

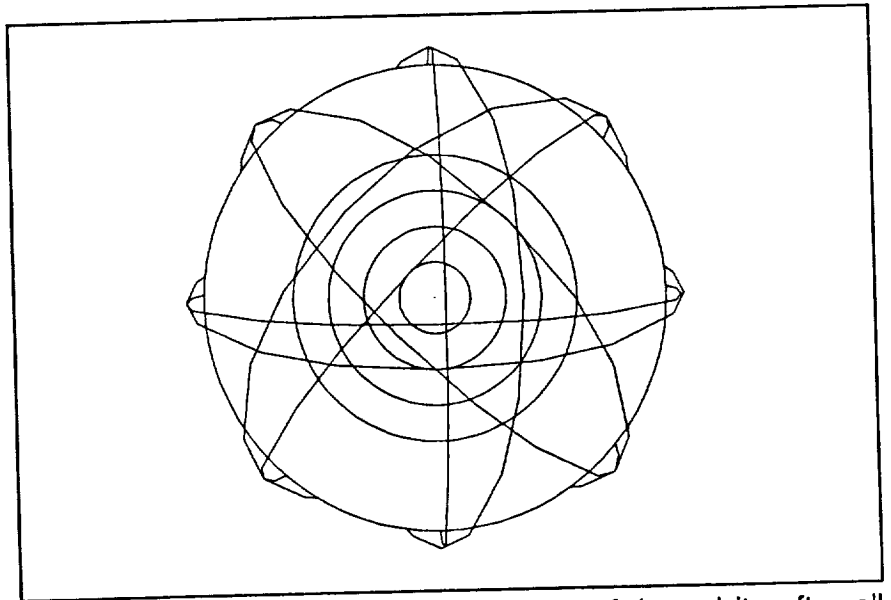


Figure 3-1 View from the North Pole of the orbits after all 8 Pegasus launches. Satellites are still in clusters of 6.

capitalizing on the effect of the earth's oblateness on orbital movement.

The earth's oblateness causes an orbit's line of nodes to regress. The regression rate is a function of altitude and inclination. By slightly changing the relative orbit inclination or altitude of each satellite, slightly different orbital regression rates will be produced. Thus, the six satellite orbits will spread out with time. This effect is shown in figure 3-2.

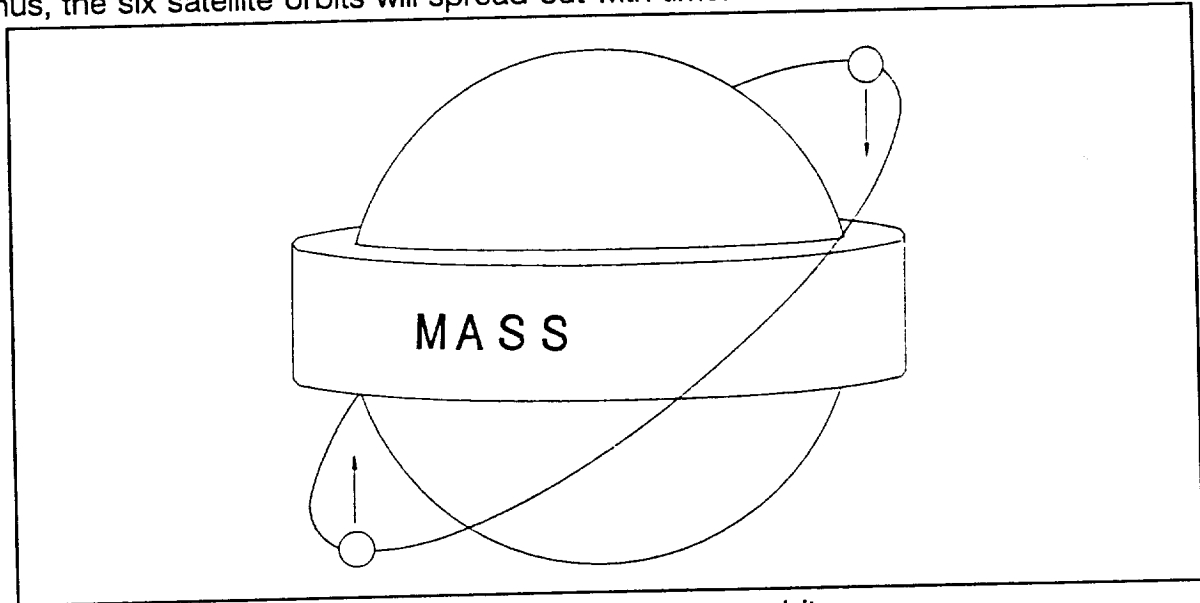


Figure 3-2 Effect of the earth's oblateness on an orbit.

At lower orbit inclinations, a satellite has a larger moment arm for the equatorial mass to tug on. This causes the orbit to precess and the line of nodes to regress. The relationship which calculates the nodal regression per second for a circular orbit is given by the following equation (1). This is the averaged effect over one orbit.

$$\dot{\Omega} = -3nJ_2 \frac{R^2}{2a^2(1-e^2)^2} \cos i$$

$$n = (\mu/a^3)^{1/2}$$

μ = earth gravitational parameter

J_2 = Oblateness effect

R = Radius of earth

i = inclination

a = semi-major axis

e = eccentricity

3.4 Inclination Versus Altitude Deployment Methods

The effects of an orbit's altitude and inclination on the monthly nodal regression are shown in figure 3-3. These effects should each be carefully examined to determine how to best use them in spreading apart the clusters of six satellites.

Figure 3-4 shows two satellites in slightly different circular orbits. These orbits vary only

by an altitude difference. The monthly relative nodal regression rate is shown as a function of the orbit inclination. The altitude separation method has the greatest effect in lower inclination orbits. As the inclination approaches the poles, the relative nodal regression goes to zero.

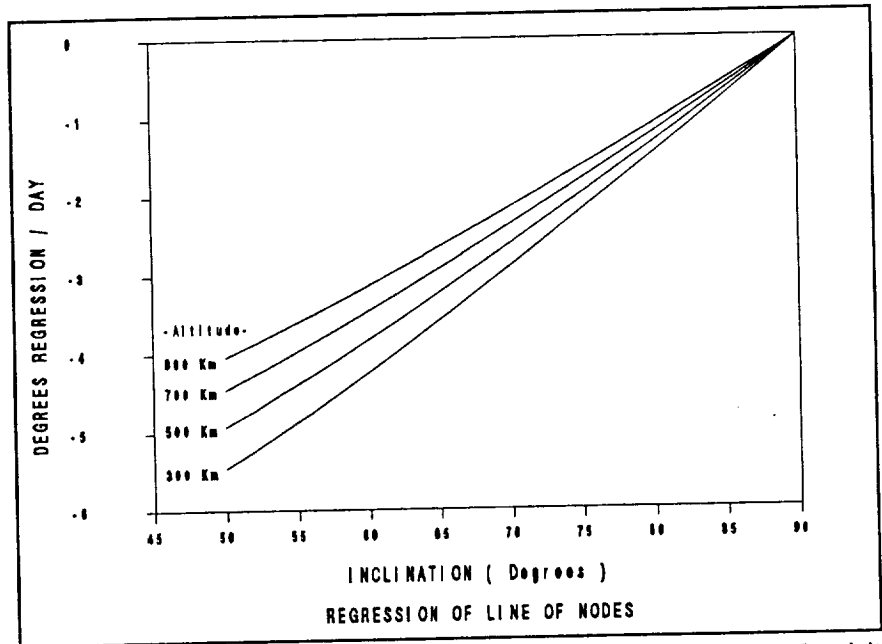


Figure 3-3 Nodal regression per day as a function of orbit altitude and inclination

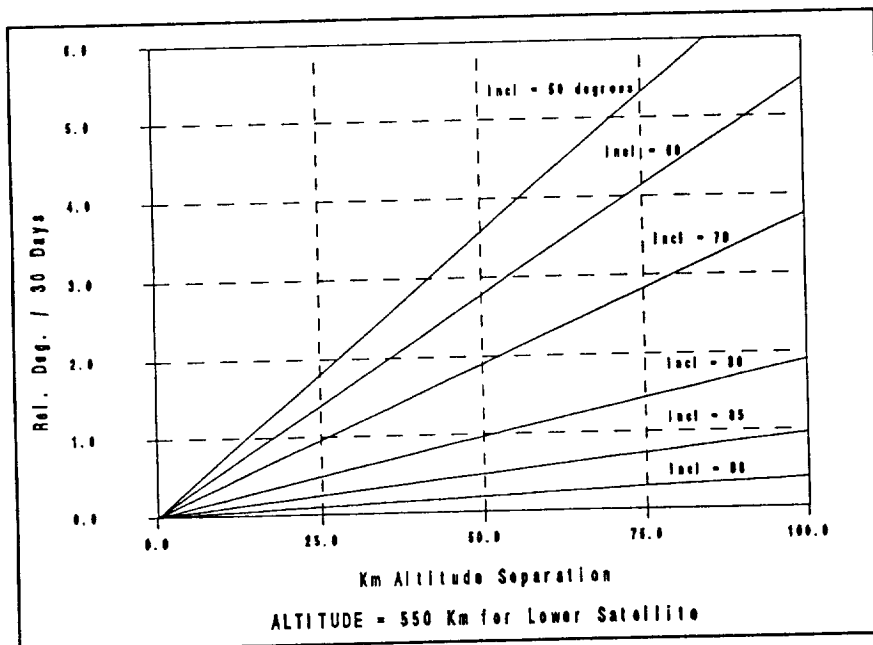


Figure 3-4 Relative altitude separation effect on the relative nodal regression of two satellites per month

The effect of relative inclination separation of two satellites can be shown in figure 3-5. Here the relative nodal regression increases near the poles. The orbit inclination has generally less of an effect on relative nodal regression with this deployment method.

A study of our orbit maneuvering capabilities shows that the maximum

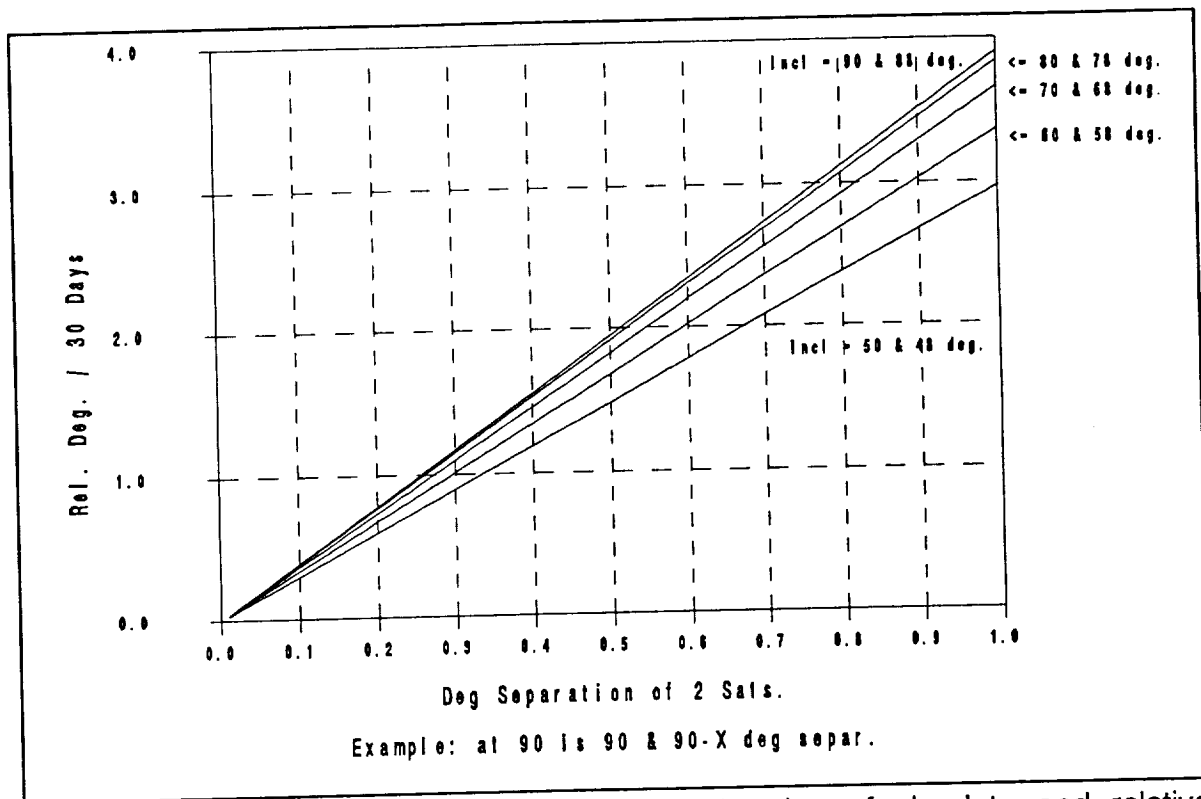


Figure 3-5 Relative nodal regression as a function of absolute and relative inclination of two satellites

achievable inclination difference between two satellites is about 0.5° . The maximum altitude difference between two circular orbiting satellites is about 75 km. The two methods may be compared in figure 3-6. This figure shows the relative nodal regression of two cases. First, the satellites are separated by an altitude of 75 km. Second, the satellites are separated by a relative inclination of 0.5° . The altitude separation method is better from 75° and below, and the inclination separation method is better from 75° and above. In order to maximize the dispersion rate of the satellites, these two methods will be employed in this manner.

There are other considerations for each deployment method. Less fuel is required to perform the altitude maneuvers. The inclination dispersion requires about twice the fuel. Another consideration is that different altitudes cause each satellite to have a slightly different period. So not only do the satellites' orbital planes gradually separate, but they quickly spread out along the orbit path and will completely disperse around the earth in about a day. For these reasons, the altitude separation method is more desirable. However, the inclination method is required near the poles.

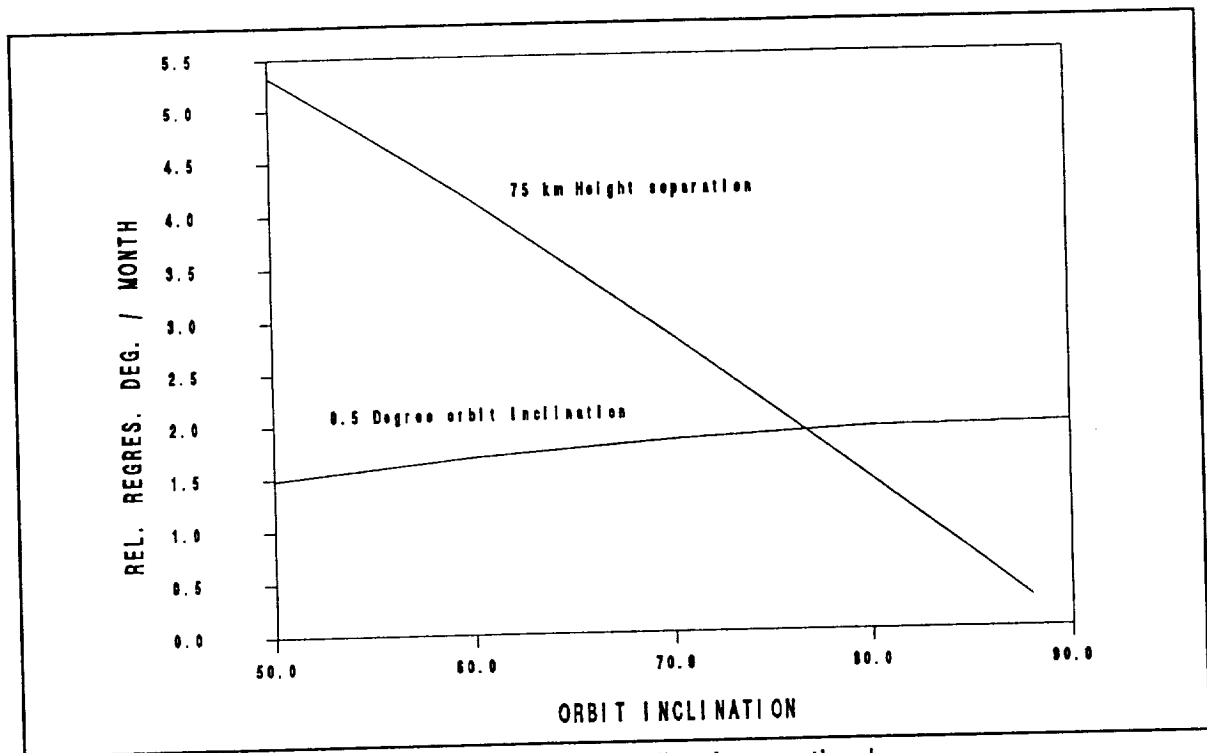


Figure 3-6 Comparison of Altitude and Inclination methods

3.5 Launch Configuration

Eight launches will insert the satellite clusters into the initial orbits shown in table 3-1 (see figure 3-1).

All 8 orbits will be circular at 550 km in order to achieve a minimum lifetime of 7 years. From these initial orbits, the orbital maneuvers will commence to place each of the six satellites into their own slightly different orbits. The inclination separated orbit clusters will be toward the poles (87° , 87.5° , 88° ...). The altitude separated orbit clusters will be spread to higher altitudes in increments of 75 km (550 km, 625 km, 700 km...). See appendix B for exact orbit descriptions.

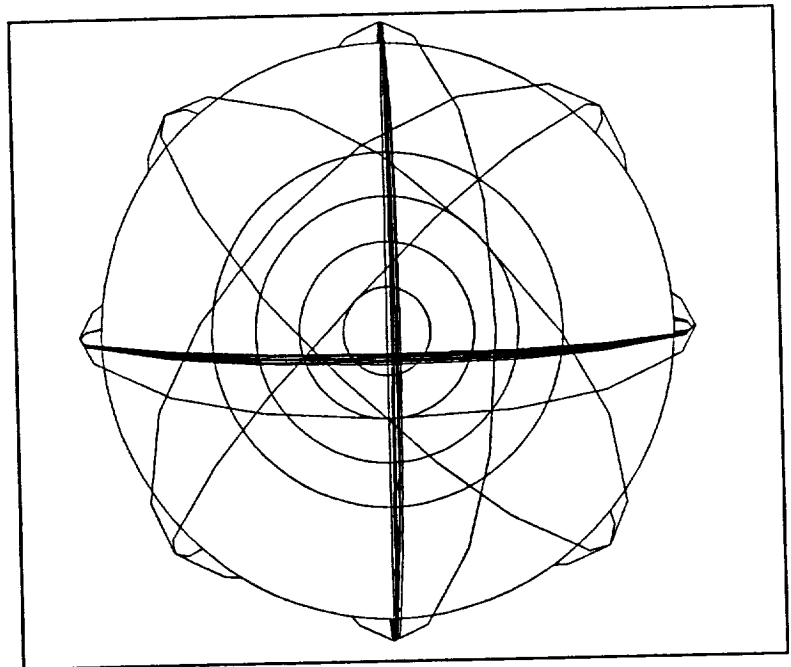


Figure 3-7 After cluster dispersion maneuvers

Table 3-1 Initial orbits for each satellite cluster

LAUNCH NUMBER	INCLINATION	TYPE OF SEPARATION
1	87°	Inclination
2	82.5°	Inclination
3	86°	Altitude
4	75°	Altitude
5	70°	Altitude
6	65°	Altitude
7	60°	Altitude
8	55°	Altitude

3.6 Constellation over time

After all orbital maneuvers have been completed, the satellites have been placed into their initial orbits and the view appears in figure 3-7. The two orbit groups nearest to pole have been dispersed by inclination separation and the other six in lower inclinations have been dispersed by altitude separation. From this time, the satellite orbit will regress at different rates to cause the constellation configuration seen in figure 3-8. This is the constellation configuration 6 months later. Each satellite's nodal regression rate per month is shown in appendix B. One concern is that this configuration will provide

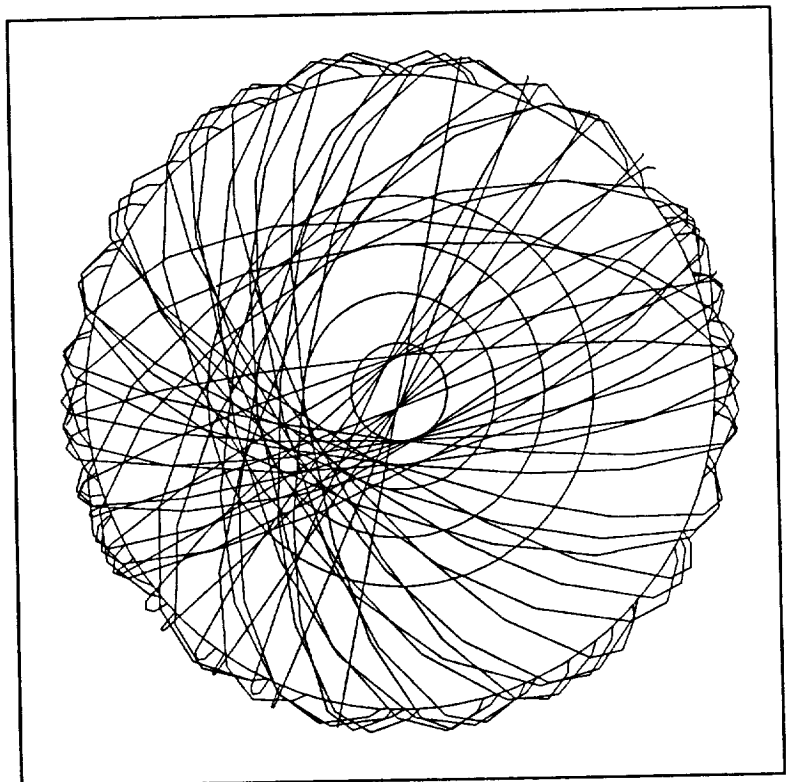


Figure 3-8 Constellation configuration after 6 months

adequate coverage of the earth in a short time span. The average orbit period is 100 minutes. Forming a global electrical field picture from 100 minutes of information might not work well if the E field is very dynamic. A shorter time frame of 20 minutes might be more desirable. Figure 3-9 shows the approximate global coverage during a 20 minute time frame. This coverage should provide adequate global coverage for our purposes.

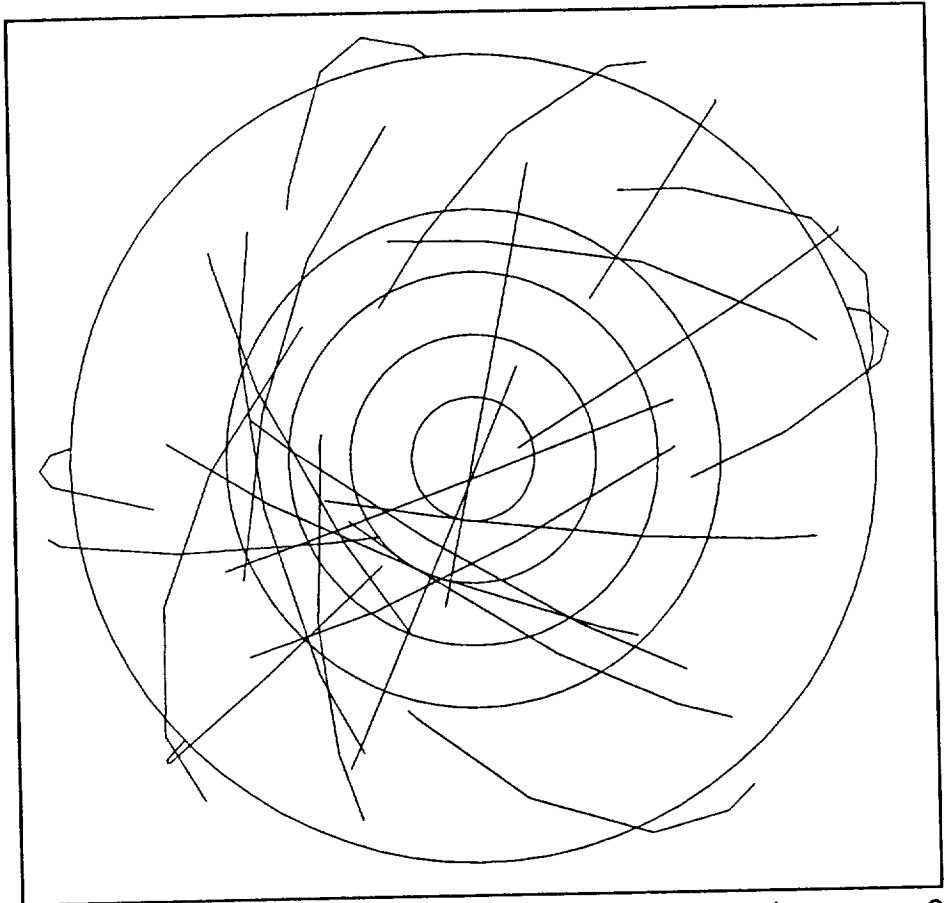


Figure 3-9 Global coverage during a 20 minute time span 6 months after deployment

REFERENCES

1. Wiesel: Spaceflight Dynamics. McGraw-Hill, 1989.

4.0 DEPLOYMENT

4.1 Launch Vehicle Selections

Fifty satellites will need to be deployed. Riding piggyback is a reasonable method to consider since the satellites have a mass of only 25 kilograms each. This is a low cost deployment method since most of the cost is paid by the main payload. We will certainly consider any piggyback opportunities which place our satellites in desirable orbits and fall within the mission time frame. However, finding enough missions to piggyback 50 satellites to the desired orbits is difficult. The orbits required are circular between 500 and 1000 km in altitude with inclinations above 55°. Also, this system must function as a whole, so the satellites must be deployed in a reasonably short amount of time (within 1 year) in order to function together.

It is possible to purchase one or two dedicated large class launchers like the Delta II or the Ariane and deploy all 50 satellites at once. However, there are great problems in spreading out a large group of satellites from a single orbit (see chapter 3.0).

McDonnell Douglas has asked USU to consider deployment of our satellite(s) on a piggyback with the Delta II. Space will be provided on the second stage where the satellite(s) will ride into an elliptical orbit of about 46° latitude. This is an excellent opportunity to launch one or several satellites. Such a deployment is particularly appealing as an opportunity to test the first satellite(s) in orbit. The Delta II orbit is not a practical one for constantly monitoring the earth's E field, but the ELF system will enjoy the chance to be proven in space.

Orbital Science's Pegasus is a smaller launching system capable of placing over 250 kg into the desired orbits. It can carry six ELF satellites into a 550 km circular orbit where they may be separated into individual orbits. The launch costs are reasonable at around 8 million dollars per launch.

The Pegasus launch vehicle has been chosen to deploy the major portion of satellites into the desired orbits. Eight Pegasus launches will deploy 6 satellites per launch for a total of 48 satellites. Realistically, Orbital Sciences Corp. cannot deploy 8 Pegasus vehicles at once, however they can deploy vehicles within weeks of each other thus achieving the goal of total constellation deployment in a short time (1).

4.2 Pegasus Launch

4.2.1 Individual Satellite Deployment Capability Each cluster of six satellites will arrive in a 550 km circular orbit. The six satellites will be connected to an interface bus which is attached to the Pegasus third stage. Each cluster then needs to be dispersed by either altitude or inclination maneuvers. Methods of maneuvering each satellite from the initial orbit to its own slightly different altitude or inclination orbit have been studied.

An ejection system was briefly considered that could eject each satellite with a single thrust. Each satellite could be thrust from the main structure by a spring or some sort of pneumatic device. The distance of applied thrust was the limiting factor, perhaps 1 m. Since the length was so short, a large acceleration would be required to achieve a sufficient delta V. This force was too large to be practical so this choice was eliminated.

Each satellite could be equipped with a small propulsion system. Solid, liquid, and electric thrusters were all considered.

Electric propulsion was eliminated because of the power requirements and the time required for dispersion. Work has been done on thrusters in the several kilowatts range (2), but our available power is only several watts. To change the orbit inclination, delta V must be applied at the equator and the thruster shut down for the rest of the orbit. Time required to significantly rotate the orbital plane with the available power was in the years.

Both solid and liquid thrusters were found to be possibilities. A liquid system might be a 70 N thruster which could thrust for about 3 minutes to achieve an appropriate delta V of perhaps 500 m/s. This delta V would sufficiently rotate the orbital plane. Solid motors were found from the Thiokol Star B series which were in the range required for an appropriate delta V.

The final ELF configuration did not allow thrusters on individual satellites because the design was simplified to the point that the satellites did not carry attitude control. The cost of providing one motor for each satellite was also high. The space debris from 48 satellites, each ejecting a motor was also an issue. There was no method of de-orbiting each motor after use. The small motors considered were in fact themselves designed to de-orbit space systems. The forces placed on the satellites by the solid motors was also questionable. The structure would have to be strengthened to carry the deployment thrust loads.

A bus system was chosen as the answer to the satellite deployment problem. This is a single vehicle with an attitude control system and one motor for orbit maneuvering. Six satellites will ride this bus and be ejected into their respective orbits. Thus, the complexity of an attitude control system and capability of thrusting to different orbits is combined into one vehicle. This simplifies the cost and complexity of the deployment system, particularly since the Pegasus third stage supplies the attitude control system.

4.2.2 Pegasus Bus System The bus system in figure 4-1 is composed of the Pegasus third stage, six ELF satellites, the interface structure, a thruster and fuel tanks. Our structure will stay attached to the Pegasus third stage so we can use its attitude control system to assist in performing our orbit maneuvers. We will provide a thruster since the third stage will, at deployment, only have attitude control fuel left.

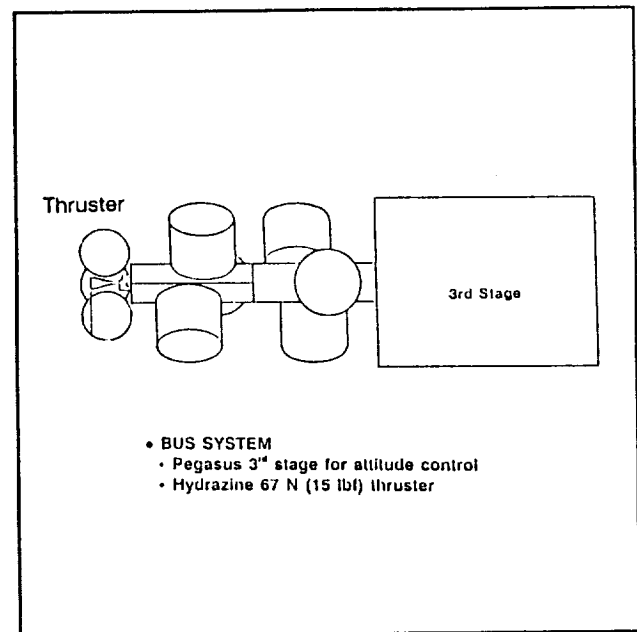


Figure 4-1 Bus system

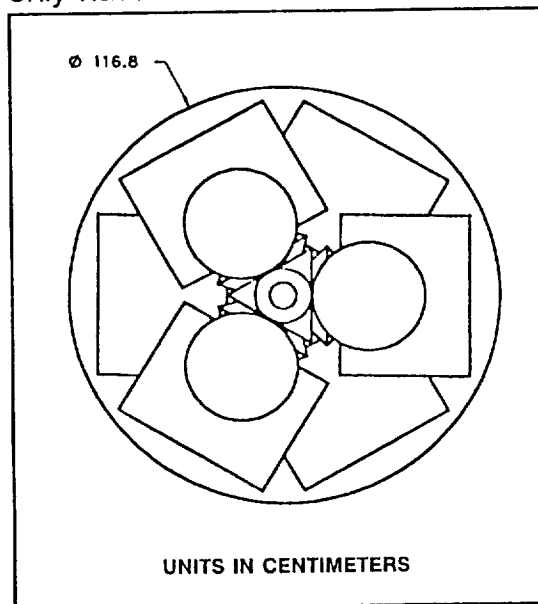


Figure 4-2 Top view of Launch Vehicle Configuration

4.2.2.1 The Interface The interface design consists of a vertical post (ALUM. 7061) with a triangular cross section (26.1 cm sides). The post is divided into two sections. These sections are offset by 60°. The satellites are wrapped around the post in a spiral manner as seen in figures 4-2 and 4-3. The mass of the center post and satellite interfaces is 63 kg. The ELF system will provide propulsion to enable the bus system to make the orbital maneuvers. A 66 N hydrazine bi-propellant motor has been chosen to meet our needs. The motor will be mounted on the top of the satellite support beam to thrust axially through the bus. Three 36 cm spherical fuel tanks will also be mounted around the perimeter of the

motor. The tanks should total about 10 kg and the fuel approximately 43 kg. The specific model of motor and thrusters is still being considered. Rocket Research has provided information on available systems (3).

4.2.2.2 Satellite Mounting Due to an instability (tumbling) problem when launching the satellites into the orbits, provisions need to be made to spin the satellites while they are being ejected from the Pegasus. Figure 4-4, (see appendix C for more details), illustrates the method used to eject and spin the satellites. The marmon clamp system consists of two conical sections bound together by a strap. This is commonly used for satellite deployment. There is an explosive placed which, when ignited, allows separation of the two sections. A catch plate (which is welded to the threaded guide) is placed between the conical sections. Spikes will serve the function of holding the satellite to the guide rod. When marmon clamp is released, the spring will force the satellite forward. At the same time the threaded rod travels through the threaded guide which causes rotation of the catch plate which spins the satellite. Employing a 70-78 N/cm spring results in a revolution of 1 RPM. Provision is provided to stop the guide rod as shown in figure 4-4.

The 67 Newton thruster is fixed to thrust axially through the third stage. However, the center of mass will not

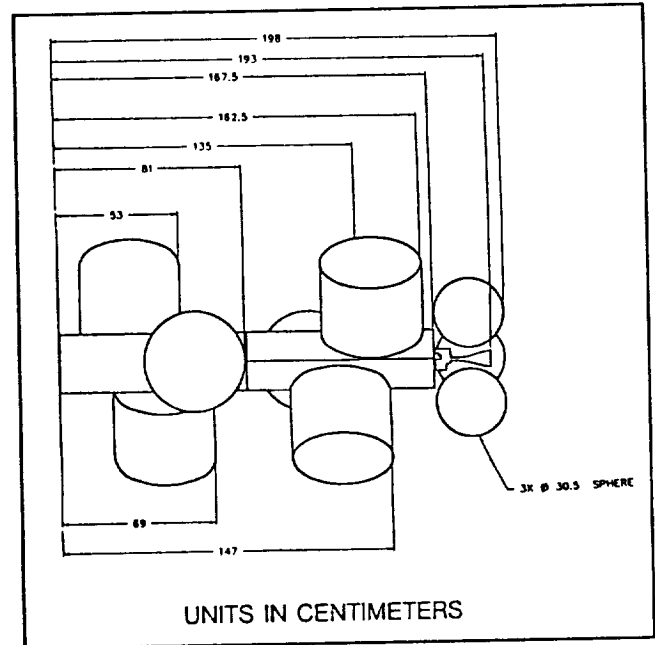


Figure 4-3 Side view of Launch Vehicle Configuration

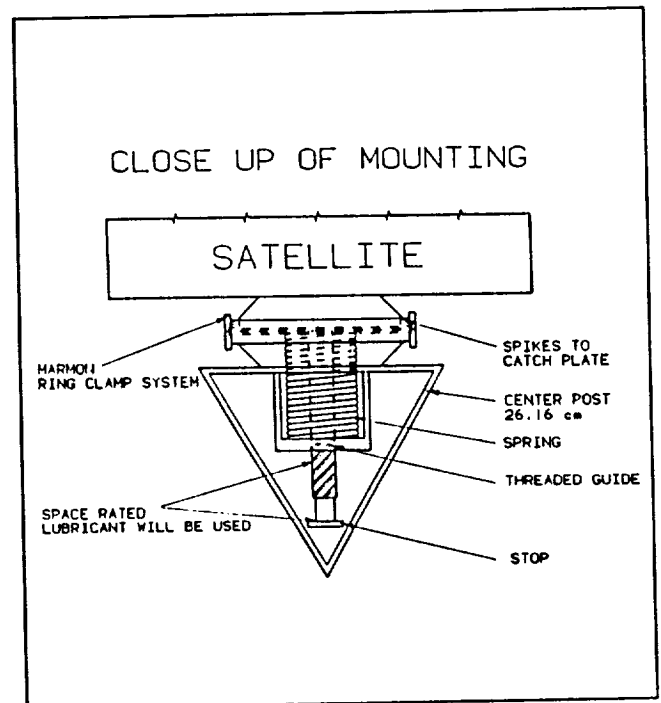


Figure 4-4 Satellite Interface System

always be located along this line. As each satellite is deployed, the center of mass shifts slightly, about 3 cm. The resulting moment is compensated for by the attitude control thrusters on the third stage.

Spiraling the satellites around the center post minimizes the orbit maneuvering time spent with an off axis center of mass. Using the spiral configuration, the center of mass will be shifted off axis with every odd number of satellites deployed. The off axis problem occurs only after the first, third, and fifth satellites are deployed. So for three of the five orbit changes, the Pegasus third stage attitude control thrusters will be needed for off axis thrust compensation.

4.2.2.3 Pegasus Modifications Our system requires the full use of the Pegasus third stage guidance system while performing maneuvers. We require about 5 hours of third stage operating time to complete orbital maneuvers. At present, the third stage is capable of operating its guidance computer for 45 minutes after launch. Orbital Sciences think this need can be met and say it is possible to modify their design for our 5 hour requirement (4).

We will need perhaps three to five times the impulse supplied by Pegasus's CO₂ attitude control thrusters. Pegasus comes equipped with 660 N-s of impulse. Orbital Sciences Corp. can add more attitude control fuel and hopefully be able to meet our needs (3).

4.2.2.4 Future Considerations of the Bus System The bus system idea appears to be undisputed in concept. The type of motor and fuel might still be improved. A solid propellant motor would require the deployment system to be different since satellites would have to deploy under about 2 g's of force. This system would be cheaper since solid systems are usually cheaper. However, a solid motor would not be capable of firing several times for altitude maneuvers. The best choice for fuel tanks needs further investigation. Three hydrazine tanks were specified to carry the required 43 kg of fuel, however, it is a possibility that two larger tanks will do the same job for less money. The satellite spiral configuration might be modified in order to fit two 42 cm spherical tanks instead of three 36 cm tanks. This would cut the cost since the 42 and 36 cm tanks each cost about the same.

4.2.3 Orbital Maneuvering and Requirements

4.2.3.1 Inclination Maneuvering Two launches will be above 80° inclination and will require the inclination separation method. Figure 4-5 shows this method.

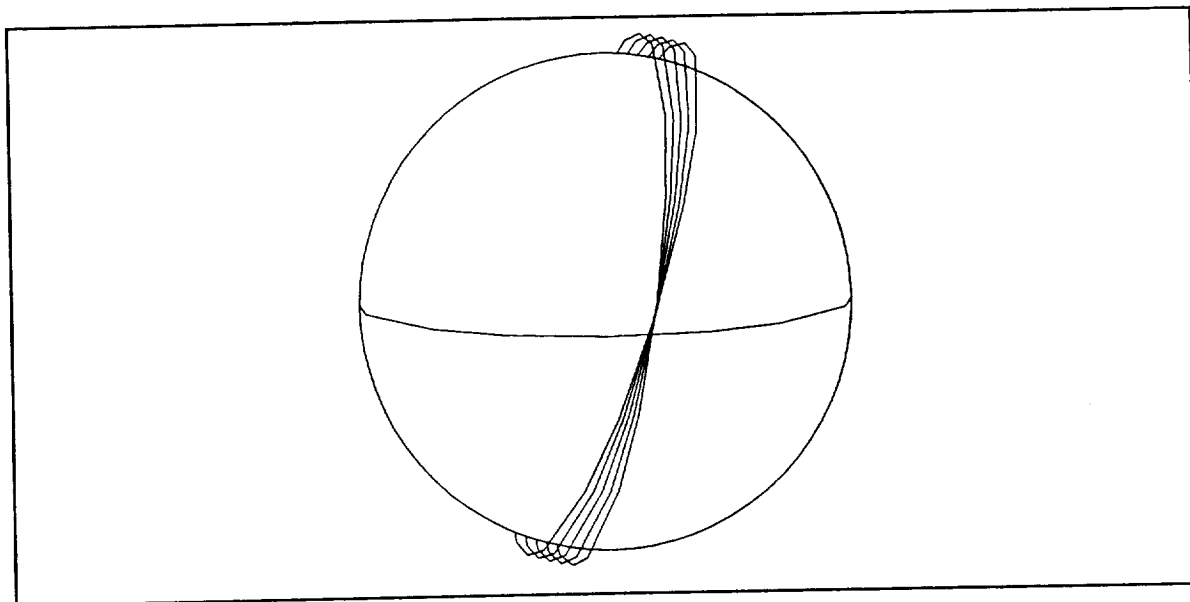


Figure 4-5 Delta V at equator for inclination separation

The inclination separation method will require releasing the first satellite into the initial Pegasus orbit. The following delta Vs must occur while passing over the equator to maximize the change in inclination per delta V. During the first pass over the equator, a delta V will be fired to rotate the orbital inclination 0.5° . The second satellite will then be released into this new orbit. Thus, the other satellites will be released one at a time at 0.5° inclination increments as the bus's orbital plane is rotated a total of 2.5° .

The circular velocity at the 550 km altitude is 7585 m/s. Thus, rotation of the bus orbit plane a total of 2.5° , requires a total delta V of 331 m/s. The motor has only 66 Newtons of thrust so it takes about 30 minutes to provide this total delta V. Since the delta V should occur over the equator, it is broken up into five small delta Vs lasting six minutes each. Thus, the total delta V is performed over five orbits at one pulse per orbit. For each orbit, the delta V causes the orbital plane to rotate 0.5° were one satellite is deployed. The total delta V required for 2.5 total degrees inclination change can be burdensome on fuel requirements. Figure 4-6 shows how much total hydrazine fuel is required for the system. Since we desire an inclination separation between each satellite of about 0.5° , this system will require around 43 kg of hydrazine.

4.2.3.2 Altitude Maneuvering Six launches below 80° inclination will require the altitude separation method.

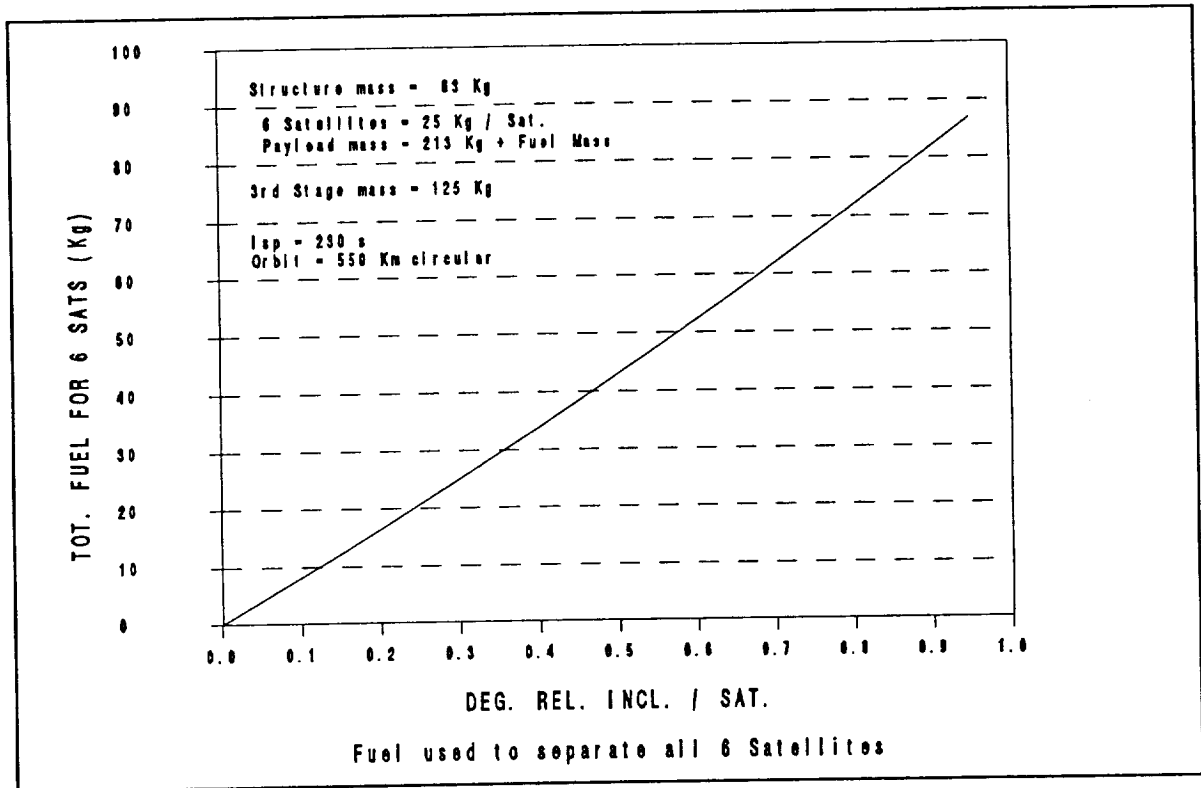


Figure 4-6 Fuel requirements for inclination maneuver

An altitude separation scheme requires leaving the first satellite in the initial Pegasus orbit. The first delta V is then used to leave the 550 km circular orbit. The bus will ride a Hohmann transfer to a maximum altitude of 625 km. A second delta V will there be used to circularize the orbit where the second satellite will be deployed. The bus will maneuver on Hohmann transfers to the rest of the orbits. A total of ten delta Vs will be used in altitude maneuvering as seen in figure 4-7. These delta Vs are considerably less fuel consuming than the inclination method since the average delta V is 20 m/s for a total of 200 m/s. For the hydrazine fuel used, and considering all the changes in mass through the orbits, a total fuel mass of 24 kg is required by this deployment scheme.

4.2.3.3 Release from Bus Upon reaching the desired altitude and inclination, the satellite will be inserted into its orbit from the bus. The satellite will be spun to approximately 1 RPM as it is released. This spin will help to initially stabilize the satellite as it moves away from the bus. As of yet a system has not been designed to begin the deployment of the booms and start the spin-up process. One possible design could be a trigger system which would actuate upon deployment from the bus. A time delay could be used to clear the satellite away from the bus. Another system could use a signal from the ground to activate the process. Preferably the

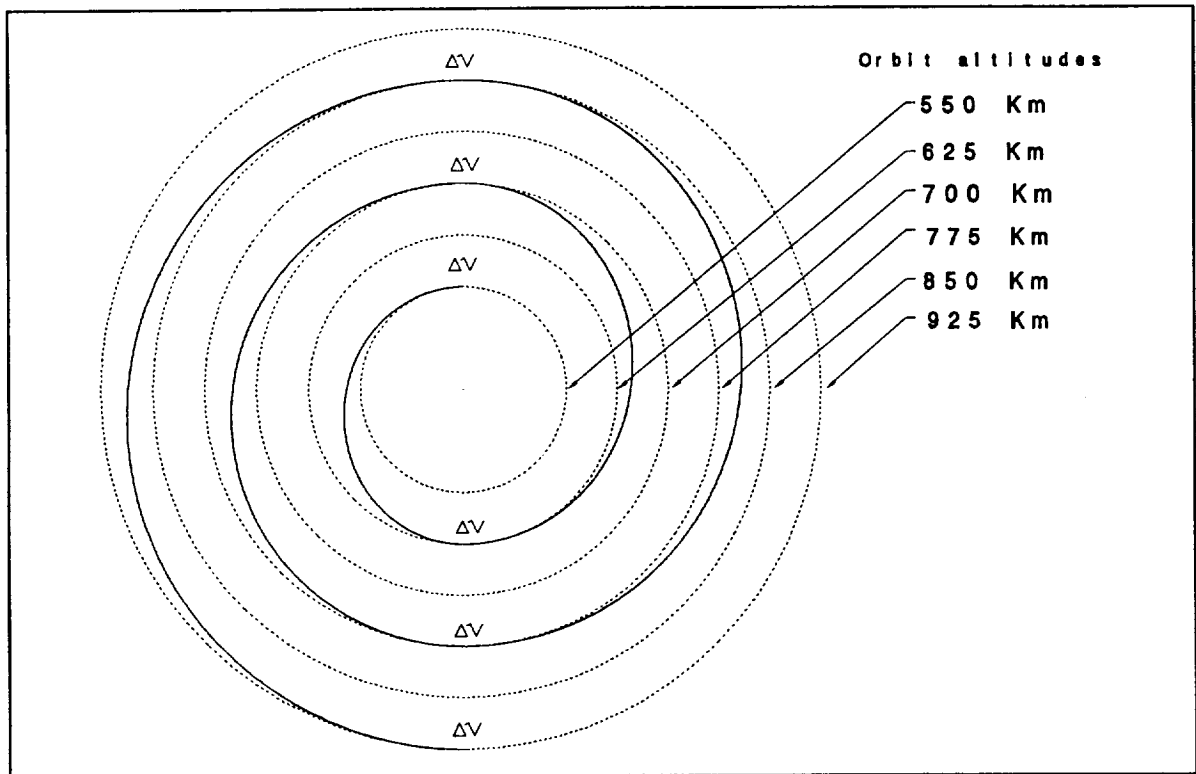


Figure 4-7 Altitude maneuvers for altitude scheme

first method would be used with the second as a backup in case the first method failed.

4.2.4 Mass Requirements of System The following is the configuration masses.

Pegasus third stage = 125 kg (Not part of payload)
 6 satellites = 150 kg
 Interface structure = 63 kg

Inclination maneuvers

Motor + 3 tanks = 10 kg
 Hydrazine fuel = 43 kg

Altitude maneuvers

Motor + 3 tanks = 5 kg
 Hydrazine fuel = 24 kg

total inclination system payload = 266 kg

total altitude system payload = 242 kg

Figure 4-8 is data provided by Orbital Sciences showing the maximum payload capacity of the Pegasus launch vehicle (5). We will launch slightly to the right of the 90° inclination line. For a 550 km orbit, the above masses are reasonable.

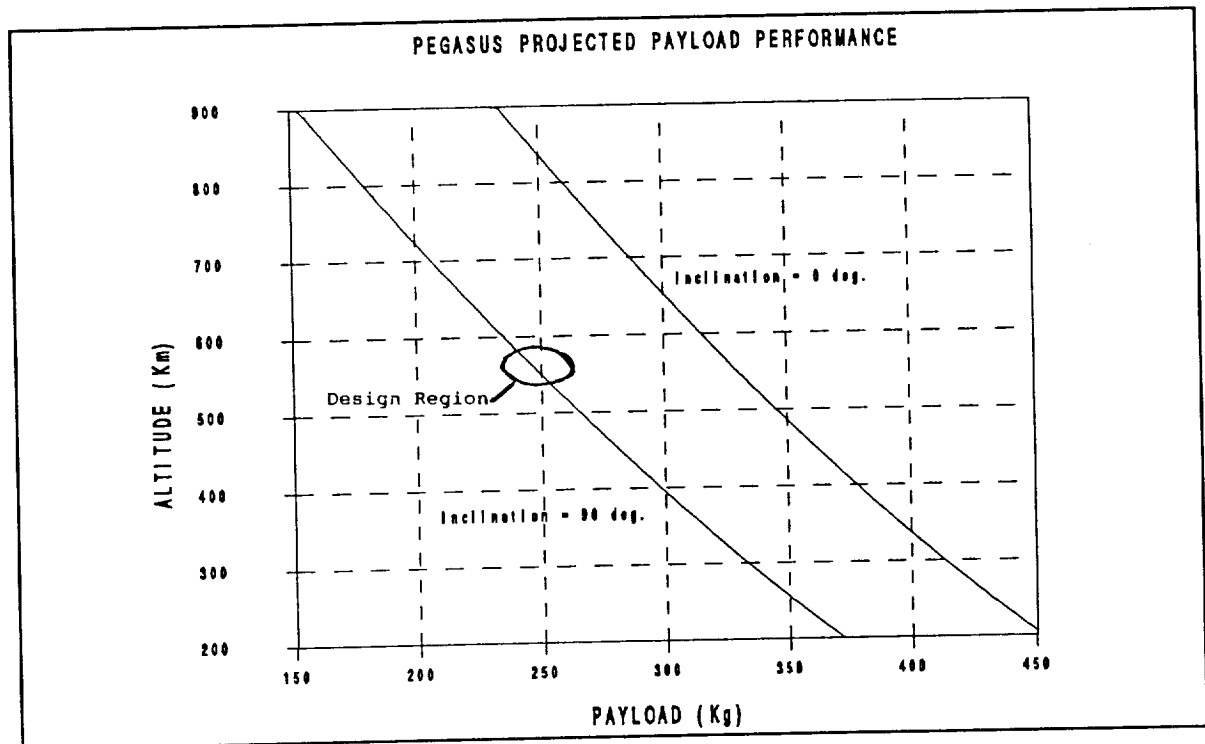


Figure 4-8 Pegasus payload capability

4.3 Delta II Launch

The Delta II is considered to be an excellent opportunity to launch some of our ELF satellites. It is proposed that the first satellite(s) be launched as a secondary payload aboard a Delta II rocket. As the secondary payload of the Delta II launch, our satellite will have an economical ride into space. The performance of the satellite will then be evaluated. If the satellite performs as designed, the remaining satellites in the constellation will be deployed.

From the "Preliminary Delta II Launch Schedule and Secondary Payload Margins (2/12/90)" all of the scheduled launches with secondary payload availability will be launched into inclinations between 28.7 and 34 degrees. However, most desirable orbits for E field sensing are circular orbits above 55° inclination and between 550 and 1000 km altitude. So, we will employ the Delta II piggyback system when

launches are available in compatible orbits. Also, will also use the Delta II system for initial ELF satellite evaluation. In selecting the launch for ELF evaluation, it is not important to choose a specific orbit which provides optimum E field measurement

Studies might be furthered on an orbit maneuvering system such as a booster on individual ELF satellites or a tether system. This system could change the ELF orbit(s) from the initial launch orbit to a more desirable orbit(s). Such an orbit maneuvering capability would broaden the selection of Delta II launches.

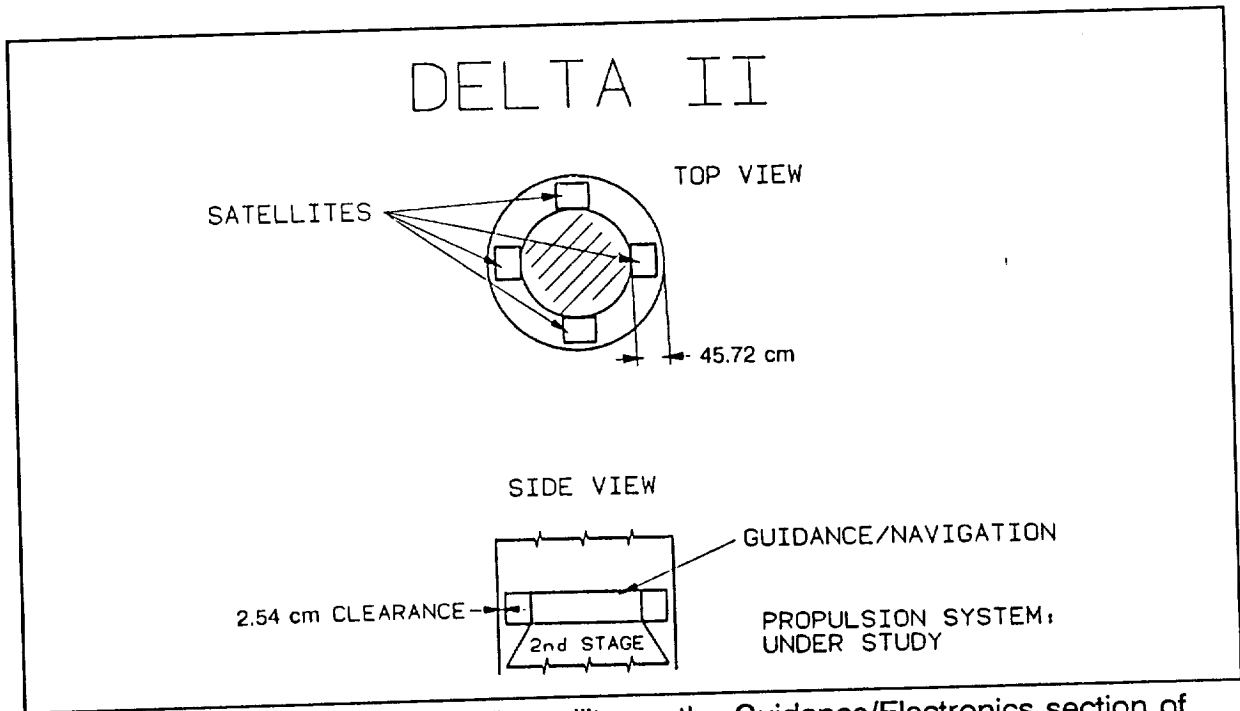


Figure 4-9 Mounting of the ELF satellite on the Guidance/Electronics section of the Delta II launch vehicle.

4.3.1 Launch Vehicle Interface Figure 4-9 shows a second stage mounting plan. The size of the ELF satellite and its booster motor creates a problem for mounting. The locations available for a secondary payload of this size must be designed into the space available for the primary payload. If a new type of satellite deployment utilizing a tether system is used, the satellite may be mounted to the guidance section of the rocket. This same mounting position may also be used if the guidance section is altered such that a booster (insertion) motor is accommodated.

The most probable mounting scheme to be used is a marmon clamp and standard pyrotechnic devices. The Delta II's computer system will be used to control the

deployment of the satellite.

The actual mounting position will be determined after a series of discussions between the McDonnell Douglas Commercial Delta Corporation, Utah State University, and the owner of the primary payload. The final details of the mounting and ejection mechanisms of the satellite are TBD after the above talks.

4.3.2 Orbital Maneuvering An orbital maneuvering system could be designed to insert our ELF satellites in desired orbits following deployment from the Delta II. We would like circular orbits above 55° inclination and between 550 and 1000 km altitude. A system could be designed to maneuver our satellites from the initial second stage orbit to an orbit more suitable for our purposes. Some options are discussed.

Consider a motor attached to each satellite. If several delta Vs needed to be performed, a restartable liquid motor would be required. This could be accomplished if space on the second stage could be found to fit both the satellite and the motor. The current ELF geometry causes difficulties fitting the motor on the satellite. Also the satellite would need an attitude control system. For ELF mission requirements, an attitude control system is not needed. Thus, additions to the satellite design would be necessary for ELF system deployment of the full constellation.

Another system presently being considered for orbit maneuvering is the tether deployment system. This system will be used to send small satellites on different trajectories from the Delta II (bus) orbit. Further investigation of this method is needed.

REFERENCES

1. Bob Lindberg, Phone conversation, Orbital Sciences, April 18, 1990.
2. NASA Technical Memorandum 102065 AIAA-89-2492: The NASA low thrust propulsion program. 25th Joint Propulsion Conference, July 10-12, 1989
3. Monopropellant hydrazine rocket engine assemblies, rocket engine modules propulsion systems. Rocket Research publication 90-H-1454, May, 1990
4. Bob Lindberg, Phone conversation, Orbital Sciences, April 1, 1990.
5. Orbital Sciences Corp.: Pegasus Payload Users Guide. December, 1988.

5.0 ATTITUDE CONTROL AND DETERMINATION SYSTEM

The attitude control system (ACS) gives the spacecraft the ability to maneuver in space. The ELF satellite will need only a minimal attitude control system. This system will spin-up or de-spin the satellite to maintain a 10 ± 2 RPM spin rate. This spin rate will provide the necessary angular speed for the electrical field sensors as well as provide the necessary stability for the satellite.

5.1 Design Requirements

The criteria for the final design were to:

- 1) know the attitude within $\pm 1^\circ$;
- 2) rotate the electrical field (e-field) sensors at 10 ± 2 RPM;
- 3) minimize the mass;
- 4) minimize the cost; and
- 5) use proven technology.

The primary driver of the final design was to know the attitude within $\pm 1^\circ$.

5.2 Design Evolution

The design of the ELF satellite has passed through many stages. The first design was made to maintain the e-field sensors as stationary as possible and to keep the communications dish always pointing towards the earth. To accommodate both requirements, a gravity gradient design was considered. This would have required an attitude control system for orbital insertion and oscillation damping. The sensors used were eight CCD Cameras. Four were used to sense the sun, and the other four were used to sense the earth's horizon. All the camera data would have been sent to the on board computer for complex data processing to determine the attitude of the satellite.

Later, we determined that the sensors needed to be rotating. To have the sensors rotating and the communications dish pointing towards the earth, a dual spinner satellite was designed. This would have required a three-axis control system as well as complicated data transferral mechanisms between the rotating boom system and the satellite bus. The same attitude determination techniques that were used on the first design, were used on this design. This system was thought to be too complicated so alternatives were considered. Relaxation of the e-field sensor spin rate requirement and

the elimination of the earth pointing antenna led to the final design concept.

For the final design, a nearly omni-directional antenna was incorporated which alleviated the requirement of having a section of the satellite always pointing towards the earth. The major requirements were then to spin stabilize the satellite and to know the attitude within $\pm 1^\circ$. To satisfy those requirements, a single-axis spin stabilized satellite was designed. This required only a single-axis control system to spin-up or de-spin the satellite.

5.3 Attitude Control Operations

The attitude control system will require three distinct systems: the attitude sensing system, the data processing and logic system, and the attitude propulsion system. Each of these systems is necessary to control the spin rate of the satellite.

The attitude sensing system will use two 2-axis magnetometers, two sun sensors, and one horizon sensor. By using different combinations of these five sensors, the attitude of the satellite can always be determined. Some of the information will be redundant but this redundancy can be used to better determine the exact attitude of the satellite.

The data processing system will analyze the information from the sensors and activate the propulsion system if necessary. Two pieces of information will be needed from the attitude system. First, the orientation of the satellite in space with respect to some inertial reference frame will be needed. Second, the spin rate of the satellite will be needed to determine the exact location of the booms. This information will be used to reconstruct the shape of the e-field and maintain a proper spin rate for the e-field sensors.

To adjust the spin rate of the satellite, a cold gas propulsion system will be used. Between 1.0 and 2.0 kg of propellant will be stored at launch time. The basic system will consist of two propellant tanks, two regulators, four valves, and four nozzles. The nozzles will be oriented about the spin axis. The logic system will pulse the thrusters if spin rate adjustments are needed.

5.4 Satellite Motion

5.4.1 Equations of Motion A model of the satellite dynamics are a necessary part of building a control system. The modeling equations are used to generate the logic for

the control system. Since the e-field sensor is made up of a three-axis, orthogonal sensing system, any orientation (attitude) may be maintained by each satellite. To derive the equations of motion for the control system, only a local coordinate system is necessary. Local in this case means a coordinate system which is unique to each satellite. The approach used in this paper is to use a body fixed coordinate system.

The equations of motion of the satellite may be described by using Euler's equations. These equations use the following assumptions:

1. The body is a rigid body.
2. The rotation of the body is equal to the rotation of the body fixed frame.
3. The largest principal moment of inertia axis will correspond with the spin axis of the satellite. And,
4. The body will rotate about the center of mass.

Using the above assumptions the Euler Equations may be written as:

$$\begin{aligned} M_1 &= A\dot{\omega}_1 + (C-B)\omega_2\omega_3 \\ M_2 &= B\dot{\omega}_2 + (A-C)\omega_1\omega_3 \\ M_3 &= C\dot{\omega}_3 + (B-A)\omega_1\omega_2 \end{aligned}$$

where

A,B,C = The principal axes of inertia

$\omega_1, \omega_2, \omega_3$ = Spin rate of the principal axes

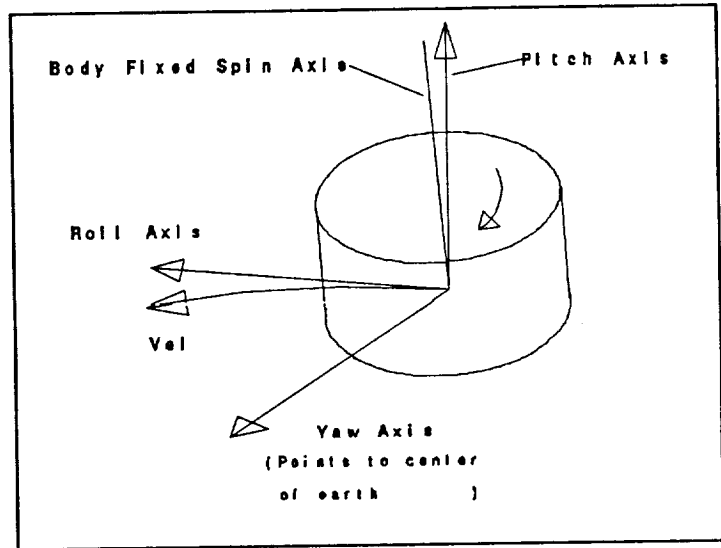
M_1, M_2, M_3 = External Torques on Satellite.

The spin axis for this configuration is C (axis 3). It will be the only controlled axis. The yaw and roll axes will depend on gyroscopic effects for their stability.

To simplify the non-linear Euler equations, assume that ω_1 and ω_2 are very small compared to ω_3 . By linearizing the Euler equations, the C-axis becomes decoupled from the other two. The system control equation for the spin axis thus becomes:

$$M_3 = C\dot{\omega}_3$$

5.4.2 Stability Analysis To visualize the motion of the satellite, a reference frame other than the body fixed reference frame must be established. One such frame is the Yaw-Pitch-Roll coordinate axes. In this coordinate system, the yaw axis points towards the center of the earth, the roll axis is parallel to the velocity vector of the satellite and the pitch axis is normal to the other two axes as shown in figure 5-1. Although this is not an inertial coordinate frame, it allows a visualization of the movement of the satellite.



To derive the equations of motion in the yaw-pitch-roll axes system, the body fixed axes must be placed through three axial rotations to align

Figure 5-1 The Yaw-Pitch-Roll coordinate axes give a reference frame to visualize the motion of the satellite.

the two coordinate systems. Also a set of Euler angle equations must be developed to convert the angular rotations in the body fixed coordinate frame to those in the yaw-pitch-roll coordinate frame. If small angles are assumed in the transformation between the two systems, the transformation matrix may be defined as:

$$\begin{bmatrix} 1 & \theta & -\phi \\ -\theta & 1 & \psi \\ \phi & -\psi & 1 \end{bmatrix}$$

and the Euler angles as

$$\begin{aligned} \omega_1 &= \dot{\psi} - \phi \dot{\omega}_0 \\ \omega_2 &= \dot{\phi} + \psi \dot{\omega}_0 \\ \omega_3 &= \dot{\theta} + \omega_0 \\ \dot{\omega}_1 &= \ddot{\psi} - \dot{\phi} \dot{\omega}_0 \\ \dot{\omega}_2 &= \ddot{\phi} + \dot{\psi} \dot{\omega}_0 \\ \dot{\omega}_3 &= \ddot{\theta} \end{aligned}$$

Upon substitution of the Euler angle equations into the Euler equations of motion, and linearization of the equations, the yaw-pitch-roll equations of motion for the satellite become:

$$\begin{aligned} M_1 - A\ddot{\psi} + [-(A+B-C)\omega_0 + (C-B)\Omega]\dot{\phi} + [(C-b)(\Omega\omega_0 + \omega_0^2)]\psi \\ M_2 = B\ddot{\phi} + [(A+B-C)\omega_0 - (C-A)\Omega]\dot{\psi} + [(C-A)(\Omega\omega_0 + \omega_0^2)]\phi \\ M_3 = C\ddot{\Omega} \end{aligned}$$

where

- ψ = Spin rate about the yaw axis
- θ = Spin rate about the pitch axis
- ϕ = Spin rate about the roll axis
- ω_0 = Angular velocity of satellite orbit about the earth
- Ω = Spin rate of Satellite about the C-axis ($\Omega = \omega_3$)

In this coordinate system, the spin axis will nominally be aligned with the pitch axis. The spin axis is the only controlled axis. The pitch and the roll axes will not be controlled by any active system.

Examination of the yaw-pitch-roll equations of motion indicates that the motion of the pitch axis is independent of the motion of the yaw and roll axes. The yaw and roll axes on the other hand are coupled. Since they are coupled, energy will be transferred between them.

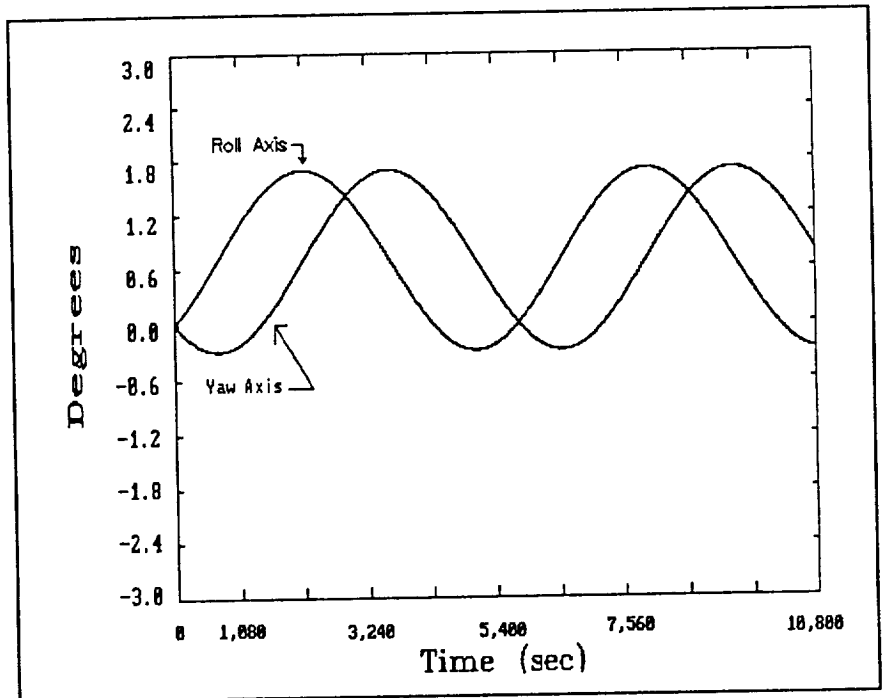


Figure 5-2 The satellite oscillates less than 1.8° about the yaw and roll axes.

Because the satellite is an oblate spinner, the motion of the satellite will be stable. Stable means that the satellite will not change its attitude drastically for small external forces. To visualize the motion of the satellite the equations of motion for the yaw and the roll axes were analyzed with the application of small external torques. To represent the nutational motion of the satellite, a program called TUTSIM (9) was used to evaluate the coupled differential equations. Figure 5-2 represents the satellite motion with a step input torque of 10^{-4} N·m in both the pitch and roll axes. The spin rate of the satellite is 10 RPM and the moments of inertia are $I_x = 9.6 \text{ kg} \cdot \text{m}^2$, $I_y = 9.6 \text{ kg} \cdot \text{m}^2$, $I_z = 16.8 \text{ kg} \cdot \text{m}^2$. The maximum deviation from either the yaw or roll axes during a three hour period is approximately 1.8° . With

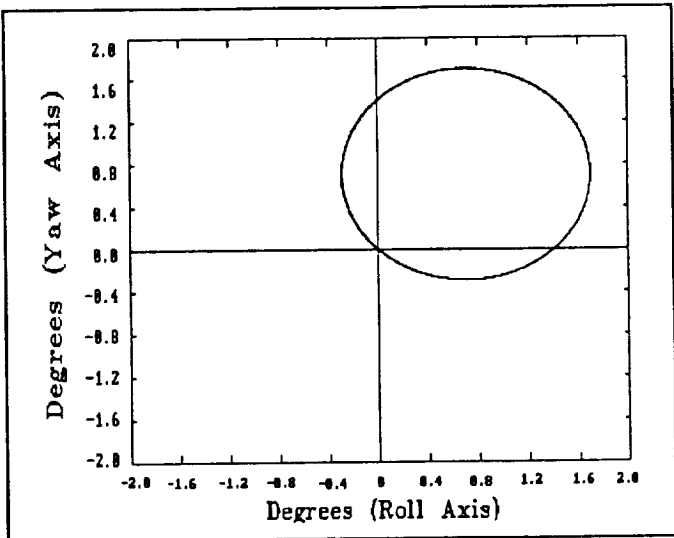


Figure 5-3 Path traced by the spin axis about the pitch axis due to the oscillations of the satellite.

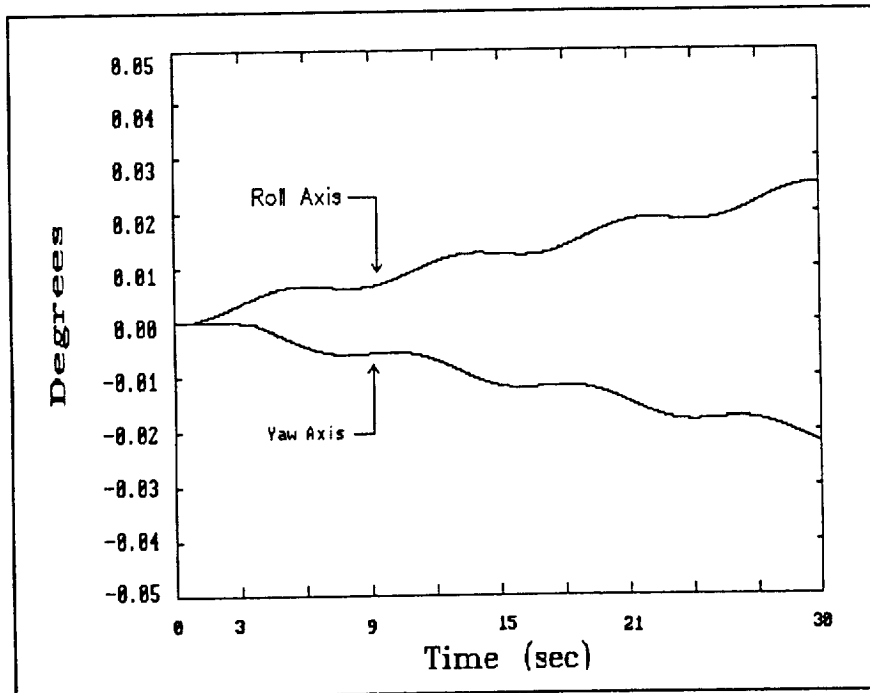


Figure 5-4 High frequency oscillations of the satellite about the roll and yaw axes.

The maximum deviation of this magnitude, the attitude would need to be determined at least three or four times per orbit to be within the $\pm 1^\circ$ limit. Figure 5-3 illustrates the motion of the spin axis due to the oscillations of the satellite about the yaw and roll axes.

Also, present in the motion of the satellite is a cupusoidal motion. The motion may be seen by viewing the oscillations of the satellite about the yaw-roll axes at a higher resolution. Figure 5-4

shows the higher frequency oscillation of the satellite. The magnitude of this oscillations is small compared to that seen in figure 5-2. Figure 5-5 demonstrates the motion of the pitch axis due to these smaller oscillations.

To visualize what figures 5-2, 5-3, 5-4 and 5-5 represent, imagine that a pencil extends through the body fixed spin axis. This pencil then plots the motion of the satellite on a paper which is in the yaw-roll plane.

The motion of the satellite would appear to plot a circle on the paper about the pitch axis.

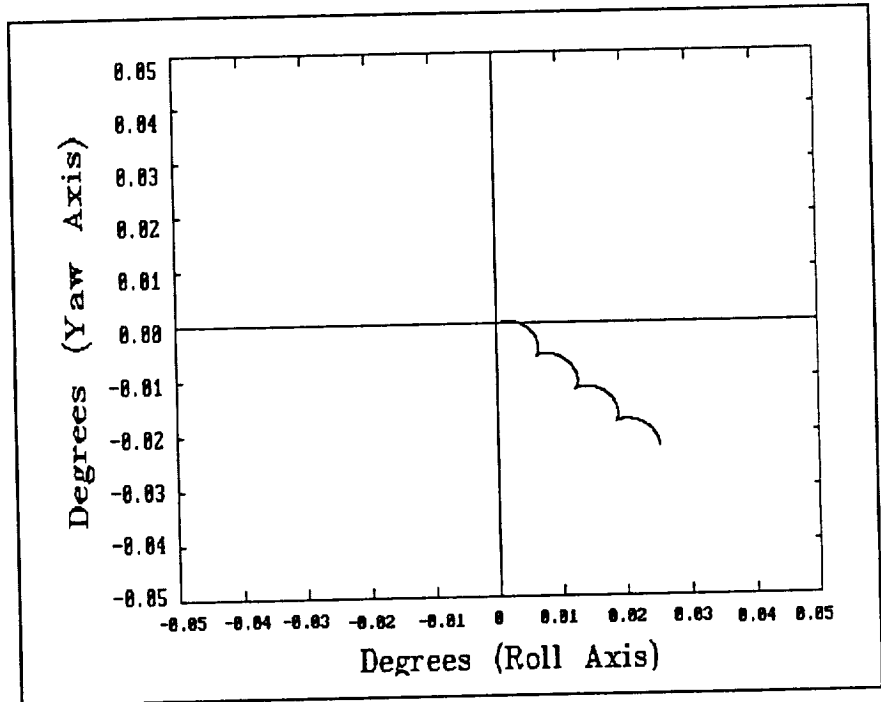


Figure 5-5 Movement of the spin axis due to the oscillations of the satellite about the yaw and roll axes.

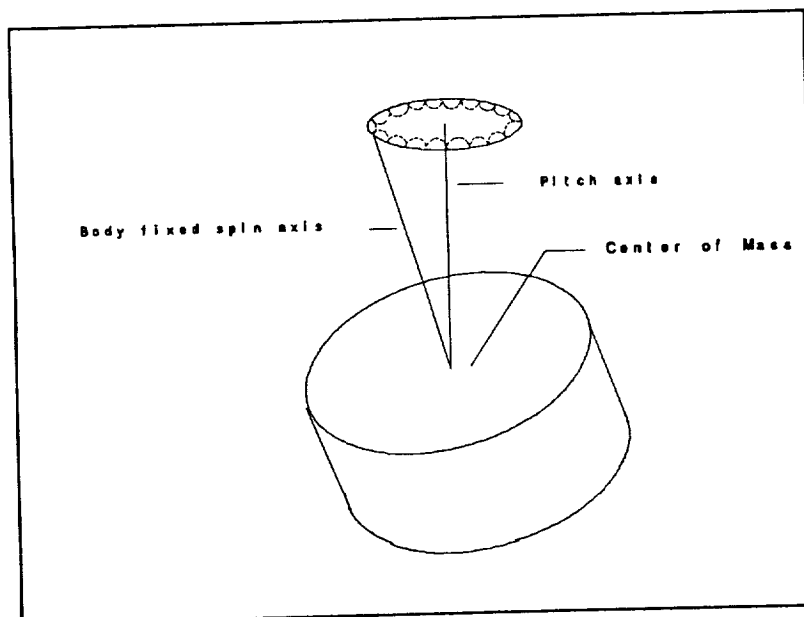


Figure 5-6 If a constant input torque is applied to the satellite in the body fixed frame, the satellite will begin to nutate as illustrated in this figure.

The pencil would trace out a cone with the point of the cone at the center of gravity of the satellite. Figure 5-6 illustrates this motion of the satellite.

The above analysis in the yaw-pitch-roll axes coordinate system does not represent the exact attitude of any of the satellites to be launched. A satellite could have any attitude. Such analysis does however give a representative motion of a satellite as it would be in its own local coordinate frame.

The analysis of the satellite motion using a single rigid body model is limited. An important characteristic of the long booms is that they will vibrate. These vibrations act as an energy damper. Over time, oscillation of the satellite about the yaw and roll axes will be damped out by the vibrations of the booms. By assuming a single rigid body for the satellite system, energy dissipation is not accounted for in the system. A better model could be made up of four non-rigid booms each attached to the satellite bus. A non-rigid boom could include damping elements. Such a model could allow for the energy dissipation of the vibrating booms.

5.5 Attitude Determination

To determine the attitude of a satellite with respect to the earth, some way is needed to determine the satellite's orientation relative to some direction in space. Sensors are used to find the angle of the reference axis in the satellite's coordinate frame. This angle defines a vector which could lie anywhere on a cone defined by the angle as illustrated in figure 5-7. To pinpoint its location on this cone another reference direction must be found. This second vector will define a second vector cone. Since the satellite attitude is common to both vectors, the cones will intersect, as seen in figure 5-8. The cones will intersect at two different points causing ambiguity in determining the exact attitude. To determine which of the two points specifies the exact orientation of the satellite, another two vectors are sampled at a later time. Now comparing all four vectors, the correct orientation can be determined. Some of the objects that are sensed are the Sun, the Moon, the stars, and the Earth. One vector can also be determined by finding the Earth's magnetic field with respect to the satellite, and comparing it to magnetic field maps of the Earth (2).

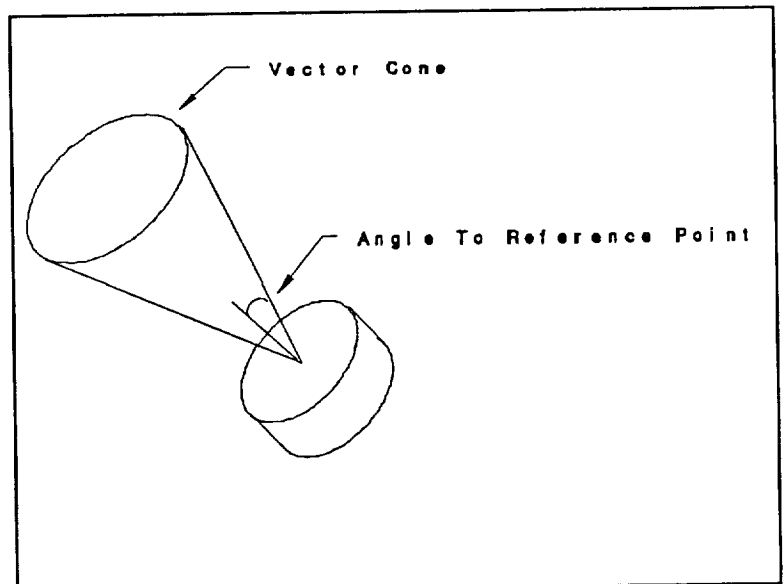


Figure 5-7 Each attitude sensor will provide one angle measurement which will define a cone in space. The attitude of the satellite could point in any direction defined by the cone.

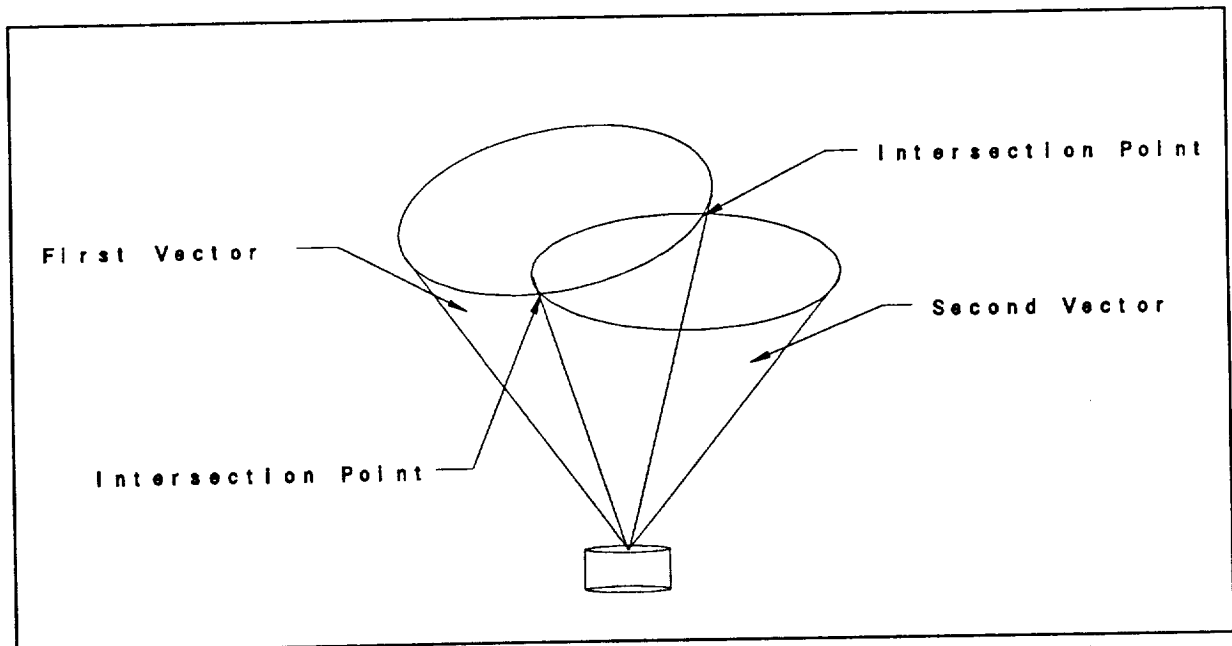


Figure 5-8 By using two different reference points, two vector cones will be defined in space. These can be used to determine the attitude of the satellite.

The velocity about the spin axis will also need to be determined. There are several sensors that can be used to find the attitude, but the sensors need to be low-cost, light-weight, low-power-consumption, and off-the-shelf technology.

5.5.1 Finding the Stars The first type of sensor that we look at is a star sensor. Sensing a star will give the highest form of accuracy and is available for low altitude orbits. It is the hardest object to find in the sky because it is so small. To find a star it takes a very complex process of searching. The star sensors are also very heavy, expensive, and use too much power.

5.5.2 Finding the Sun The sun does not give as high an accuracy as finding a star but it is an easy object to find, being the brightest object in the sky, and is also one of the biggest. In a worst case scenario, the sun would only be visible for 60% of the orbit. There are many devices used by industry to sense the sun.

One way is using a charge-coupled device (CCD) array, where the sun comes through an optic lens and shines somewhere on a CCD array. Then the CCD array is scanned by an on board computer to find out where the brightest spot lies on the array. Then, knowing the position of that point, the angle of entry can be extracted. With those two pieces of information, two vectors can be determined in space relative to the sun. The drawback with this system is the large amount of time it takes to determine the vectors.

A second way to find the sun is to use silicon photo detectors. When these detectors are arranged in a pyramid configuration, as in figure 5-9, they give a wide field of view. Each side of the pyramid can fit up to three photo detectors. This will help in the accuracy of the measurement. The pyramid is enclosed in a fused silica dome on a printed circuit board. Each detector outputs a cosine function. This function peaks at 600 microamps when the sun is normal to its face. Each side of the pyramid puts out a cosine function that is 45° out of phase from the sensor on the opposite side. This will give some cross-coupling geometry that will not affect the final output. The difference between opposite detectors is used to create a voltage that is linear to plus or minus 45° and provides a polarity past plus or minus 90° . When all four outputs are summed together, it will give a 2π steradian (hemisphere) field of view.

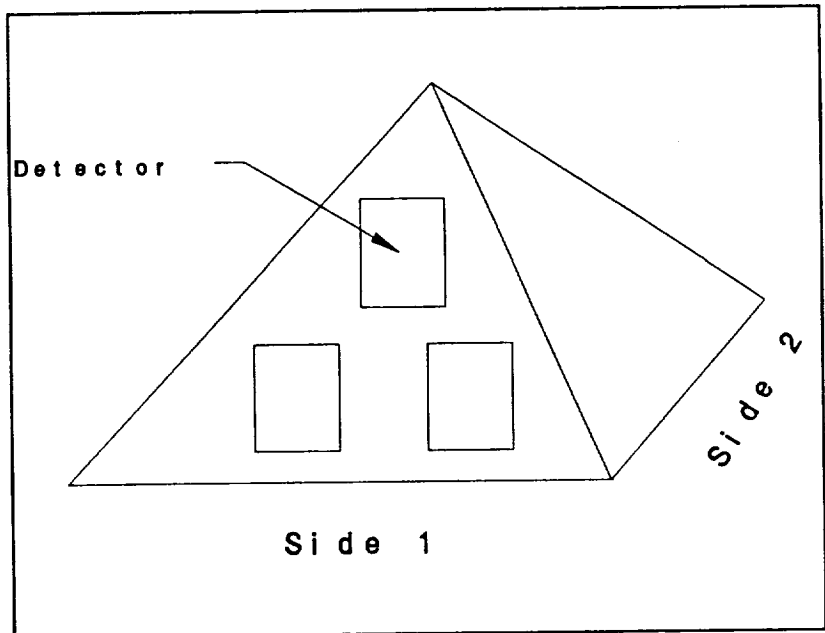


Figure 5-9 Sun Sensor Detectors

This means that two sensors are needed, one on top and the other on the bottom of the satellite, to cover 4π steradian (sphere) field of view.

5.5.3 Finding the Earth The earth is the biggest object and always in the field of view, making it the easiest target to find. There are two basic ways to sense the earth that we looked at.

The first is using the light from the sun reflected off the earth. The brightest point is where the earth meets space called the horizon. The sensor is placed 90° off the spin axis. Therefore, when the satellite spins around and the sensor crosses the horizon, it can start a real time clock. When it crosses the other side of the horizon, it will turn off the clock. The attitude can be calculated by using the horizon crossing time. This sensor is also ideal to calculate the velocity of the spin axis. Instead of recording the time across the earth, the sensor will record the time it takes it to make one revolution. From this time the angular velocity can be determined and fed to the control system.

The second method does not look at the reflected light, but at the CO₂. The CO₂ is also detected at the horizon and the attitude is calculated about the same way. The big difference is that the sensor does not depend on the reflection of direct sunlight to calculate the attitude. This makes it possible to sense the attitude in all orbits, all the time.

5.5.4 Finding the Earth's Magnetic Field A 3-axis magnetometer sensor can detect its position relative to the Earth's magnetic field. The Earth's magnetic field is known to 0.4 degrees per axis. The maps of the magnetic field are even less accurate at the polar regions because that is where the Orion belts come closest to the Earth. This can make the uncertainty of the magnetic field more than 0.4 degrees. Knowing the magnetic field and where the satellite position is with respect to that field, one attitude vector can be determined. The magnetometer has many advantages. The first is that it is not dependent on orbit or sun position. The second is that it has a very low power consumption. As long as there is power on board, the magnetometer could help in sensing the attitude. The third reason is that magnetometers are light weight and can also give additional data on orbit dynamics.

5.5.5 Using Gyroscopes and Accelerometers The big advantages to using gyroscopes and accelerometers are that no external sensing device is needed and they are orbit independent. They are relatively easy to obtain an attitude vector from. The main drawback of these sensors is that they tend to drift and have to be updated often. Highly accurate gyros and accelerometers are quite complex, heavy, and require relatively high power consumption.

5.5.6 Sensors Used Two different sensors are needed to determine the attitude within $\pm 1^\circ$. We have decided on using three sensors instead of two sensors for two reasons. First, if an ELF satellite is behind the earth (not visible to the sun), then a sun sensor will not work. Using a magnetometer and a horizon sensor for this situation could work, but the magnetometer may not be within $\pm 1^\circ$ of accuracy. All three sensors can be used on the sunny side of the earth to accurately calculate the attitude. The magnetometer and horizon can be used on the dark side. The second reason for using three sensors is that the redundancy of data can help to more accurately determine the attitude using statistical methods.

The Ithaco Bullseye Horizon Crossing Computer (BHCC) will be used for the horizon sensor (12). It has a very low mass of 500 grams. The BHCC can scan the earth, sun, or moon. It uses an optical head to focus the radiant energy in a narrow band width. This sensor also has a built in period measurement. This will determine the velocity of the ELF satellites. It has a power consumption of 750 mW.

The selected sun sensor is made by Lockheed Missiles & Space Company. This sensor uses the silicon photo detector in a pyramid configuration as explained earlier. It is called the Wide Angle Sun Sensor (WASS) (13). There will be two of these sensors used: one located on the top, and one on the bottom of the satellite. This will give a 4π steradian field of view. This sensor weighs only 132 grams, and has a power consumption of 70 mW. The accuracy is $\pm 0.5^\circ$.

The magnetometer will be a 2-axis Ithaco Magnetometer (12). Two (2-axis) magnetometers will be used to build an orthogonal 3-axis measuring system. This will give one axis of redundancy. The drawback of using this magnetometer is that it has an accuracy of $\pm 1^\circ$. This is compounded with only knowing the earth's magnetic field to 0.4° (7). This makes the uncertainty over 1° . It weighs only 350 grams and consumes 30 mW of power. The details of each sensor are given in table 5-1. Appendix D contains additional literature on the sensors.

5.5.7 Totals The numbers in table 5-1 only represent one sensor. The totals in table 5-2 show the total values for all of the sensors used.

Table 5-1 Sensor information (12,13).

	Sun Sensor (WASS)	Horizon Sensor (BHCC)	Magnetometer (2-axis)
Manufacturer	Lockheed	Ithaco	Ithaco
# used on ELF	2	1	2
Size (cm)	6.6x5.8x5.1	3.8x12.7x5.8 (optical) 2.9x15.3x15.3 (Electronics)	4.3x13.3x6.7
Mass (kg)	0.132	0.3 (optical) 0.5 (Elect.)	0.350
Power (mW)	70	750	30
Accuracy	0.5°	0.053°	1°
Operational Temperature	-100 to $+85^\circ\text{C}$	-20 to $+70^\circ\text{C}$	0 to 60°C
Position	(1) Top (1) Bottom	90° off spin axis	Inside ELF

Table 5-2 Totals for all of the sensors.

	Totals for all sensors used
Weight of all instruments (Not including all wires)	1.764 kg
Power (100 % Duty cycle) (60 % Duty cycle)	810 mW 140 mW
Accuracy (Worst case) (Best case)	1° 0.5°

5.5.8 Position of Sensors The position of the sensors was a critical factor in the design. The horizon crossing sensor is placed 90 degrees off the spin axis, as shown in figure 5-10. It was placed there because as the satellite spins around it can scan the horizon. This position will work in all orientations except one. When the spin axis is exactly parallel with the horizon, the sensor will not be able to see the horizon. This can occur only briefly in each orbit however. This will not affect the attitude determination because there will be the Sun sensor and the magnetometer to determine the attitude. The two Sun sensors are placed on the top and bottom of the spacecraft in order to insure that one of the WASS can find the sun, as the horizon is being scanned by the BHCC. The two 2-axis magnetometer will be placed on the opposite side of the electronics. This will reduce any false readings due to the magnetic fields caused by the electronics.

5.6 Closed Loop Control System

The control was a very complicated full order system when we were controlling the dual spin satellite. The control system had to keep the dish pointing to the Earth at all times. Since with the simple spinner, we are only concerned with controlling the rate of the spin axis, and not concerned with controlling the position of the satellite, the only equation used was the spin axis equation:

$$M_3 = C\dot{\omega}_3$$

where

M_3 = External Torques on Satellite

C = The principal axis of inertia

ω_3 = Spin rate of axis

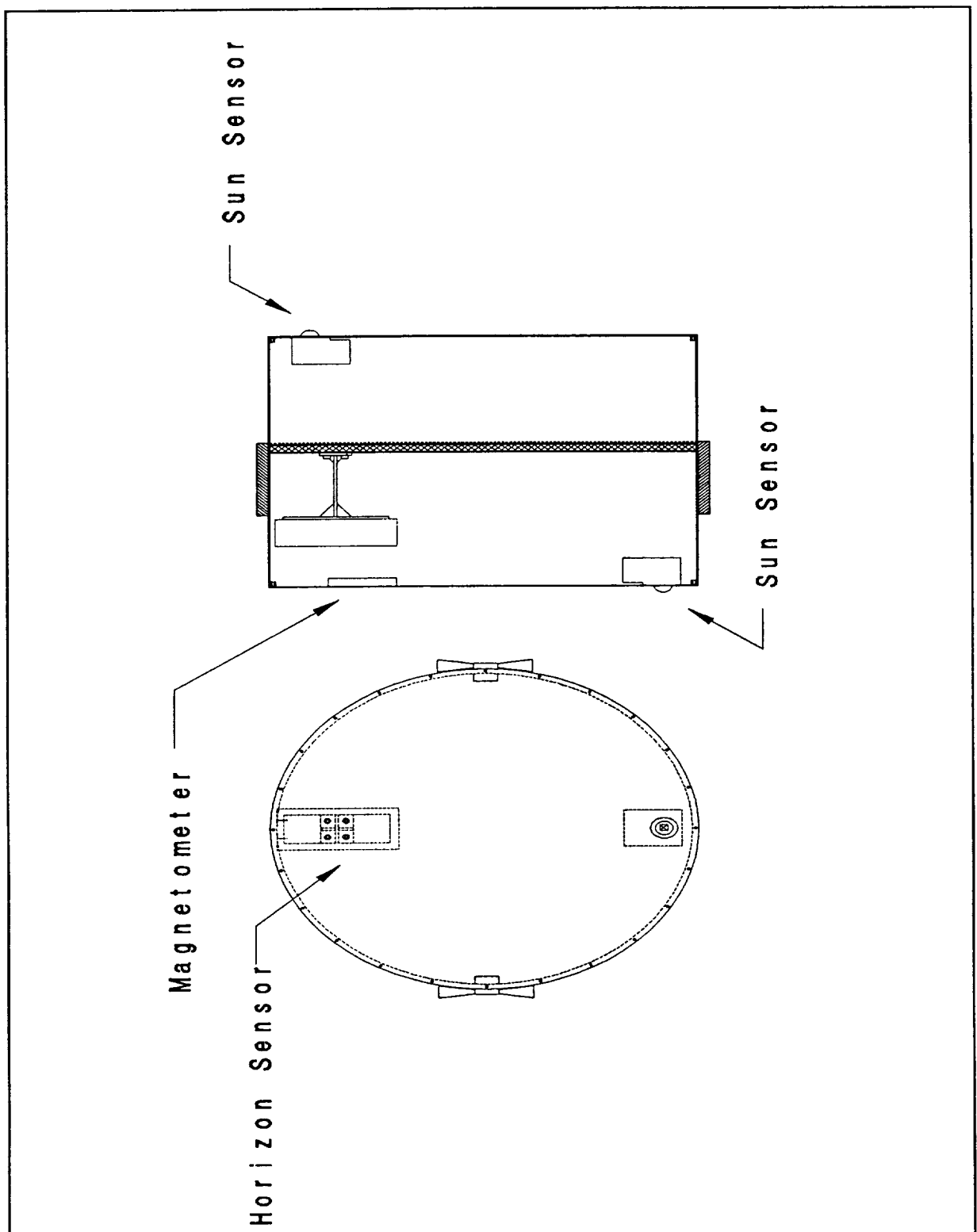


Figure 5-10 Sensor placement in the ELF satellite.

This equation gives the dynamics of the spin axis. Figure 5-11 illustrates the second order control loop for this equation.

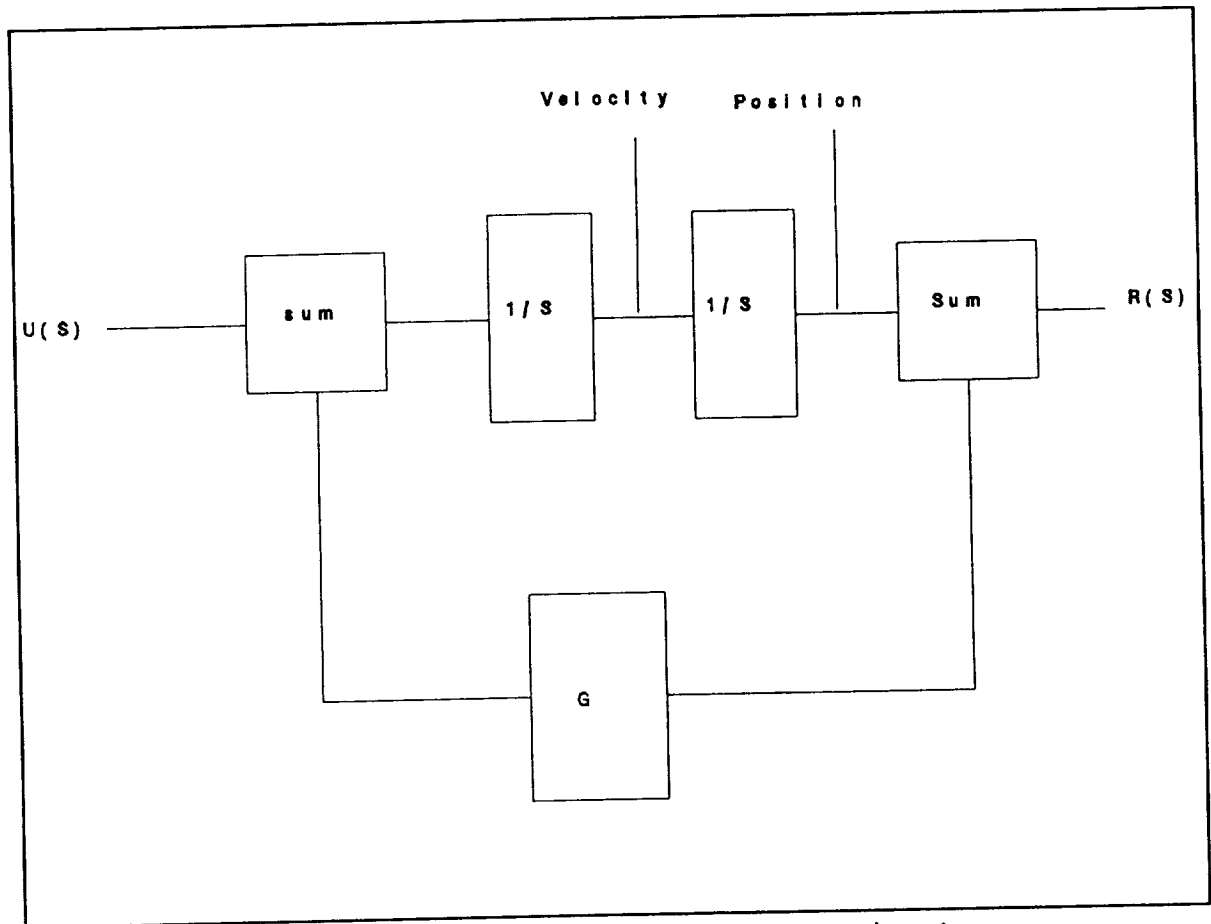


Figure 5-11 Second order control loop for attitude control system.

Where

- $U(s)$ = The input to the system
- $R(s)$ = The output to the system
- $1/S$ = Integrator
- SUM = Summer
- G = The closed loop gain.

By taking the transfer function and reducing it, the following equation can be represented:

$$T(s) = \frac{\frac{1}{s^2}}{1 + \frac{H}{s^2}} = \frac{1}{s^2 + H}$$

This transfer function is representative of the system we need to control. Since the position of the satellite is not controlled, we are only concerned with feeding back the velocity and not the position. The velocity will be calculated by using a horizon crossing sensor as stated earlier. This will simplify the block diagram from a second order system to a first order. Figure 5-12 illustrates the first order system block diagram.

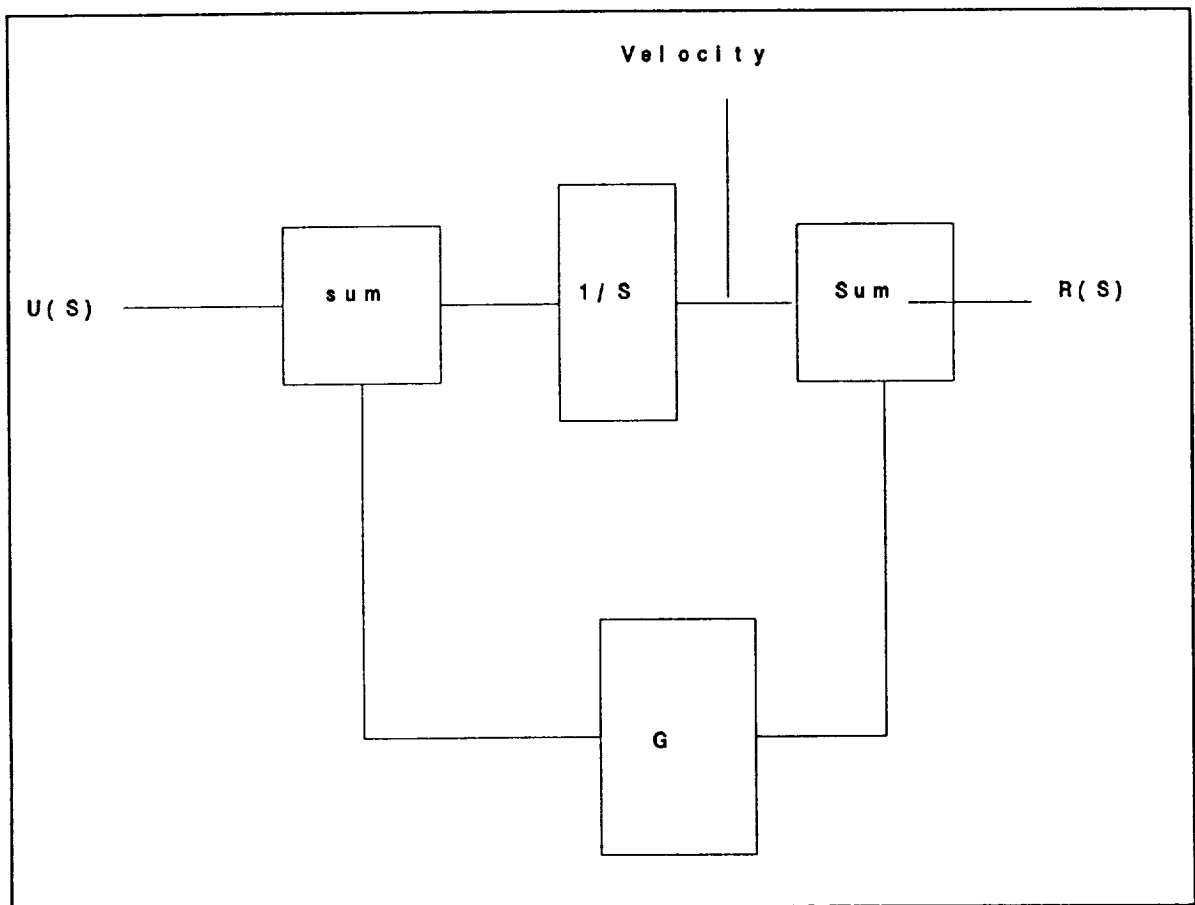


Figure 5-12 First order block diagram for the ELF attitude control system.

The first order transfer function is represented by the following equation:

$$T(s) = \frac{\frac{1}{s}}{1 + \frac{H}{s}} = \frac{1}{s+H}$$

The gain (G) in the transfer function is the torque applied by the cold gas thrusters which is 0.405 (0.405 N·m).

The satellite needs to spin at a rate of 10 RPM. To save propellant, a dead band of ± 2 RPM will be implemented. To implement this dead band, a hysteresis algorithm will be used. The hysteresis will not allow the control system loop to close unless the spin rate is greater than 12 RPM, or less than 8 RPM. Figure 5-13 illustrates the attitude control block diagram with the hysteresis block added.

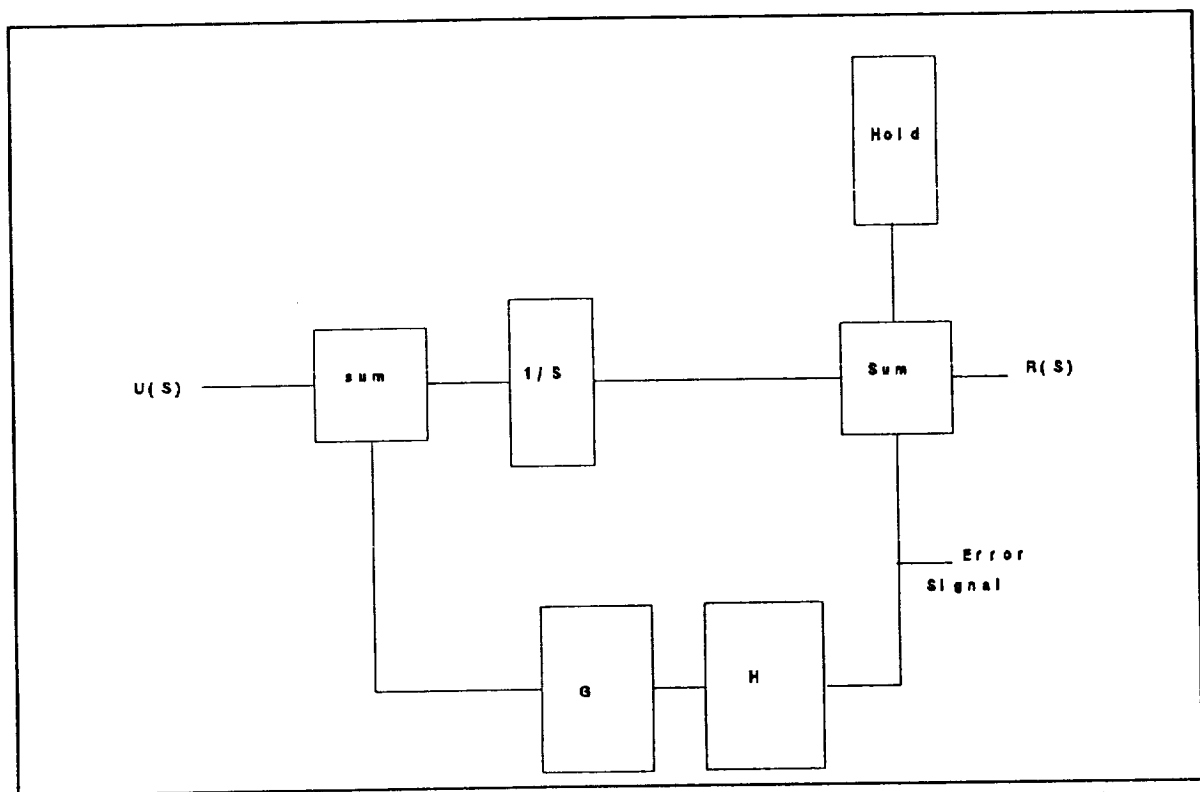


Figure 5-13 The hysteresis block is added to the control system to provide a ± 2 RPM dead band. This will conserve the propellant.

Where

$U(s)$ = The input to the system

$R(s)$ = The output to the system

$1/S$ = Integrator

SUM = Summer

HOLD = Hold the spin rate at 10 RPM

H = Hysteresis function (Dead Band of ± 2 RPM)

G = The closed loop gain.

Once the satellite has been spun-up to 10 RPM, the second SUM block will add the velocity of the spinning satellite (10 RPM) to the HOLD block. The HOLD block represents a -10 RPM. This will make the sum (error signal) zero when the satellite is spinning at 10 RPM. Now the error signal will multiply the control loop by zero, and essentially remove the control loop. When external forces increase the spin rate of the satellite the error will become positive. At this point the hysteresis will continue to keep the control loop from closing until the velocity exceeds 12 RPM. The hysteresis will then allow the loop to close, firing the thruster, which will bring the spin rate back to 10 RPM. This also works when the satellite slows down and the error becomes negative. Then the hysteresis will not close the loop until the spin rate has dropped below 8 RPM. The hysteresis curve is shown in figure 5-14.

This hysteresis curve shows that the thrusters will not be activated between 8 and 12 RPM. Thus, if the spin rate does exceed these numbers it will fire the thrusters to either speed up or slow the ELF satellite. Since there is an on-board computer, the implementation of a hysteresis curve will be an easy task.

One desirable characteristic for the spin rate control is the ability to increase and decrease the dead band or the spin rate of the satellite. Since the on-board computer will control the attitude system, new commands or software can be communicated from the ground station. These directions can then be stored into the EEPROM (Electrically Erasable Programmable ROM) which stores the control system software.

5.7 Propulsion system

5.7.1 Tank and Nozzle Design The ELF satellite will use a nitrogen cold gas system for the initial spin-up and for maintaining the spin rate of the satellite. Figure 5-15 illustrates the position of the basic components of the attitude control system. This system was chosen for its simplicity.

The tanks for the cold gas system may be obtained from Aerojet Corporation (11). The Aerojet tank is made from a composite material and has a mass of approximately 0.25 kg. The rated pressure for the tank is approximately 69 MPa. The tank has a total length of 22.86 cm and a diameter of 7.62 cm. The geometry consists of a cylinder with hemispherical

ends. Two tanks of this size will be installed in the satellite. The total volume of the two tanks is 1853 cm^3 . The current design separates the tanks into two independent systems. In the advent that a valve became stuck, only one tank would lose its propellant.

The tank pressure was analyzed using the ideal gas law $PV = mRT$. Table 5-3 gives the pressure in the tanks for various masses and temperatures. Just under 1.5 kg of nitrogen could be used with these tanks.

To regulate the flow of the compressed gas, six pneumatic regulators will be needed. This will allow for each tank to have its own regulating system. Each regulating system requires three pressure regulators. The first regulator (P/N 400414) will reduce the 69 MPa tank pressure to 21 MPa. The second regulator (P/N 400414) will reduce the pressure from 21 MPa to 0.69 MPa. The third regulator (P/N 400432) (See appendix D) will then reduce the 0.69 MPa to the 0.35 MPa needed by the nozzles (10). Multiple stages are needed for the pressure regulators to provide a steady flow to the nozzles. Currently a design to interconnect the two tanks is being considered due to the cost of the regulating systems.

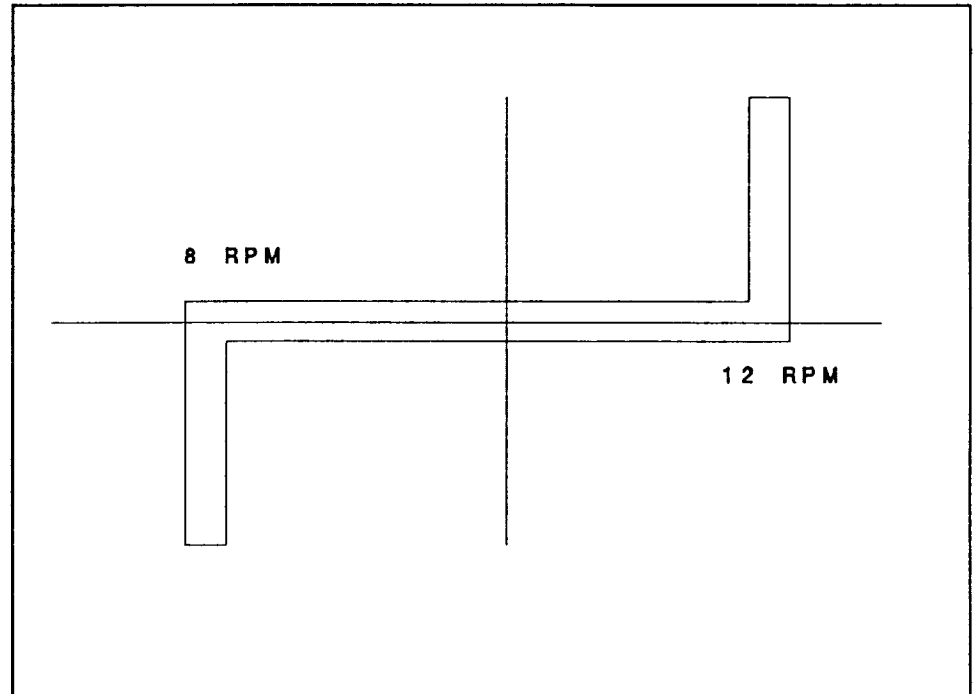


Figure 5-14 The hysteresis block will not recognize the spin rate error signal until the 10 ± 2 RPM has been sensed. Once the 10 ± 2 RPM is reached, the thrusters will be activated and the spin rate will be moved back to 10 RPM

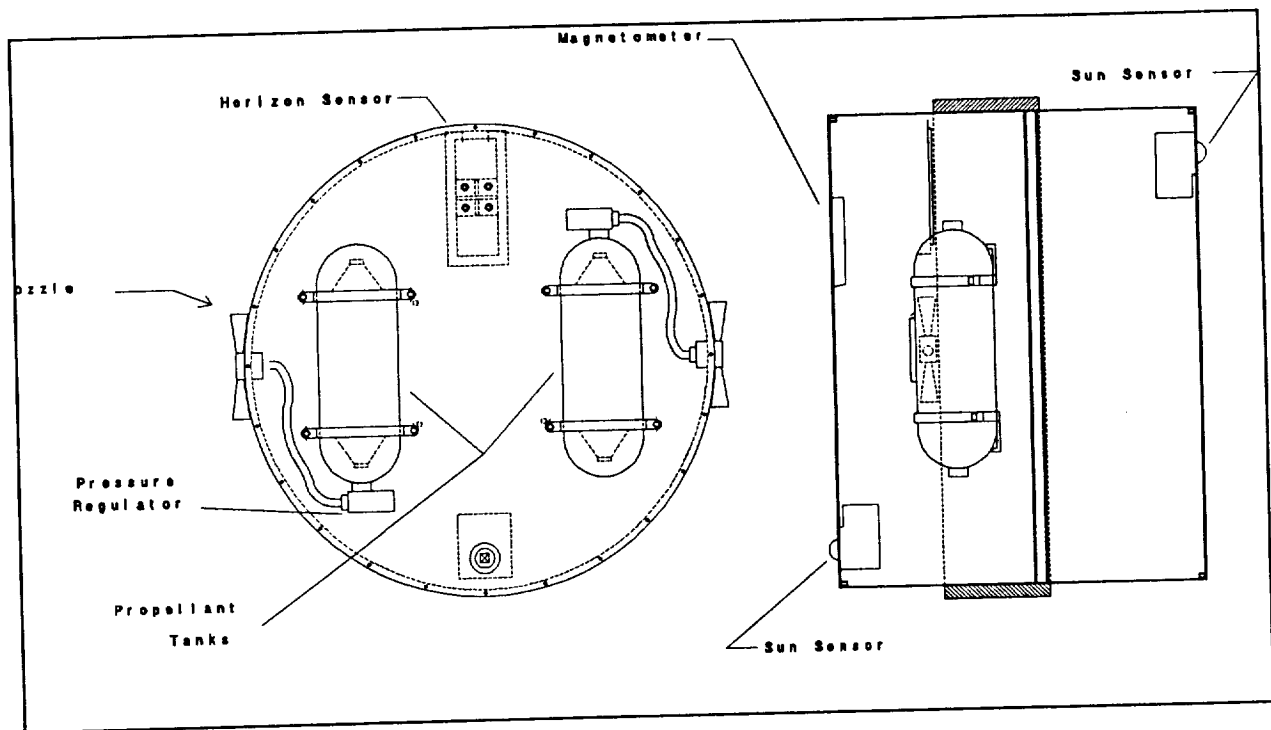


Figure 5-15 Propulsion system layout.

Four 0.9 N thrusters will control the spin rate of the satellite. All four will be oriented about the spin axis so the satellite can be spun-up or de-spun. A redundant double

Table 5-3 Using the ideal gas law $PV = mRT$, the tank pressure is calculated for various temperatures and masses. R for nitrogen is $296.8 \text{ J/kg} \cdot ^\circ\text{K}$.

Mass (kg)	Temperature ($^\circ\text{K}$)	Pressure (MPa)
1.0	250	40
1.0	300	48
1.5	250	60
1.5	300	72
2.0	250	80
2.0	300	96

valve is recommended for each nozzle. This will reduce the amount of gas which will leak while the thrusters are not in use. Conservation of propellant mass is important for this system. Futurecraft has a nozzle which could work in the ELF satellite with some modifications to the nozzle. The nozzles, pressure regulators, and valves can be bought

through Futurecraft in California (10). Table 5-4 gives a summary of the components of the propulsion system.

Table 5-4 The following items will be used for the attitude control propulsion system (10,11).

	Tank	Nozzle	Pressure Regulator	Pressure Regulator
P/N	?	200915	400414	400432
Mass (kg)	0.25	0.17	0.11	0.098
Volts	N/A	28	N/A	N/A
Amps (W)	N/A	60	N/A	N/A
Number	2	4	4	2
Cost/item	?	\$2000	\$5000	\$5000
Company	Aerojet	Futurecraft	Futurecraft	Future-craft

5.7.2 Propellant Expenditures The amount of mass to spin-up or de-spin the satellite may be found by determining the amount of time to change the angular velocity ω of the satellite. That time is then multiplied by the mass flow rate through the nozzles. Δt may be determined from the equation of motion of the pitch axis by integrating with respect to time. The spin up time may thus be determined by the following equation

$$\Delta t = C \frac{\Delta \omega_3}{M_3}$$

The mass flow rate may be found from

$$\dot{m} = \frac{Thrust}{I_{sp}}$$

where

I_{sp} = Specific impulse

Thrust = Thrust of Nozzles

The total mass used may then be found using the above values.

$$m = \dot{m} \Delta t$$

For a cold gas system using nitrogen, the theoretical I_{sp} is 785 N·m/kg. Since the radius of the satellite is 0.225 m, the torque applied to the satellite by two thrusters is 0.405 N·m.

The propulsion system will be used for two duties. Its first duty will be to initially spin up the satellite after orbital insertion. This will require a spin-up from 1 to 10 RPM. The second will be to maintain the spin rate at 10 RPM. Since the dead band for the control system will be ± 2 RPM, the time to change the spin rate by 2 RPM is used to calculate spin-up and de-spin mass usage. Table 5-5 lists the theoretical mass usage for the initial spin-up of the satellite and for subsequent spin rate adjustments.

Table 5-5 By knowing the flow rate through nozzle, the amount of mass for each duty may be determined if the amount of time to perform the duty is known.

Initial Spin-up (1 to 10 RPM)	0.08956 kg
Spin-up (8 to 10 RPM)	0.01990 kg
De-spin (12 to 10 RPM)	0.01990 kg

Table 5-6 shows the theoretical number of de-spins or spin-ups which may be performed for a given propellant mass.

The main drawback to the cold gas system is that the propellant is an expendable item. The amount of times that the propulsion system will need to be used has been difficult to determine. The effects of the solar pressures and gravity gradients on such a small satellite as this are very small. Therefore, to de-spin or spin-up the satellite should only need to be done occasionally. To try to approximate how many times the propulsion system will be used, solar pressure torques were applied to the TUTSIM model. The solar pressure torques had to be increased 1000 times to require the use of the propulsion system to de-spin the satellite once in a ten day period. This analysis

indicates that 30 or 40 de-spins should be more than sufficient over a 7 year period. It is recommended, however, that more analysis be done in this area.

Table 5-6 The number of spin-ups or de-spins is calculated by first subtracting the initial spin-up mass from the total mass at launch time. The difference is then divided by the de-spin (spin-up) mass.

Propellant (kg)	# of Spin-up or De-spins
1.0	46
1.5	71
2.0	96

5.8 Conclusion

The attitude control and determination system is a minimum level system used only to control the spin rate of the satellite and sense the attitude. The sensor system will consist of one horizon sensor, two sun sensors and one magnetometer. Combinations of these sensors will be able to determine the attitude of the satellite at all times. The

Table 5-7 Mass and cost totals for the attitude control system (11,12,13).

	Number	Mass (Tot) kg	Cost (Tot)
Magnetometer	2	0.700	?
Sun Sensor	2	0.264	?
Horizon Sensor	1	0.500	?
Tank	2	0.500	?
Nozzle	4	0.680	\$8,000
Pressure Regulator (400414)	4	0.440	\$20,000
Pressure Regulator (400432)	2	0.197	\$10,000
Totals	17	3.281	\$38,000 ⁺

propulsion system will use a cold gas nitrogen system. Initial estimates indicate that 1.5 kg of propellant will be sufficient for the 7 year mission of the satellite. Table 5-7 gives the totals for the complete system.

REFERENCES

1. Agrawal, Brij N.: Design of Geosynchronous Spacecraft. Prentice-Hall, 1986.
2. Computer Sciences Corporation: Spacecraft Attitude Determination and Control. Kluwer Academic Publisher, 1988.
3. Kaplan, Marshall H.: Modern Spacecraft Dynamics and Control. John Wiley & Sons, 1976.
4. Sutton, George P.: Rocket Propulsion Elements. John Wiley & Sons, 5th Edition, 1986.
5. Wiesel, William E.: Spaceflight Dynamics. McGraw-Hill, 1989.
6. Greenwood, Donald T.: Principles of Dynamics. Prentice-Hall, 1988.
7. Martel, F., Pal, P. K., and Psiaki, M. L.: Three-axis attitude determination via kalman filtering of magnetometer data. Paper No. 17 for the Flight Mechanics/Estimation Theory Symposium, NASA/Goddard Space Flight Center, May 10 & 11, 1988.
8. May, D.: AMSAT phase IV propulsion and attitude control systems conceptual design. AIAA/Utah State University Conference on Small Satellite, 1989.
9. TUTSIM, Copyright of TUTSIM Products, 1988.
10. Promotional Literature, Drawing Numbers 200915 (Nozzle), 900620 (double redundant Regulator). Futurecraft, City of Industry, CA.
11. Dr. Young, Phone conversation, Aerojet Corp., CA, April 1990.
12. Promotional Literature, Fact Sheet Ithaco Magnetometer, Fact Sheet Ithaco Bullseye Horizon Sensor. Ithaco Inc., Ithaca, NY.
13. Promotional Literature, Fact Sheet Sun Sensors (WASS). Lockheed Missiles and Space Company, Sunnyvale, CA.

6.0 DATA PROCESSING SYSTEM

The data processing system provides control and processing for the active satellite subsystems. These include electrical field sensing, attitude sensing and control, communications, power control, and thermal control. In addition, the data processing system will perform various housekeeping tasks such as monitoring internal temperatures and NiCad cell states of charge.

This chapter will describe the data processing system hardware, including the functions of each section. As well, we will outline the available alternatives, provide a rationale for selection, and justify the choices made. Although due consideration was given to software implications of hardware specifications, no software development has been done, and so no software description will be offered.

6.1 System Requirements

The ELF satellite acquires electrical field samples periodically, at known intervals and at known attitudes. Samples, in the form of voltages, are converted to a digital representation. Along with timing and attitude information, these samples are stored on board the satellite, to be forwarded to earth twice daily. Other "state-of-the-satellite" information is appended to the transmission as requested. The data processing system supports these functions.

In addition, the satellite operation may need to be altered on command from earth. The system provides that flexibility. For example, the electrical field samples can be offset and scaled as desired, the operating software can be modified, and NiCad cell banks can be disconnected from the main power bus for cycling to restore capacity.

6.2 System Components

A basic data processing or microprocessor system will include a microprocessor, external memory, and simple logic functions (these direct, gate, store, and invert signals to assure correct system operation and are often known as "glue logic"). Often, where large amounts of data must be stored, a mass storage device or system is included. Peripheral components, which reduce the need for microprocessor attention by independently performing functions such as input/output (I/O) and timing, may also be used. An integrated approach to this microprocessor system encompasses the other satellite systems to a degree, because of the interdependence of the systems.

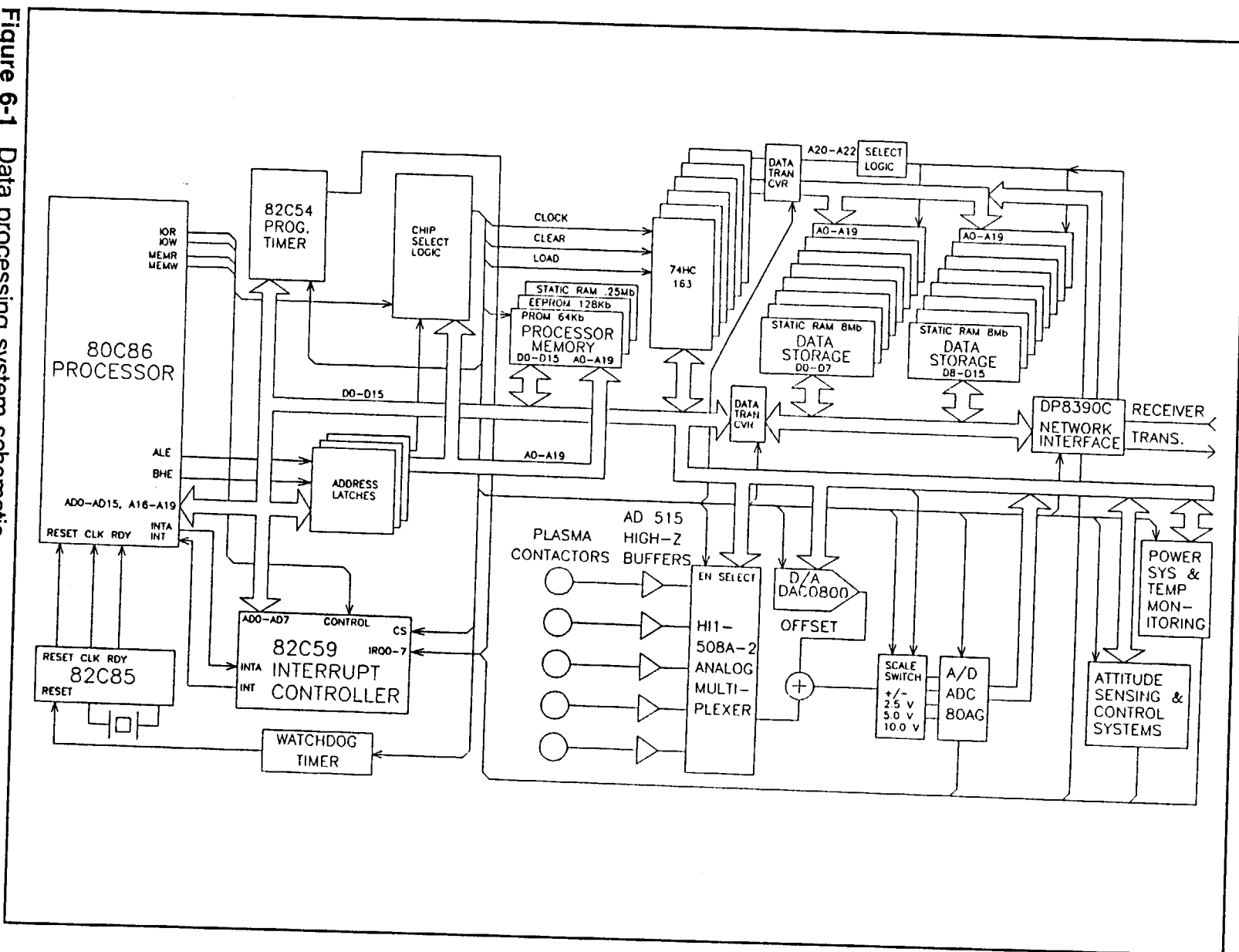
The ELF microprocessor system comprises a processor, general purpose processor memory, data storage memory, and peripherals including a communications interface, a programmable timer, a watchdog timer, and a programmable interrupt controller. The schematic of the complete data processing system is shown in figure 6-1. The component specifications may be found in appendix E.

6.2.1 Processor Several microprocessors were considered for the system; among these were the Intel family processors 80C85, 80C86, 80186, and 80C286, and the Motorola MC-68HC000. In addition, we looked at the data bus size (at least 16 bits wide for the electrical field sensor), the physical address space (the amount of memory the processor can handle-8 Mbytes for the data storage memory), the power consumption, speed, and radiation tolerance. In time, the drivers of the choice proved to be radiation tolerance, followed by power consumption. Both the 80C86 and 80186 are 16 bit (data bus) processors; also, they are both manufactured in a rad-hard process by Harris Semiconductor. Of these two, the 80C86 had lower power consumption. Neither have the physical addressing required for the data storage, but alternatives exist. Were radiation hardness not a factor, either the 80C286 or the MC-68HC000 processor would be preferable due to the 16 Mbyte physical address space they both possess.

6.2.2 Processor Memory The processor memory incorporates 64 Kbytes of programmable read-only memory (PROM) to preserve the fundamental routines of the operating system program. 128 Kbytes of electrically erasable programmable read-only memory (EEPROM) affords the option of reprogramming high level routines, and 256 Kbytes of static random access memory (SRAM) provides the standard storage required by the processor. (The term static refers to the fact that the information will be retained so long as power is applied to the memory. The alternative, dynamic RAM, must be "refreshed" or rewritten every 200 ms or so, or it will "forget". This requires a great deal more power.) The amount of memory may be changed to suit design needs, but the sizes given will serve for this application.

6.2.3 Data Storage Data storage is accomplished in 8 Mbytes of static RAM. The ELF satellite will take samples from 5 probes 10 times per second. In a 12 bit digital representation, the samples are a source of $5 \times 10 \times 12$ or 600 bits per second. Given that a byte equals 8 bits, this corresponds to 75 bytes per second or 6.48 Mbytes per day. Since timing and attitude information should add less than one Mbyte per day, 8 Mbytes of memory will suffice. Although transmission of data to earth is possible twice per day, 24 hours of storage provides a margin of safety. For instance, if 2 satellites are spaced closely and pass over the ground station at the same time, sufficient time may not be available to gather the data from both satellites on one pass.

Figure 6-1 Data processing system schematic



6.2.3.1 Options for Data Storage Memory Our options for data storage memory were magnetic media and semiconductor memory. We considered using a small hard disk drive, but the power requirement was high and the lifetime short. We decided to increase reliability by avoiding moving parts if possible. The largest available semiconductor memory is a 512 Kbyte hybrid CMOS SRAM, the WS-512K8-120, made by White Technology. Though 8 Mbytes of SRAM will require 16 packages, the board area needed is still less than 1/4 of the area available on the circuit board. The power requirement of each device is 3.6 mA at standby and 52 mA in operation at 5 Mhz. By keeping each device at standby unless being written to or read from, power drain can be reduced from 832 mA to 106 mA. Whether in operation or in standby, all information is preserved.

6.2.3.2 Expansion of Data Storage Memory As the 80C86 can address only one Mbyte of memory, other means were employed to enable addressing of the 8 Mbytes of data storage. Six 4-bit counters are used to address the data storage. Each counter will carry overflow to the next most significant counter, so the counters act together as a single 24-bit counter. This allows addressing of a maximum of 16 Mbytes of memory.

The processor can load any desired address to the counters, clear the counters to zero, and increment the counters by means of the clock line. Through the address load, clear, and clock operations, the processor can control the storage of data.

6.2.4 Communication System Interface To send the contents of the data storage memory to earth as the satellite passes the ground station, the microprocessor system must be able to send data to the communication system at a speed of 1 Mbit/second. A National Semiconductor DP8390C is a network interface controller for local area networks (LAN) which is capable of this data transmission rate. It provides a communications interface with direct memory access (DMA) capability. This capability allows the controller to send data with a minimum of assistance from the microprocessor which permits sampling of the electrical field while data is being sent to earth. During this time, the samples will be stored in the processor memory, to be moved to the data storage when communications have concluded. As this device is not radiation tolerant, alternative devices are under consideration.

6.2.5 Programmable Timer A programmable timer, a Harris 82C54, provides for a variable sample rate. The timer signals the processor that a sample is to be taken. If desired, a change in the sample rate can be made on command from earth.

6.2.6 Watchdog Timer A watchdog timer insures that software errors do not permanently disable satellite operation. Radiation can cause a temporary change of state in a memory cell; this can occur in either SRAM processor memory or in the registers within the microprocessor. Depending on the location changed, this can halt the program being run or send it into an endless loop. Normally, the watchdog timer is continually being reset by a program. If a software error occurs, the timer will not receive the reset pulse; it will timeout and reset the processor. As the basic programs are contained in PROM, which is programmed by "blowing fuses", these programs are not susceptible to corruption by radiation.

6.2.7 Programmable Interrupt Controller The Harris 82C59 is a programmable interrupt controller. It prioritizes the demands for processing made by various satellite components. It also is a rad-hard component.

6.3 Raw Data Storage

During the course of our design work, we realized that maximum scientific benefit would be obtained from the data if it arrived on earth in an unprocessed form. The voltages at the plasma contactors, or probes, only remotely resemble the earth's electrical field. Error voltages, such as those induced by the passage of the satellite through the earth's magnetic field, and photoelectric currents caused by solar radiation striking the probes, are also present. These errors must be removed to obtain valid information about the earth's electrical field. This processing can be done using either the limited resources of the satellite, or on earth, which has effectively a limitless supply of processing power.

We determined that all data should be stored in a raw form, with any serious processing to be done on earth. However, maximum resolution can be obtained in the A/D (analog to digital) conversion process when the maximum value of the voltage sample is close to but does not exceed the maximum range of the A/D converter (positive and negative 2.5 volts). To permit this, we decided to provide for adjustments to the voltage sample before conversion. The sample may be offset by shifting it to center the variations around 0 volts and may be scaled by multiplying the sample by different constants to obtain a maximum value just within the range of the A/D converter.

6.4 Hazards to the System

Hazards of orbital injection and of the space environment demand an emphasis on reliability. Mechanical stresses during lift-off and flight are reduced by the rigidity of the supporting framework and by elimination of mechanical resonances below 2000 Hz, the region where launch vehicle vibration becomes most severe.

6.4.1 Van Allen Radiation Belts Major hazards to electronic systems in space are charged particles and gamma radiation. The Van Allen radiation belts are toroidal energetic trapped particle fields encompassing the earth. The particles in these fields move rapidly along the earth's magnetic flux lines, oscillating between the earth's magnetic poles. They closely approach the earth in the polar regions. The polar trajectory of the ELF satellites places them within these fields in the regions above 65 degrees of latitude (magnetic).

6.4.2 Ionizing Radiation The energy of ionizing radiation, such as these particles, deposited in the silicon of the semiconductors, forms additional charge carriers, some of which accumulate and eventually alter the operation of the material. In addition, ionizing radiation can both activate low impedance paths from the voltage supply to ground in CMOS technology (called latchup) and can cause memory cells to change state (referred to as a soft error, or single event upset).

6.5 Radiation Damage Prevention

To prevent radiation damage to the semiconductors of the data processing system, such measures as are necessary will be taken, such as the use of rad hard components where available, 3/16" aluminum plate shielding, and seals and connectors which prevent the entry of radiation into the housing for the data processing system.

REFERENCES

1. CIGD Data Book: Rad-Hard/Hi-Rel. Harris Corporation, 1987.
2. Data Communications Local Area Networks UARTS Handbook. National Semiconductor Corporation, 1988.
3. WS-512K8-120 Data Sheet. White Technology, Inc., 1988.
4. MC68HC000 Microprocessors User's Manual. Motorola, Inc., Prentice Hall, 1989.
5. Military Products Handbook, Vol I. Intel Corporation, 1989.
6. Linear Data Book 2, Revision 1. National Semiconductor Corporation, 1988.
7. Burr-Brown Integrated Circuits Data Book, Vol 33. Burr-Brown Corporation, 1989.

7.0 COMMUNICATION SYSTEM

7.1 Requirements

The functional requirements of this system are to:

- 1) communicate with the ground station from any attitude; and
- 2) establish a data link with the ground station.

7.2 Antennae

7.2.1 ELF Satellite Antenna A functional requirement unique to the communication system is to be able to transfer stored data from the satellite to the ground from any attitude. This is because each satellite in the cluster will have a different orientation with respect to the earth. In order to meet this requirement the antenna on the satellite must be virtually omni-directional.

Figure 7-1 illustrates the position of the stripline wraparound antenna, Model 55-XXX, on the ELF satellite. It was designed by Physical Science Laboratory at New Mexico State University. This antenna will meet the above stated requirement of virtual omni-directionality. It has a total mass of 1.36 kg and costs \$6000 per unit (1). It uses a 1 kg transmitter, Model T-1024S, manufactured by AydinVictor that costs an additional \$6000 per unit (2).

The cross-sectional side view of the radiated pattern is shown in figure 7-2 and the cross-sectional top view is shown in figure 7-3. The side view has a typical butterfly shape with a

-40 dBi null at the top and bottom of the pattern. This null is narrow in that signal is

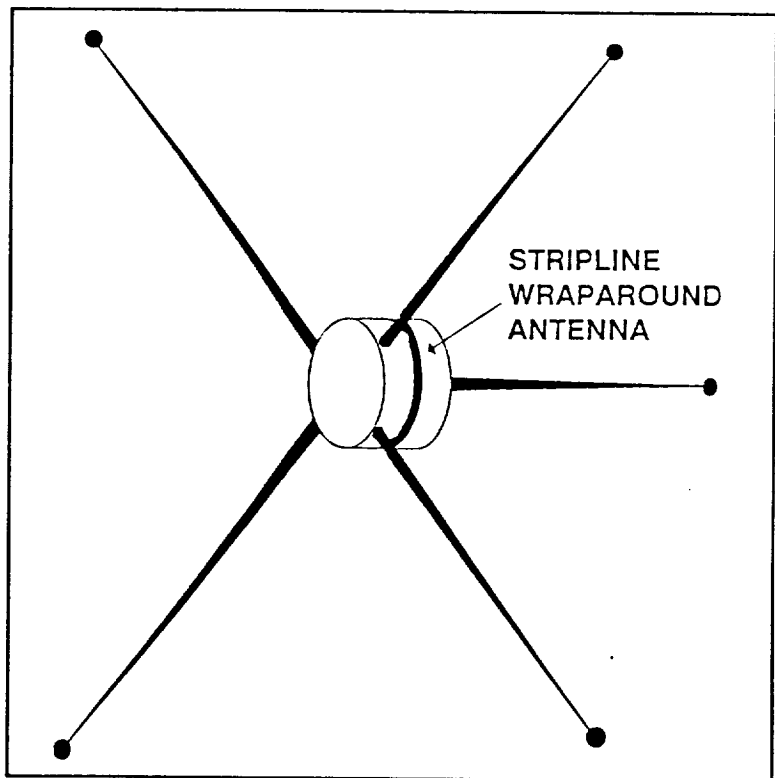


Figure 7-1 Location of the stripline wraparound antenna on the ELF satellite

back to full power within 5° of either side of the vertical axis. At the sides, nulls as great as -5 dBi exist. The top view illustrates nulls of at most -3 dBi (1). This radiated pattern is close enough to omnidirectionality to meet the functional requirement of being able to communicate from any attitude. Admittedly, there may be times when a satellite would be oriented so that the top or bottom null is pointing toward the ground station making the downlink improbable. Such occurrences should be temporary, rare, and relatively unimportant since there will be a sufficient number of other satellites in the cluster able to transmit.

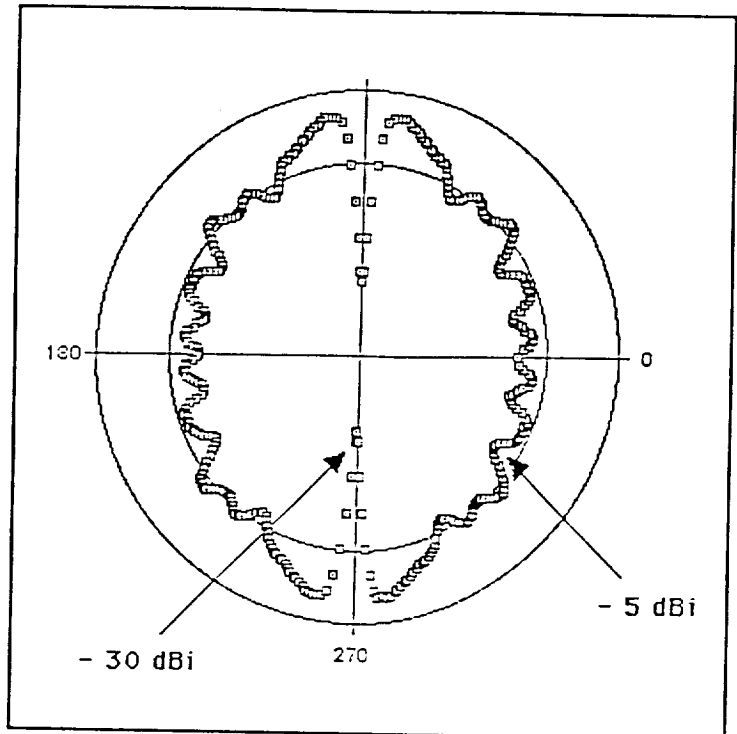


Figure 7-2 Cross-sectional side view of the stripline wraparound antenna radiation pattern

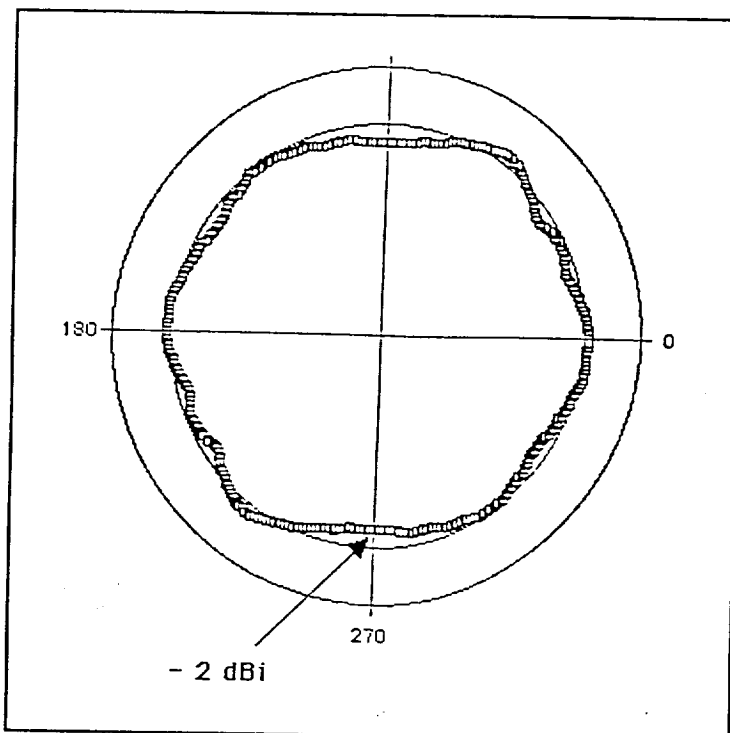


Figure 7-3 Cross-sectional top view of the stripline wraparound antenna radiation pattern

7.2.2 Ground Station Antenna

Each of the satellites will be tracked by a dish antenna on the ground as it passes overhead. The downloading of stored data and the transmitting of various commands from the ground station will occur at this time.

Although a complete statistical analysis of exactly how many satellites will be able to download daily has not been done, initial observations indicate that enough satellites will succeed in transferring stored data so that a accurate model of the earth's electrical field can be constructed.

These initial observations include the following:

- 1) Each satellite will pass over the ground station twice daily. And,
- 2) The total transmission time (detailed below) is relatively short allowing time for several simultaneously occurring satellites to download data.

There is a trade off between the size of the ground station antenna and the power of the transmitter on the satellites. Since the power available for transmission is relatively small, a ground station antenna with a high gain is desirable. We have chosen a 4.3 m diameter parabolic dish antenna that has a gain of 39 dB. This antenna, Model 2P14, is built by Anderson Manufacturing, Idaho Falls, Idaho. It costs \$1500 for the dish and receiver (3). Additional equipment for the ground station such as tracking control unit and computer hardware/software has yet to be determined.

7.2.3 Off-The-Shelf Technology Wraparound antennae are commonly used for simple spinner satellites and sounding rockets. The technology has been tested and the antenna are readily available. Parabolic dish antennae have been used for years to receive/transmit data to and from satellites.

7.3 ELF Data Link

7.3.1 RF Downlink The transfer of information from one point in space to another using electromagnetic wave propagation requires a transfer of energy. Each operation in the data link contributes a gain or a loss to the energy transfer. These operations can be expressed as an equation that will detail the data link budget (4).

In quantifying the link budget, we use an equation that yields a margin of safety or signal margin (M):

$$M = \frac{P_t G_t G_r}{(E_b/N_o) k T B L_s L_a L_o}$$

This equation is often expressed in Db:

$$M = P_t (dBW) + G_t (dB) + G_r - (E_b/N_o)_{req} (dB) \\ - B (dBb/s) + 228.6 dB - T (dB^\circ K) \\ - L_s (dB) - L_a (dB) - L_o (dB)$$

where,

- P_t = power of transmitter
- G_t = gain of transmitter
- G_r = gain of receiver
- $(E_b/N_o)_{req}$ = required bit error rate
- B = bandwidth
- k = Boltzmann's constant (1.38×10^{-23})
- T = receiving noise temperature (degrees kelvin)
- L_s = free space loss
- L_a = atmospheric attenuation of the wave
- L_o = non-ideal system components loss (5, also Appendix G)

Using the transmitter and receiver stated above and frequency shift keying, the least efficient digital signal modulation method, the signal margin for the ELF data link is 5 dB at 2200 MHz. This is the worst case. There are other modulation/demodulation schemes that would yield a higher signal margin. For details of the signal margin computation refer to the spreadsheet output in appendix F.

7.3.2 Transmission At the beginning of a transmission, a training sequence is necessary to verify that the data link has been established. During this sequence the identity of the individual satellite is relayed.

Precise transmission of digital information via an RF link requires the consideration of probability of bit error. At frequencies in the S-band region, a bit error rate of 12.5 dB is necessary for the probability of bit error (P_e) to be 10^{-4} . This P_e is sufficient if the data is validated, using handshaking, every 16 kbits. Handshaking is accomplished using parity and/or overflow checking. The following is a breakdown of total transmission time.

Transmission of 8 MBytes Stored Data

Bandwidth = 1 MHz
Delay = 8 m sec each way
Training Sequence = 10 sec
Handshaking every 16 K bits
(Total 500 handshakes)
Check Time = 8 sec
(500 x 2 x 8 msec)

Transmission Time

Training sequence =	10 sec
Data transfer =	64 sec
Handshaking =	<u>8 sec</u>
Total =	82 sec

7.3.3 RF Uplink The data downlink process is reversible in that commands from the ground station antenna will be received by the stripline wraparound antenna on the ELF satellite. The uplink frequency will be within the 10 MHz bandwidth of the antenna eliminating the need for an additional antenna on the satellite. The Transmitter/Receiver switching unit that is necessary to do this is part of the onboard communication system.

REFERENCES

1. Williamson, J., Telephone Conference, Physical Science Laboratory, New Mexico State University, May, 1990.
2. Lane, K., Telephone Conference, Physical Science Laboratory, New Mexico State University, May, 1990.
3. Telephone Conference, Anderson Manufacturing, Idaho Falls, Idaho, April, 1990.
4. Sperry: Data Link Basics - The Link Budget. p. 1.
5. Baker, K.: Communications link analysis. Electrical Engineering Dept., Utah State University, p. 1-3, 1984.

8.0 POWER SYSTEM

The top level requirements for the satellite are to:

- 1) generate and distribute power;
- 2) minimize weight and cost; and
- 3) use off-the-shelf technology.

The functional requirements of the satellite are to:

- 1) meet the power requirements of the other subsystems for a minimum of 7 years life span; and
- 2) handle single point failures

8.1 Solar Cells

To get maximum power generation from a small craft like this, we needed to put as many solar cells on the craft as physically possible without adding complexity in the size or shape of the craft. The preferred craft shape, as far as the power generation is concerned, would be a sphere. This would give constant power generation regardless of the orientation of the craft to the sun. The problem is that this shape of craft would be difficult to manufacture, also the antenna design would be much simpler if the craft had a flat ground plane to direct the signal to the earth, so a sphere is not the overall best choice. The next best shaped craft would be a "tuna can." With the proper dimensions, this craft would give equal power generated by the side as it would by one end. To determine this size, we set the area of the side equal to the area of one end and solved for r and h. Using r as the radius of the craft and h as the height of the craft. The equation is as follows:

$$\pi r^2 = 0.40[2\pi r(h-10)]$$

The 0.4 is a power generation factor for a curved surface. This means that power generated from 40% of the side should equal the power generated from one end of the craft. The -10 is to account for the width of the stripline wrap-around antenna. Solving for r and h yields

$$r = .8h - 8$$

or

$$h = 1.25r + 10$$

The size of the launch vehicle determined the final size of the craft (35 cm high, 45 cm diameter), but it was close to the calculated value for r and h (38 cm high, 22.5 cm radius).

This shape craft gives us a total area of 4948 cm^2 for the side, and 1590 cm^2 for one end. The antenna is 10 cm wide and wrapped around the side of the craft. This takes up 1413 cm^2 of solar cells on the side of the craft. A curved surface can only generate 40% of the power that a flat surface can, thus reducing the effective area of the side to 1414 cm^2 . The area of the top of the craft is 1590 cm^2 , which will give us pretty close to equal power generation from the top or the side.

The power that is generated by solar cells is determined by the angle at which the sun strikes the cells as shown in figure 8-1. This has a value of 100% at 0° to the sun, and

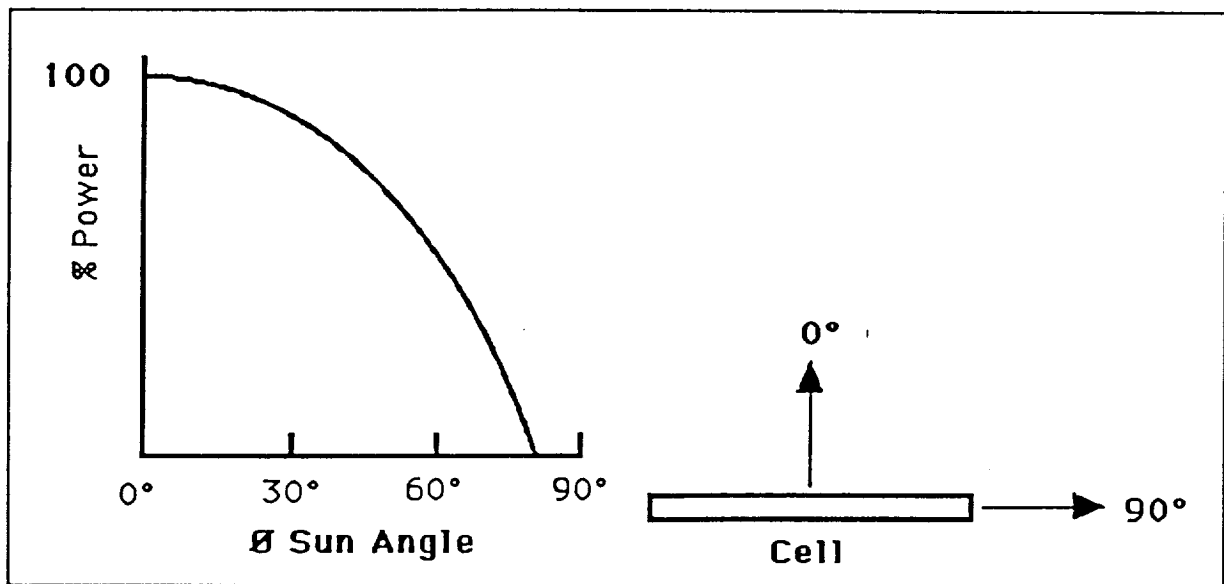


Figure 8-1 Percent output of the solar cells versus angle of sun light

decreases as a cosine function to 0 at 90° from the sun. If one side of the craft is receiving full sunlight (ie. 0°) then neither end will be receiving any light. As this angle is rotated so both the top and the side are receiving power, then the percent of power from the side and from the end can be determined. Since the cosine of $45^\circ = 0.707$, then a maximum power will be produced when the sun is at 45° to the craft as shown in figure 8-2. This also means that the minimum power production will be at 0° to the craft, and the actual power will be somewhere between these two angles.

The power output of the solar cells can be calculated by knowing a few constants. The solar constant of the sun for a satellite in orbit about the earth has an average value of 1400 W/m^2 . The current conversion efficiency is 14%, and the packing efficiency of cells is 85%. Multiplying these numbers together gives a power output of 16.66 mW/cm^2 . This would give us a

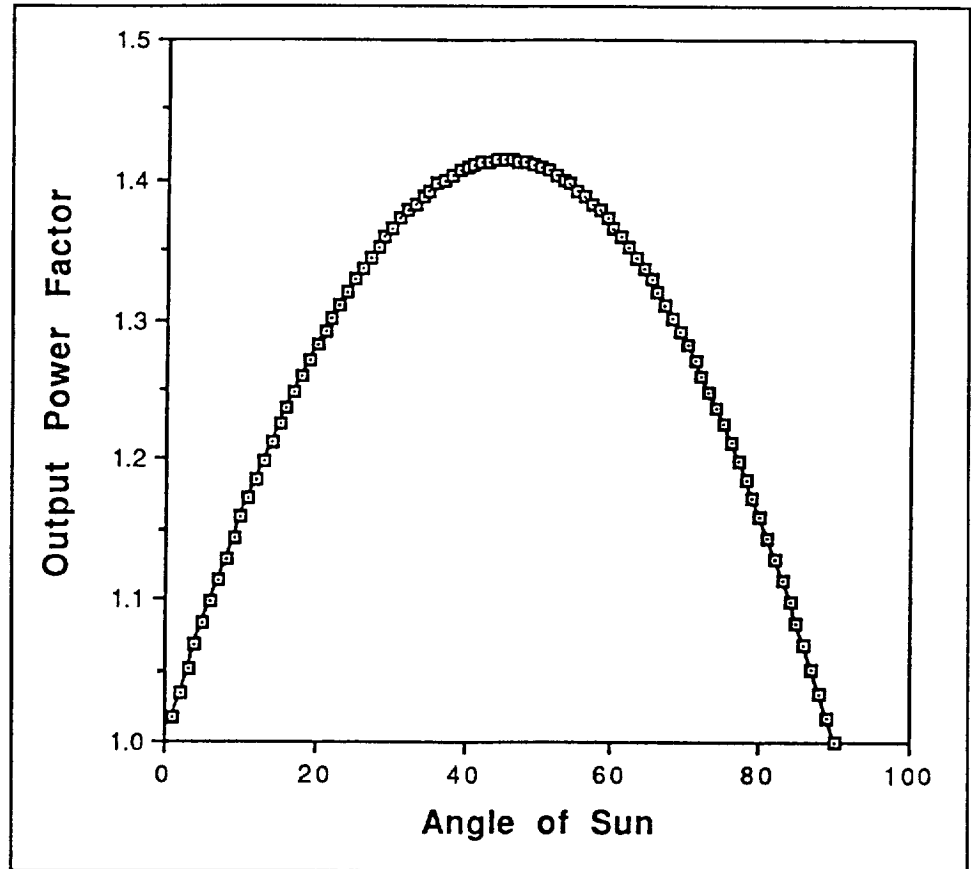


Figure 8-2 Output versus angle of the sun

minimum power output from the solar cells of 23.56 W Beginning of Life (BOL) from the side of the craft, and a maximum output of 35.38 W BOL with the sun at 45° to the craft.

This is only the power available at the cells. There is also a 85% DC to DC power conversion efficiency which will cut back on our total power, and a 25% cell degradation over a 7 year life span. Taking these factors into account, gives a minimum of 15.02 W End of Life (EOL) and a maximum of 22.56 W EOL. With a charging constant of 85% for the NiCad batteries, we will have 12.77 W minimum EOL, and 19.17 W maximum EOL. Because of the random orbits of the 50 satellites, the attitude of any one craft will be different from every other craft, so the output from all crafts will range between the minimum and maximum.

Solar cells can be very expensive, heavy, and require sub-structure to attach them to the craft. Because of the cost as well as the weight factor, we have chosen to use ultra-light weight wrap-around solar cells manufactured by Sovonics (4). These cells have not been flight tested, but they are easy to install, very light weight and cheap compared to

glass covered cells. If it is shown at a later date that these are inadequate for our design we will have to re-evaluate the design criteria and select a different type of cell. The weight on these cells is 21.7 grams/m², which will give us a total weight of 14.57 grams which is considerably less than the average for standard cells. The cost of these cells is about 1/10th the cost of standard cell, making them very attractive. Arrangements for a sample for the first flight tested satellite can be made, and a discount for quantities is also available.

8.2 Batteries

The subsystem power requirements are detailed in table 8-1. These power requirements

Table 8-1 Power Requirements

Subsystem	Power (W)	Duty Cycle
Sensors	1.5	continuous
Computer	2.0	continuous
Attitude Sensing	0.810 0.140	continuous 60%
Thermal Control	3.0	40%
Communication	25.0	0.0069%
Attitude Control	20.0	$1.28 \times 10^{-4}\%$

determine the number of batteries that will be needed to maintain the craft through the earth's shadow. One orbit of the earth will take 90 minutes. As a worst case orbit, the craft will be in the shade for a maximum of 36 minutes. This means that the craft has to have a battery reserve to handle 36 minutes of darkness. It must also be able to charge the batteries during 54 minutes of sunlight before entering darkness again.

To determine the number of batteries needed, we assumed worst case where everything turned on in the shade. Using the equation: Power = Current x Voltage, and knowing the power and voltage, we solved for the current, and determined the Amp hours needed. With a maximum voltage of 12 volts (except for the attitude control, which uses 20 V at 1 A every 3 months for 10 seconds), and the power requirements given in table 8-1, we get a current of 480 mA. With a maximum depth of discharge for a 7 year

battery life of only 25%, this requires a minimum of 2.54 amp hours of batteries. Using AA-sized NiCad batteries rated at 600 mA hours and 1.2 V, we need a minimum of 4 batteries in parallel. To give the satellite a reasonable safety factor and to account for battery failure we chose to use 5 batteries in parallel, which will give us 3 Amp hours of power in the shade.

To get the required voltage for the craft, we have to connect batteries in series. This will increase the output voltage, but not affect the current output. To get 12 volts, a minimum of 10 batteries is needed. Because we want to regulate the power at 12 volts, there needs to be a supply voltage greater than 12 Volts, so we chose to use 12 batteries connected in series, giving us 14.4 volts maximum. Using 12 batteries per pack, and 5 packs of batteries, this gives us a total of 60 batteries. AA-sized batteries weigh 26 grams each, giving a total weight of 1.56 kg.

8.3 Single Point Failures

The worst possible failure of the power system would be a direct short in any of the satellite subsystems. If the computer or any of the electrical field sensors go into a direct short then the satellite is useless, so there are no provisions to handle either of these cases. If a solar cell, a battery pack, attitude sensor, or one of the electric field sensors goes into a direct short, then we need to be able to remove it from the power supply so that it will not drain the power for the rest of the craft. To do this, the craft will need a bank of latching relays. At launch, all systems will be off, except for the computer which will power up the subsystems after deployment. If one of the subsystems then fails, we can remove it from the power supply by turning off its relay. If it goes into a direct short, then it may drain all the power from the craft before the computer or ground control could remove it from the power supply. To handle this, the craft will have a bank of diodes to isolate each subsystem. These diodes will have a slight power drain, but they will also automatically isolate a subsystem with a direct short, and give us time to remove that subsystem from the power supply.

REFERENCES

1. Hanak, J.J.: Ultralight Monolithic Photovoltaic Modules of Amorphous Silicon Alloys. Proceedings of the Eighteenth IEEE Photovoltaic Specialists Conference, Las Vegas, Nevada, October 21-25, 1985.
2. Space Craft Systems Design and Engineering: Solar Photovoltaic Arrays.
3. Cockron, C.D.: Space Handbook. Air Command and Staff College, Air University Press, Maxwell Air Force Base, Alabama, January, 1985.
4. Joseph Hanak, Iowa State University, (515) 294-2296.

9.0 ELF STRUCTURE AND CONFIGURATION

9.1 System Requirements

The requirements for the structure are to:

- 1) keep the total mass under 25 kg;
- 2) keep the structure under 15 kg;
- 3) fit six on Pegasus launch vehicle;
- 4) use off-the-shelf technology; and
- 5) last at least 7 years.

9.2 Design Phases

9.2.1 Gravity Gradient Because of its inherent stability, we first designed a gravity gradient satellite as shown in figure 9-1. In our initial configuration the satellite was cylindrical and symmetric about the major axis. When deployed the satellite resembled a dumbbell with the two major masses connected by a three meter beryllium copper coiled boom also known as a stacer boom.

9.2.2 Dual-Spin Satellite Later, it was determined that the sensor booms must rotate. The design then changed from a gravity gradient to a dual spinner satellite.

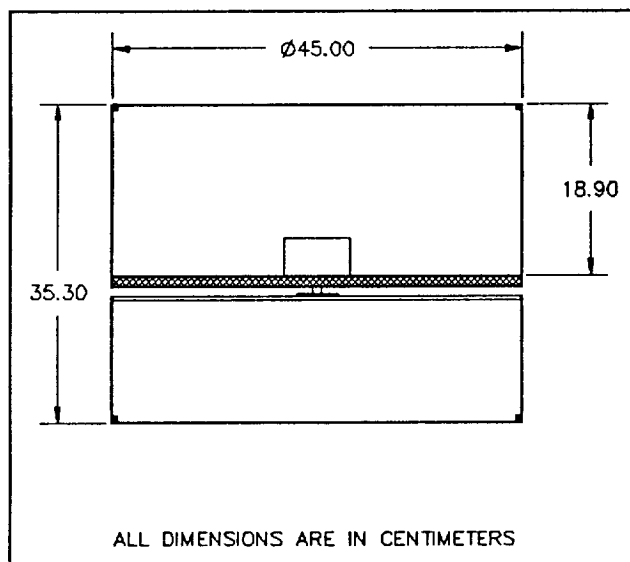


Figure 9-2 Dual spinner satellite design

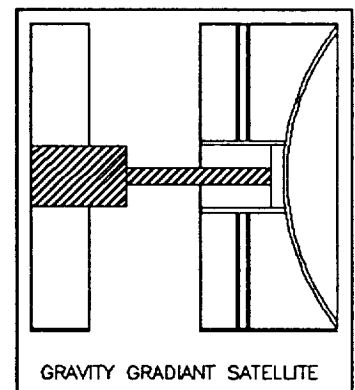


Figure 9-1 Gravity gradient satellite design

This allowed the communications dish to point to the earth at all times and the booms to rotate. We were able to maintain the basic structure, but removed the stacer boom and replaced it with a DC brushless motor. The dual spin design was discarded after the preliminary design review because of complications in passing data through the spinning joint. The design requirements were also relaxed on the antenna which allowed us

to change the dual spin satellite into a simple spinning satellite. Figure 9-2 shows the basic dual spin satellite.

9.2.3 Simple Spinner Following the critical design review, we changed the satellite design to a simple spin satellite. The dimensions of the previous design fit our requirements, so they were not changed. A launch support interface was added to allow the satellite to be attached and launched from the launch bus. Figure 9-3 shows the final structure and its dimensions.

9.3 Materials

Initially G-10 was used for our outer skin with aluminum honeycomb for the primary support plate. We decided against the G-10 because information was not available on its resistance to atomic oxygen or its durability in a space environment. We also needed to provide a heat conductive material at the perimeter (G-10 is a good insulator) for thermal control. With the decision against G-10, we moved to aluminum 6061-T6 because of its thermal properties, its low density, and the fact that it has been proven in a space environment.

The materials finally chosen are:

- 1) for the outer skin: 0.16cm thick aluminum 6061-T6;
- 2) for the support plate: 1.25cm thick POLYCORE 420-5056 aluminum honeycomb from Pollux Corporation;
- 3) for the hardware mounts: milled aluminum 6061-T6;
- 4) for the radiation shield: milled aluminum 0.635cm thick 6061-T6;
- 5) for the mounting screws: stainless steel; and
- 6) for the honeycomb screw pads: aluminum 6061-T6 0.93cm thick.

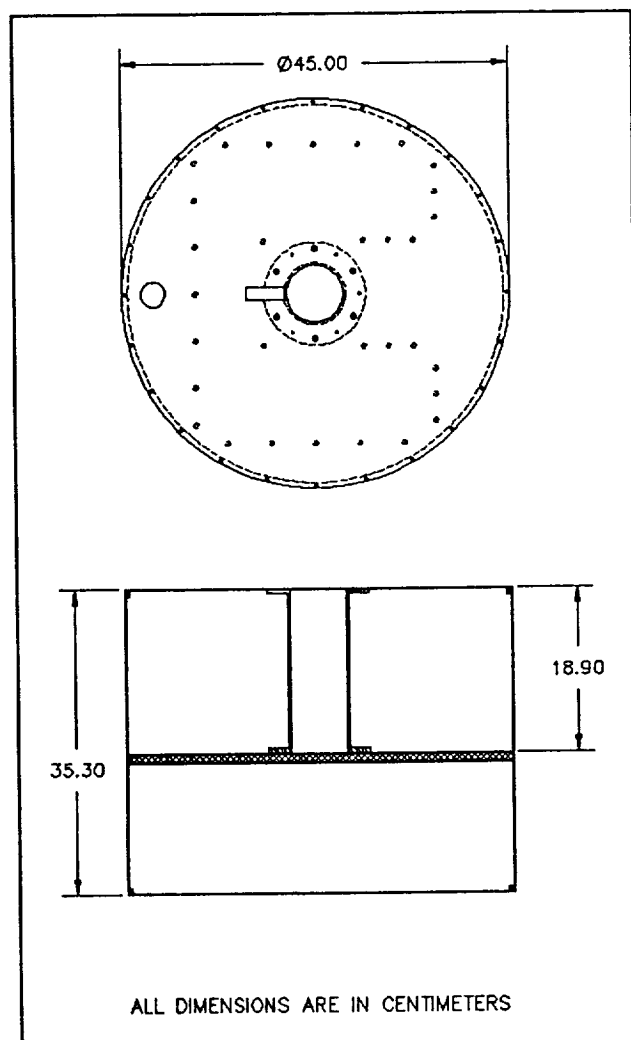


Figure 9-3 Final ELF satellite design

Figure 9.4 shows the basic satellite with hardware locations and materials called out.

9.4 Sensor Booms

With the gravity gradient satellite, tape booms were being used because of their simplicity. It was determined that if the tape were insulated, excluding the last two inches, the required measurements could be taken.

When the requirements changed, we searched for an alternate type of sensing boom. Mehrdad Roosta from Utah State University's Space Dynamics Laboratory (SDL) recommended Robert Weitzmann's Electrical Field Booms. A detailed description of the

Weitzmann booms is given in appendix G. These booms flew on the SPEAR mission for SDL. After contacting Robert Weitzmann and discussing our application, he recommended his Quadrapole design. For the on-axis boom, Mr. Weitzmann recommended using a 1.9 meter stacer boom. This sensor boom will fit in the launch support interface and has been successfully flown on other missions. The following is quoted from material Mr. Weitzmann sent us. "The Weitzmann Quadrapole and STACER booms are made from a beryllium copper spring material. The strip material is formed to a fixed coil diameter and helix angle, selected to provide significant overlap of the

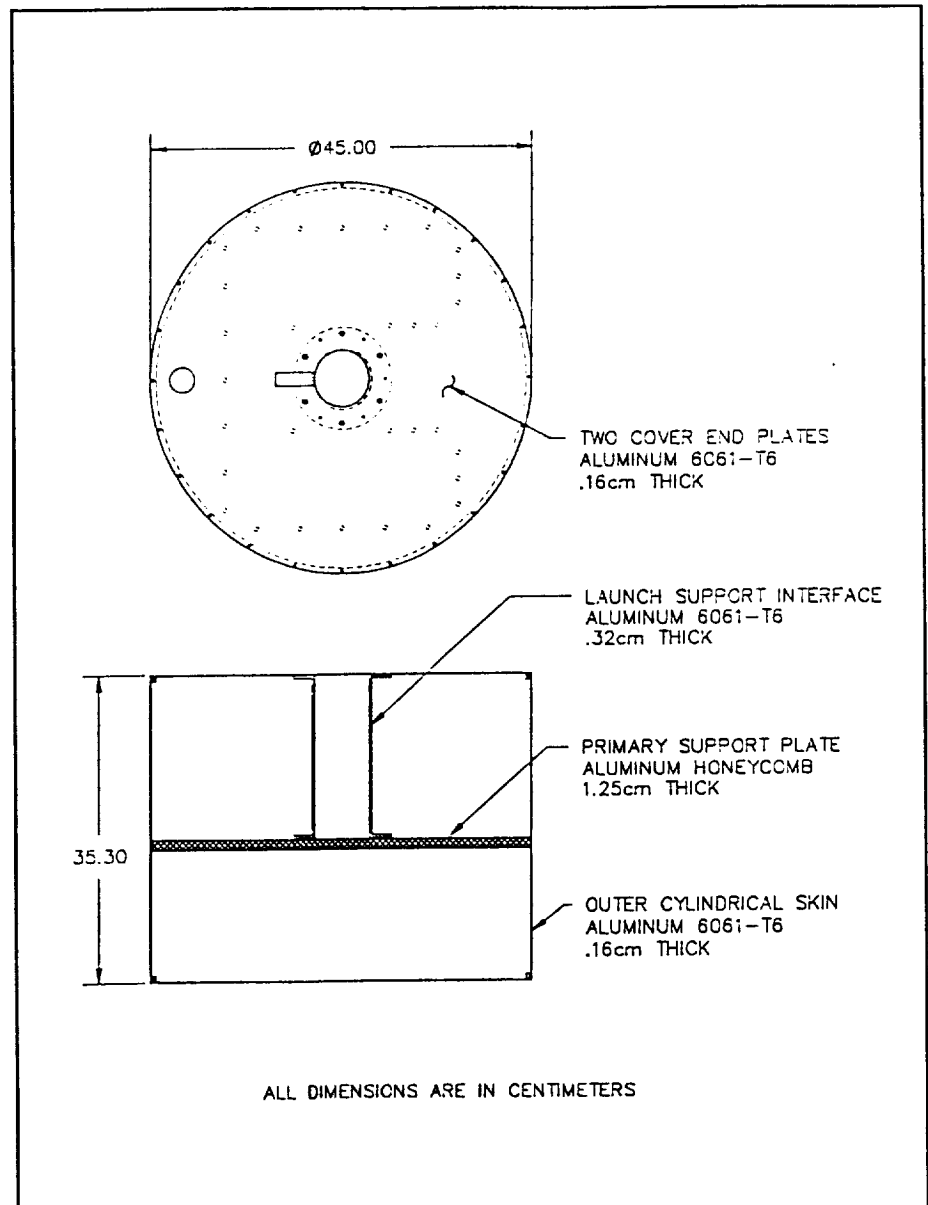


Figure 9-4 Basic ELF satellite structure and materials

adjacent coils. The spring energy of the stowed booms cause it to self extend when released. The element forms one coil at a time, such that a fully formed tubular element emerges from the housing. The extended boom behaves like a continuous thin walled tube, exhibiting cantilever bending stiffness, and is subject to failure by localized buckling. In this application, the strip material will be coated on the outside with an organically bonded molybdenum disulfide film to reduce surface reflectivity, and to provide a lubricating film between coils. Deployment will be initiated by a ICI Americas electro-explosive pin puller." (1) The Quadrapole unit weights 6.36 kg and can be deployed while the satellite is spinning from 0 to 210 RPM. The stacer unit weights 0.85 kg and can be deployed with spin rates ranging from 0-45 RPM. Both units will need to be isolated from ground, this will be accomplished by using 0.305 cm thick sheet of teflon. Figure 9.5 shows the basic structure and the Weitzmann boom locations.

9.5 Subsystem Placement

Several considerations were made in the placement of the subsystems. Some of the subsystems require a specific location, others allow some variance in location. For the latter, dimensional constraints and the location of center of mass dictated their position. The center of mass calculations and results are located in appendix G.

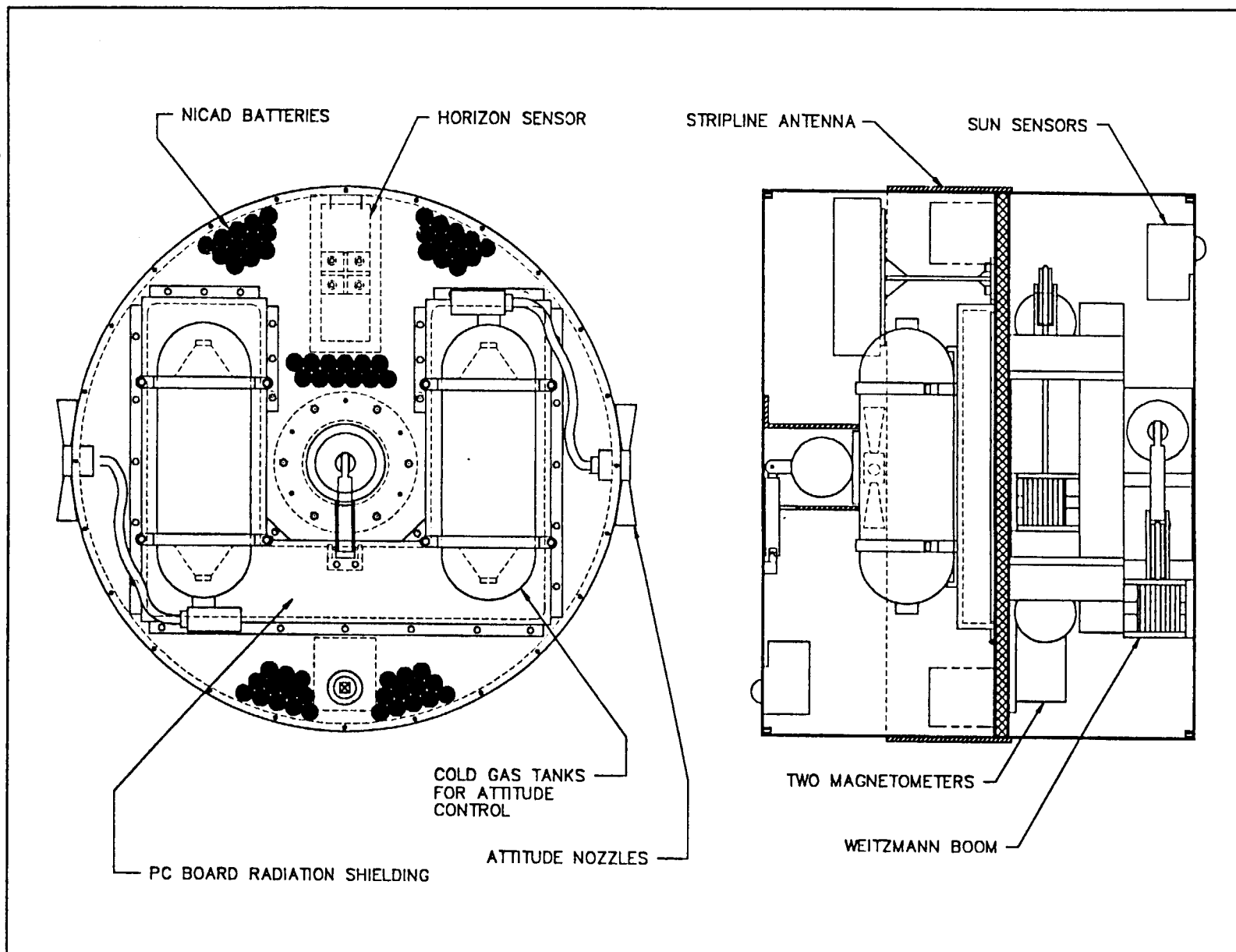
The sensors which are included within the attitude sensing and control system require definite locations. Two sun sensors, each located on a flat side of the satellite, have a mass of 132 grams and dimensions of 6.6 x 5.8 x 5.1 cm each. One horizon sensor, located on the perimeter of the satellite, has a mass of 300 grams and dimensions of 12.7 x 5.8 x 3.8 cm. Two magnetometers, placed against the outer skin of the satellite to prevent interference from circuit electronics, have a mass of 350 grams and dimensions of 4.3 x 13.3 x 6.7 cm.

The circuit board is mounted on the honeycomb plate to take advantage of the aluminum in the plate to shield against radiation. A radiation shield of milled aluminum which weighs 1.35 kg gives the board a 0.5 cm thick protective shield to the remaining sides.

Two cold gas tanks are mounted to the circuit board radiation shield. Each tank has a dry mass of 0.25 kg and will initially contain 2 kg of N_2 . The tanks have a length of 23 cm and a diameter of 7.5 cm each.

The batteries for the power subsystem consist of 5 groups of 12 AA-size batteries. The flexibility in placement of the battery packs allows us to use them as balance weights. Situating the batteries as shown in figure 9.5, we are able to locate the center of mass

Figure 9-5 Subsystem placement on ELF satellite structure



along the spin axis.

The stripline antenna is made of a 2 mm thick by 100 mm wide copper strap. It is located on the perimeter of the satellite and has a mass of 0.1 kg.

9.6 Conclusions

The satellite has a total mass of 19.1 kg with the structure making up 13.4 kg of the total. Included in the mass of the structure are the masses of the outer shell, the honeycomb plate, the Weitzmann booms, and the circuit board radiation shield. The satellite design allows us to fly 6 on a Pegasus launch vehicle or 4 piggybacking on the Delta II. All components in the design have been developed and flight tested, and all materials used last longer than 7 years in space.

REFERENCES

1. Weitzmann, Robert H., Correspondence. Wietzmann Consulting, Inc., Aerospace Engineering, San Francisco, CA, April, 1990.

10.0 THERMAL CONTROL

This chapter describes the heat flow analysis through the ELF satellite and determination of the component temperatures. If a component was not within the required temperature range, then the thermal control techniques necessary to maintain the component within its allowable temperature range were determined. Table 10-1 is a list of the key components inside the satellite and their operating temperature ranges.

Table 10-1 List of the satellite components and their operating temperature ranges.

Batteries	250 K to 320 K
Electronics	250 K to 320 K
Sun Sensors	190 K to 350 K
Horizon Crossing Sensor	250 K to 330 K
Cold Gas Tanks	T < 320 K
Magnetometers	270 K to 330 K

The booms and the electrical field sensors were not included in the list because, according to their manufacturers, they are thermally self-sufficient. Also, there was no exact data on the surface thermal properties of the booms. The beryllium-copper booms, which are coated with molybdenum disulfide, are now undergoing intense testing at Goddard Space Flight Center and the results should be released the summer of 1991. Weitzmann Inc., the manufacture of the booms, suggested an α/ϵ range of 0.9 to 1.3 as a good approximation. The symbol α refers to the absorbtivity of a substance and the symbol ϵ refers to the emissivity of a substance.

Figure 10-1 shows the heat flux inputs into the satellite system. Q_{sun} is the average direct solar flux and was assumed to be 1400 W/m. $Q_{\text{reflected}}$ is the amount of solar flux that is reflected off the earth onto the satellite. Q_{earth} is the radiation exchange with earth, which is assumed to be a black-body object. Q_{space} is the energy radiated to space. Q_{internal} is the internal heat generation by components inside the satellite. The equation used in the energy balance of the satellite was:

$$\dot{Q}_{\text{SUN}} + \dot{Q}_{\text{REFLECTED}} + \dot{Q}_{\text{EARTH}} + \dot{Q}_{\text{INTERNAL}} - \dot{Q}_{\text{SPACE}}$$

where:

$$\begin{aligned}\dot{Q}_{\text{SUN}} &= \alpha_s A_s I_s \\ \dot{Q}_{\text{REFLECTED}} &= \alpha_s F_{s,e} A_s I_s \\ \dot{Q}_{\text{EARTH}} &= \sigma \epsilon_s F_{s,e} A_s (T_s^4 - T_e^4) \\ \dot{Q}_{\text{SPACE}} &= \sigma \epsilon_s F_{s,sp} A_s (T_s^4 - T_{sp}^4)\end{aligned}$$

where:

- A_{\perp} = the orbit-average spacecraft projected area perpendicular to the sun
- A_s = the surface area of the satellite
- a = the albedo of the earth which was assumed to be 0.3 ± 0.02 , which is a yearly average
- α_s = the absorptivity of the satellite (for silicon-carbide solar cells, $\alpha = 0.7$)
- ϵ_s = the emissivity of the satellite (for silicon-carbide solar cells, $\epsilon = 0.82$)
- ϵ_e = the emissivity of the earth, which for a black-body object is 1
- $F_{s,se}$ = the radiation exchange view factor of spacecraft to sunlit earth
- $F_{s,e}$ = the view factor of spacecraft to earth
- $F_{s,sp}$ = the view factor of spacecraft to space ($F_{s,e} + F_{s,sp} = 1$)
- I_s = the solar flux at earth
- σ = the Stefan-Boltzman constant which equals $5.67E-08 \text{ W}/(\text{mK}^4)$.

Solving the energy balance equation for T_s , the outside surface temperature of the satellite, yields the equation:

$$T_s = \left[\frac{I_s (A_{\perp} + a F_{s,se} A_s)}{\sigma A_s} \right]^{1/4}$$

α/ϵ versus T_s is plotted for varying Q_{internal} in figure 10-2. This plot is for a worst case scenario in which the satellite is in an orbit in which one side is always facing the sun, called a hot case.

For a worst case scenario where one side of the satellite never

sees the sun, the direct sunlight and sunlight reflected off the earth is removed from the above equation. This yields the equation for a cold case:

Internal heat generation versus surface temperature from this equation is plotted in figure 10-3.

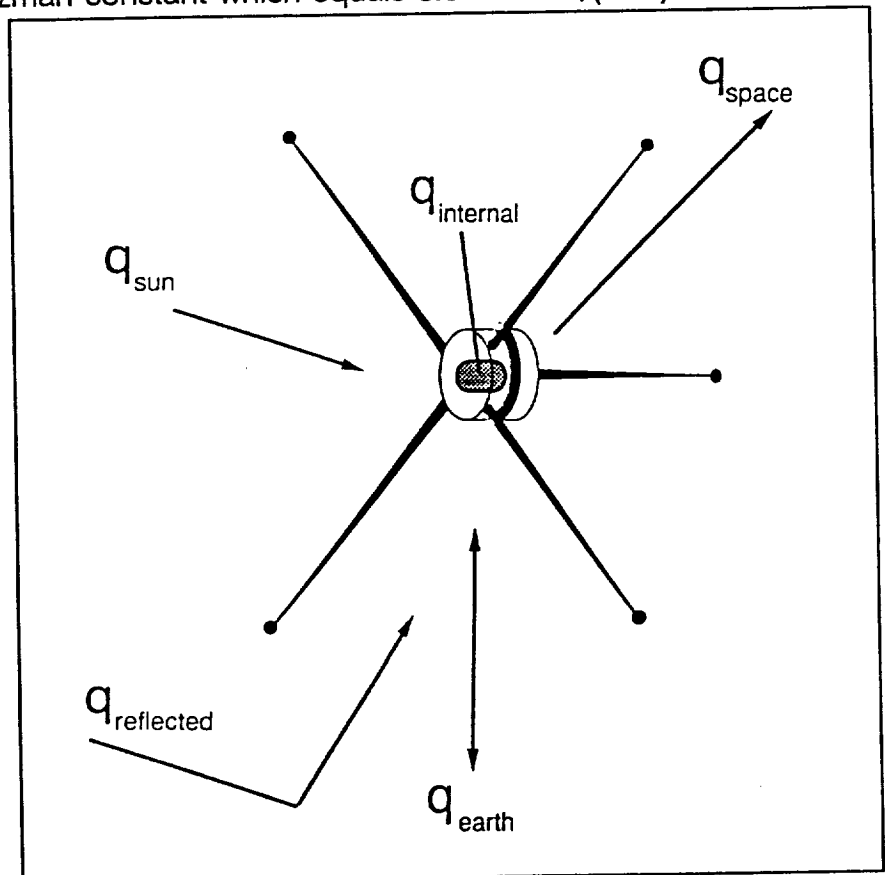


Figure 10-1. Diagram of Heat Flux Inputs to the Satellite System.

This initial evaluation of the surface temperature of the satellite showed that for a steady-state case in which one side of the satellite was always facing the sun, the temperature would be in the desired range for a surface coated with solar-cells (α/ϵ of about .8).

For the cold case, in which one side of the satellite never sees the sun, the surface temperature was below the required range. From this initial analysis, a range of possible maximum and minimum surface

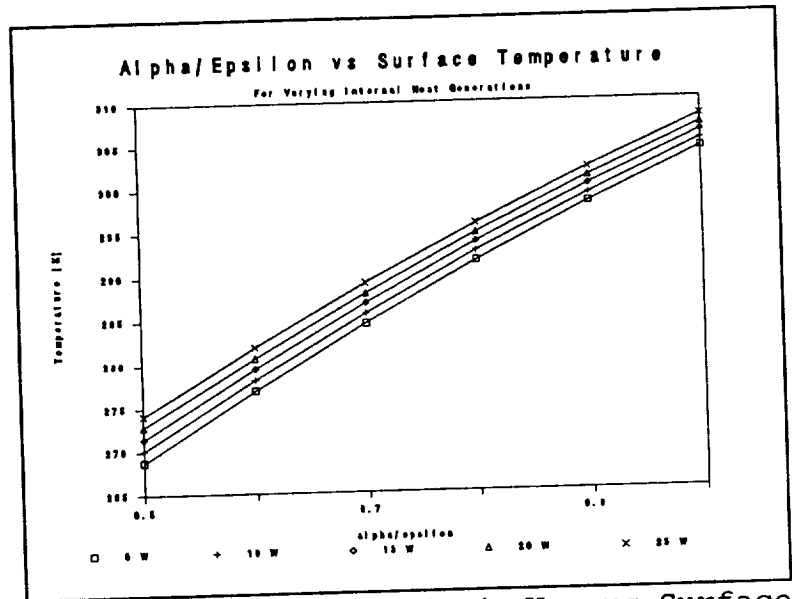


Figure 10-2. A plot of α/ϵ Versus Surface Temperature of the ELF Satellite for Varying Internal Heat Generations.

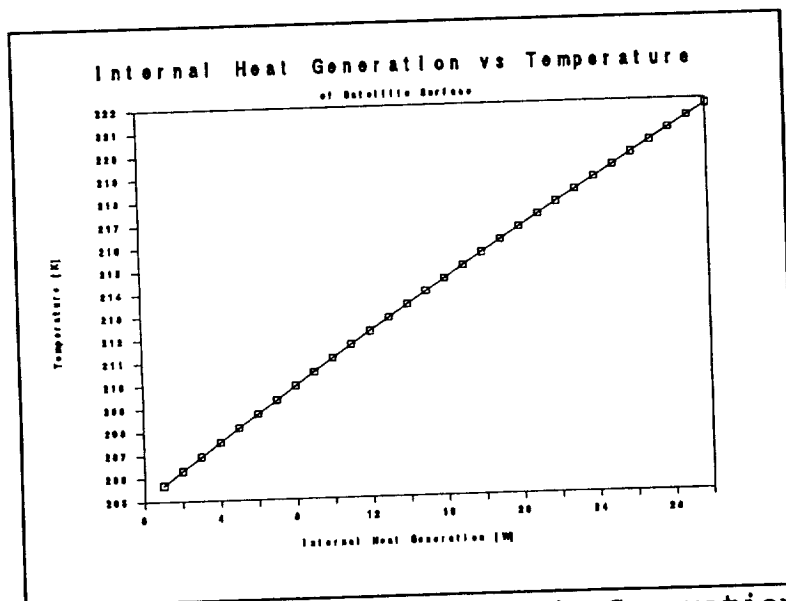


Figure 10-3. Internal Heat Generation Versus Surface Temperature of Elf Satellite.

temperatures was established. The maximum temperature expected was about 310 K and the minimum temperature expect was about 220 K. The minimum temperature was below the operating temperature range of some of the instruments.

For a more indepth thermal analysis, a SINDA 1987/ANSI computer model was developed. Figure 10-4 shows the external nodal break-up of the satellite and figure 10-5 shows the internal satellite and boom nodal break-up. Table H-1, located in Appendix

H1, contains a listing of the nodes and their corresponding descriptions.

In order to run simplified steady-state simulations, two extreme cases were chosen: a hot orbit in which the orbit plane and flat plate of the satellite were perpendicular to the solar radiation, as shown in figure 10-6; and a cold orbit in which the orbital plane of the satellite was parallel to the solar radiation and the satellite was in the shade of the earth approximately 40% of the time, as shown in figure 10-7. For the hot case, simulations

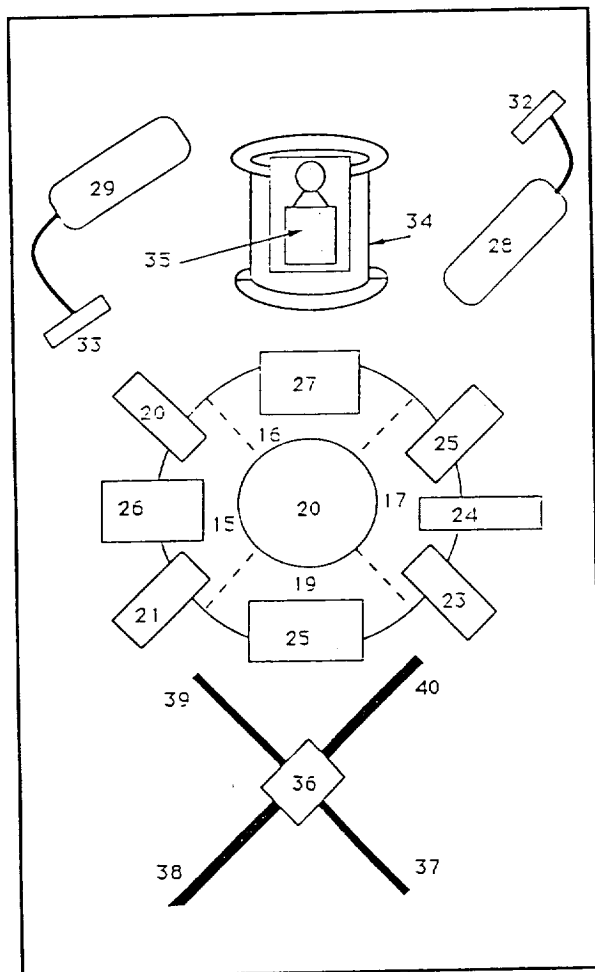


Figure 10-5 Nodal Break-up of the Internal Components of the Satellite and Booms.

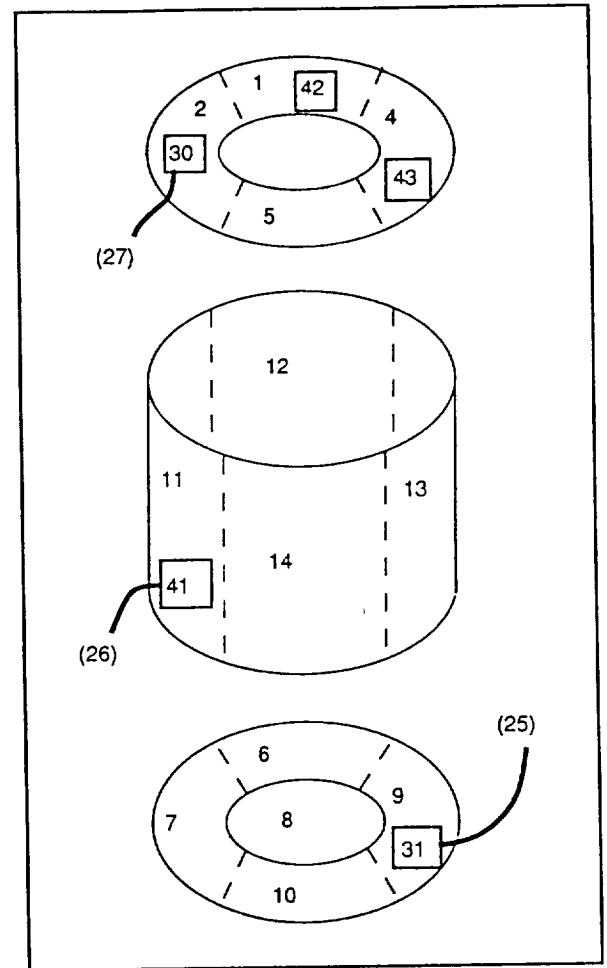


Figure 10-4 Nodal Break-up of External Part of Satellite.

were run with the quadrapole side facing the sun and also with the monopole side facing the sun. A sample of the SINDA program and a sample copy of the generated output is located in appendix H2.

In order to account for the spin of the satellite with a steady-state model, the rotation of the satellite was modeled as a sinusoidal wave. Figure 10-8 shows the sine wave and the corresponding time locations of the satellite. During the positive part of the sine wave, a given point on the satellite would see some portion of the sun. On the

negative part of the sine wave, the point would not be able to see the sun. In effect, the cyclic portion of the sun would be a half-rectified sine wave. The average sunlight that a point on the satellite would see over one cycle was assumed to be the root-mean square value:

$$f(t)_{rms} = \sqrt{\frac{1}{T} \int_0^T f(t)^2 dt}$$

where $f(t)$ is any function of time and T is the period of averaging. In order to verify the root-mean square assumption for direct sunlight on the spinning side of the satellite,

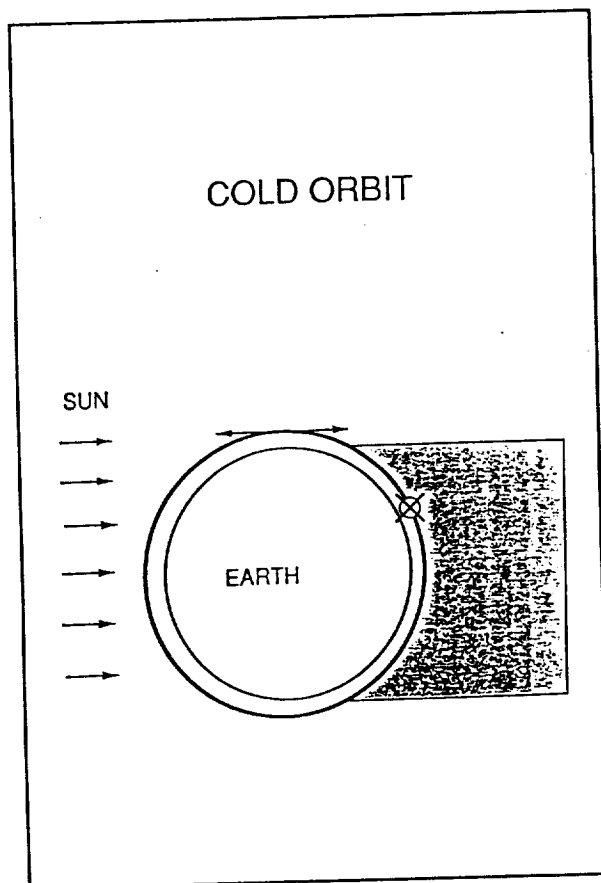


Figure 10-7 Cold Orbit Worst Case Scenario for SINDA Computer Model.

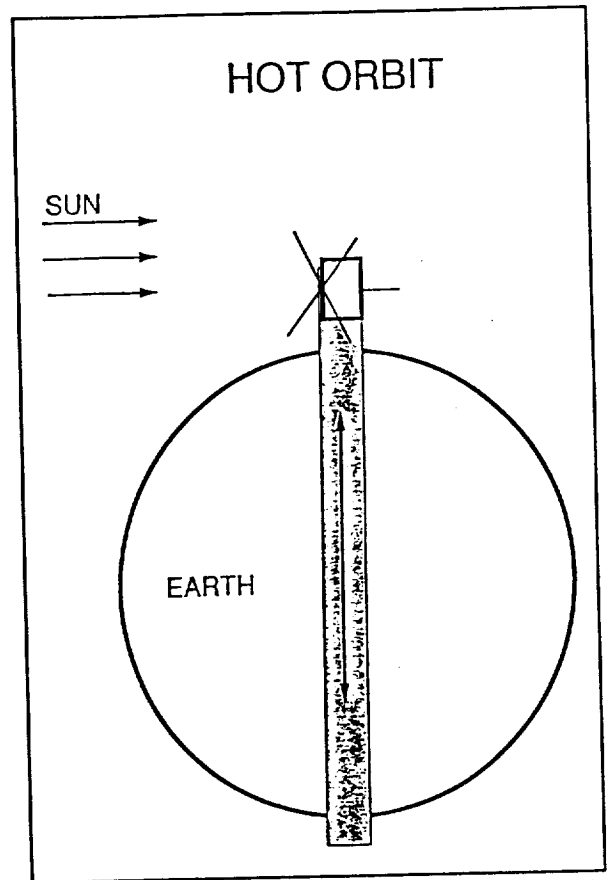


Figure 10-6 Hot Orbit Worst Case Scenario for SINDA Computer Model.

a transient analysis was performed on a cylinder. This cylinder, shown in figure 10-9a, had both ends open. The transient analysis was based on an energy balance of the cylinder. The change in energy of the control volume is:

$$mC_p \frac{\partial T}{\partial t} = \dot{q}_{sun} + \dot{q}_{earth} + \dot{q}_{space} + \dot{q}_{conduction} + \dot{q}_{convection}$$

Figure 10-9b shows the energy transferred into and out of the control volume by conduction, convection and radiation. The transient analysis was also set up to be run at different spin rates. This transient analysis showed the shell temperature to be about

335 K. This temperature was slightly higher than the satellite temperature calculated with the SINDA program. This was to be expected since the shell model did not include the end plates. If the end plates had been included, radiation to space with no

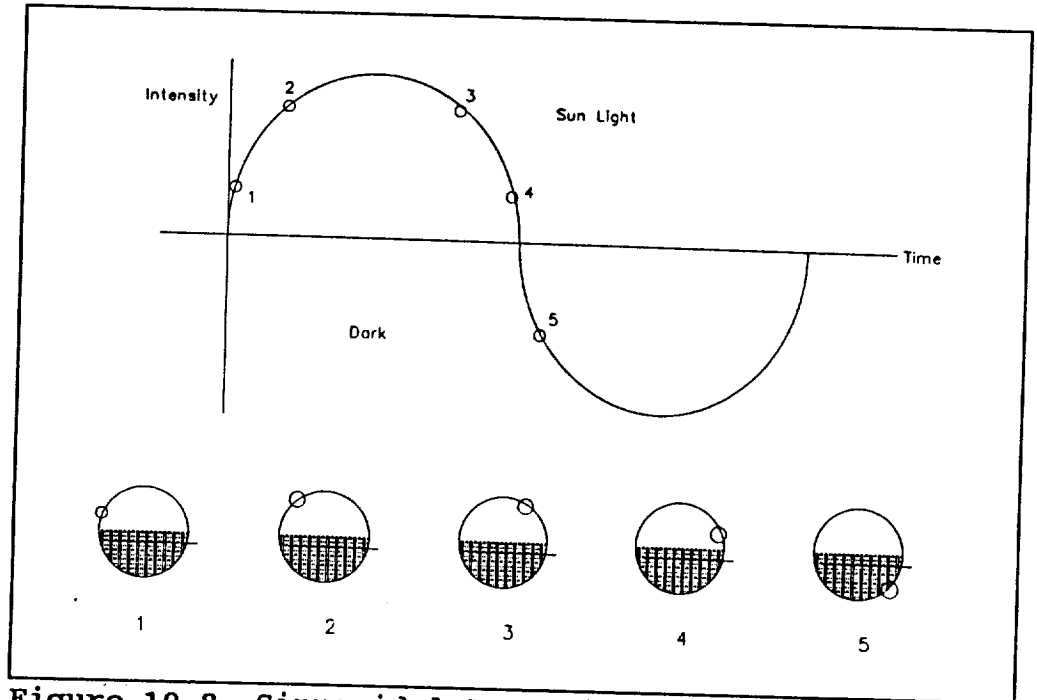


Figure 10-8 Sinusoidal Approximation of the Spinning Satellite and the Corresponding Time Locations of a Point on the Satellite.

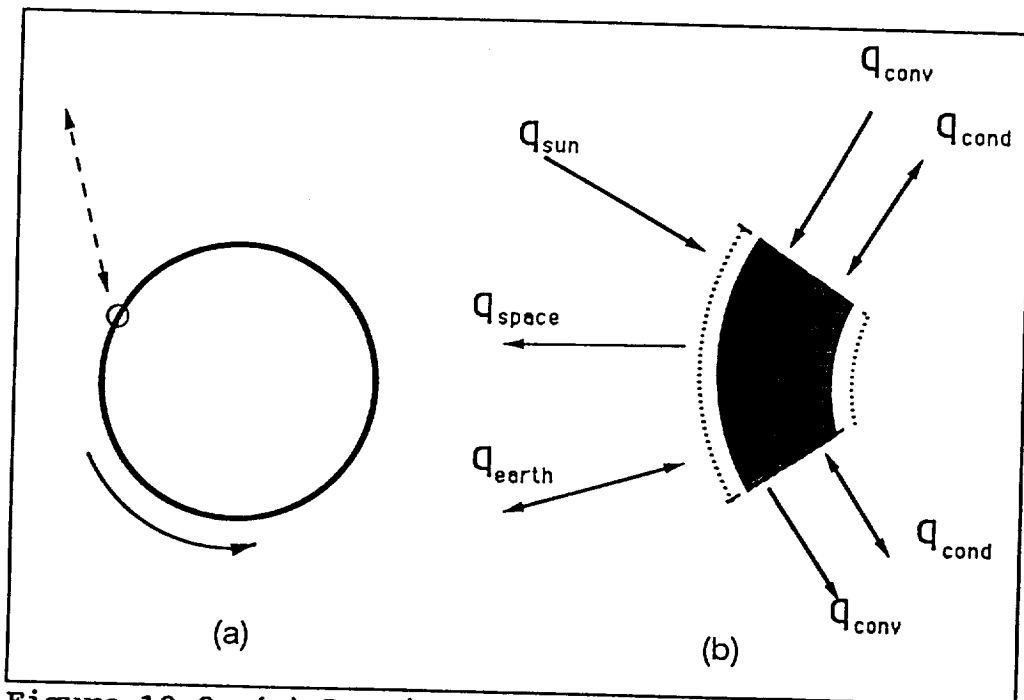


Figure 10-9 (a) Drawing of Cylinder Used in Root-Mean Square Radiation Verification. (b) Energy Flow Through Cylinder Element.

heat input would have lowered the satellite temperature.

Another way to support the root-mean square energy flux assumption was found in a paper written by Preuss et al (1). This paper dealt with the surface temperature of a spinning

satellite versus distance from sun for different values of α/ϵ . A graph of their results is shown in figure 10-10. The value at $\alpha/\epsilon = 0.8$ and 1 astronomical unit resulted in a surface temperature of the satellite of about 290 K. This value was very close to the temperature found in the initial calculations.

After an initial run of the computer model, it was discovered that with the given design of the satellite the internal component temperatures would be less than the given requirements. At this point, different thermal control techniques were examined to determine what could be done to raise the component temperatures to the desired values. In order to add more heat energy to the satellite system, three 1 Watt resistance heaters were equally dispersed over the surface of the electronic component radiation shielding. The heaters would add energy to the center of the satellite system which contained components that were below the temperature ranges. Each heater would be equipped with its own on/off regulating switch. The switch would be a simple bimetallic strip set up to turn on at temperatures below 250 K and turn off at 270 K composed of two flat strips connected one on top of the other. One strip would be made of a metal with a higher thermal expansion coefficient than the other strip so that with temperature changes, the metal with the higher coefficient would expand or contract more, causing the combined strip to bend. The switch would be designed such that at temperatures below 250 K, the strips of metal would complete a connection and turn the heaters on and at temperatures above 260 K, the strips would bend far enough to break the connection and turn the heaters off. There is enough excess power to run the heaters for their duty cycle of approximately 40%. The heaters would only be needed when the satellite was in the earth's shadow.

Another source of heat input into the satellite was developed by assuming that the cold-gas nozzles were made of aluminum and coated with black nickel oxide, which has an absorbtivity of 0.92 and an emissivity of 0.08. With the black nickel oxide coating, the cold-gas nozzles could absorb large amounts of heat compared to the amount that they radiate out to space. The thermal energy would be transported to the center of the satellite via 1 by 0.1 cm copper straps that are 12 cm long which connect the nozzles to the electronic radiation shielding.

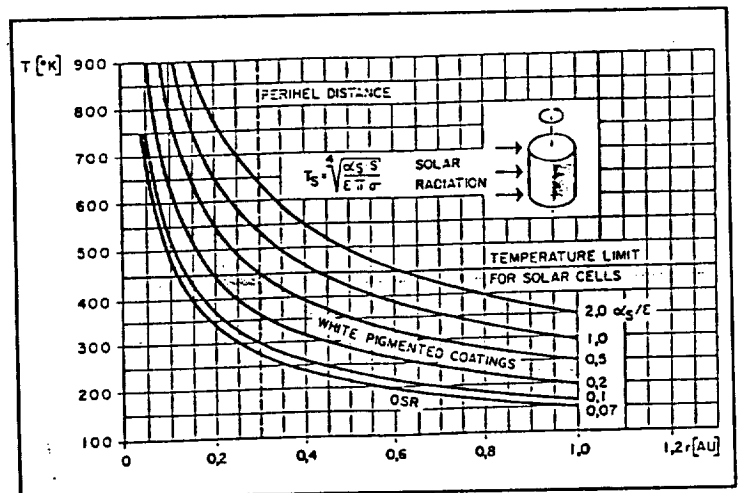


Figure 10-10 Spinning Satellite Surface Temperature Versus Distance From Sun For Different Values of α/ϵ [1].

In order to keep the attitude determination sensors within their required temperature ranges, a 0.159 cm diameter copper strap, 15 cm long, was attached from the sensors to the radiation shielding. The straps were required to add additional heat energy to the sensors because they could radiate some of their heat out to space since they are located on the outside edges of the satellite and exposed to space. The additional heat conducted by the copper straps was enough to keep the sensors within their temperature requirements for both cases investigated.

After the thermal control techniques described above were added to the SINDA model, the simulations were run again. The generated component temperatures were compared with the required operating temperature ranges. Table 10-2 is a list of the component temperatures for the hot case, quadrupole side facing the sun; table 10-3 is a list of the component temperatures for the hot case, monopole side facing the sun; and table 10-4 is a list of the component temperatures for the cold case.

Table 10-2 Component temperatures calculated by the SINDA model for the hot case, quadrupole side facing the sun.

Batteries	309.62 K
Electronics	309.93 K
Sun Sensors	309.93 K
Horizon Crossing Sensor	310.03 K
Cold Gas Tanks	306.94 K
Magnetometers	308.17 K

Table 10-3 Component temperatures calculated by the SINDA Model for the hot case, single boom side facing the sun.

Batteries	291.51 K
Electronics	291.70 K
Sun Sensors	291.69 K
Horizon Crossing Sensor	291.73 K
Cold Gas Tanks	291.65 K
Magnetometers	297.26 K

Table 10-4 Component temperatures calculated by the SINDA computer model for the cold case.

Batteries	265.05 K
Electronics	265.04 K
Sun Sensors	265.62 K
Horizon Crossing Sensor	265.63 K
Cold Gas Tanks	270.33 K
Magnetometers	264.93 K

All components appeared to be in the required temperature ranges except for the magnetometers. In the cold-case scenario the magnetometers were at 264.93 K which is about 5-6 K below the minimum operating temperature value of 270 K. For the actual flight model of the satellite, either different magnetometers must be used with lower operating temperature range or a way must be found to increase the thermal energy of the magnetometers when the satellite is in the earth's shadow.

A possible source of error in the component temperatures generated by the SINDA program could be due to fasteners. For the thermal analysis performed here, the fasteners of the satellite structure were not specified, so it was assumed that the connections between different nodes in the satellite were the minimum cross-sectional areas of contact. Another source of error could possibly be eliminated by performing a transient analysis with the SINDA program. Due to the complexity of the SINDA program associated with performing a transient analysis and a lack of time, only a steady state analysis was performed. This steady state analysis employed different assumptions, such as the root-mean square average solar flux into the satellite system, which could simulate a transient condition but also could be incorrect. With a transient analysis, different orbital configurations could be evaluated instead of just the worst case scenario orbits evaluated with the steady state analysis.

In conclusion, the initial calculations gave an expected temperature range 220 K to 310 K. The SINDA computer program was then used to run a steady state analysis of a 3-dimensional satellite model. In order to simulate a transient energy flux into the satellite, the assumption of a root-mean square value of a half rectified sinusoidal wave was used. This assumption was verified by two different sources: a transient analysis of a simple cylinder and the results of a paper by Preuss et al. In order to achieve the required component temperature ranges for both the hot case and the cold case, three 1-Watt heaters were connected to the electronic component radiation shielding and all three

heaters would be equipped with self-contained control switches. The cold-gas nozzles were then assumed to be coated with black nickel oxide and the heat absorbed by the nozzles was transported to the radiation shielding via copper straps. Copper straps were also used to thermally connect the radiation shielding to the attitude sensors. The resultant component temperatures were all within the required ranges except for the magnetometers which were about 10 K below their operating range during the cold case.

It is recommended that for a flight model, a transient analysis be performed with SINDA or with another heat transfer computer program. A different program would be recommended because with the 43 node model used, the SINDA program was almost overloaded and it required more than 10 minutes to run each simulation. Also, the fasteners need to be specified for a final thermal analysis.

REFERENCES

1. Preuss et al: Proceedings of the 2nd International Conference on Space Engineering: Investigation of low α/ϵ coatings in a simulated space environment. Springer-Verlag, New York Inc., New York, NY, 1969.
2. Incropera, F. P. and De Witt, D. P.: Introduction to Heat Transfer. John Wiley & Sons, Inc., New York, NY, 1985.
3. Bird, R. B., Stewart, W. E., and Lightfoot, E. N.: Transport Phenomena. John Wiley & Sons, Inc., New York, NY, 1960.
4. Dr. Warren Phillips, Personal Conversation, 15 April, 1990.
5. SINDA 1987/ANSI, Network Analysis Associates, Inc., P.O. Box 8007, Fountain Valley, California 92708. Phone (714) 641-8945 Fax (714) 641-8945.

APPENDIX A

ELECTRICAL FIELD SENSING SYSTEM

APPENDIX A1

```
10  ! GROVER CLEVELAND SMITH
20  ! UTAH STATE UNIVERSITY 1990
100 DECLARE REAL P(1900),EROR(1900),TIM.(1900),ANG(1900),X(1800)
200 L=2.75
210 Y=0
220 X=0
230 T=0
240 M=.25
250 V1=8050
260 V2=3
270 E=.5
1000 FOR T=0 TO 1800 STEP 60
1010 T1=T
1020 A=(PI/2700)*T1
1030 A1=A/2*PI
1040 IF A1<=PI/2 THEN B=(2*Y/PI)*A
      ELSE IF A1<=PI THEN B=((1-2*Y)/PI)*A
      ELSE IF A1<=-(3/2*PI) THEN B=-(2*Y/PI)*A
      ELSE IF A1<=2*PI THEN B=-((1-2*Y)/PI)*A
      END IF
1050 C=(PI*T1/3+(PI*X/180))
1060 MX=M*COS(2*A)*COS(B)
1070 MY=M*COS(2*A)*SIN(B)
1080 MZ=M*SIN(2*A)
1090 VX=V1*COS(A)*COS(B)+V2*COS(A)*COS(C-PI*X/180)
1100 VY=V1*COS(A)*SIN(B)+V2*COS(A)*COS(C-PI*X/180)
1110 VZ=V1*SIN(A)+V2*SIN(C-PI*X/180)
1120 LX=L*COS(A)*COS(C)
1130 LY=L*COS(A)*SIN(C)
1140 LZ=L*SIN(A)
1150 EX=E*COS(A)*COS(B-PI)
1160 EY=E*COS(A)*SIN(B-PI)
1170 EZ=E*SIN(B-PI)
1180 EXVB=VY*MZ-VZ*MY
1190 EYVB=VZ*MX-VX*MZ
1200 EZVB=VX*MY-VY*MX
1210 PX=EX*LX+EXVB*LX
1220 PY=EY*LY+EYVB*LY
1230 PZ=EZ*LZ+EZVB*LZ
1240 TEMP=SQRT (PX^2+PY^2+PZ^2)
```

```

1250 IF PX=0 THEN PX=PX+1000 END IF
1260 TANG=(PX/PY)
2000 FOR X=1 TO 45
2010 T1=Y
2020 A=(PI/2700)*T1
2030 A1=A/2*PI
2040 IF A1<=PI/2 THEN B=(2*X/PI)*A
      ELSE IF A1<=PI THEN B=((1-2*X)/PI)*A
      ELSE IF A1<=-(3/2*PI) THEN B=(2*X/PI)*A
      ELSE IF A1<=2*PI THEN B=-((1-2*X/PI)*A
      END IF
2050 C=PI*T1/3+(PI*X/180)
2060 MX=M*COS(2*A)+COS(B)
2070 MY=M*COS(2*A)+SIN(B)
2080 MZ=M*SIN(2*A)
2090 VX=V1*COS(A)*COS(B)+V2*COS(A)*COS(C-PI*X/180)
2100 VY=V1*COS(A)*SIN(B)+V2*COS(A)*SIN(C-PI*X/180)
2110 VZ=V1*SIN(A)+V2*SIN(C-PI*X/180)
2120 LX=L*COS(A)*COS(C)
2130 LY=L*COS(A)*SIN(C)
2140 LZ=L*SIN(A)
2150 EX=E*COS(A)*COS(B-PI)
2160 EY=E*COS(A)*SIN(B-PI)
2170 EZ=E*SIN(B-PI)
2180 EXVB=VY*MZ-VZ*MY
2190 EYVB=VZ*MX-VX*MZ
2200 EZVB=VX*MY-VY*MX
2210 PX=EX*LX+EXVB*LX
2220 PY=EY*LY+EYVB*LY
2230 PZ=EZ*LZ+EZVB*LZ
2240 P(T1)=SQRT(PX^2+PY^2+PZ^2)
2250 DELTAP=P(T1)-TEMP
2260 IF PX=0 THEN PX=1000
2270 ANG(T1)=PX/PY
2280 IF TANG=0 THEN TANG=1000
2290 ERANG(T1)=(ANG(T1)-TANG)/TANG
2300 IF P(T)=0 THEN P(T)=1000
2380 IF TEMP=0 THEN TEMP=1000
2390 EROR(T1)=DELTAP/TEMP
2400 TIM.(T1)=T
2410 X(T1)=X
2420 IF ERANG(T1)>=.01 GOTO 4200

```

```
2430 IF EROR(T1)>=.01 GOTO 4200
2440 NEXT X
2450 NEXT T
2460 FOR T1=0 TO 1800 STEP 60
2470 PRINT #1 USING "####,###,###.####,###.####,###.####",
    TIM.(T1),X(T1),EROR(T1),ERANG(T1),P(T1)
2480 NEXT T1
2490 CLOSE #1
2500 END
```

APPENDIX A2

Error due to spacecraft rotation

$$\alpha_{\omega} = \frac{\omega k T_e}{e E} \left[\left(1 + \frac{8 k T_i}{\pi m_i v^2} \right) \left(\frac{k T_i}{2 \pi m_i} + \frac{v^2}{16} + \frac{i_{ph}}{4 n e} \right) \right]^{-\frac{1}{2}}$$

Error due to particle screening

$$\alpha_d = \frac{10^6 k^3 T_e^2 T A}{2 \pi d^5 E^3 e^3 n} \left[\frac{k T_i}{2 \pi m_i} + \frac{v^2}{16} + \frac{i_{ph}}{4 n e} \right]^{-\frac{1}{2}}$$

Symbol	Quantity	Units	Value
ω	angular velocity	s ⁻¹	1.05
e	elementary charge	C	1.60x10 ⁻¹⁹
k	Boltzmann's constant	J/K	1.58x10 ⁻²³
m_i	ion mass	kg	2.65x10 ⁻²⁶
m_e	electron mass	kg	9.11x10 ⁻³¹
v	forward velocity	m/s	7.35x10 ³
n	electron density	m ⁻³	10 ⁹
d	boom length	m	2.75 1.65
T	amplifier temperature	K	323
A	amplifier bandwidth	Hz	100
i_{ph}	photoelectric constant	A/m ²	10 ⁻⁴
E	ambient electric field	V/m	.002
T_i	ambient ion temperature	K	800
T_e	ambient electron temperature	K	--

APPENDIX B

MISSION DESCRIPTION

APPENDIX B

Individual satellites are referred to by two numbers such as 3,1. The first number is the launch number and the second is the satellite of that launch in order of deployment. Thus 3,1 is the third launch and the first satellite to be deployed from that cluster.

Satellite	Deployment Type	Inclination Degrees	Altitude km	Nodal Regression per Month (deg)
1,1	Inclination	87.0	550	-11.7
1,2	Inclination	87.5	550	-9.8
1,3	Inclination	88.0	550	-7.8
1,4	Inclination	88.5	550	-5.9
1,5	Inclination	89.0	550	-3.9
1,6	Inclination	89.5	550	-2.0
2,1	Inclination	82.5	550	-29.2
2,2	Inclination	83.0	550	-27.3
2,3	Inclination	83.5	550	-25.3
2,4	Inclination	84.0	550	-23.4
2,5	Inclination	84.5	550	-21.4
2,6	Inclination	85.0	550	-19.5
3,1	Altitude	80.0	550	-38.8
3,2	Altitude	80.0	625	-37.4
3,3	Altitude	80.0	700	-36.0
3,4	Altitude	80.0	775	-34.7
3,5	Altitude	80.0	850	-33.5
3,6	Altitude	80.0	925	-32.3

Satellite	Deployment Type	Inclination Degrees	Altitude km	Nodal Regression per Month (deg)
4,1	Altitude	75.0	550	-57.9
4,2	Altitude	75.0	625	-55.7
4,3	Altitude	75.0	700	-53.7
4,4	Altitude	75.0	775	-51.8
4,5	Altitude	75.0	850	-49.9
4,6	Altitude	75.0	925	-48.1
5,1	Altitude	70.0	550	-76.5
5,2	Altitude	70.0	625	-73.7
5,3	Altitude	70.0	700	-71.0
5,4	Altitude	70.0	775	-68.4
5,5	Altitude	70.0	850	-65.9
5,6	Altitude	70.0	925	-63.6
6,1	Altitude	65.0	550	-94.5
6,2	Altitude	65.0	625	-91.0
6,3	Altitude	65.0	700	-87.7
6,4	Altitude	65.0	775	-84.5
6,5	Altitude	65.0	850	-81.5
6,6	Altitude	65.0	925	-78.6

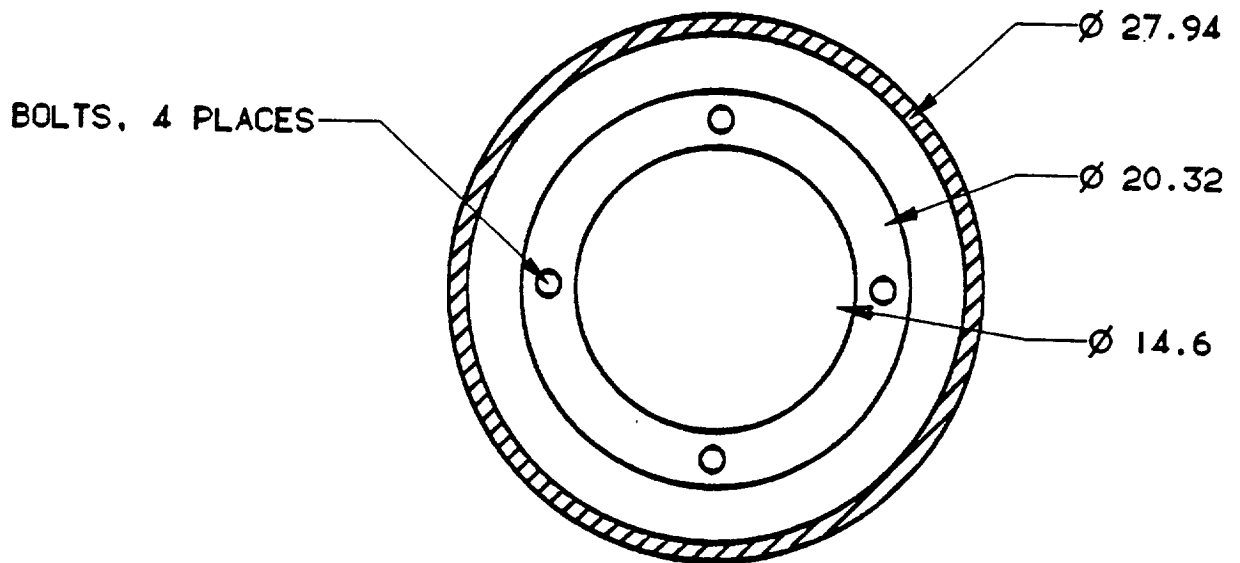
Satellite	Deployment Type	Inclination Degrees	Altitude km	Nodal Regression per Month (deg)
7,1	Altitude	60.0	550	-111.8
7,2	Altitude	60.0	625	-107.7
7,3	Altitude	60.0	700	-103.7
7,4	Altitude	60.0	775	-100.0
7,5	Altitude	60.0	850	-96.4
7,6	Altitude	60.0	925	-93.0
8,1	Altitude	55.0	550	-128.3
8,2	Altitude	55.0	625	-123.5
8,3	Altitude	55.0	700	-119.0
8,4	Altitude	55.0	775	-114.7
8,5	Altitude	55.0	850	-110.6
8,6	Altitude	55.0	925	-106.7

APPENDIX C

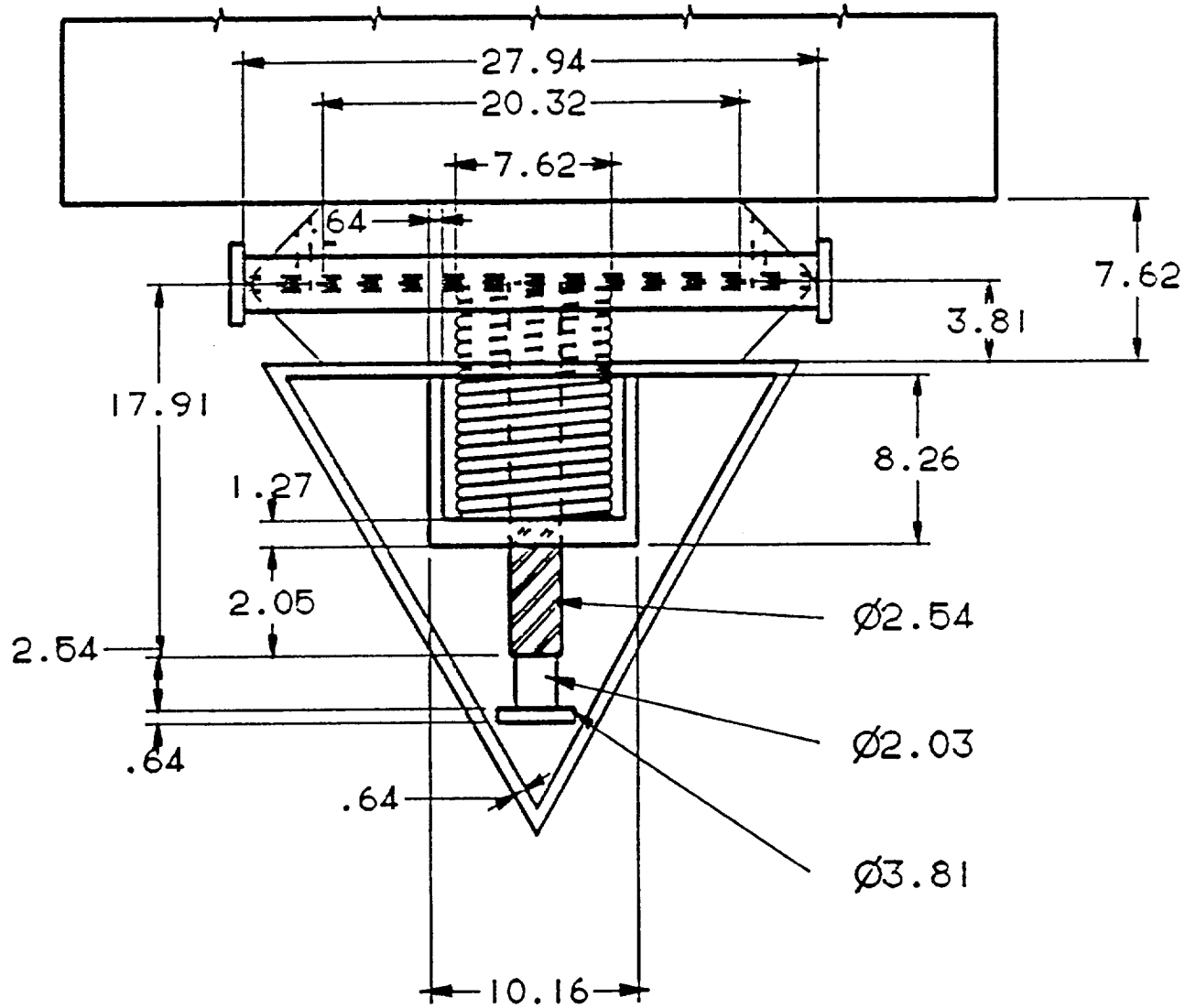
ELF CONSTELLATION DEPLOYMENT

MARMON CLAMP

SIDE VIEW



TOP VIEW



APPENDIX D

ATTITUDE CONTROL AND DETERMINATION SYSTEM

VALVE COMPONENTS FOR MISSILE AND SPACE APPLICATION

VALVE TYPE	FUTURECRAFT P/N	DESCRIPTION	PROJECT/CUSTOMER/YEAR	WEIGHT (LBS.)	AREA WEIGHT
<u>THRUSTERS,</u> SOLENOID OPERATED	200733	2.0 LBF NOM. THRUST, 0.067" ESEO, 465 PSIA OP. PRESS., COAXIAL TYPE	BLOCK 5D G.E., RAYTHEON DIV., MARQUARDT, 1976	0.28	0.013
	200886	30.0 LBF THRUST, (F/C EQUIV. TO 200895)	F/C, 1977	0.87	
	200895	* 30.0 LBF THRUST	SSTTP PENETRATION AIDS LAUNCHER "B", 1977 AVCO, SPACE DATA		
	2009157	* 30.2 LBF, 50 PSIA OP. PRESS. COAXIAL TYPE, 1/4" TUBE STUB, GASEOUS NITROGEN SERVICE, 10 M. SEC. MAX. RESPONSE, <u>DUAL SERIES REDUNDANT</u> SOLENOID VALVES	ROCKWELL INT'L, (P-80-1 SATELLITE) TEAL RUBY SENSOR, 1978	0.75	

ORIGINAL PAGE IS
OF POOR QUALITY

*New product announcement
from Futurecraft
Corporation*

PULLOS PREVUES

*by
Alex Pullos*

Phone (818) 330-1611
TWX 910-584-1330
FAX 818-336-1878
P.O. BOX 3929



January 10, 1989

Attention:

NEW PRODUCT ANNOUNCEMENT

PRESSURE REGULATOR: P/N 400432

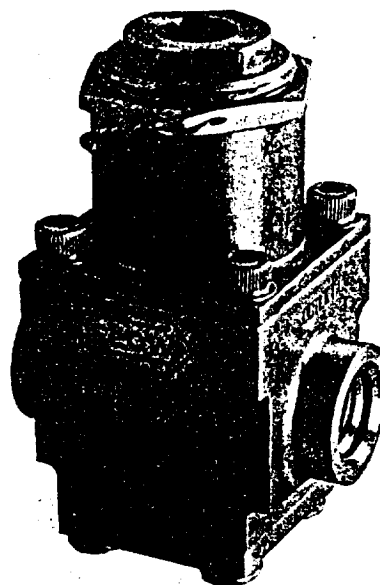
APPLICATION: Space Project, Cold Gas
Pressurization System

WEIGHT: 7 Ounces

OPERATING PRESSURE: 6,000 PSIA Inlet,
1,015±20 PSIA Outlet

FLUID MEDIA: Gaseous Nitrogen

SIZE: 1.4" Sq. X 2.8"



This Pressure Regulator performs accurately when operated "Slam Start" with a Pyro Start Valve.

Futurecraft Corporation designs and manufactures space project fluid devices for the full range of pressures and fluid service. Valves include Solenoid Valves, Thrusters, Isolation Valves, Ball Valves, Fill and Vent Valves, and Squib operated Start Valves. Please let me know if you would like more information on these products.

Watch for our next new product announcement.

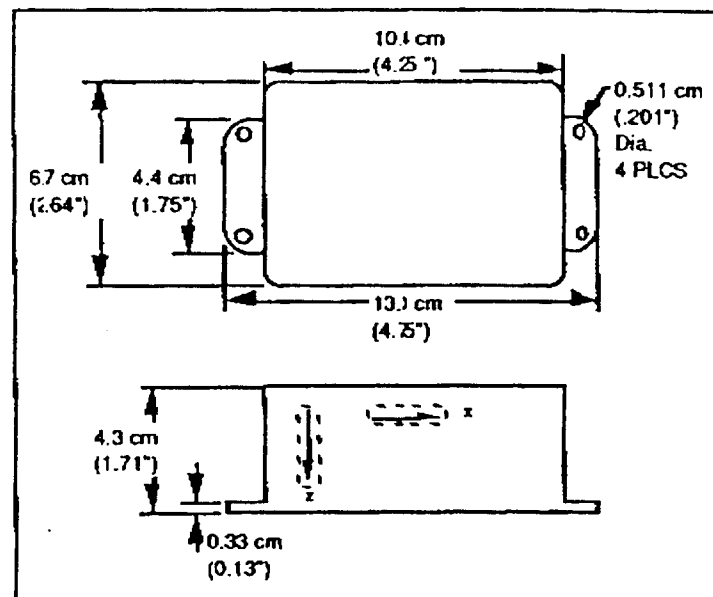
Sincerely yours,

FUTURECRAFT CORPORATION

Alex Pullos

MAGNETOMETER

Number of Axes	Two, orthogonal
Orthogonality	$\pm 0^\circ$, axis to axis and axes to reference surface
Zero Field Output	Selectable
Sensitivity	Selectable
Linear Measurement Range	Selectable
Noise Level	$9 \text{ nT}/\sqrt{\text{Hz}}$
Linearity	$\pm 1\%$ FS
Power Consumption	30 milliwatt (Maximum)
Weight	350 grams (0.77 lb) with case 60 grams (0.13 lb) without case
Dimensions (Less Connector)	43 cm x 13.3 cm x 6.7 cm (1.71" x 4.75" x 2.64") Flange Mounted

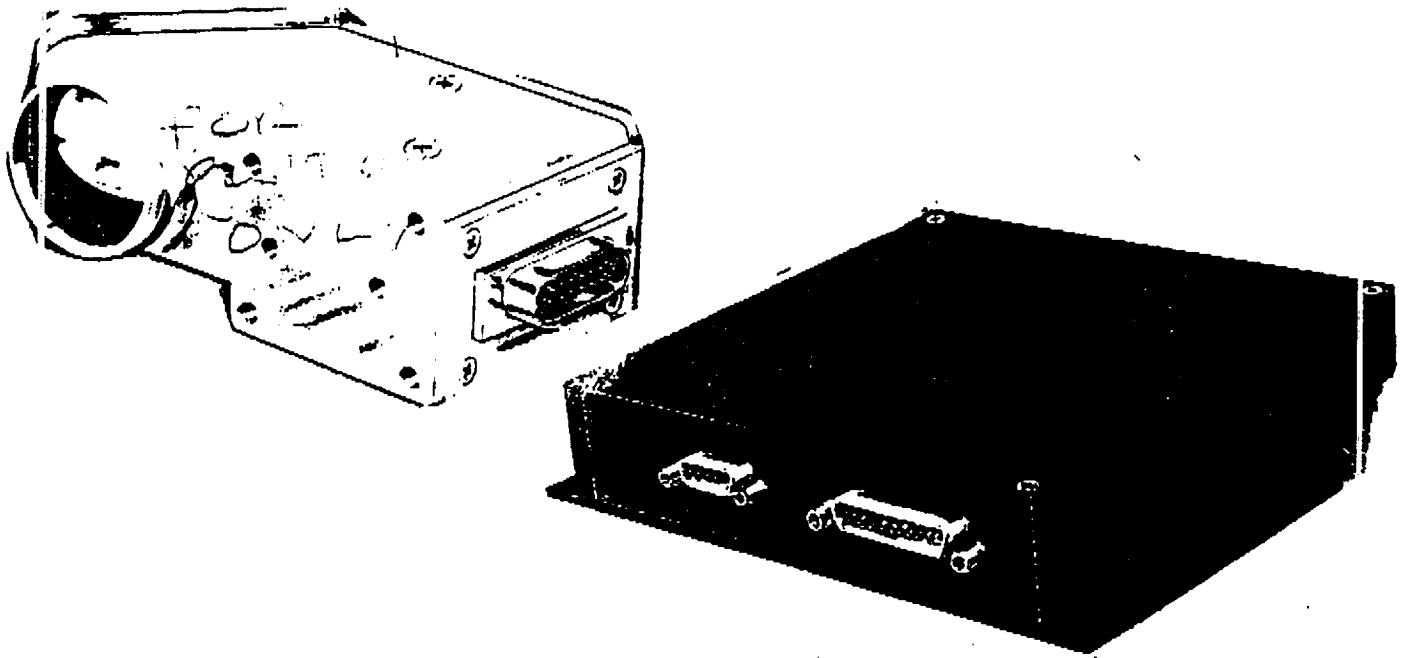


ITHACO

ATTITUDE IS EVERYTHING

#93829 - 1/18/90

BULLSEYE HORIZON CROSSING COMPUTER (BHCC)



DESCRIPTION

The BULLSEYE™ Horizon Crossing Computer (BHCC) is an accurate and versatile instrument used for timing measurements and attitude determination on spinning spacecraft. Its unique optical computing detector allows it to be used to accurately reference the spacecraft to the Earth over a wider dynamic range of speeds and geometries than offered by any other known instrument of comparable simplicity and cost.

Each BHCC is comprised of two components. A small sensor head (SH) contains the optics, the detector, and a preamplifier. A separate Electronics Assembly (EA) contains the associated electronics to process the SH output into accurately referenced timing pulses for use by any spacecraft. The SH assembly utilizes only a small portion of the precious external surface of the spacecraft. The separate EA can be mounted inside the spacecraft at a convenient location.

ORIGINAL PAGE IS
OF POOR QUALITY

ITHACO
SPACE SYSTEMS

PRINCIPLE OF OPERATION

Spacecraft rotation scans the BHCC's Field of View through space and across a celestial body such as the earth, sun, or moon. Incident radiant energy emanating from the celestial body is collected through the BH's aperture, focused by a 90° off-axis paraboloidal mirror through an extremely narrow band (14.25 to 15.65 micron) meniscus spectral filter and input to the Bullseye Pyroelectric Optical Computer.

As illustrated below in Figure 1, the Bullseye Optical Computer possesses two coaxial Fields of View comprised of an inner circular area circumscribed by an outer annular ring. As the coaxial fields are scanned across a celestial body, two distinct wave-

forms are generated as illustrated in Figure 2. The convolution of the outer ring with the celestial body produces an "hourglass" waveform while the inner circular area yields a nearly linear "S" curve. Simple subtraction yields a waveform closely matching the waveform that would result from double differentiation (electronically) of the signal from a more conventional detector. By accomplishing the differentiation optically rather than electronically, the BHCC circumvents noise and bandwidth problems faced by electronic differentiation. As a result, the BHCC is able to accommodate an unusually wide dynamic range of geometries and spin speeds without degrading accuracy and noise performance.

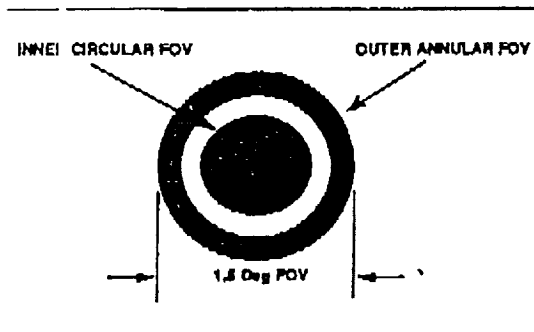


FIGURE 1

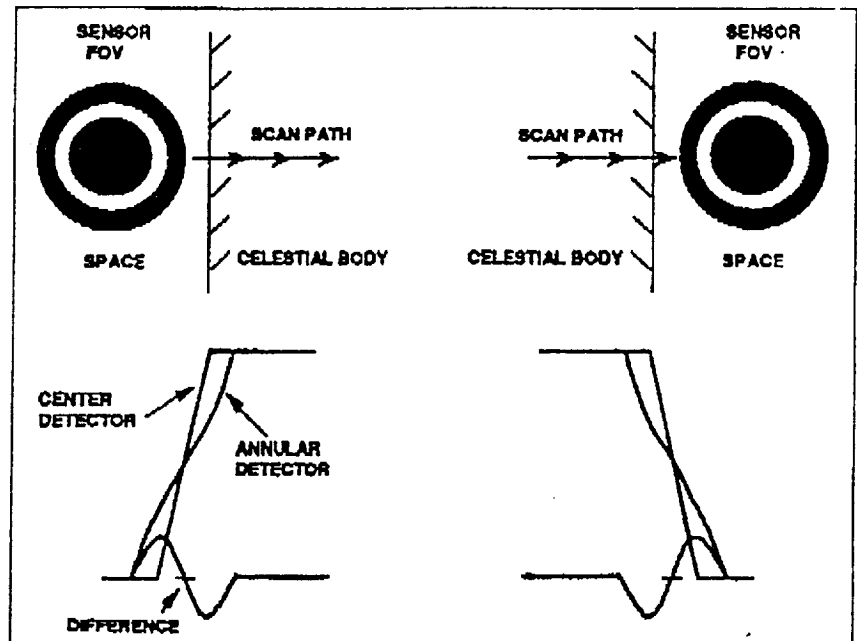


FIGURE 2 WAVEFORMS

SPECIFICATION SUMMARY

Power Consumption		0.75 Watts
Mass	Optical Head	300 g
	Electronics Assembly	500 g
Dimensions	Optical Head	38mm (h) x 127mm (w) x 58mm (d)
	Electronics Assembly	29mm (h) x 153mm (w) x 153mm (d)
Radiation Hardness		10 ⁵ Rads (si)
Random Vibration		21 g's rms
Operational Temperature		-20°C to +70°C
Parts Program		To "S" Level Components
Design Life		15 Years (Minimum)

APPLICATION

The BHCC can be used for precision timing purposes on any spinning spacecraft operating in Low Earth Orbit (LEO) to beyond Geostationary Earth Orbit (GEO). In use, the SH is mounted on the surface of the spacecraft so that the FOV has a clear view of the celestial sphere. The FOV is usually aimed at an angle between 45 and 90 degrees from the anticipated spin axis of the spacecraft, depending upon the application and the intended orbit. The EA is mounted at a convenient location inside the spacecraft. Because the EA is separate, small sized, and can be located several feet from the SH, its location can be chosen to advantage by the spacecraft designer.

The simplest application of the BHCC is a timing application. The BHCC is used to activate and deactivate an experiment when it views a hot object. For example, if an experiment is designed to take data when viewing the Earth, it is desirable to deactivate when viewing deep space to save power or to avoid damage from viewing the Sun or Moon. The BHCC FOV can be aligned with that of the instrument or mounted so that it leads the instrument by a predetermined angle. The BHCC outputs can then be used to safely gate the experiment.

Another typical application of the BHCC is spin phase and period measurement. In this application, the BHCC is mounted at an angle (90 degrees or less)

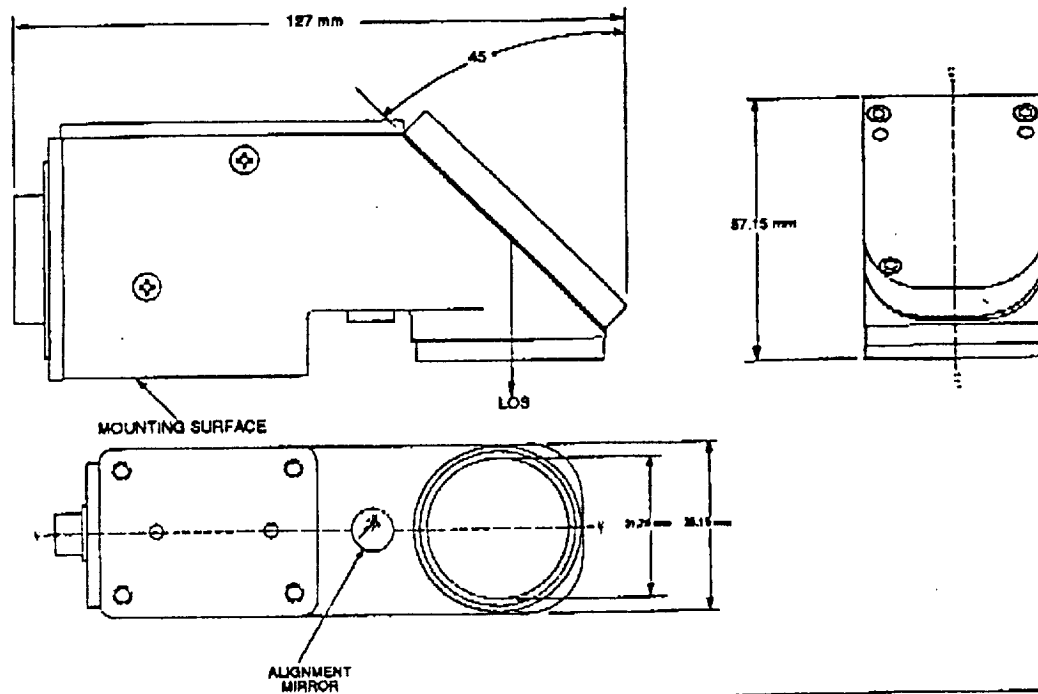
relative to the spin axis of the spacecraft. As the spacecraft rotates, the BHCC FOV sweeps across the Earth. When the FOV sweeps onto the Earth, the EA quickly processes the optical signals into a pulse which is delayed by a carefully calibrated time delay. The same delay applies to the signal generated by the Earth/space crossing. The mean time between the two crossings represents the instant when the FOV was viewing closest to nadir. The mean time is nearly independent of spacecraft attitude and altitude. The time interval between these "Bottom Dead Center" instants is a superb measurement of the spacecraft spin period. The spacecraft rotation phase angle can be accurately determined from the period and the time of the last Bottom Dead Center.

The BHCC is often used to determine the orientation of the spin axis. If the SH is mounted so that the FOV is aimed at an angle less than 90 degrees relative to the spin axis, the duration that the FOV sees the Earth will depend upon the spin axis orientation relative to the Earth and the spacecraft altitude. If the altitude is known, the spin axis orientation may be determined. Alternatively, a second BHCC mounted at another angle can be used. Since the altitude is common to both sensors, its effect can be removed.

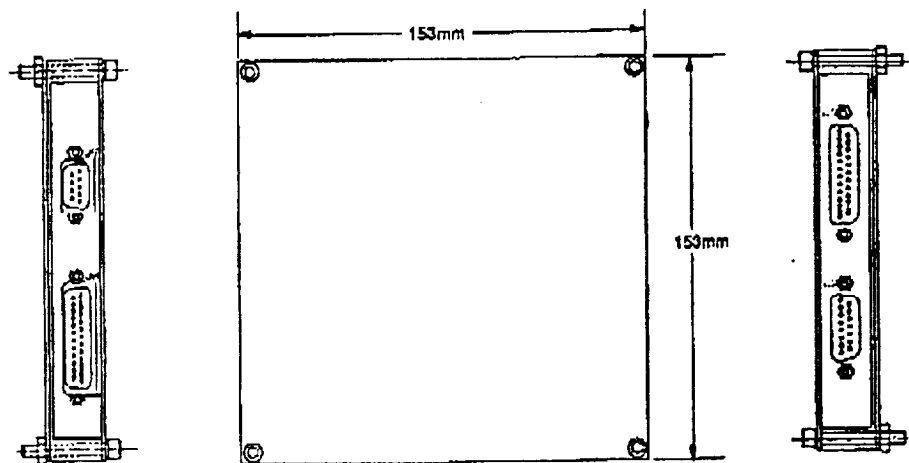
ON ORBIT PERFORMANCE (TYPICAL)

Instrument Errors	
Noise Equivalent Angle	0.005°
Alignment	0.016°
Component Variations	0.005°
Spin Rate Variation	0.005°
Total	0.018°
Radiation Error	
USAF 1976 Standard January/July Profiles	0.020° (typical) 0.050° (worst case)
On-Orbit Accuracy	
	0.027° (typical) 0.053° (worst case)

SENSOR OUTLINE



ELECTRONICS OUTLINE



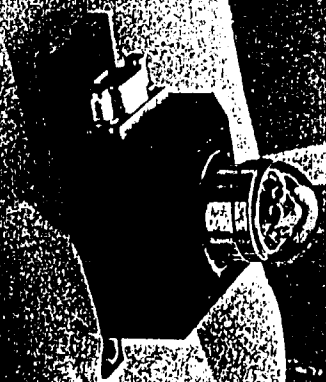
ITHACO

ATTITUDE IS EVERYTHING

735 West Clinton Street, Box 6437, Ithaca NY 14851-6437 USA
Tel: (607) 272-7640 (800) 847-2080 FAX: (607) 272-0804 TWX: 510-255-9307

SUN SENSORS

FACT SHEET



Active outputs of several detectors, Sun sensors are used for attitude control, safemode operation, and solar array pointing.

Lockheed Missiles & Space Company, Inc. (LMSC) has been producing sun sensors for spacecraft for over 20 years. Sun sensors are used to determine the relative angle between the spacecraft and the sun. This is accomplished by "sensing" the radance from the sun and determining the vector from the rel-

since supported SEASAT, Space Telescope, and many other Lockheed space programs. Over 100 sensors of this type have been delivered or are in production.

After designing and flying several special purpose sun sensors, a family of Wide Angle Sun Sensors (WASS) was developed. The development of WASS started in 1974 and WASS has

As well as WASS, LMSC has developed an Intermediate Sun Sensor (ISS) to be used for pointing experiments. The ISS has been used successfully in over 40 flights.

 *Lockheed Missiles & Space Company*

Wide Angle Sun Sensors (WASS)

The basic components of WASS are small (0.070 inch) silicon photo detectors mounted on a pyramid, as illustrated in Figure 1. For most applications, the output is a combination of the short circuit current of the detectors that depends on specific sensor functions. The pyramid is enclosed in a fused silica dome and the detectors are wired to a standard integrated circuit header for mounting on a printed circuit board. The pyramid is sized so that up to 3 detectors per face may be mounted. This allows for full redundancy within each package.

Each detector output is a cosine function peaked at 600 microamps when the sun is normal to its face. This function is shifted 45 degrees to the sun sensor pointing axis, as shown in Figure 2. When the difference between opposing detectors is used, as shown in Figure 3, a control signal is created which is nearly linear to ± 45 degrees and provides polarity past ± 90 degrees. When used in a two-axis configuration, there is some cross-coupling from the geometry involved. If the outputs of the detectors are summed, as in Figure 4, then a monitor or sun presence signal with a 2π steradian field of view (FOV) (hemisphere) is obtained. For monitor sen-

sors with a narrower FOV, a single detector is mounted behind a circular aperture to create a conical FOV.

WASS come in several configurations. The basic housing, with a pyramid-dome assembly, is illustrated in Figure 5. The detectors may be wired as a single-axis or two-axis control sensor or as a hemispherical sensor.

The model shown in Figure 6 is used for safemode operation and has a two-axis control sensor and three conical FOV monitor sensors. The FOV monitor sensors are used to determine loss of solar illumination in a "2 out of 3" configuration. A control sensor may be mounted alone in a minimum size package (as shown on the cover for SEASAT). This sensor is also produced with amplifying electronics.

Accuracy of the WASS depends on the type of application. A typical control sensor can be set to a null accuracy of 0.5° to 1.5° . Depending on orbital altitude, there could be bias to this value from Earth albedo. Aging and thermal effects may cause a scale factor error for both the control and monitor sensors. However, most of these effects on the control sensor can be eliminated in the using software. The remainder of the effects must be accounted for in setting thresholds. The sensors can also be affected by reflections from vehicle structure. This effect can be minimized by applying a guard ring around the base of the dome. The WASS are designed to be very reliable and have been qualified for most current launch vehicle environments. They have been qualified for a thermal operating range of -100°C to 85°C . A new WASS design has been nuclear hardened by a special selection of material and the addition of shorting diodes for protection against SGEMP. Since every WASS has 100 percent internal redundancy and a small number of parts, there are no single point failures and all failure rates are extremely low.

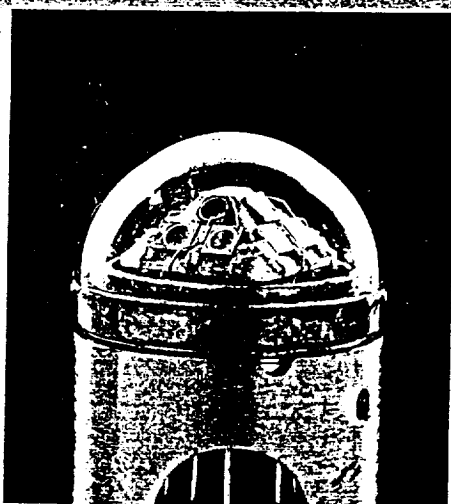


Figure 1. Wide Angle Sun Sensor Detector Assembly

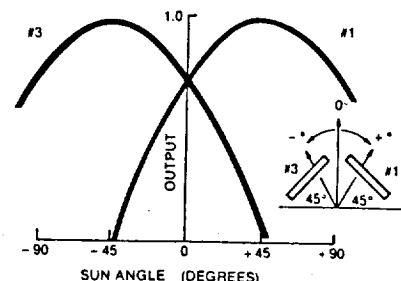


Figure 2. Individual Detector Outputs

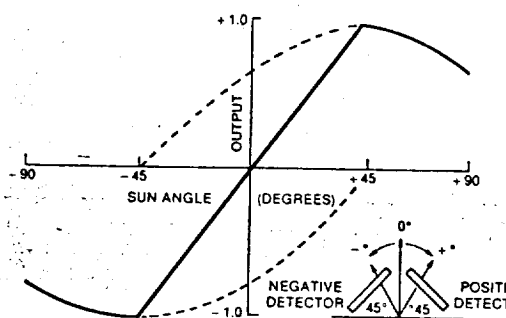


Figure 3. Control Sensor Output

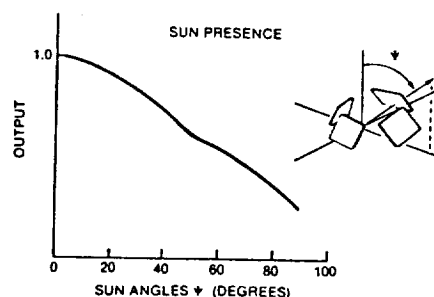


Figure 4. Spherical Sensor Output

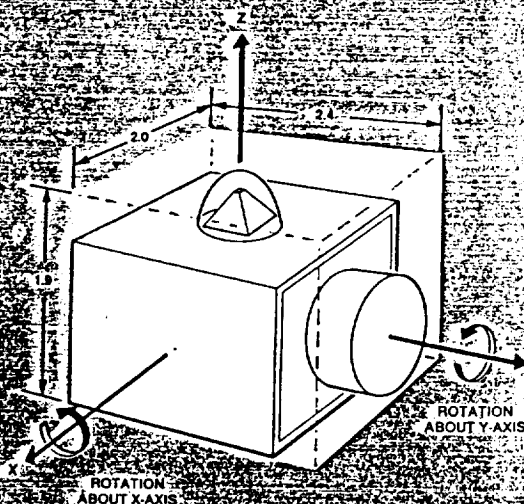


Figure 5. WASS Axes Definitions and Size

Intermediate Sun Sensor (ISS)

The Lockheed ISS, shown in Figure 7, is a 2-axes high accuracy sensor used for solar pointing experiments. The ISS accuracy is determined by aperture masks mounted on each end of a fused silica block.

The entrance aperture is a square and the exit aperture covers five detectors, four of which are arranged around a central detector used for sun presence

This arrangement provides a long term null accuracy of ± 6 arc sec, a linear range of ± 180 arc min, and a polarity range of ± 20 degrees. The sun presence range is ± 11 degrees. The ISS sensor has built-in electronics which provide outputs of 3.6 volts/degree. The ISS was designed for use on the NASA sounding rocket programs and has been used successfully on over 40 flights.

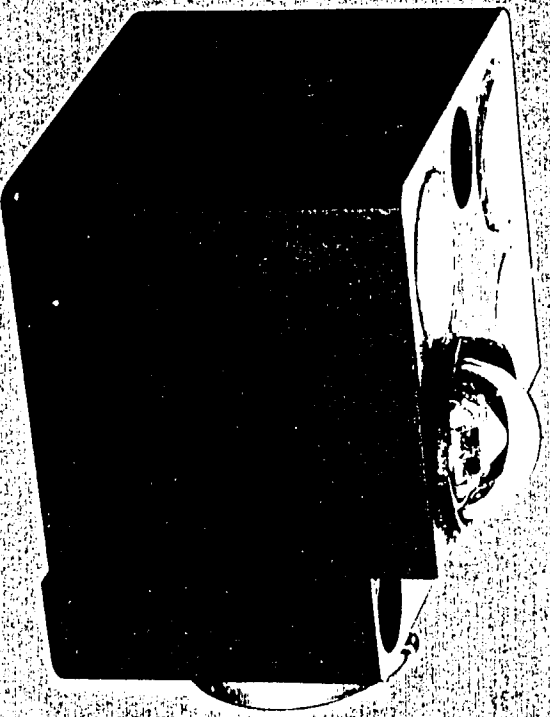


Figure 7. Intermediate Sun Sensor

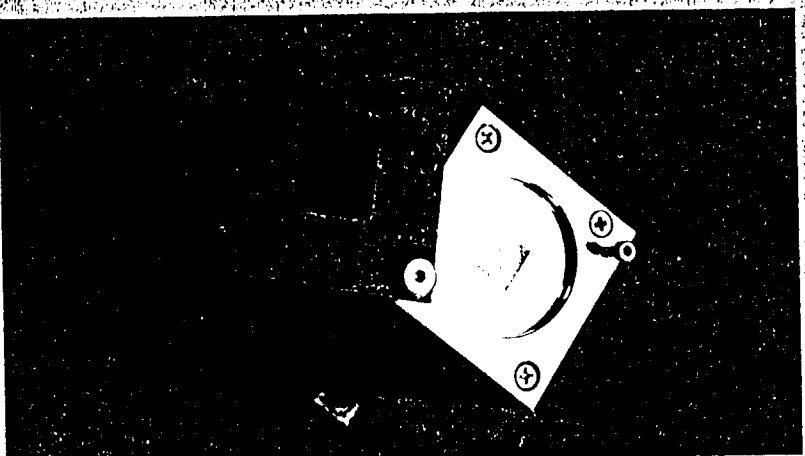


Figure 8. Test Facility



Figure 9. Assembly in Microelectronics Facility

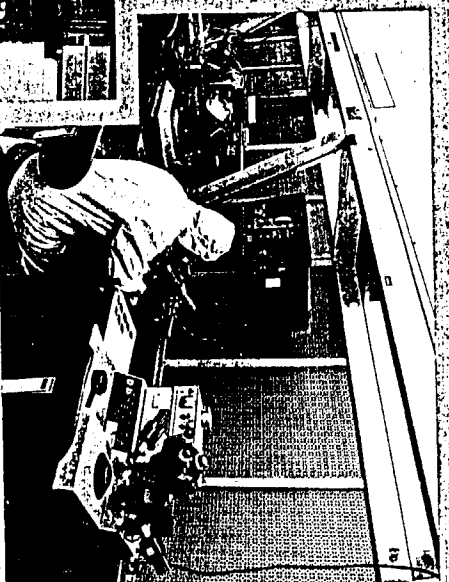


Figure 6. Control and Monitor Sun Sensor

Test Facilities

LMSC has excellent sun sensor test facilities, with flight-proven calibration standards, as shown in Figure 8. Functional tests are performed with an accurately collimated 1/100 sun source. Environmental tests are performed with 100 percent data monitoring capability. All tests are performed at LMSC.

Manufacture of the detector/pyramid assemblies is performed, using full industry standard techniques, at LMSC's Microelectronics facilities, as illustrated in Figure 9. The remaining work on the assembly is performed at the sensor electronics manufacturing shop.

New Products

EMSC is currently working on development of a microprocessor-operated linear CCD sun sensor, as shown in Figure 10. It has a very large dynamic range (20,000:1) and has a demonstrated noise-equivalent angle of 2 arc sec over a range of 100 degrees. The absolute accuracy, depending on precision and tangent function calibrations, is 0.01 degrees. A development model of this sensor has been flown on an Altobee rocket experimental flight. This CCD sun sensor will be developed for both spin-stabilized and 3-axes stabilized operations.

EMSC Sun Sensors

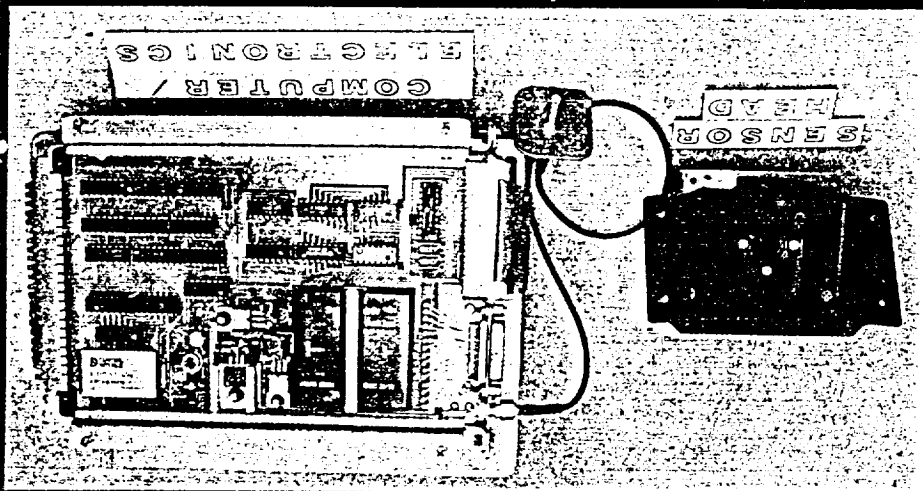


Figure 10: Development Model CCD Sun Sensor

WASS	WASS	SEASAT	ISS	Digital SS (Proposed)
------	------	--------	-----	-----------------------

Size (in.)	Weight	Power	Output (max)	Accuracy (at null)	Range
2.4x2.0x1.9	155g	None	620 μ A	1/2°	2 π Sr.
2.6x2.3x2.0	132g	70mW	5V	1/2°	2 π Sr.
2.1x1.0x1.4	37g	None	620 μ A	1/2°	2 π Sr.
1.4x1.4x3.0	225g	90mW	1mV/arc sec	6 arc sec	\pm 20°
2x4x6	1000g	1W	digital	0.01°	100°

For further information please contact:
 G.F. Turner, Manager, Aerospace Products (408) 756-5216
 L.E. Florant, Manager, Electro-Optical Products (408) 742-7610
 E.L. Becker, Business Development (408) 742-3483
 G.J. Welik, Solar Array Products (408) 742-3187

Lockheed Missiles & Space Company

P.O. Box 508 Sunnyvale, California 94088

APPENDIX E

DATA PROCESSING SYSTEM

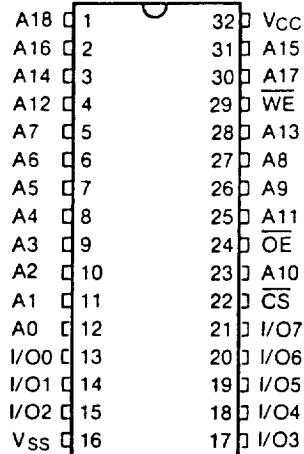


FIGURE 1—Pin Configuration

A0 - A16	Address Inputs
I/O0 - I/O7	Data Input/Output
CS	Chip Select
OE	Output Enable
WE	Write Enable
V _{CC}	+5.0V Power
V _{SS}	Ground

Pin Description

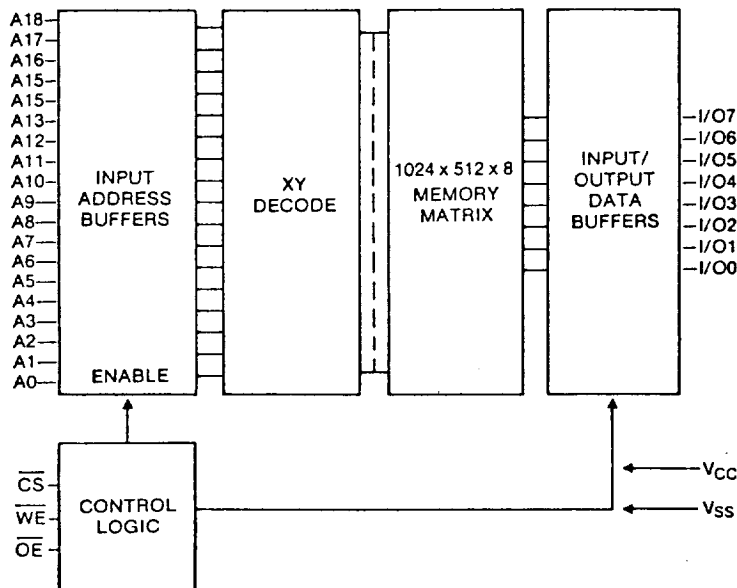


FIGURE 2—Block Diagram

PRELIMINARY WS-512K8-120

512K x 8 BIT
CMOS SRAM

FEATURES

- 5 Volt Operation
- All CMOS Fully Static Design
- Hermetic Ceramic Package
- Operating Current: 13 mA/MHz @ 25°C
- Standby Current: 3.6 mA @ 25°C
- Access Time: 120 nS
- Battery Back-Up Operation
- Temperature Ranges:
 - Military; -55°C to +125°C
 - Industrial; -40°C to +85°C

DESCRIPTION

The White Technology model WS-512K8-120 is a CMOS SRAM housed in a hermetically sealed ceramic 32 pin package. Featuring JEDEC standard pinouts the device provides 512K bytes of read/write low power memory. The device is well suited for battery backed operation and will retain data at voltages as low as 2.0 volts.

Designed for use in demanding applications, the memory packaging and construction is well suited for military and severe industrial applications. Screening and burn in to military standards are available options.

The advanced 512K x 8 SRAM is constructed using co-fired ceramic packaging and high density CMOS memory. The module also features internal power supply bypass capacitors to enhance performance.

Inputs and outputs are TTL compatible. The logic levels and drive capabilities permit the memory to interface with most digital logic systems. Since the device is all CMOS, low power operation for standby applications such as battery backed systems is straightforward. The normal operating range for V_{CC} includes standard TTL levels.

The memory features low power consumption. Typical values for operating current are 52 mA
(continued)

ABSOLUTE MAXIMUM RATINGS

Operating Temperature	-55°C to +125°C
WS-512K-120 CM	-40°C to +85°C
WS-512K-120 CI	
Storage Temperature Range	-65°C to +150°C
Supply Voltage	-0.5V to 7.0V
Signal Voltages Any Pin	-0.5V to 7.0V
Power Dissipation	1.0 Watt
Continuous Current Per Output	20 mA

DESCRIPTION (continued)

at 25°C while cycling at 5 MHz. In standby, the memory has a typical supply current of 3.6 mA at 25°C. In typical systems where multiple modules are operating using chip select to activate each device, the overall current requirement is only slightly above that for one unit. Those units not selected require only standby current.

Since the device is a fully static memory refreshing is not needed. The memory read and write cycles are compatible with virtually all microprocessors. The maximum read access time from address change or chip enable is 120 nS. The write cycle also features typical times of 120 nS. The data may be written over a wide range of times and is not critical.

The rugged ceramic package features a welded metal cover and co-fired construction to assure maximum integrity and hermetic seal. The package is designed and rated to meet military specifications.

The memory has nineteen address lines A0 through A18. These lines combine to select a specific byte from the memory array of 512K (524,288 bytes). The data input and output share a common read/write data bus I/O0 through I/O7. Additional control lines with inverse sense logic are \overline{CS} (Chip Select), \overline{WE} (Write Enable), and \overline{OE} (Output Enable).

When asserted low, the chip enable line selects the memory and permits response to the write enable and output enable lines. When the chip enable line is high the memory is deactivated and current drain is sharply reduced. The write enable line permits data storage to the memory when asserted low. To permit the memory to place the data on the I/O bus the output enable line is asserted low. When this line is high the output of the memory is set to high impedance and no data is presented to the I/O bus.

The timing diagrams of Figures 4 and 5 illustrate the preferred timing sequence and timing specifications for the memory. The output enable line is high during write cycles while the write enable line is high during read cycles.

The memory is designed to operate over the normal TTL voltage range and interface with TTL logic levels and CMOS. The memory will also retain data at lower levels of V_{CC} . Figure 6 shows a typical battery backup schematic. The battery size determines the data retention duration. The memory has low power drain at both room and elevated temperatures.

Figure 7 illustrates a technique to realize a eight megabyte battery backed up SRAM system. Sixteen of the WS-512K8-120 memory modules are used to expand the total storage to 8,388,608 bytes. Additional banks of memories could be employed to expand the memory space further. For the sixteen memories and the decoder, a total board space of only 19.34 square inches (5.53 x 3.5 inches) is needed.

RECOMMENDED OPERATING CONDITIONS

$$V_{DD} = 5.0V \pm 10\%, V_{SS} = 0V, T_A = 25^\circ C$$

Parameter	Sym.	Min.	Max.	Unit
Supply Voltage	V_{CC}	4.5	5.5	V
Input High Voltage	V_{IH}	2.2	$V_{CC} + .3$	V
Input Low Voltage	V_{IL}	-0.3	0.8	V
Operating Temp. (Mil.)	T_A	-55	+125	°C
Operating Temp. (Ind.)	T_A	-40	+85	°C

TRUTH TABLE

\overline{CS}	\overline{OE}	\overline{WE}	A0-A18	Mode	Data I/O	Device Current
H	X	X	X	Standby	High Z	Standby
L	L	H	Stable	Read	Data Out	Active
L	H	L	Stable	Write	Data In	Active
L	H	H	Stable	Out Disable	High Z	Active

DATA RETENTION CHARACTERISTICS

Parameter	Sym.	Min.	Max.	Unit
Data Retention Supply Voltage	V_{DDR}	2.0	5.5	V
Data Retention Current $V_{DD} = 3V, CS \geq V_{DDR} - .2V$	I_{DD2}		400	μA

NOTES

1. All voltages referenced to V_{SS} (Gnd).
2. All I/O transitions are measured ± 200 mV from steady state with loading as specified in "Load Test Circuits."
3. Typical limits are at $V_{CC} = 5.0V, T_A = 25^\circ C$, with specified loading.

DC AND OPERATING CHARACTERISTICS

Parameter	Symbol	Conditions	Min.	Typ.	Max.	Unit
Input Leakage Current	I_{LI}	$V_{CC} = \text{Max.}, V_{IN} = \text{Gnd. or } V_{CC}$			15	μA
Output Leakage Current	I_{LO}	$\overline{CS} = V_{IH}, \overline{OE} = V_{IH}, V_{OUT} = \text{Gnd. to } V_{CC}$			15	μA
Static Supply Current	I_{CC1}	$\overline{CS} = V_{IH}, \overline{OE} = V_{IH}, \text{Duty Cycle} = 0$			25	mA
Dynamic Supply Current	I_{CC2}	$\overline{CS} = V_{IL}, \overline{OE} = V_{IH}, \text{Duty Cycle} = \text{Max.}$			160	mA
Standby Current	I_{SB1}	$\overline{CS} = V_{DD}, \overline{OE} = V_{IH}, \text{Duty Cycle} = \text{Max.}$			2.0	mA
Standby Current	I_{SB2}	$\overline{CS} = V_{DD}, \overline{OE} = V_{IH}, \text{Duty Cycle} = \text{Max.}, T_A = \text{Max.}$			5.5	mA
Output Low Voltage	V_{OL}	$I_{OL} = 4.0 \text{ mA}$			0.4	V
Output High Voltage	V_{OH}	$I_{OH} = -4.0 \text{ mA}$	2.4			V
Input Capacitance	C_{IN}	$V_{IN} = 0\text{V}, f = 1.0 \text{ MHz}$			40	pF
Output Capacitance	C_{OUT}	$V_{OUT} = 0\text{V}, f = 1.0 \text{ MHz}$			40	pF

AC CHARACTERISTICS

(At Recommended Operating Conditions; see table on previous page.)

 $T_A = -55^\circ\text{C to } +125^\circ\text{C}$

Parameter	Symbol		Min.	Typ.	Max.	Unit
Read Cycle Time	t_{RC}	Figure 4, (1)	120			nS
Address Access Time	t_{ACC}	Figure 4, (2)			120	nS
\overline{CS} Access Time	t_{ACS}	Figure 4, (3)			120	nS
Output Hold From Address Change	t_{OH}	Figure 4, (4)	10			nS
Chip Select To Output In Low Z	t_{CLZ}	Figure 4, (5)	10			nS
Chip Select To Output In High Z	t_{CHZ}	Figure 4, (6)			40	nS
Output Enable To Output Valid	t_{OE}	Figure 4, (7)			60	nS
Output Enable To Output In Low Z	t_{OLZ}	Figure 4, (8)	5.0			nS
Output Enable To Output In High Z	t_{OHZ}	Figure 4, (9)			40	nS
Write Cycle Time	t_{WC}	Figure 5, (10)	120			nS
Address Set Up Time	t_{AS}	Figure 5, (11)	0			nS
Write Pulse Width	t_{WP}	Figure 5, (12)	80			nS
Write Recovery Time	t_{WR}	Figure 5, (13)	0			nS
Write Enable To Output In High Z	t_{WHZ}	Figure 5, (14)	0		40	nS
Data Valid To End Of Write	t_{OW}	Figure 5, (15)	50			nS
Data Hold Time	t_{OH}	Figure 5, (16)	0			nS
Output Active From End Of \overline{WE}	t_{OW}	Figure 5, (16)	10			nS
Chip Select Time	t_{CW}	Figure 5, (12)	85			nS
Address Valid To End Of Write	t_{AW}	Figure 5, (17)	85			nS
Input Pulse Levels			0.6		2.4	V
Input Rise And Fall Times					5.0	nS
Input Timing Reference Level				1.5		V
Output Reference Level				1.5		V
Output Load		See Figure 3		10		pF

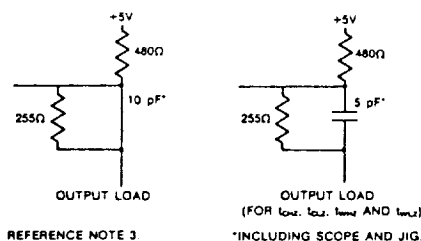


FIGURE 3—Load Test Circuits

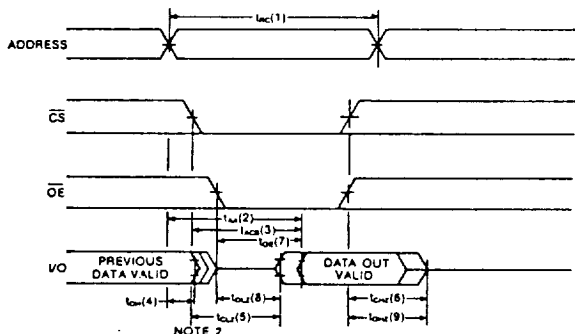


FIGURE 4—Read Cycle Timing Diagram

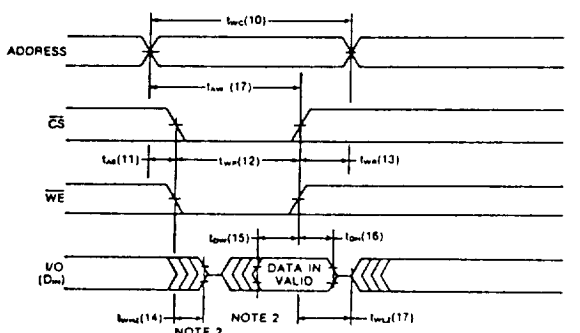


FIGURE 5—Write Cycle Timing Diagram

ORDERING INFORMATION

PACKAGE OPTIONS

C Ceramic DIP

TEMPERATURE RANGE OPTIONS

M Military -55°C to +125°C
I Industrial -40°C to +85°C

WS-512K8-120CM

PROCESSING:
M = Military
I = Industrial
PACKAGE:
C = Ceramic Side Braided
ACCESS/CYCLE TIME
BITS PER WORD
NUMBER OF WORDS
STATIC RAM
White Technology

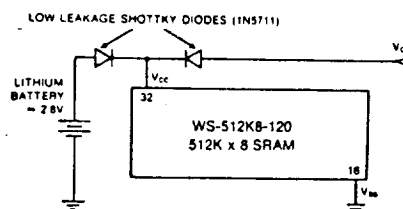


FIGURE 6—Backup Battery Hookup

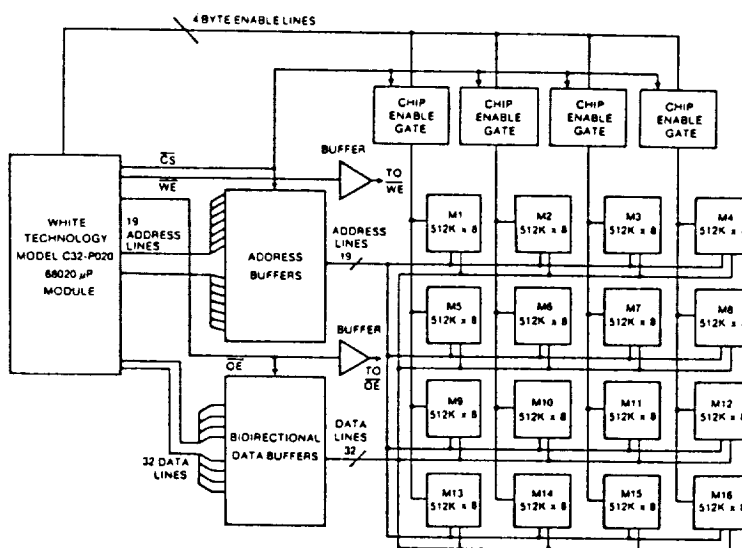
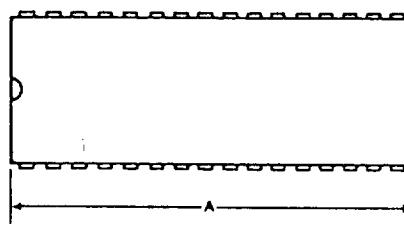
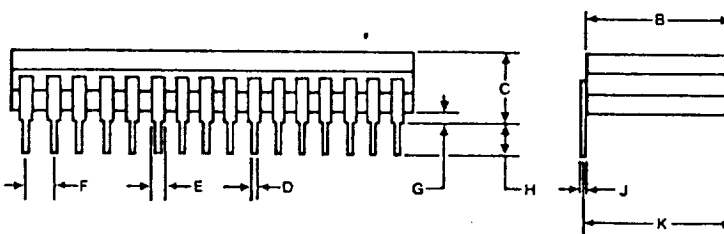


FIGURE 7—Eight Megabyte SRAM System

PACKAGE OUTLINE



DIM.	INCHES		MILLIMETERS	
	MIN	MAX	MIN	MAX
A	1.654	1.686	42.0	42.8
B	0.580	0.600	14.7	15.2
C	0.235	0.275	6.0	7.0
D	0.018	0.020	0.4	0.5
E	0.045	0.055	1.1	1.4
F	0.100 TYP		2.5 TYP	
G	0.040	0.060	1.0	1.5
H	0.125 MIN		3.2 MIN	
J	0.008	0.012	0.2	0.3
K	0.590	0.610	15.0	15.5





AD515

AD515

2

OPERATIONAL AMPLIFIERS

FET-Input Electrometer OPERATIONAL AMPLIFIER

FEATURES

- ULTRA-LOW BIAS CURRENT: 0.075pA max
- LOW POWER: 1.5mA max
- LOW OFFSET: 1mV max
- LOW DRIFT: 15 μ V/ $^{\circ}$ C max
- LOW COST
- REPLACES ANALOG DEVICES AD515

APPLICATIONS

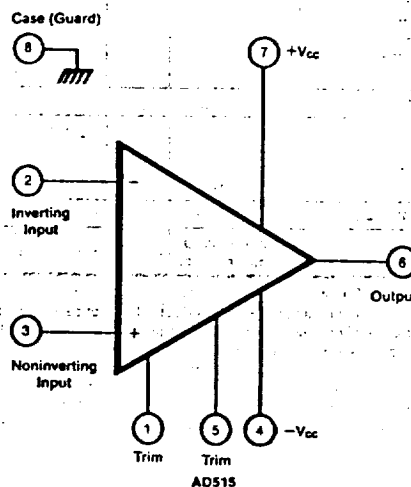
- pH SENSORS
- INTEGRATORS
- TEST EQUIPMENT
- ELECTRO-OPTICS
- CHARGE AMPLIFIERS
- GAS DETECTORS

DESCRIPTION

The Burr-Brown AD515 is a monolithic pin-for-pin replacement for the hybrid Analog Devices AD515 ultra-low bias current operational amplifier.

Laser-trimmed offset voltage and very-low bias current are important features of this popular amplifier. Monolithic construction allows lower cost and higher reliability than hybrid designs.

The AD515 is available in three electrical grades; all are specified over 0 $^{\circ}$ C to +70 $^{\circ}$ C and supplied in a TO-99 hermetic package.



International Airport Industrial Park - P.O. Box 11400 - Tucson, Arizona 85734 - Tel. (602) 746-1111 - Twx: 910-952-1111 - Cable: BURCORP - Telex: 66-649

PDS-654A

SPECIFICATIONS

ELECTRICAL

At $V_{CC} = \pm 15VDC$ and $T_A = +25^\circ C$ unless otherwise noted. Pin 8 connected to ground.

PARAMETER	CONDITIONS	AD515J			AD515K			AD515L			UNITS
		MIN	TYP	MAX	MIN	TYP	MAX	MIN	TYP	MAX	
OPEN-LOOP GAIN, DC											
Open-Loop Voltage Gain ⁽¹⁾	$R_L \geq 2k\Omega$	20k			40k			25k			V/V
	$R_L \geq 10k\Omega$	40k			100k			50k			V/V
	T_{MIN} TO T_{MAX} , $R_L = 2k$	15k			40k			25k			V/V
RATED OUTPUT											
Voltage Output: $R_L = 2k\Omega$	T_{MIN} TO T_{MAX}	± 10	± 12		*	*		*	*		V
$R_L = 10k\Omega$	T_{MIN} TO T_{MAX}	± 12	± 13		*	*		*	*		V
Load Capacitance Stability	Gain = +1		1000		*	*		*	*		pF
Short Circuit Current		10	25	50	*	*	*	*	*	*	mA
FREQUENCY RESPONSE											
Unity Gain, Small Signal Full Power Response	20V p-p, $R_L = 2k$	5	350		*	*		*	*		kHz
Slew Rate	$V_O = \pm 10V$, $R_L = 2k$, Gain = -1		16		*	*		*	*		kHz
Overload Recovery	Gain = -1	0.3	1.0	100	*	*	*	*	*	*	V/ μs
INPUT											
OFFSET VOLTAGE ⁽²⁾	$V_{CM} = 0VDC$		0.4	3.0		*	1.0		*	1.0	mV
Input Offset Voltage	T_{MIN} TO T_{MAX}			50			15			25	$\mu V/^\circ C$
Average Drift	T_{MIN} TO T_{MAX}	68	86	400	80		100	74		200	dB
Supply Rejection			50								$\mu V/V$
BIAS CURRENT ⁽²⁾	$V_{CM} = 0VDC$			300			150			75	IA
Input Bias Current											
Either Input											
IMPEDANCE											
Differential			$10^{12} \parallel 1.6$			*			*		$\Omega \parallel pF$
Common-Mode			$10^{12} \parallel 0.8$			*			*		$\Omega \parallel pF$
VOLTAGE RANGE ⁽³⁾											
Differential Input Range		± 20	± 11		*	*		*	*		V
Common-Mode Input Range		± 10	94		*	*		*	*		V
Common-Mode Rejection	$V_{IN} = \pm 10VDC$	66		80			70				dB
NOISE											
Voltage: 0.1Hz to 10Hz			4.0		*	*		*	*		μV p-p
$f_o = 10Hz$			75		*	*		*	*		nV/ \sqrt{Hz}
$f_o = 100Hz$			55		*	*		*	*		nV/ \sqrt{Hz}
$f_o = 1kHz$			50		*	*		*	*		nV/ \sqrt{Hz}
Current: 0.1Hz to 10Hz			0.003		*	*		*	*		pA p-p
$f_o = 10Hz$ to 10kHz			0.01		*	*		*	*		pA rms
POWER SUPPLY											
Rated Voltage			± 15		*	*		*	*		VDC
Voltage Range,		± 5		± 18	*	*		*	*		VDC
Derated Performance				1.5	*	*		*	*		VDC
Current, Quiescent	$I_o = 0mA$		0.8		*	*		*	*		mA
TEMPERATURE RANGE											
Specification Range	Ambient temp.	0		+70	*	*		*	*		$^\circ C$
Storage	Ambient temp.	-65		+150	*	*		*	*		$^\circ C$

* Specification same as AD515J.

* Specification same as AD515J.

NOTES: (1) With or without nulling of V_{OS} . (2) Offset voltage, offset current, and bias current are measured with the units fully warmed up. (3) It is possible for the input voltage to exceed the supply voltage, a series protection resistor should be added to limit input current to 0.5mA. The input devices can withstand overload currents of 0.3mA indefinitely without damage.

ORDERING

Basic model
Performance
J, K, L
Package
H = TO

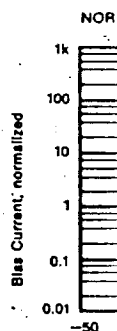
CONNECT

Top View

Offset

TYPICAL

$T_A = +25^\circ C$, $V_O = 0V$

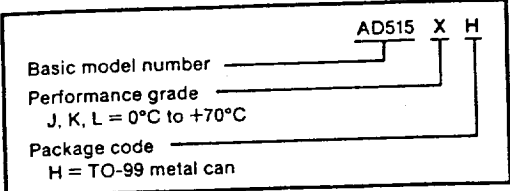


Burr-Brown

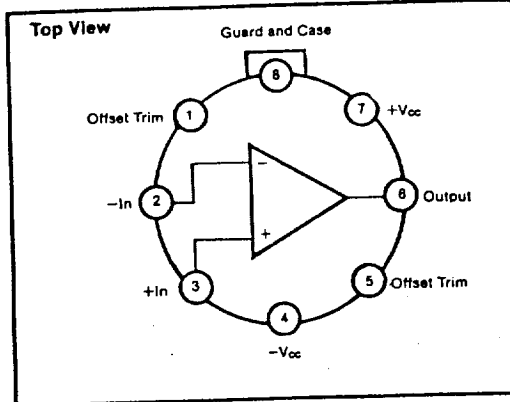
AD515L		
TYP	MAX	UNITS
		V/V
		V/V
		V/V
		V
		V
		pF
		mA
		kHz
		kHz
		V/ μ s
		μ s
	1.0	mV
	25	μ V/ $^{\circ}$ C
	200	dB
		μ V/V
	75	IA
		Ω pF
		Ω pF
		V
		V
		dB
		μ V p-p
		nV/ $\sqrt{\text{Hz}}$
		nV/ $\sqrt{\text{Hz}}$
		pA p-p
		pA rms
		VDC
		VDC
		mA
		$^{\circ}$ C
		$^{\circ}$ C

armed up. (3) If it is possible for it devices can withstand overload

ORDERING INFORMATION

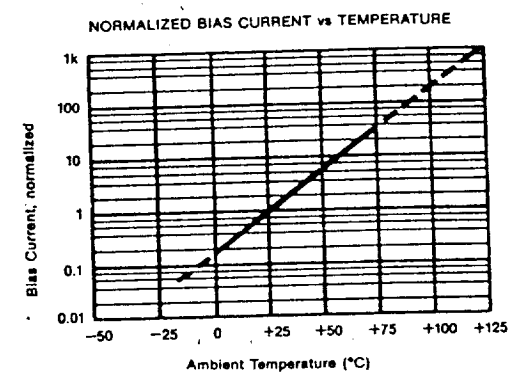


CONNECTION DIAGRAM



TYPICAL PERFORMANCE CURVES

$T_A = +25^{\circ}\text{C}$, $V_{CC} = \pm 15\text{VDC}$ unless otherwise noted.



ABSOLUTE MAXIMUM RATINGS

Supply	$\pm 18\text{VDC}$
Internal Power Dissipation ⁽¹⁾	500mW
Differential Input Voltage ⁽²⁾	$\pm 36\text{VDC}$
Input Voltage Range ⁽³⁾	$\pm 18\text{VDC}$
Storage Temperature Range	-65°C to $+150^{\circ}\text{C}$
Operating Temperature Range	-55°C to $+125^{\circ}\text{C}$
Lead Temperature (soldering, 10 seconds)	$+300^{\circ}\text{C}$
Output Short Circuit Duration ⁽³⁾	Continuous
Junction Temperature	$+175^{\circ}\text{C}$

NOTES: (1) Packages must be derated based on $\theta_{JA} = 150^{\circ}\text{C/W}$ or $\theta_{JA} = 200^{\circ}\text{C/W}$. (2) For supply voltages less than $\pm 18\text{VDC}$ the absolute maximum input voltage is equal to the supply voltage. (3) Short circuit may be to power supply common only. Rating applies to $+25^{\circ}\text{C}$ ambient. Observe dissipation limit and T_J .

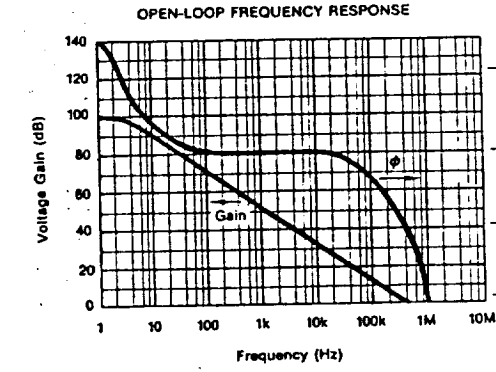
MECHANICAL

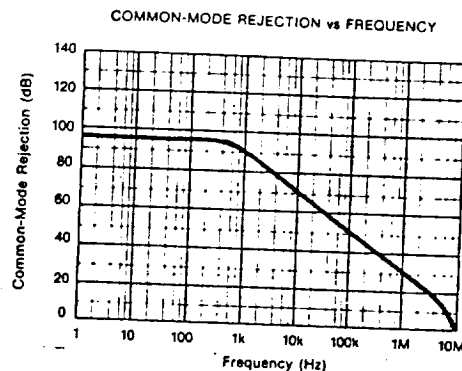
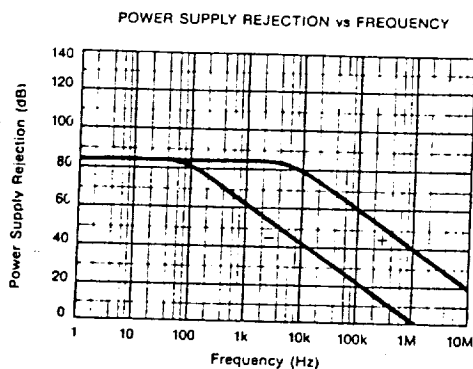
"H" PACKAGE

NOTE: Leads in true position within .010" (.25mm) R at MMC at seating plane. Pin numbers shown for reference only. Numbers may not be marked on package. Pin material and plating composition conform to Method 2003 (solderability) of MIL-STD-883 (except paragraph 3.2).

TO-99 (Hermetic)

DIM	INCHES		MILLIMETERS	
	MIN	MAX	MIN	MAX
A	.325	.370	8.51	9.40
B	.308	.325	7.75	8.51
C	.165	.185	4.19	4.70
D	.016	.021	0.41	0.52
E	.010	.040	0.25	1.02
F	.010	.040	0.25	1.02
G	.508 BASIC			
H	.026	.034	0.71	0.86
J	.029	.048	0.74	1.14
K	.900	-	22.7	-
L	.110	.160	2.78	4.06
M	.45° BASIC			
N	.096	.109	2.41	2.67





APPLICATIONS INFORMATION

OFFSET VOLTAGE ADJUSTMENT

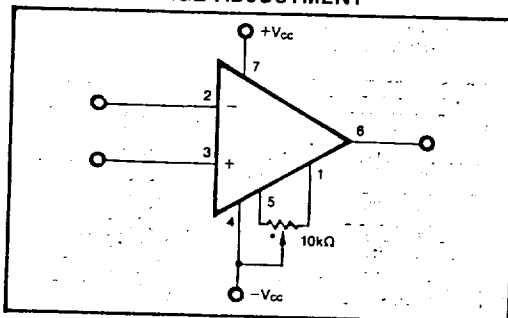


FIGURE 1. Offset Voltage Trim.

INPUT PROTECTION

The AD515 requires input protection only if the source is not current limited. Limiting input current to 0.5mA with a series resistor is recommended when input voltage exceeds supply voltage.

Static damage can cause subtle changes in amplifier input characteristics without necessarily destroying the device. In precision operational amplifiers (both bipolar and FET types), this may cause a noticeable degradation of offset voltage and drift.

Static protection is recommended when handling any precision IC operational amplifier.

GUARDING AND SHIELDING

As in any situation where high impedances are involved, careful shielding is required to reduce "hum" pickup in input leads. If large feedback resistors are used, they should also be shielded along with the external input circuitry.

Leakage currents across printed circuit boards can easily exceed the bias current of the AD515. To avoid leakage problems, it is recommended that the signal input lead of the AD515 be wired to a Teflon standoff. If the lead is to be soldered directly into a printed circuit board, utmost care must be used in planning the board layout.

A "guard" pattern should completely surround the high impedance input leads and should be connected to a low impedance point which is at the signal input potential. The amplifier case should be connected to any input shield or guard via pin 8. This insures that the amplifier itself is fully surrounded by guard potential, minimizing both leakage and noise pickup (see Figure 2).

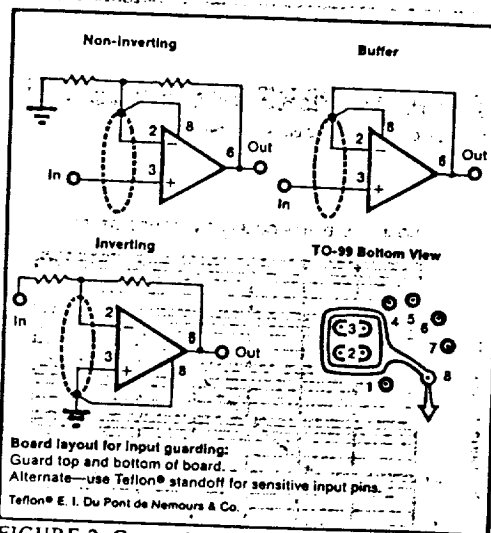


FIGURE 2. Connection of Input Guard.

BURR
BROWN

FEATURES

- -55°C TO +125°C
- 30nA MAX. BIAS CURRENT
- ±8mV, MAX. OFFSET VOLTAGE
- ±5μV/°C TYP. OFFSET DRIFT
- 12MHz BANDWIDTH
- HERMETIC PACKAGING (741-TYPE)

DESCRIPTION

These precision operational amplifiers are designed for applications from dc to extremely high frequencies. They are used in gain blocks, comparators, amplifiers, high-speed integrators, and

You're assured of performance from the -55°C to +125°C. Our screening procedures are in accordance with MIL-883, method 2000. Our solderability tests are in accordance with both destructive and non-destructive

International Air Products



HARRIS

HS-80C86RH

ADVANCE INFORMATION

Radiation Hardened CMOS
16 Bit Microprocessor

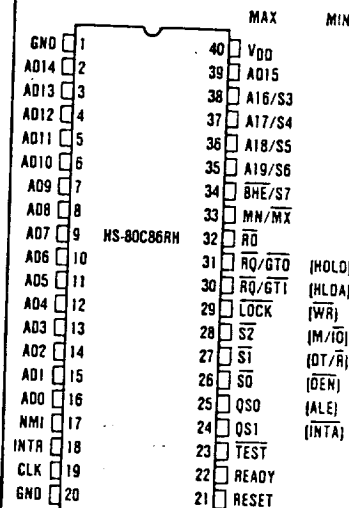
Features

- Pin Compatible with NMOS 8086 and Harris 80C86
- Radiation Hardened (Guaranteed)
 - ▶ Latch Up Free Epi-CMOS
 - ▶ Total Dose > 100K Rad(Si)
 - ▶ Transient Upset > 10⁸ Rad(Si)/sec
 - ▶ Functional after 1 x 10⁶ Rad(Si) Total Dose
- Completely Static Design
 - ▶ DC to 5MHz
- Low Power Operation
 - ▶ ICCSB = 500μA Maximum
 - ▶ ICCOP = 10mA/MHz Typical
- 1 Mbyte of Direct Memory Addressing Capability
- 24 Operand Addressing Modes
- Bit, Byte, Word, and Block Move Operations
- 8 and 16 Bit Signed/Unsigned Arithmetic
 - ▶ Binary or Decimal
 - ▶ Multiply and Divide
- Bus-hold Circuitry Eliminates Pull-up Resistors
- Hardened Field, Self Aligned, Junction Isolated CMOS Process
- Single 5V Power Supply
- Military Temperature Range

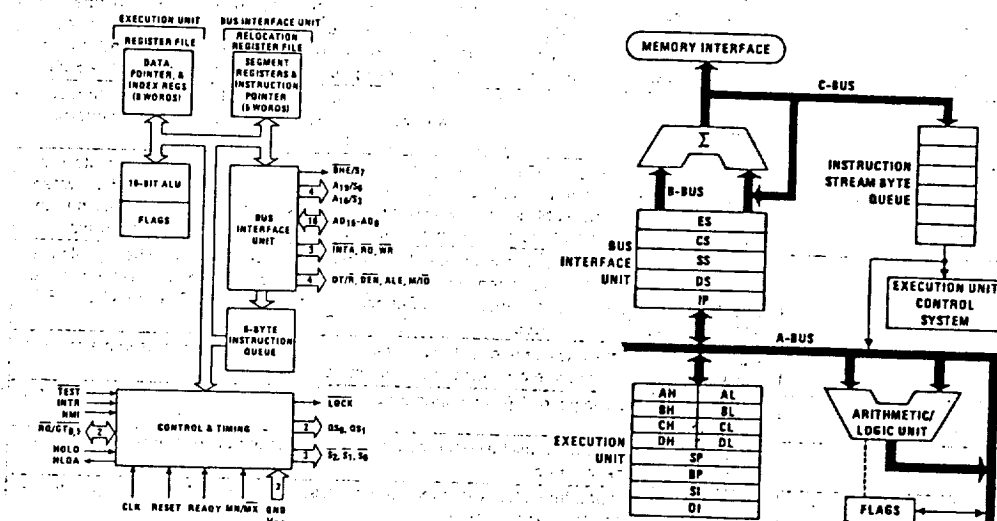
Description

The Harris HS-80C86RH high performance radiation hardened 16 bit CMOS CPU is manufactured using a hardened field, self-aligned silicon gate CMOS process. Two modes of operation, MINimum for small systems and MAXimum for larger applications such as multi-processing, allow user configuration to achieve the highest performance level. Full TTL compatibility and industry standard operation allow use of existing NMOS 8086 hardware and software designs.

Pinout DIP TOP VIEW



Functional Diagram



CAUTION: Electronic devices are sensitive to electrostatic discharge. Proper I.C. handling procedures should be followed.

HS-80C86RH

Pin Description

The following pin function descriptions are for HS-80C86RH systems in either minimum or maximum mode. The "Local Bus" in these descriptions is the direct multi-

plexed bus interface connection to the HS-80C86RH (without regard to additional bus buffers).

SYMBOL	PIN NUMBER	TYPE	DESCRIPTION
AD ₁₅ -AD ₀	2-16, 39	I/O	ADDRESS DATA BUS: These lines constitute the time multiplexed memory/I/O address (T ₁) and data (T ₂ , T ₃ , T _W , T ₄) bus. A ₀ is analogous to BHE for the lower byte of the data bus, pins D ₇ -D ₀ . It is LOW during T ₁ when a byte is to be transferred on the lower portion of the bus in memory or I/O operations. Eight-bit oriented devices tied to the lower half would normally use A ₀ to condition chip select functions (See BHE). These lines are active HIGH and are held at high impedance to the last valid logic level during interrupt acknowledge and local bus "hold acknowledge" or "grant sequence".
A ₁₉ /S ₆ A ₁₈ /S ₅ A ₁₇ /S ₄ A ₁₆ /S ₃	35-38	O	ADDRESS/STATUS: During T ₁ , these are the four most significant address lines for memory operations. During I/O operations these lines are low. During memory and I/O operations, status information is available on these lines during T ₂ , T ₃ , T _W , T ₄ . S ₆ is always zero. The status of the interrupt enable FLAG bit (S ₅) is updated at the beginning of each CLK cycle. S ₄ and S ₃ are encoded as shown in (Table 1). This information indicates which segment register is presently being used for data accessing. These lines are held at high impedance to the last valid logic level during local bus "hold acknowledge" or "grant sequence".
BHE/S ₇	34	O	BUS HIGH ENABLE/STATUS: During T ₁ the bus high enable signal (BHE) should be used to enable data onto the most significant half of the data bus, pins D ₁₅ -D ₈ . Eight bit oriented devices tied to the upper half of the bus would normally use BHE to condition chip select functions. BHE is LOW during T ₁ for read, write, and interrupt acknowledge cycles when a byte is to be transferred on the high portion of the bus. The S ₇ status information is available during T ₂ , T ₃ and T ₄ . The signal is active LOW, and is held at high impedance to the last valid logic level during interrupt acknowledge and local bus "hold acknowledge" or "grant sequence"; it is LOW during T ₁ for the first interrupt acknowledge cycle. (See Table 2).
RD	32	O	READ: Read strobe indicates that the processor is performing a memory or I/O read cycle, depending on the state of the M/ $\overline{\text{IO}}$ or S ₂ pin. This signal is used to read devices which reside on the HS-80C86RH local bus. RD is active LOW during T ₂ , T ₃ and T _W of any read cycle, and is guaranteed to remain HIGH in T ₂ until the 80C86 local bus has floated. This line is held at a high impedance logic one state during "hold acknowledge" or "grant sequence".
READY	22	I	READY: is the acknowledgement from the addressed memory or I/O device that will complete the data transfer. The RDY signal from memory or I/O is synchronized by the HS-82C85RH Clock Generator to form READY. This signal is active HIGH. The HS-80C86RH READY input is not synchronized. Correct operation is not guaranteed if the Setup and Hold Times are not met.
INTR	18	I	INTERRUPT REQUEST: is a level triggered input which is sampled during the last clock cycle of each instruction to determine if the processor should enter into an interrupt acknowledge operation. If so, an interrupt service routine is called via an interrupt vector lookup table located in system memory. INTR is internally synchronized and can be internally masked by software resetting the interrupt enable bit. This signal is active HIGH.
TEST	23	I	TEST: input is examined by the "Wait" instruction. If the TEST input is LOW execution continues, otherwise the processor waits in an "Idle" state. This input is synchronized internally during each clock cycle on the leading edge of CLK.
NMI	17	I	NON-MASKABLE INTERRUPT: is an edge triggered input which causes a type 2 interrupt. An interrupt service routine is called via an interrupt vector lookup table located in system memory. NMI is not maskable internally by software. A transition from LOW to HIGH initiates the interrupt at the end of the current instruction. This input is internally synchronized.
RESET	21	I	RESET: causes the processor to immediately terminate its present activity. The signal must change from LOW to HIGH and remain active HIGH for at least four clock cycles. It restarts execution, as described in the Instruction Set description, when RESET returns LOW. RESET is internally synchronized.
CLK	19	I	CLOCK: provides the basic timing for the processor and bus controller. It is asymmetric with a 33% duty cycle to provide optimized internal timing.
VDD	40		VDD: +5V power supply pin. A 0.1 μ F capacitor between pins 20 and 40 is recommended for decoupling.
GND	1, 20		GND: Ground. Note: both must be connected. A 0.1 μ F capacitor between pins 1 and 20 is recommended for decoupling.
MN/MX	33	I	MINIMUM/MAXIMUM: Indicates what mode the processor is to operate in. The two modes are discussed in the following sections.

Pin Description

The following pin function descriptions are for HS-80C86RH systems in either minimum or maximum mode.

SYMBOL	PIN NUMBER
S ₀ , S ₁ , S ₂	26, 27, 28
RO/GT ₀ RO/GT ₁	31, 32
LOCK	29
QS ₁ , QS ₀	24, 25

TABLE 1

S ₄	S ₃	CHARACTERISTICS
0	0	Alternate
0	1	Stack
1	0	Code
1	1	Data

HS-80C86RH

Pin Description

The following pin function descriptions are for the HS-80C86RH system in maximum mode (i.e., MN/MX = GND).

Only the pin functions which are unique to maximum mode are described below.

SYMBOL	PIN NUMBER	TYPE	DESCRIPTION															
$\overline{S_0}, \overline{S_1}, \overline{S_2}$	26-28	O	STATUS: is active during T ₄ , T ₁ and T ₂ and is returned to the passive state (1, 1, 1) during T ₃ or during T _W when READY is HIGH. This status is used by the 82C88 Bus Controller to generate all memory and I/O access control signals. Any change by $\overline{S_2}, \overline{S_1}$ or $\overline{S_0}$ during T ₄ is used to indicate the beginning of a bus cycle, and the return to the passive state in T ₃ or T _W is used to indicate the end of a bus cycle. These status lines are encoded as shown in Table 3. These signals are held at a high impedance logic one state during "grant sequence".															
$\overline{RQ}/\overline{GT_0}$ $\overline{RQ}/\overline{GT_1}$	31, 30	I/O	REQUEST/GRANT: pins are used by other local bus masters to force the processor to release the local bus at the end of the processor's current bus cycle. Each pin is bi-directional with $\overline{RQ}/\overline{GT_0}$ having higher priority than $\overline{RQ}/\overline{GT_1}$. $\overline{RQ}/\overline{GT}$ has an internal pull-up bus hold device so it may be left unconnected. The request/grant sequence is as follows (see $\overline{RQ}/\overline{GT}$ Sequence Timing) <ol style="list-style-type: none">1. A pulse of 1 CLK wide from another local bus master indicates a local bus request ("hold") to the HS-80C86RH (pulse 1).2. During a T₄ or T₁ clock cycle, a pulse 1 CLK wide from the HS-80C86RH to the requesting master (pulse 2) indicates that the HS-80C86RH has allowed the local bus to float and that it will enter the "grant sequence" state at the next CLK. The CPU's bus interface unit is disconnected logically from the local bus during "grant sequence".3. A pulse 1 CLK wide from the requesting master indicates to the HS-80C86RH (pulse 3) that the "hold" request is about to end and that the HS-80C86RH can reclaim the local bus at the next CLK. The CPU then enters T₄ (or T₁ if no bus cycles pending). Each Master-Master exchange of the local bus is a sequence of 3 pulses. There must be one idle CLK cycle after each bus exchange. Pulses are active low. If the request is made while the CPU is performing a memory cycle, it will release the local bus during T ₄ of the cycle when all the following conditions are met: <ol style="list-style-type: none">1. Request occurs on or before T₂.2. Current cycle is not the low byte of a word (on an odd address).3. Current cycle is not the first acknowledge of an interrupt acknowledge sequence.4. A locked instruction is not currently executing. If the local bus is idle when the request is made the two possible events will follow: <ol style="list-style-type: none">1. Local bus will be released during the next cycle.2. A memory cycle will start within three clocks. Now the four rules for a currently active memory cycle apply with condition number 1 already satisfied.															
LOCK	29	O	LOCK: output indicates that other system bus masters are not to gain control of the system bus while LOCK is active LOW. The LOCK signal is activated by the "LOCK" prefix instruction and remains active until the completion of the next instruction. This signal is active LOW, and is held at a HIGH impedance logic one state during "grant sequence". In MAX mode, LOCK is automatically generated during T ₂ of the first INTA cycle and removed during T ₂ of the second INTA cycle.															
QS ₁ , QS ₀	24, 25	O	QUEUE STATUS: The queue status is valid during the CLK cycle after which the queue operation is performed. QS ₁ and QS ₀ provide status to allow external tracking of the internal HS-80C86RH instruction queue. Note that QS ₁ , QS ₀ never become high impedance. <table><tr><td>QS₁</td><td>QS₀</td><td></td></tr><tr><td>0</td><td>0</td><td>No Operation</td></tr><tr><td>0</td><td>1</td><td>First Byte of Op Code from Queue</td></tr><tr><td>1</td><td>0</td><td>Empty the Queue</td></tr><tr><td>1</td><td>1</td><td>Subsequent Byte from Queue</td></tr></table>	QS ₁	QS ₀		0	0	No Operation	0	1	First Byte of Op Code from Queue	1	0	Empty the Queue	1	1	Subsequent Byte from Queue
QS ₁	QS ₀																	
0	0	No Operation																
0	1	First Byte of Op Code from Queue																
1	0	Empty the Queue																
1	1	Subsequent Byte from Queue																

TABLE 1

TABLE 1.

S ₄	S ₃	CHARACTERISTICS
0	0	Alternate Data
0	1	Stack
1	0	Code or None
1	1	Data

TABLE 2.

BHE	A ₀	CHARACTERISTICS
0	0	Whole word
0	1	Upper byte from/to odd address
1	0	Lower byte from/to even address
1	1	None

TABLE 3.

$\overline{S_2}$	$\overline{S_1}$	$\overline{S_0}$	CHARACTERISTICS
0	0	0	Interrupt Acknowledge
0	0	1	Read I/O Port
0	1	0	Write I/O Port
0	1	1	Halt
1	0	0	Code Access
1	0	1	Read Memory
1	1	0	Write Memory
1	1	1	Passive

HS-80C86RH

Pin Description

The following pin function descriptions are for the HS-80C86RH in minimum mode (i.e. MN/MX = VDD). Only the

pin functions which are unique to minimum mode are described; all other pin functions are as described below.

SYMBOL	PIN NUMBER	TYPE	DESCRIPTION
M/ $\overline{\text{IO}}$	28	O	STATUS LINE: logically equivalent to $\overline{\text{S}}_2$ in the maximum mode. It is used to distinguish a memory access from an I/O access. M/ $\overline{\text{IO}}$ becomes valid in the T ₄ preceding a bus cycle and remains valid until the final T ₄ of the cycle (M = HIGH, IO = LOW). M/ $\overline{\text{IO}}$ is held to a high impedance logic zero during local bus "hold acknowledge".
$\overline{\text{WR}}$	29	O	WRITE: indicates that the processor is performing a write memory or write I/O cycle, depending on the state of the M/ $\overline{\text{IO}}$ signal. $\overline{\text{WR}}$ is active for T ₂ , T ₃ and TW of any write cycle. It is active LOW, and is held to high impedance logic one during local bus "hold acknowledge".
$\overline{\text{INTA}}$	24	O	INTERRUPT ACKNOWLEDGE: is used as a read strobe for interrupt acknowledge cycles. It is active LOW during T ₂ , T ₃ and TW of each interrupt acknowledge cycle. Note that $\overline{\text{INTA}}$ is never floated.
ALE	25	O	ADDRESS LATCH ENABLE: is provided by the processor to latch the address into the 82C82 latch. It is a HIGH pulse active during clock LOW of T ₁ of any bus cycle. Note that ALE is never floated.
DT/ $\overline{\text{R}}$	27	O	DATA TRANSMIT/RECEIVE: is needed in a minimum system that desires to use a data bus transceiver. It is used to control the direction of data flow through the transceiver. Logically, DT/ $\overline{\text{R}}$ is equivalent to $\overline{\text{S}}_1$ in maximum mode, and its timing is the same as for M/ $\overline{\text{IO}}$ (T = HIGH, R = LOW). DT/ $\overline{\text{R}}$ is held to a high impedance logic one during local bus "hold acknowledge".
$\overline{\text{DEN}}$	26	O	DATA ENABLE: provided as an output enable for a bus transceiver in a minimum system which uses the transceiver. $\overline{\text{DEN}}$ is active LOW during each memory and I/O access and for $\overline{\text{INTA}}$ cycles. For a read or $\overline{\text{INTA}}$ cycle it is active from the middle of T ₂ until the middle of T ₄ , while for a write cycle it is active from the beginning of T ₂ until the middle of T ₄ . $\overline{\text{DEN}}$ is held to a high impedance logic one during local bus "hold acknowledge".
HOLD HLDA	31, 30	I O	HOLD: indicates that another master is requesting a local bus "hold". To be acknowledged, HOLD must be active HIGH. The processor receiving the "hold" will issue a "hold acknowledge" (HLDA) in the middle of a T ₄ or T ₁ clock cycle. Simultaneously with the issuance of HLDA, the processor will float the local bus and control lines. After HOLD is detected as being LOW, the processor will lower HLDA, and when the processor needs to run another cycle, it will again drive the local bus and control lines. HOLD is not an asynchronous input. External synchronization should be provided if the system cannot otherwise guarantee the setup time.

Functional Description

Static Operation

All HS-80C86RH circuitry is of static design. Internal registers, counters and latches are static and require no refresh as with dynamic circuit design. This eliminates the minimum operating frequency restriction placed on other microprocessors. The CMOS HS-80C86RH can operate from DC to 5MHz. The processor clock may be stopped in either state (HIGH/LOW) and held there indefinitely. This type of operation is especially useful for system debug or power critical applications.

The HS-80C86RH can be single stepped using only the CPU clock. This state can be maintained as long as is necessary. Single step clock operation allows simple interface circuitry to provide critical information for bringing up your system.

Static design also allows very low frequency operation (down to DC). In a power critical situation, this can provide extremely low power operation since HS-80C86RH

power dissipation is directly related to operating frequency. As the system frequency is reduced, so is the operating power until, ultimately, at a DC input frequency, the HS-80C86RH power requirement is the standby current, (500 μ A maximum).

Internal Architecture

The internal functions of the HS-80C86RH processor are partitioned logically into two processing units. The first is the Bus Interface Unit (BIU) and the second is the Execution Unit (EU) as shown in the CPU functional diagram.

These units can interact directly but for the most part perform as separate asynchronous operational processors. The bus interface unit provides the functions related to instruction fetching and queuing, operand fetch and store, and address relocation. This unit also provides the basic bus control. The overlap of instruction pre-fetching

provided by the BIU to keep the BIU queue empty. Up to 6 bytes of data are available to the BIU while waiting for the EU to complete its operation.

The instruction queue in the BIU to keep the BIU queue empty. Whenever there is a data transfer, the BIU will attempt to fill the queue, which greatly reduces the number of times the EU must wait for data. The queue acts as a buffer between the EU and the BIU. When the queue is empty (i.e., the first byte of data is available to the BIU), the first byte of data is available to the BIU.

The execution unit (EU) is the BIU queue and the BIU queue is addressed to the BIU. The BIU for processing the BIU for storage.

Memory Organization

The processor provides a memory organization which locates the memory as a linear address space. The memory is organized as a linear address space of 00000000 to FFFFFFFF, logically divided into segments of up to 64K bytes, falling on 16-byte boundaries.

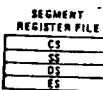


FIGURE 1. HS-80C86RH

TYPE OF MEMORY REFERENCE

Instruction Fetch
Stack Operation
Variable (except following)

String Source
String Destination
BP Used As Base Register

HS-80C86RH

provided by this unit serves to increase processor performance through improved bus bandwidth utilization. Up to 6 bytes of the instruction stream can be queued while waiting for decoding and execution.

The instruction stream queuing mechanism allows the BIU to keep the memory utilized very efficiently. Whenever there is space for at least 2 bytes in the queue, the BIU will attempt a word fetch memory cycle. This greatly reduces "dead-time" on the memory bus. The queue acts as a First-In-First-Out (FIFO) buffer, from which the EU extracts instruction bytes as required. If the queue is empty (following a branch instruction, for example), the first byte into the queue immediately becomes available to the EU.

The execution unit receives pre-fetched instructions from the BIU queue and provides un-relocated operand addresses to the BIU. Memory operands are passed through the BIU for processing by the EU, which passes results to the BIU for storage.

Memory Organization

The processor provides a 20-bit address to memory, which locates the byte being referenced. The memory is organized as a linear array of up to 1 million bytes, addressed as 00000(H) to FFFFF(H). The memory is logically divided into code, data, extra and stack segments of up to 64K bytes each, with each segment falling on 16-byte boundaries. (See Figure 1).

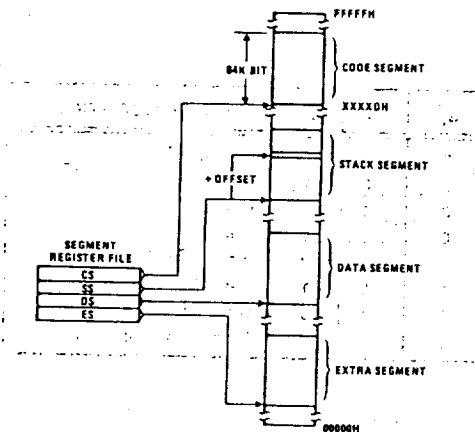


FIGURE 1. HS-80C86RH MEMORY ORGANIZATION

TABLE 4.

TYPE OF MEMORY REFERENCE	DEFAULT SEGMENT BASE	ALTERNATE SEGMENT BASE	OFFSET
Instruction Fetch	CS	None	IP
Stack Operation	SS	None	SP
Variable (except following)	DS	CS, ES, SS	Effective Address
String Source	DS	CS, ES, SS	SI
String Destination	ES	None	DI
BP Used As Base Register	SS	CS, DS, ES	Effective Address

All memory references are made relative to base addresses contained in high speed segment registers. The segment types were chosen based on the addressing needs of programs. The segment register to be selected is automatically chosen according to the specific rules of Table 4. All information in one segment type share the same logical attributes (e.g. code or data). By structuring memory into relocatable areas of similar characteristics and by automatically selecting segment registers, programs are shorter, faster and more structured. (See Table 4).

Word (16-bit) operands can be located on even or odd address boundaries and are thus not constrained to even boundaries as is the case in many 16-bit computers. For address and data operands, the least significant byte of the word is stored in the lower valued address location and the most significant byte in the next higher address location. The BIU automatically performs the proper number of memory accesses, one if the word operand is on an even byte boundary and two if it is on an odd byte boundary. Except for the performance penalty, this double access is transparent to the software. The performance penalty does not occur for instruction fetches; only word operands.

Physically, the memory is organized as a high bank (D15-D8) and a low bank (D7-D0) of 512K bytes addressed in parallel by the processor's address lines.

Byte data with even addresses is transferred on the D7-D0 bus lines while odd addressed byte data (A₀ HIGH) is transferred on the D15-D8 bus lines. The processor provides two enable signals, BHE and A₀, to selectively allow reading from or writing into either an odd byte location, even byte location, or both. The instruction stream is fetched from memory as words and is addressed internally by the processor at the byte level as necessary.

In referencing word data, the BIU requires one or two memory cycles depending on whether the starting byte of the word is on an even or odd address, respectively. Consequently, in referencing word operands performance can be optimized by locating data on even address boundaries. This is an especially useful technique for using the stack, since odd address references to the stack may adversely affect the context switching time for interrupt processing or task multiplexing.

Certain locations in memory are reserved for specific CPU operations (See Figure 2). Locations from address FFFF0H through FFFFFH are reserved for operations including a jump to the initial program loading routine. Following RESET, the CPU will always begin execution at location FFFF0H where the jump must be located. Locations 00000H through 003FFH are reserved for interrupt operations. Each of the 256 possible interrupt service routines is accessed through its own pair of 16-bit pointers - segment address pointer and offset address pointer. The first pointer, used as the offset address, is loaded into the IP and the second pointer, which designates the base address is loaded into the CS. At this point program control is transferred to the interrupt routine.

HS-80C86RH

The pointer elements are assumed to have been stored at the respective places in reserved memory prior to occurrence of interrupts.

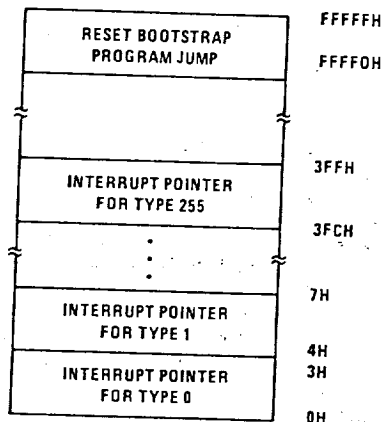


FIGURE 2. RESERVED MEMORY LOCATIONS

Minimum and Maximum Operation Modes

The requirements for supporting minimum and maximum HS-80C86RH systems are sufficiently different that they cannot be met efficiently using 40 uniquely defined pins. Consequently, the HS-80C86RH is equipped with a strap pin (MN/MX) which defines the system configuration. The definition of a certain subset of the pins changes, dependent on the condition of the strap pin. When the MN/MX pin is strapped to GND, the HS-80C86RH defines pins 24 through 31 and 34 in maximum mode. When the MN/MX pin is strapped to VDD, the HS-80C86RH generates bus control signals itself on pins 24 through 31 and 34.

Bus Operation

The HS-80C86RH has a combined address and data bus commonly referred to as a time multiplexed bus. This technique provides the most efficient use of pins on the

processor while permitting the use of a standard 40-lead package. This "local bus" can be buffered directly and used throughout the system with address latching provided on memory and I/O modules. In addition, the bus can also be demultiplexed at the processor with a single set of 82C82 latches if a standard non-multiplexed bus is desired for the system.

Each processor bus cycle consists of at least four CLK cycles. These are referred to as T₁, T₂, T₃ and T₄ (see Figure 3). The address is emitted from the processor during T₁ and data transfer occurs on the bus during T₃ and T₄. T₂ is used primarily for changing the direction of the bus during read operations. In the event that a "NOT READY" indication is given by the addressed device, "Wait" states (TW) are inserted between T₃ and T₄. Each inserted wait state is the same duration as a CLK cycle. Idle periods occur between HS-80C86RH driven bus cycles whenever the processor performs internal processing.

During T₁ of any bus cycle, the ALE (Address Latch Enable) signal is emitted (by either the processor or the 82C88 bus controller, depending on the MN/MX strap). At the trailing edge of this pulse, a valid address and certain status information for the cycle may be latched.

Status bits $\overline{S_0}$, $\overline{S_1}$ and $\overline{S_2}$ are used by the bus controller, in maximum mode, to identify the type of bus transaction according to Table 5.

TABLE 5.

$\overline{S_2}$	$\overline{S_1}$	$\overline{S_0}$	CHARACTERISTICS
0	0	0	Interrupt
0	0	1	Read I/O
0	1	0	Write I/O
0	1	1	Halt
1	0	0	Instruction Fetch
1	0	1	Read Data from Memory
1	1	0	Write Data to Memory
1	1	1	Passive (no bus cycle)

CLK

ALE

$\overline{S_2}$ - $\overline{S_0}$

ADDR/
STATUS

ADDR/DATA

\overline{RD} , \overline{INTA}

READY

DT/R

\overline{DEN}

WP



PRELIMINARY

DP8390C-1/NS32490C-1 Network Interface Controller

General Description

The DP8390C-1/NS32490C-1 Network Interface Controller (NIC) is a microCMOS VLSI device designed to ease interfacing with CSMA/CD type local area networks such as StarLAN. The NIC implements all Media Access Control (MAC) layer functions for transmission and reception of packets in accordance with the IEEE 802.3 Standard. Unique dual DMA channels and an internal FIFO provide a simple yet efficient packet management design. To minimize system parts count and cost, all bus arbitration and memory support logic are integrated into the NIC.

The DP8390C-1 is software compatible with the DP8390.

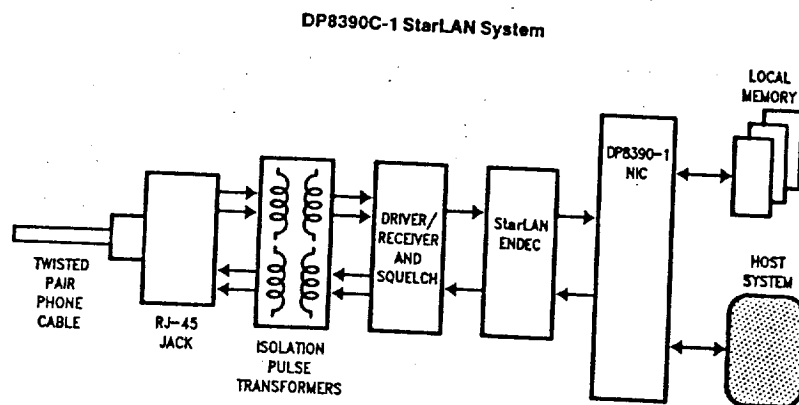
Features

- Compatible with IEEE 802.3 StarLAN (1 Mb/s)
- Interfaces with 8-, 16- and 32-bit microprocessor systems
- Implements simple, versatile buffer management
- Requires single 5V supply
- Utilizes low power microCMOS process
- Includes
 - Two 16-bit DMA channels
 - 16-byte internal FIFO with programmable threshold
 - Network statistics storage
- Supports physical, multicast, and broadcast address filtering
- Provides loopback diagnostics
- Utilizes independent system and network clocks

Table of Contents

- 1.0 SYSTEM DIAGRAM
- 2.0 BLOCK DIAGRAM
- 3.0 FUNCTIONAL DESCRIPTION
- 4.0 TRANSMIT/RECEIVE PACKET ENCAPSULATION/DECAPSULATION
- 5.0 PIN DESCRIPTIONS
- 6.0 DIRECT MEMORY ACCESS CONTROL (DMA)
- 7.0 PACKET RECEPTION
- 8.0 PACKET TRANSMISSION
- 9.0 REMOTE DMA
- 10.0 INTERNAL REGISTERS
- 11.0 INITIALIZATION PROCEDURES
- 12.0 LOOPBACK DIAGNOSTICS
- 13.0 BUS ARBITRATION AND TIMING
- 14.0 PRELIMINARY ELECTRICAL CHARACTERISTICS
- 15.0 SWITCHING CHARACTERISTICS
- 16.0 PHYSICAL DIMENSIONS

1.0 System Diagram



TL/F/9345-1

RELIMINARY

troller

ENCAPSULATION/

TROL (DMA)

RACTERISTICS

TL/F/9345-1

2.0 Block Diagram

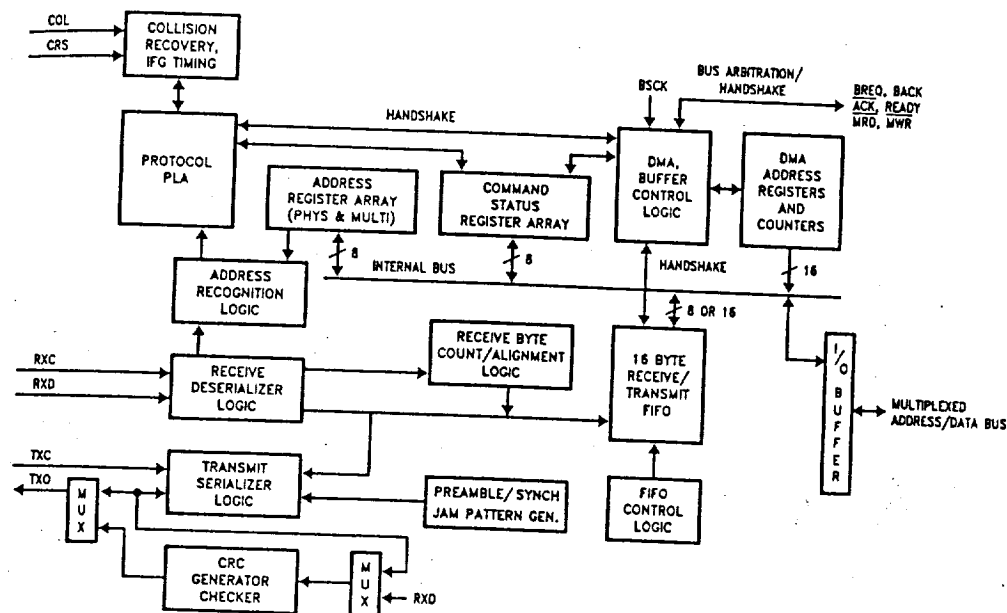


FIGURE 1

TL/F/9345-2

3.0 Functional Description

(Refer to Figure 1)

RECEIVE DESERIALIZER

The Receive Deserializer is activated when the input signal Carrier Sense is asserted to allow incoming bits to be shifted into the shift register by the receive clock. The serial receive data is also routed to the CRC generator/checker. The Receive Deserializer includes a synch detector which detects the SFD (Start of Frame Delimiter) to establish where byte boundaries within the serial bit stream are located. After every eight receive clocks, the byte wide data is transferred to the 16-byte FIFO and the Receive Byte Count is incremented. The first six bytes after the SFD are checked for valid comparison by the Address Recognition Logic. If the Address Recognition Logic does not recognize the packet, the FIFO is cleared.

CRC GENERATOR/CHECKER

During transmission, the CRC logic generates a local CRC field for the transmitted bit sequence. The CRC encodes all fields after the synch byte. The CRC is shifted out MSB first following the last transmit byte. During reception the CRC logic generates a CRC field from the incoming packet. This local CRC is serially compared to the incoming CRC appended to the end of the packet by the transmitting node. If the local and received CRC match, a specific pattern will be generated and decoded to indicate no data errors. Transmission errors result in a different pattern and are detected, resulting in rejection of a packet.

TRANSMIT SERIALIZER

The Transmit Serializer reads parallel data from the FIFO and serializes it for transmission. The serializer is clocked by the transmit clock. The serial data is also shifted into the

CRC generator/checker. At the beginning of each transmission, the Preamble and Synch Generator append 62 bits of 1,0 preamble and a 1,1 synch pattern. After the last data byte of the packet has been serialized the 32-bit FCS field is shifted directly out of the CRC generator. In the event of a collision the Preamble and Synch generator is used to generate a 32-bit JAM pattern of all 1's.

ADDRESS RECOGNITION LOGIC

The address recognition logic compares the Destination Address Field (first 6 bytes of the received packet) to the Physical address registers stored in the Address Register Array. If any one of the six bytes does not match the pre-programmed physical address, the Protocol Control Logic rejects the packet. All multicast destination addresses are filtered using a hashing technique. (See register description) If the multicast address indexes a bit that has been set in the filter bit array of the Multicast Address Register Array the packet is accepted, otherwise it is rejected by the Protocol Control Logic. Each destination address is also checked for all 1's which is the reserved broadcast address.

FIFO AND FIFO CONTROL LOGIC

The NIC features a 16-byte FIFO. During transmission the DMA writes data into the FIFO and the Transmit Serializer reads data from the FIFO and transmits it. During reception the Receive Deserializer writes data into the FIFO and the DMA reads data from the FIFO. The FIFO control logic is used to count the number of bytes in the FIFO so that after a preset level, the DMA can begin a bus access and write/read data to/from the FIFO before a FIFO underflow overflow occurs.

3.0 Functional Description (Continued)

Because the NIC must buffer the Address field of each incoming packet to determine whether the packet matches its Physical Address Registers or maps to one of its Multicast Registers, the first local DMA transfer does not occur until 8 bytes have accumulated in the FIFO.

To assure that there is no overwriting of data in the FIFO, the FIFO logic flags a FIFO overrun as the 13th byte is written into the FIFO; this effectively shortens the FIFO to 13 bytes. In addition, the FIFO logic operates differently in Byte Mode than in Word Mode. In Byte Mode, a threshold is indicated when the $n+1$ byte has entered the FIFO; thus, with an 8-byte threshold, the NIC issues Bus Request (BREQ) when the 9th byte has entered the FIFO. For Word Mode, BREQ is not generated until the $n+2$ bytes have entered the FIFO. Thus, with a 4 word threshold (equivalent to an 8-byte threshold), BREQ is issued when the 10th byte has entered the FIFO.

PROTOCOL PLA

The protocol PLA is responsible for implementing the IEEE8023 protocol, including collision recovery with random backoff. The Protocol PLA also formats packets during transmission and strips preamble and synch during reception.

DMA AND BUFFER CONTROL LOGIC

The DMA and Buffer Control Logic is used to control two 16-bit DMA channels. During reception, the Local DMA stores packets in a receive buffer ring, located in buffer memory. During transmission the Local DMA uses programmed pointer and length registers to transfer a packet from local buffer memory to the FIFO. A second DMA channel is used as a slave DMA to transfer data between the local buffer memory and the host system. The Local DMA and Remote DMA are internally arbitrated, with the Local DMA channel having highest priority. Both DMA channels use a common external bus clock to generate all required bus timing. External arbitration is performed with a standard bus request, bus acknowledge handshake protocol.

4.0 Transmit/Receive Packet Encapsulation/Decapsulation

A standard IEEE 802.3 packet consists of the following fields: preamble, Start of Frame Delimiter (SFD), destination address, source address, length, data, and Frame Check Sequence (FCS). The typical format is shown in Figure 2. The packets are Manchester encoded and decoded by the StarLAN ENDEC and transferred serially to the NIC using NRZ data with a clock. All fields are of fixed length except for the data field. The NIC generates and appends the preamble, SFD and FCS field during transmission. The Preamble and SFD fields are stripped during reception. (The CRC is passed through to buffer memory during reception.)

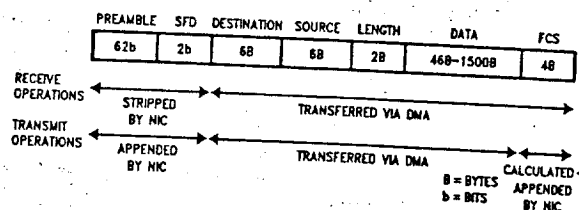


FIGURE 2

TL/F/9345-3

PREAMBLE AND START OF FRAME DELIMITER (SFD)

The Manchester encoded alternating 1,0 preamble field is used by the StarLAN ENDEC to acquire bit synchronization with an incoming packet. When transmitted each packet contains 62 bits of alternating 1,0 preamble. Some of this preamble will be lost as the packet travels through the network. The preamble field is stripped by the NIC. Byte alignment is performed with the Start of Frame Delimiter (SFD) pattern which consists of two consecutive 1's. The NIC does not treat the SFD pattern as a byte, it detects only the two bit pattern. This allows any preceding preamble within the SFD to be used for phase locking.

DESTINATION ADDRESS

The destination address indicates the destination of the packet on the network and is used to filter unwanted packets from reaching a node. There are three types of address formats supported by the NIC: physical, multicast, and broadcast. The physical address is a unique address that corresponds only to a single node. All physical addresses have an MSB of "0". These addresses are compared to the internally stored physical address registers. Each bit in the destination address must match in order for the NIC to accept the packet. Multicast addresses begin with an MSB of "1". The NIC filters multicast addresses using a standard hashing algorithm that maps all multicast addresses into a six bit value. This six bit value indexes a 64 bit array that filters the value. If the address consists of all 1's it is a broadcast address, indicating that the packet is intended for all nodes. A promiscuous mode allows reception of all packets: the destination address is not required to match any filters. Physical, broadcast, multicast, and promiscuous address modes can be selected.

SOURCE ADDRESS

The source address is the physical address of the node that sent the packet. Source addresses cannot be multicast or broadcast addresses. This field is simply passed to buffer memory.

LENGTH FIELD

The 2-byte length field indicates the number of bytes that are contained in the data field of the packet. This field is not interpreted by the NIC.

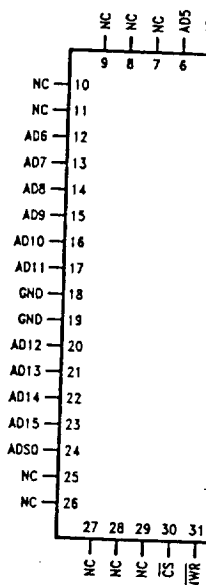
DATA FIELD

The data field consists of anywhere from 46 to 1500 bytes. Messages longer than 1500 bytes need to be broken into multiple packets. Messages shorter than 46 bytes will require appending a pad to bring the data field to the minimum length of 46 bytes. If the data field is padded, the number of valid data bytes is indicated in the length field. The NIC does not strip or append pad bytes for short packets, or check for oversize packets.

4.0 Transmit/Receive FCS FIELD

The Frame Check Sequence (FCS) is calculated and appended to the end of the packet to allow detection of errors with reception, error free packets.

Connection Diagram



g 1,0 preamble field is
uire bit synchronization
nsmitted each packet
reamble. Some of this
ravel through the net-
by the NIC. Byte align-
Frame Delimiter (SFD)
ecutive 1's. The NIC
yte, it detects only the
eding preamble within
l.

the destination of the filter unwanted packages. There are three types of address filters: unicast, multicast, and broadcast. Unicast is a unique address that identifies a specific physical address. Multicast addresses are compared to the destination address of the packets. Each bit in the destination address of the filter for the NIC to accept or reject a packet begins with an MSB of 1, indicating that the packet is using a standard broadcast address. Multicast addresses into a 64-bit array that contains all 1's. It is a packet intended for reception of all packets. Broadcast is required to match any address. Multicast and promiscuous address filters are used to filter unwanted packets.

ess of the node that
not be multicast or
ly passed to buffer

umber of bytes that
ket. This field is not

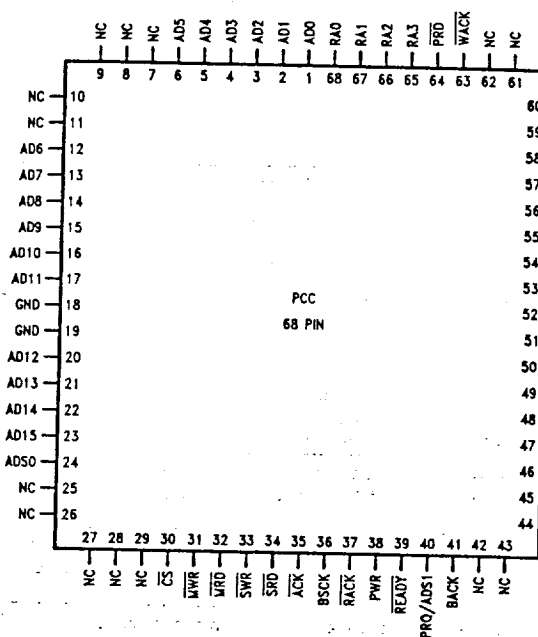
146 to 1500 bytes. If a packet is to be broken into fragments, each fragment must be at least 46 bytes. The number of fragments is determined by the number of bytes in the packet divided by the maximum fragment size. The NIC will then send the fragments in order. The NIC will also send short packets.

FCS FIELD

The Frame Check Sequence (FCS) is a 32-bit CRC field calculated and appended to a packet during transmission to allow detection of errors when a packet is received. During reception, error free packets result in a specific pattern in

the CRC generator. Packets with improper CRC will be rejected. The AUTODIN II ($X^{32} + X^{26} + X^{23} + X^{22} + X^{16} + X^{12} + X^{11} + X^{10} + X^8 + X^7 + X^5 + X^4 + X^2 + X^1 + 1$) polynomial is used for the CRC calculations.

Plastic Chip Carrier



TUF/9345-5

AD0	1	48	RA0
AD1	2	47	RA1
AD2	3	46	RA2
AD3	4	45	RA3
AD4	5	44	PRD
A05	6	43	WACK
AD6	7	42	INT
AD7	8	41	RESET
AD8	9	40	COL
AD9	10	39	RXD
AD10	11	38	CRS
AD11	12	37	RXC
GND	13	36	V _{CC}
AD12	14	35	LBK
AD13	15	34	TXD
AD14	16	33	TXC
AD15	17	32	TXE
A0S0	18	31	BREQ
CS	19	30	BACK
WWR	20	29	PRQ/ADS1
WRO	21	28	READY
SWR	22	27	PWR
SRD	23	26	RACK
ACK	24	25	BSCK

TV/F/9345-4

Order Number DP8390CN-1 or DP8390CV-1
See NS Package Number N48A or V68A

BUS INTERFACE PINS

Symbol	DIP Pin No	Function	Description
AD0-AD15	1-12 14-17	I/O,Z	MULTIPLEXED ADDRESS/DATA BUS: <ul style="list-style-type: none"> Register Access, with DMA inactive, \overline{CS} low and \overline{ACK} returned from NIC, pins AD0-AD7 are used to read/write register data. AD8-AD15 float during I/O transfers. SRD, SWR pins are used to select direction of transfer. Bus Master with BACK input asserted <ul style="list-style-type: none"> During t1 of memory cycle AD0-AD15 contain address During t2, t3, t4 AD0-AD15 contain data (word transfer mode). During t2, t3, t4 AD0-AD7 contain data, AD8-AD15 contain address (byte transfer mode). Direction of transfer is Indicated by NIC on \overline{MWR}, \overline{MRD} lines.
ADS0	18	I/O,Z	ADDRESS STROBE 0 <ul style="list-style-type: none"> Input with DMA inactive and \overline{CS} low, latches RA0-RA3 inputs on falling edge. If high, data present on RA0-RA3 will flow through latch. Output when Bus Master, latches address bits (A0-A15) to external memory during DMA transfers.

5.0 Pin Descriptions (Continued)

BUS INTERFACE PINS (Continued)

Symbol	DIP Pin No	Function	Description
\overline{CS}	19	I	CHIP SELECT: Chip Select places controller in slave mode for μP access to internal registers. Must be valid through data portion of bus cycle. RA0-RA3 are used to select the internal register. \overline{SWR} and \overline{SRD} select direction of data transfer.
\overline{MWR}	20	O,Z	MASTER WRITE STROBE: Strobe for DMA transfers, active low during write cycles (t_2 , t_3 , t_w) to buffer memory. Rising edge coincides with the presence of valid output data. TRI-STATE* until BACK asserted.
\overline{MRD}	21	O,Z	MASTER READ STROBE: Strobe for DMA transfers, active during read cycles (t_2 , t_3 , t_w) to buffer memory. Input data must be valid on rising edge of \overline{MRD} . TRI-STATE until BACK asserted.
\overline{SWR}	22	I	SLAVE WRITE STROBE: Strobe from CPU to write an internal register selected by RA0-RA3.
\overline{SRD}	23	I	SLAVE READ STROBE: Strobe from CPU to read an internal register selected by RA0-RA3.
ACK	24	O	ACKNOWLEDGE: Active low when NIC grants access to CPU. Used to insert WAIT states to CPU until NIC is synchronized for a register read or write operation.
RA0-RA3	45-48	I	REGISTER ADDRESS: These four pins are used to select a register to be read or written. The state of these inputs is ignored when the NIC is not in slave mode (\overline{CS} high).
\overline{PRD}	44	O	PORT READ: Enables data from external latch onto local bus during a memory write cycle to local memory (remote write operation). This allows asynchronous transfer of data from the system memory to local memory.
\overline{WACK}	43	I	WRITE ACKNOWLEDGE: Issued from system to NIC to indicate that data has been written to the external latch. The NIC will begin a write cycle to place the data in local memory.
INT	42	O	INTERRUPT: Indicates that the NIC requires CPU attention after reception transmission or completion of DMA transfers. The interrupt is cleared by writing to the ISR. All interrupts are maskable.
RESET	41	I	RESET: Reset is active low and places the NIC in a reset mode immediately, no packets are transmitted or received by the NIC until STA bit is set. Affects Command Register, Interrupt Mask Register, Data Configuration Register and Transmit Configuration Register. The NIC will execute reset within 10 BUSK cycles.
BREQ	31	O	BUS REQUEST: Bus Request is an active high signal used to request the bus for DMA transfers. This signal is automatically generated when the FIFO needs servicing.
BACK	30	I	BUS ACKNOWLEDGE: Bus Acknowledge is an active high signal indicating that the CPU has granted the bus to the NIC. If immediate bus access is desired, BREQ should be tied to BACK. Tying BACK to Vcc will result in a deadlock.
PRQ, ADS1	29	O,Z	PORT REQUEST/ADDRESS STROBE 1 <ul style="list-style-type: none"> • 32 BIT MODE: If LAS is set in the Data Configuration Register, this line is programmed as ADS1. It is used to strobe addresses A16-A31 into external latches. (A16-A31 are the fixed addresses stored in RSAR0, RSAR1.) ADS1 will remain at TRI-STATE until BACK is received. • 16 BIT MODE: If LAS is not set in the Data Configuration Register, this line is programmed as PRQ and is used for Remote DMA Transfers. In this mode PRQ will be a standard logic output. NOTE: This line will power up as TRI-STATE until the Data Configuration Register is programmed.
READY	28	I	READY: This pin is set high to insert wait states during a DMA transfer. The NIC will sample this signal at t_3 during DMA transfers.

5.0 Pin Descriptions (Continued)

BUS INTERFACE PINS (Continued)

Symbol	DIP Pin No
\overline{PWR}	
RACK	
BSCK	
NETWORK INTERFACE PINS	
COL	
RXD	3
CRS	3
RXC	3
LBK	3
TXD	3
TXC	3
TXE	32
POWER	
Vcc	36
GND	13

6.0 Direct Memory Access

The DMA capabilities of the DP8390C-1 in typical applications transfer data between the CPU and memory. In transmission, the packet is sent in bursts. Should a collision occur, the packet is retransmitted with a random delay. In reception, packets are DMA transfered (as explained below).

A remote DMA channel can be used to accomplish transfers between the CPU and memory. The two DMA channels are combined to form a single channel.

DUAL DMA CONFIGURATION

An example configuration of the DP8390C-1 DMA channels is shown in Figure 6-1.

5.0 Pin Descriptions (Continued)

BUS INTERFACE PINS (Continued)

Symbol	DIP Pin No	Function	Description
PWR	27	O	PORT WRITE: Strobe used to latch data from the NIC into external latch for transfer to host memory during Remote Read transfers. The rising edge of PWR coincides with the presence of valid data on the local bus.
RACK	26	I	READ ACKNOWLEDGE: Indicates that the system DMA or host CPU has read the data placed in the external latch by the NIC. The NIC will begin a read cycle to update the latch.
BCK	25	I	This clock is used to establish the period of the DMA memory cycle. Four clock cycles (t1, t2, t3, t4) are used per DMA cycle. DMA transfers can be extended by one BCK increments using the READY input.

NETWORK INTERFACE PINS

COL	40	I	COLLISION DETECT: This line becomes active when a collision has been detected on the coaxial cable. During transmission this line is monitored after preamble and synch have been transmitted. At the end of each transmission this line is monitored for CD heartbeat.
RXD	39	I	RECEIVE DATA: Serial NRZ data received from the ENDEC, clocked into the NIC on the rising edge of RXC.
CRS	38	I	CARRIER SENSE: This signal is provided by the ENDEC and indicates that carrier is present. This signal is active high.
RXC	37	I	RECEIVE CLOCK: Re-synchronized clock from the ENDEC used to clock data from the ENDEC into the NIC.
LBK	35	O	LOOPBACK: This output is set high when the NIC is programmed to perform a loopback through the StarLAN ENDEC.
TXD	34	O	TRANSMIT DATA: Serial NRZ Data output to the ENDEC. The data is valid on the rising edge of TXC.
TXC	33	I	TRANSMIT CLOCK: This clock is used to provide timing for internal operation and to shift bits out of the transmit serializer. TXC is nominally a 1 MHz clock provided by the ENDEC.
TXE	32	O	TRANSMIT ENABLE: This output becomes active when the first bit of the packet is valid on TXD and goes low after the last bit of the packet is clocked out of TXD. This signal connects directly to the ENDEC. This signal is active high.

POWER

VCC	36		+ 5V DC is required. It is suggested that a decoupling capacitor be connected between these pins. It is essential to provide a path to ground for the GND pin with the lowest possible impedance.
GND	13		

6.0 Direct Memory Access Control (DMA)

The DMA capabilities of the NIC greatly simplify use of the DP8390C-1 in typical configurations. The local DMA channel transfers data between the FIFO and memory. On transmission, the packet is DMA'd from memory to the FIFO in bursts. Should a collision occur (up to 15 times), the packet is retransmitted with no processor intervention. On reception, packets are DMAed from the FIFO to the receive buffer ring (as explained below).

A remote DMA channel is also provided on the NIC to accomplish transfers between a buffer memory and system memory. The two DMA channels can alternatively be combined to form a single 32-bit address with 8- or 16-bit data.

DUAL DMA CONFIGURATION

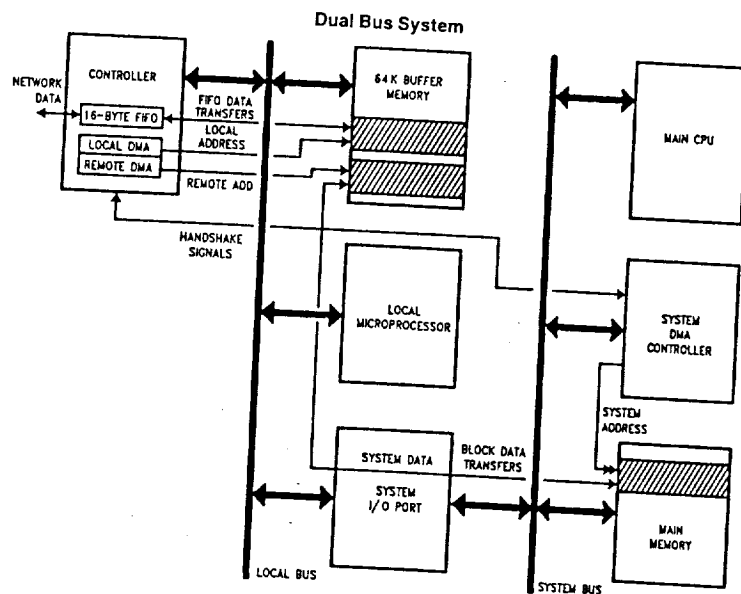
An example configuration using both the local and remote DMA channels is shown below. Network activity is isolated

on a local bus, where the NIC's local DMA channel performs burst transfers between the buffer memory and the NIC's FIFO. The Remote DMA transfers data between the buffer memory and the host memory via a bidirectional I/O port. The Remote DMA provides local addressing capability and is used as a slave DMA by the host. Host side addressing must be provided by a host DMA or the CPU. The NIC allows Local and Remote DMA operations to be interleaved.

SINGLE CHANNEL DMA OPERATION

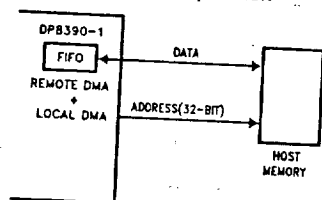
If desirable, the two DMA channels can be combined to provide a 32-bit DMA address. The upper 16 bits of the 32-bit address are static and are used to point to a 64 kbyte (or 32k word) page of memory where packets are to be received and transmitted.

6.0 Direct Memory Access Control (DMA) (Continued)



TL/F/9345-8

32-Bit DMA Operation

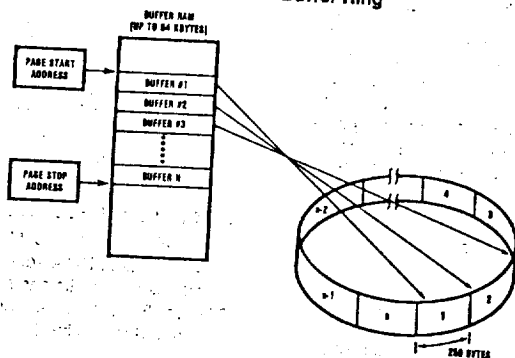


TL/F/9345-7

7.0 Packet Reception

The Local DMA receive channel uses a Buffer Ring Structure comprised of a series of contiguous fixed length 256 byte (128 word) buffers for storage of received packets. The location of the Receive Buffer Ring is programmed in two registers, a Page Start and a Page Stop register. Ethernet packets consist of a distribution of shorter link control packets and longer data packets, the 256 byte buffer length provides a good compromise between short packets and longer packets to most efficiently use memory. In addition these buffers provide memory resources for storage of back-to-back packets in loaded networks. The assignment of buffers

NIC Receive Buffer Ring



TL/F/9345-8

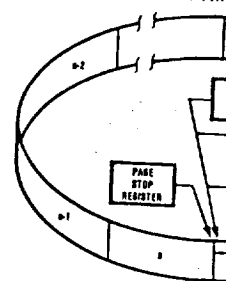
7.0 Packet Reception

for storing packets is contained in the NIC. The Buffer Memory performs basic functions: linking received packets, recovery of buffers when a packet is received. At initialization, a portion of address space is reserved for eight bit registers, the Page Start Register (PSTART) and the Page Stop Register (PSTOP). The NIC treats the list of buffers as a circular list. The DMA address reaches the end of the list and is reset to the Page Start Address.

INITIALIZATION OF THE BUFFER RING

Two static registers and two dynamic registers are used in the operation of the Buffer Ring. The static registers are the Page Start Register (PSTART) and the Page Stop Register (PSTOP). The dynamic registers are the Current Page Register (CPR) and the Boundary Register (BR). The CPR stores a packet and is used to store the status to the Buffer Ring or for the event of a Runt packet error. The Boundary Register is not yet read by the host. When the CPR reaches the Boundary, reception of a packet and is advanced to the next buffer. A simple analogy to remember is that the Current Page Register is the Boundary Pointer acts as a pointer to the next buffer. Note: At initialization, the Page Start and Page Stop registers both the Current Page Register.

Receive Buffer Ring



BEGINNING OF RECEPTION

When the first packet begins arrival at the NIC, the packet is placed at the location pointed to by the Page Start Register.

7.0 Packet Reception (Continued)

for storing packets is controlled by Buffer Management logic in the NIC. The Buffer Management logic provides three basic functions: linking receive buffers for long packets, recovery of buffers when a packet is rejected, and recirculation of buffer pages that have been read by the host.

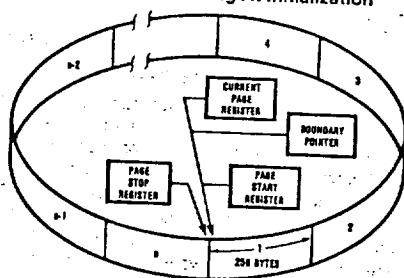
At initialization, a portion of the 64 kbyte (or 32k word) address space is reserved for the receive buffer ring. Two eight bit registers, the Page Start Address Register (PSTART) and the Page Stop Address Register (PSTOP) define the physical boundaries of where the buffers reside. The NIC treats the list of buffers as a logical ring; whenever the DMA address reaches the Page Stop Address, the DMA is reset to the Page Start Address.

INITIALIZATION OF THE BUFFER RING

Two static registers and two working registers control the operation of the Buffer Ring. These are the Page Start Register, Page Stop Register (both described previously), the Current Page Register and the Boundary Pointer Register. The Current Page Register points to the first buffer used to store a packet and is used to restore the DMA for writing status to the Buffer Ring or for restoring the DMA address in the event of a Runt packet, a CRC, or Frame Alignment error. The Boundary Register points to the first packet in the Ring not yet read by the host. If the local DMA address ever reaches the Boundary, reception is aborted. The Boundary Pointer is also used to initialize the Remote DMA for removing a packet and is advanced when a packet is removed. A simple analogy to remember the function of these registers is that the Current Page Register acts as a Write Pointer and the Boundary Pointer acts as a Read Pointer.

Note: At initialization, the Page Start Register value should be loaded into both the Current Page Register and the Boundary Pointer Register.

Receive Buffer Ring At Initialization

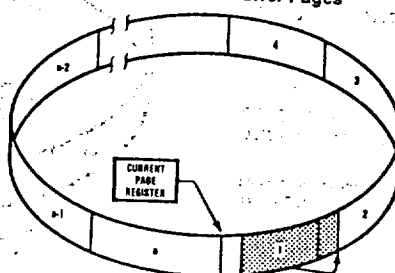


TL/F/9345-9

BEGINNING OF RECEPTION

When the first packet begins arriving the NIC begins storing the packet at the location pointed to by the Current Page

Linking Receive Buffer Pages



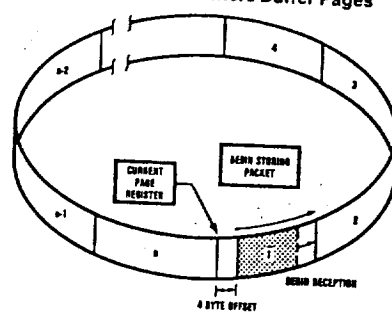
- 1) Check for = to PSTOP
- 2) Check for = to Boundary

TL/F/9345-10

ORIGINAL PAGE IS OF POOR QUALITY

Register. An offset of 4 bytes is saved in this first buffer to allow room for storing receive status corresponding to this packet.

Received Packet Enters Buffer Pages



TL/F/9345-11

LINKING RECEIVE BUFFER PAGES

If the length of the packet exhausts the first 256-byte buffer, the DMA performs a forward link to the next buffer to store the remainder of the packet. For a maximal length packet the buffer logic will link six buffers to store the entire packet. Buffers cannot be skipped when linking, a packet will always be stored in contiguous buffers. Before the next buffer can be linked, the Buffer Management Logic performs two comparisons. The first comparison tests for equality between the DMA address of the next buffer and the contents of the Page Stop Register. If the buffer address equals the Page Stop register, the buffer management logic will restore the DMA to the first buffer in the Receive Buffer Ring value programmed in the Page Start Address register. The second comparison tests for equality between the DMA address of the next buffer address and the contents of the Boundary Pointer register. If the two values are equal the reception is aborted. The Boundary Pointer register can be used to protect against overwriting any area in the receive buffer ring that has not yet been read. When linking buffers, buffer management will never cross this pointer, effectively avoiding any overwrites. If the buffer address does not match either the Boundary Pointer or Page Stop address, the link to the next buffer is performed.

Linking Buffers

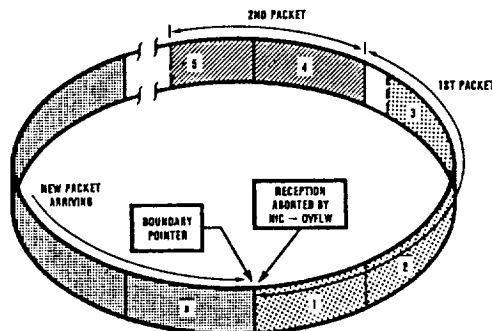
Before the DMA can enter the next contiguous 256-byte buffer, the address is checked for equality to PSTOP and to the Boundary Pointer. If neither are reached, the DMA is allowed to use the next buffer.

DP8390C-1/NS32490C-1

1

7.0 Packet Reception (Continued)

Received Packet Aborted If It Hits Boundary Pointer



TL/F/9345-12

Buffer Ring Overflow

If the Buffer Ring has been filled and the DMA reaches the Boundary Pointer Address, reception of the incoming packet will be aborted by the NIC. Thus, the packets previously received and still contained in the Ring will not be destroyed.

In a heavily loaded network environment the local DMA may be disabled, preventing the NIC from buffering packets from the network. To guarantee this will not happen, a software reset must be issued during all Receive Buffer Ring overflows (indicated by the OVW bit in the Interrupt Status Register). The following procedure is required to recover from a Receiver Buffer Ring Overflow.

1. Issue the STOP mode command (Command Register = 21H). The NIC may not immediately enter the STOP mode. If it is currently processing a packet, the NIC will enter STOP mode only after finishing the packet. The NIC indicates that it has entered STOP mode by setting the RST bit in the Interrupt Status Register.
2. Clear the Remote Byte Counter Registers (RBCR0, RBCR1). The NIC requires these registers to be cleared before it sets the RST bit.

Note: If the STP is set when a transmission is in progress, the RST bit may not be set. In this case, the NIC is guaranteed to be reset after the longest packet time (1500 bytes = 1.2 ms). For the DP8390C (but not for the DP8390B), the NIC will be reset within 2 microseconds after the STP bit is set and Loopback mode 1 is programmed.

3. Poll the Interrupt Status Register for the RST bit. When set, the NIC is in STOP mode.
4. Place the NIC in LOOPBACK (mode 1 or 2) by writing 02H or 04H to the Transmit Configuration Register. This step is required to properly enable the NIC onto an active network.
5. Issue the START mode command (Command Register = 22H). The local receive DMA is still inactive since the NIC is in LOOPBACK.
6. Remove at least one packet from the Receive Buffer Ring to accommodate additional incoming packets.
7. Take the NIC out of LOOPBACK by programming the Transmit Configuration Register back to its original value and resume normal operation.

Note: If the Remote DMA channel is not used, you may eliminate step 6 and remove packets from the Receive Buffer Ring after step 1. This will reduce or eliminate the polling time incurred in step 3.

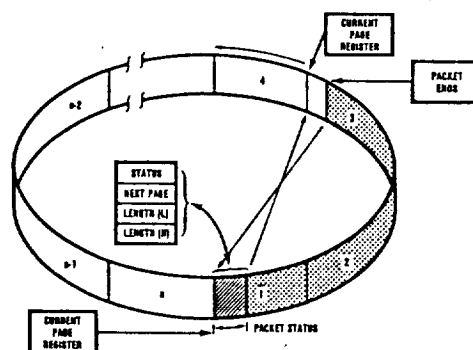
END OF PACKET OPERATIONS

At the end of the packet the NIC determines whether the received packet is to be accepted or rejected. It either branches to a routine to store the Buffer Header or to another routine that recovers the buffers used to store the packet.

SUCCESSFUL RECEPTION

If the packet is successfully received as shown, the DMA is restored to the first buffer used to store the packet (pointed to by the Current Page Register). The DMA then stores the Receive Status, a Pointer to where the next packet will be stored (Buffer 4) and the number of received bytes. Note that the remaining bytes in the last buffer are discarded and reception of the next packet begins on the next empty 256-byte buffer boundary. The Current Page Register is then initialized to the next available buffer in the Buffer Ring. (The location of the next buffer had been previously calculated and temporarily stored in an internal scratchpad register.)

Termination of Received Packet—Packet Accepted

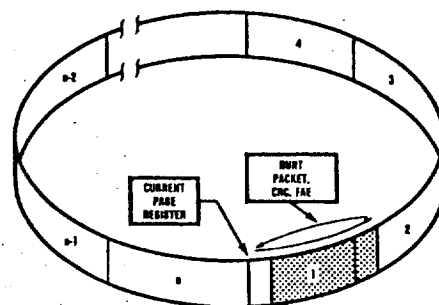


TL/F/9345-13

BUFFER RECOVERY FOR REJECTED PACKETS

If the packet is a runt packet or contains CRC or Frame Alignment errors, it is rejected. The buffer management logic resets the DMA back to the first buffer page used to store the packet (pointed to by CURR), recovering all buffers that had been used to store the rejected packet. This operation will not be performed if the NIC is programmed to accept either runt packets or packets with CRC or Frame Alignment errors. The received CRC is always stored in buffer memory after the last byte of received data for the packet.

Termination of Received Packet—Packet Rejected



TL/F/9345-14

7.0 Packet Reception

Error Recovery

If the packet is rejected the NIC by reprogramming the next packet to be received by the Current Page Register.

REMOVING PACKETS FROM THE BUFFER RING

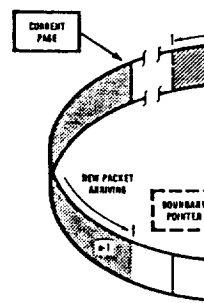
Packets are removed from the Buffer Ring by the NIC or an external device. When a Send Packet command is received, the DMA is automatically pointed to by the Boundary Pointer. After the packet is received, the NIC moves the Boundary Pointer to the next empty buffer for reception. The Boundary Pointer is moved manually by programming the Boundary Pointer. Care should be taken to ensure that the Boundary Pointer is one buffer behind the Current Page Register. The following is a suggested routine for the Receive Buffer Ring pointer.

1. At initialization, set up the Boundary Pointer to indicate where the next packet will be loaded.
2. When initializing the NIC, set the Boundary Pointer to the next empty buffer. $BNDRY = PSTART$. $CURR = PSTART + 1$. $next_pkt = PSTART$.
3. After a packet is DMA'd, update the Next Page Pointer. $next_pkt = Next Page$. $BNDRY = Next Page$. If $BNDRY < PSTART$, then $BNDRY = PSTART$.

Note the size of the Receive Buffer Ring; this will be 256 bytes of the NIC.

In StarLAN applications using a clock rate of less than 4 MHz, the NIC does not provide information properly because the network and bus clock speeds are divided twice into the third byte of the header and the upper byte of the data. The byte count, however, can be used to determine the next page pointer (second byte of the header). The following routine can be used to allow StarLAN applications to operate at speeds. $next_pkt$ is defined as:

1st Received Packet



7.0 Packet Reception (Continued)

Error Recovery

If the packet is rejected as shown, the DMA is restored by the NIC by reprogramming the DMA starting address pointed to by the Current Page Register.

REMOVING PACKETS FROM THE RING

Packets are removed from the ring using the Remote DMA or an external device. When using the Remote DMA the Send Packet command can be used. This programs the Remote DMA to automatically remove the received packet pointed to by the Boundary Pointer. At the end of the transfer, the NIC moves the Boundary Pointer, freeing additional buffers for reception. The Boundary Pointer can also be moved manually by programming the Boundary Register. Care should be taken to keep the Boundary Pointer at least one buffer behind the Current Page Pointer.

The following is a suggested method for maintaining the Receive Buffer Ring pointers.

1. At initialization, set up a software variable (`next_pkt`) to indicate where the next packet will be read. At the beginning of each Remote Read DMA operation, the value of `next_pkt` will be loaded into RSAR0 and RSAR1.

2. When initializing the NIC set:

`BNDRY = PSTART`

`CURR = PSTART + 1`

`next_pkt = PSTART + 1`

3. After a packet is DMAed from the Receive Buffer Ring, the Next Page Pointer (second byte in NIC buffer header) is used to update `BNDRY` and `next_pkt`.

`next_pkt = Next Page Pointer`

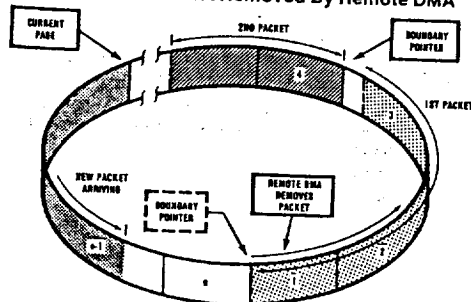
`BNDRY = Next Page Pointer - 1`

If `BNDRY < PSTART` then `BNDRY = PSTOP - 1`

Note the size of the Receive Buffer Ring is reduced by one 256-byte buffer; this will not, however, impede the operation of the NIC.

In StarLAN applications using bus clock frequencies greater than 4 MHz, the NIC does not update the buffer header information properly because of the disparity between the network and bus clock speeds. The lower byte count is copied twice into the third and fourth locations of the buffer header and the upper byte count is not written. The upper byte count, however, can be calculated from the current next page pointer (second byte in the buffer header) and the previous next page pointer (stored in memory by the CPU). The following routine calculates the upper byte count and allows StarLAN applications to be insensitive to bus clock speeds. `Next_pkt` is defined similarly as above.

1st Received Packet Removed By Remote DMA



TL/F/9345-15

`upper byte count = next page pointer - next_pkt - 1`
 if (upper byte count) < 0 then
`upper byte count = (PSTOP - next_pkt)`
`+ (next page pointer - PSTART) - 1`
 if (lower byte count > 0 fch) then
`upper byte count = upper byte count + 1`

STORAGE FORMAT FOR RECEIVED PACKETS

The following diagrams describe the format for how received packets are placed into memory by the local DMA channel. These modes are selected in the Data Configuration Register.

Storage Format

AD15	AD8	AD7	AD0
Next Packet Pointer		Receive Status	
Receive Byte Count 1		Receive Byte Count 0	
Byte 2		Byte 1	

`BOS = 0, WTS = 1` in Data Configuration Register.

This format used with Series 32000 808X type processors.

AD15	AD8	AD7	AD0
Next Packet Pointer		Receive Status	
Receive Byte Count 1		Receive Byte Count 0	
Byte 1		Byte 2	

`BOS = 1, WTS = 1` in Data Configuration Register.

This format used with 68000 type processors.

Note: The Receive Byte Count ordering remains the same for `BOS = 0` or `1`

AD7	AD0
Receive Status	
Next Packet Pointer	
Receive Byte Count 0	
Receive Byte Count 1	
Byte 0	
Byte 1	

`BOS = 0, WTS = 0` in Data Configuration Register.

This format used with general 8-bit CPUs.

8.0 Packet Transmission

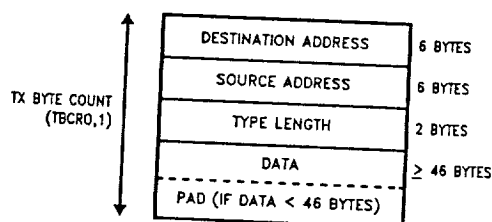
The Local DMA is also used during transmission of a packet. Three registers control the DMA transfer during transmission, a Transmit Page Start Address Register (TPSR) and the Transmit Byte Count Registers (TBCR0,1). When the NIC receives a command to transmit the packet pointed to by these registers, buffer memory data will be moved into the FIFO as required during transmission. The NIC will generate and append the preamble, synch and CRC fields.

8.0 Packet Transmission (Continued)

TRANSMIT PACKET ASSEMBLY

The NIC requires a contiguous assembled packet with the format shown. The transmit byte count includes the Destination Address, Source Address, Length Field and Data. It does not include preamble and CRC. When transmitting data smaller than 46 bytes, the packet must be padded to a minimum size of 64 bytes. The programmer is responsible for adding and stripping pad bytes.

General Transmit Packet Format



TL/F/9345-16

TRANSMISSION

Prior to transmission, the TPSR (Transmit Page Start Register) and TBCRO, TBCR1 (Transmit Byte Count Registers) must be initialized. To initiate transmission of the packet the TXP bit in the Command Register is set. The Transmit Status Register (TSR) is cleared and the NIC begins to prefetch transmit data from memory (unless the NIC is currently receiving). If the interframe gap has timed out the NIC will begin transmission.

CONDITIONS REQUIRED TO BEGIN TRANSMISSION

In order to transmit a packet, the following three conditions must be met:

1. The Interframe Gap Timer has timed out the first 6.4 μ s of the Interframe Gap (See appendix for Interframe Gap Flowchart)
 2. At least one byte has entered the FIFO. (This indicates that the burst transfer has been started)
 3. If the NIC had collided, the backoff timer has expired.
- In typical systems the NIC has already prefetched the first burst of bytes before the 6.4 μ s timer expires. The time during which NIC transmits preamble can also be used to load the FIFO.

Note: If carrier sense is asserted before a byte has been loaded into the FIFO, the NIC will become a receiver.

COLLISION RECOVERY

During transmission, the Buffer Management logic monitors the transmit circuitry to determine if a collision has occurred. If a collision is detected, the Buffer Management logic will reset the FIFO and restore the Transmit DMA pointers for retransmission of the packet. The COL bit will be set in the TSR and the NCR (Number of Collisions Register) will be incremented. If 15 retransmissions each result in a collision the transmission will be aborted and the ABT bit in the TSR will be set.

Note: NCR reads as zeroes if excessive collisions are encountered.

TRANSMIT PACKET ASSEMBLY FORMAT

The following diagrams describe the format for how packets must be assembled prior to transmission for different byte ordering schemes. The various formats are selected in the Data Configuration Register.

D15	D8 D7	D0
DA1		DA0
DA3		DA2
DA5		DA4
SA1		DA0
SA3		DA2
SA5		DA4
T/L1		T/L0
DATA 1		DATA 0

BOS = 0, WTS = 1 in Data Configuration Register.

This format is used with Series 32000, 808X type processors.

D15	D8 D7	D0
DA0		DA1
DA2		DA3
DA4		DA5
SA0		SA1
SA2		SA3
SA4		SA5
T/L0		T/L1
DATA 0		DATA 1

BOS = 1, WTS = 1 in Data Configuration Register.

This format is used with 68000 type processors.

D7	D0
DA0	
DA1	
DA2	
DA3	
DA4	
DA5	
SA0	
SA1	
SA2	
SA3	

BOS = 0, WTS = 0 in Data Configuration Register.

This format is used with general 8-bit CPUs.

Note: All examples above will result in a transmission of a packet in order of DA0, DA1, DA2, DA3... bits within each byte will be transmitted least significant bit first.

DA = Destination Address

SA = Source Address

T/L = Type/Length Field

9.0 Remote

The Remote DMA...
ets for transmission...
the Receive Buffer...
purpose slave DMA...
commands between...
There are three mod...
Read, or Send Pack...

Two register pairs a...
Remote Start Addr...
Byte Count (RBCRO...
dress register pair p...
moved while the Byt...
cate the number of b...
logic is provided to m...
and a bidirectional I/...

REMOTE WRITE

A Remote Write tran...
from the host into loc...
will read data from th...
local buffer memory b...
The DMA address will...
will be decremented a...
nated when the Rem...
count of zero.

REMOTE READ

A Remote Read tran...
from local buffer mem...
sequentially read dat...
ning at the Remote Sta...
port. The DMA address...
Counter will be decrem...
is terminated when the...
zero.

D0
DA0
DA2
DA4
DA0
DA2
DA4
T/L0
DATA 0

Configuration Register.

000, 808X type proces-

D0
DA1
DA3
DA5
SA1
SA3
SA5
T/L1
DATA 1

Configuration Register.
processors.

9.0 Remote DMA

The Remote DMA channel is used to both assemble packets for transmission, and to remove received packets from the Receive Buffer Ring. It may also be used as a general purpose slave DMA channel for moving blocks of data or commands between host memory and local buffer memory. There are three modes of operation, Remote Write, Remote Read, or Send Packet.

Two register pairs are used to control the Remote DMA, a Remote Start Address (RSAR0, RSAR1) and a Remote Byte Count (RBCR0, RBCR1) register pair. The Start Address register pair point to the beginning of the block to be moved while the Byte Count register pair are used to indicate the number of bytes to be transferred. Full handshake logic is provided to move data between local buffer memory and a bidirectional I/O port.

REMOTE WRITE

A Remote Write transfer is used to move a block of data from the host into local buffer memory. The Remote DMA will read data from the I/O port and sequentially write it to local buffer memory beginning at the Remote Start Address. The DMA address will be incremented and the Byte Counter will be decremented after each transfer. The DMA is terminated when the Remote Byte Count register reaches a count of zero.

REMOTE READ

A Remote Read transfer is used to move a block of data from local buffer memory to the host. The Remote DMA will sequentially read data from the local buffer memory, beginning at the Remote Start Address, and write data to the I/O port. The DMA address will be incremented and the Byte Counter will be decremented after each transfer. The DMA is terminated when the Remote Byte Count register reaches zero.

SEND PACKET COMMAND

The Remote DMA channel can be automatically initialized to transfer a single packet from the Receive Buffer Ring. The CPU begins this transfer by issuing a "Send Packet" Command. The DMA will be initialized to the value of the Boundary Pointer register and the Remote Byte Count register pair (RBCR0, RBCR1) will be initialized to the value of the Receive Byte Count fields found in the Buffer Header of each packet. After the data is transferred, the Boundary Pointer is advanced to allow the buffers to be used for new receive packets. The Remote Read will terminate when the Byte Count equals zero. The Remote DMA is then prepared to read the next packet from the Receive Buffer Ring. If the DMA pointer crosses the Page Stop register, it is reset to the Page Start Address. This allows the Remote DMA to remove packets that have wrapped around to the top of the Receive Buffer Ring.

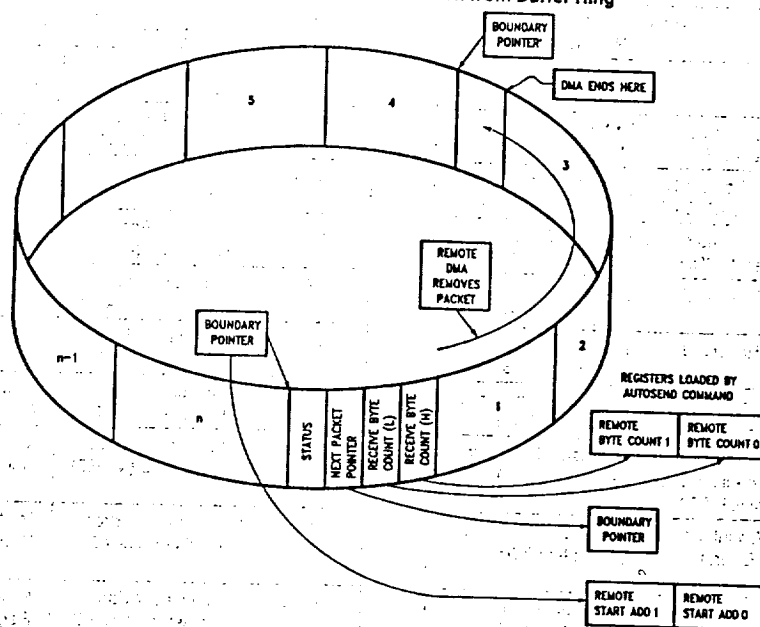
Note 1: In order for the NIC to correctly execute the Send Packet Command, the upper Remote Byte Count Register (RBCR1) must first be loaded with 0FH.

Note 2: The Send Packet command cannot be used with 88000 type processors.

10.0 Internal Registers

All registers are 8-bit wide and mapped into two pages which are selected in the Command register (PS0, PS1). Pins RA0-RA3 are used to address registers within each page. Page 0 registers are those registers which are commonly accessed during NIC operation while page 1 registers are used primarily for initialization. The registers are partitioned to avoid having to perform two write/read cycles to access commonly used registers.

Remote DMA Autoinitialization from Buffer Ring



APPENDIX F

COMMUNICATION SYSTEM

APPENDIX F: SATELLITE-TO-GROUND LINK BUDGET

• 4/3 Earth model		
Ground Elevation angle (E)		1.0°
Earth Radius (r), in 4/3 model		8500 km
Satellite elevation angle (B)		20.9°
Satellite altitude (h)		600 km
Slant Range (S)		3105 km
Frequency		2200 MHz
• Transmitter		
Transmitter power	25.0 W =	44.0 dBm
RF Line losses		-0.2 dB
Antenna gain		-5.0 dBi
EIRP		38.0 dBm
(effective isotropic radiated power)		
• Channel		
Free space loss		-169.1 dB
Atmospheric losses		0.0 dB
Signal strength @ receiver		-130.4 dBm
• Receiver RF		
Antenna gain		38.0 dBi
RF line loss (L)		-0.2 dB
Total RF carrier power (S)		-92.6 dB
• Receiver Demodulator		
Rec. noise figure (F)	290 K	2.0 dB
Total sky temp (T_a)	500 K	
T_{rec}	170 K	
T_{sys}	660 K	
kT		-170.4 dBm/Hz
Symbol rate (R_s)		1000.0 ks/s
E_b/N_o available ($S/(kT \cdot R_s)$)		17.9 dB
E_b/N_o required		2.5 dB
Signal Margin (Safety Factor)		5.4 dB

COMMUNICATIONS LINK ANALYSIS

RF Link

The maximum power P_r collected by an antenna a distance d from a transmitting antenna radiating P_t watts can be expressed

$$P_r = \frac{P_t G_t}{4\pi d^2} A_{er} \quad (1)$$

Where G_t is the gain of the transmitting antenna and A_{er} is the effective aperture of the receiving antenna. The gain (also sometimes called the directivity) is defined as the ratio of power density (W/m^2) in the direction of maximum radiation to the average power density over all directions. Gain is sometimes defined to include the efficiency of the antenna system but here we will assume 100 % efficiency and include losses due to impedance mismatch and other losses by a term to be added later. The product $P_t G_t$ is often given as the effective isotropic radiated power denoted EIRP or PEIRP.

The effective aperture A_{er} (m^2) is defined as the ratio of received power (when the antenna is oriented to extract maximum power) to the power density of the received wave. It is not simply the physical area of the antenna but it is closely related to it. The relationship between effective aperture and gain for an antenna at wavelength λ is

$$G = \frac{4\pi A_e}{\lambda^2} \quad (2)$$

The gain can also be expressed in terms of the radiation pattern of the antenna. For a pattern with a single lobe of radiation with a total solid angle Ω between half-power surfaces, $G = 4\pi/\Omega$. A useful approximation in terms of the half-power, full angle beam width in two orthogonal planes (Φ and Θ in radians or Φ° and Θ° in degrees) is

$$G \approx \frac{4\pi}{\Phi\Theta} \approx \frac{4.1 \times 10^4}{\Phi^\circ \Theta^\circ} \quad (3)$$

Table 1 lists parameters for several common antenna types.

Table 1. Antenna Parameters.

Antenna	Gain	Effective Aperture, m^2	Half-Power Beamwidth, deg
Isotropic	1	$0.079\lambda^2$	---
Half-Wave Dipole	1.64	$0.13\lambda^2$	78
Parabolic Dish (circular)	$5.5D_\lambda^2$	$0.44D^2$	$86/D_\lambda$
Rectangular Horn (optimal)	$10A_\lambda$	$0.56A$	$60/L_\lambda$
Helix (N-turn $N > 3$, $D = 0.31\lambda$, $\alpha = 12.5^\circ$)	$3.2N$	$0.25N\lambda^2$	$112/\sqrt{N}$

Note: D_λ , L_λ , A_λ are in units of wavelengths, i.e. D/λ , A/λ^2 , etc.

For example, for a 2-meter diameter parabolic dish at 2-GHz ($\lambda = 0.15$ m):

$$D_{\lambda} = 13.3; \quad G = 980 \Rightarrow 30 \text{ dB}; \quad A_e = 1.8 \text{ m}^2; \quad \text{Beam width} = 6.5^\circ$$

Now back to Equation (1) written in terms of the gain of the receiving antenna G_r ,

$$P_r = \frac{P_t G_t G_r}{L_s} \quad (4)$$

where $L_s = (4\pi d/\lambda)^2$ = the free space path loss.

So far the equations have been written for the ideal situation, i.e., no additional real world loss terms such as those due to

(1) atmospheric attenuation of the wave, which is primarily due to water vapor, O_2 and precipitation.

(2) non-ideal system components.

Allowing for terms to represent these losses L_a for (1) and L_o for (2) gives

$$P_r = \frac{P_t G_t G_r}{L_s L_a L_o} \quad (5)$$

Usually it is not the received power that is most important but the signal-to-noise ratio S/N at the detector. The available noise in an effective noise bandwidth B Hz is

$$N = kTB \quad (6)$$

where k = Boltzmann's constant (1.38×10^{-23} J/°K)
 T = Receiving system noise temperature in °K

T is the sum of two components, the antenna and receiver noise temperatures, T_a and T_e , respectively. T_e is related to the receiver noise figure F at a standard reference temperature of 290 °K

$$T_e = 290(F - 1) \text{ °K} \quad (7)$$

Introducing the noise expression (6) into Equation (5) gives

$$\frac{S}{N} = \frac{P_r}{N} = \frac{P_t G_t G_r}{kTB L_s L_a L_o} \quad (8)$$

Digital Communication Systems

In a digital communication system the quality of the recovered data at the detector output is best described in terms of the probability of bit error P_e (or bit error rate). P_e is a function of the ratio of energy per bit E_b to the noise power spectral density N_o , which for white noise is simply N/B . The exact relationship of E_b/N_o required to give a certain probability of bit error is a function of the type of modulation and demodulation systems, but the link analysis can be written in terms of a required value of E_b/N_o to give the desired P_e for

a given system. For example a 10^{-4} probability of error requires a E_b/N_o of around 10 dB for an optimum system. Denoting the required value as $[E_b/N_o]_{req}$ and assuming that all the received power is in the modulation (bits) results in $P_r = E_b R$ where R is the bits/sec. Substituting this value for P_r in Equation (8) gives

$$[E_b/N_o]_{req} = \frac{P_t G_t G_r}{k T R L_a L_s L_o} \quad (9)$$

Introducing a multiplicative safety factor called the link margin M , Equation (9) can be written

$$M = \frac{P_t G_t G_r}{k T R L_a L_s L_o [E_b/N_o]_{req}} \quad (10)$$

The link margin is most often expressed in dB. Converting Equation (10) to dB gives

$$M(\text{dB}) = P_t(\text{dBW}) + G_t(\text{dB}) + G_r(\text{dB}) - R(\text{dB b/S}) + 228.6 \text{ dB} \\ - T(\text{dB } ^\circ\text{K}) - L_a(\text{dB}) - L_s(\text{dB}) - L_o(\text{dB}) - [E_b/N_o]_{req}(\text{dB}) \quad (11)$$

As an example of the link analysis assume the following system parameters:

$$f = 2 \text{ GHz } (\lambda = 0.15 \text{ m})$$

$$T_a = 30 \text{ } ^\circ\text{K}$$

$$d = 1000 \text{ km}$$

$$F = 2 \text{ dB}$$

$$P_t = 5 \text{ W}$$

$$G_r = 3 \text{ dB}$$

$$G_t = 3 \text{ dB}$$

$$[E_b/N_o]_{req} = 10 \text{ dB}$$

$$R = 30 \text{ kb/s}$$

$$L_a = 0.3 \text{ dB}; L_o = 1 \text{ dB}$$

$$L_s = (4\pi d/\lambda)^2 = [4\pi(10^6)/0.15]^2 \Rightarrow 158 \text{ dB}$$

$$T_e = 290(F - 1) = 290(1.58 - 1) = 170 \text{ } ^\circ\text{K}$$

$$T = 30 + 170 = 200 \text{ } ^\circ\text{K} \Rightarrow 23.0 \text{ dB}$$

Now using Equation (12)

$$M = 7.0 + 3 + 3 - 44.8 + 228.6 - 23.0 - 158 - 0.3 - 1.0 - 10 = 4.5 \text{ dB}$$

Effect of Different Signalling Modes

The required (energy per bit)/(noise spectral density), $[E_b/N_o]_{req}$ for a specified bit error rate depends on the methods of modulation and demodulation of the digital signal. Table 2 and Figure 1 give the error performance for some of the most common digital signalling methods:

- (1) OOK - On-Off Keying
- (2) BPSK - Binary Phase-Shift Keying (coherent detection only)
- (3) FSK - Frequency Shift Keying

- (4) DPSK - Differential Phase-Shift Keying
- (5) QPSK - Quadrature Phase-Shift Keying (coher. det. only)

In each case, ideal detection is assumed, i.e. no bit or carrier synchronization errors, matched filters, etc. Actual systems will be degraded somewhat from these optimum comparison numbers. In several cases a choice exists between coherent detection (requiring the carrier with proper frequency and phase) and simpler incoherent detection with somewhat degraded performance. The tradeoff is the complexity required with the coherent detection schemes. The last column in Table 2 gives the required E_b/N_o for a probability of bit error of 10^{-4} for optimum signalling systems. Note from inspection of Figure 1 that for all of these systems, an order of magnitude decrease in P_e only requires about a 1 dB increase in (E_b/N_o) for P_e less than about 10^{-4} .

Table 2. Comparison of Signalling Modes

Signalling method	Bandwidth required	Error rate, P_e	$[E_b/n_o]$ (dB) for $P_e = 10^{-4}$
OOK(noncoher.)	R	$\frac{1}{2}\{\text{Exp}[-\frac{1}{2}(E_b/N_o)]\}$	11.9
OOK (coherent)	R	$Q(\sqrt{E_b/N_o})$	11.4
BPSK (coherent)	R	$Q(\sqrt{2E_b/N_o})$	8.4
FSK (noncoher.)	$2\Delta f + R$	$\frac{1}{2}\{\text{Exp}[-\frac{1}{2}(E_b/N_o)]\}$	12.5
FSK (coherent)	$2\Delta f + R$	$Q(\sqrt{E_b/N_o})$	11.4
DPSK (coherent)	R	$\frac{1}{2}\{\text{Exp}[-(E_b/N_o)]\}$	9.3
QPSK (coherent)	R/2	$Q(\sqrt{2E_b/N_o})$	8.4

Note: The function Q is defined $Q(z) = (1/\sqrt{2\pi}) \int_z^{\infty} \exp(-x^2/2) dx$. Numerical values of $Q(z)$ are found in mathematical tables.

Sky-Noise Temperature and Atmospheric Effects

It is convenient to represent an antenna connected to the input of a receiver as a resistor (matched to the receiver input) whose temperature represents the effective noise of the sky as seen through the antenna. This average antenna temperature then will depend primarily on the frequency and the pointing direction of the antenna (often taken as 15° elevation for reference). The main sources of sky noise (antenna temperature) are shown in Figure 2. In the 1 MHz to 1 GHz region the dominant source is galactic noise, which is a maximum in the direction of the galactic plane. Beyond 1 GHz, noise due to atmospheric water vapor and oxygen becomes increasingly important and is also a strong function of the elevation angle of the antenna. The atmospheric noise is caused by the absorption of energy by the atmospheric constituents that then reradiate. Since the atmosphere absorbs energy in the GHz region it also is important to consider the effect of this attenuation on radio signals traversing the atmosphere.

The region between 300 MHz and 10 GHz is called the radio window. Impairments in communications signals occur due to the atmosphere even in this so-called window region. Atmospheric absorption is due primarily to (1) molecular oxygen (2) water vapor (uncondensed) (3) water in rain, fog, clouds, snow and hail (4) free electrons in the ionosphere.

Figure 3 shows the attenuation coefficients for O_2 and H_2O given in dB/km as functions of frequency. Note the strong absorption peaks at 21 GHz due to H_2O and at 60 GHz due to O_2 . The total one-way attenuation due to O_2 and water vapor for a radio wave passing vertically through the atmosphere is shown in Figure 4 for the GHz range. Figure 5 shows the O_2 and H_2O absorption for several elevation angles of propagation through the atmosphere. A more detailed set of curves for the 1 to 20-GHz region for various elevation angles is shown in Figure 6 for O_2 and water vapor absorption. A composite plot of the atmospheric absorption due to free electrons, O_2 and water vapor is shown in Figure 7.

Attenuation due to precipitated water in the atmosphere is shown in Figures 8 and 9 for radiowaves from 1 to 100 GHz passing through the atmosphere at various elevation angles. This absorption can be extreme under conditions of heavy precipitation at frequencies beyond about 10 GHz.

All of the attenuation factors described above are small at frequencies below about 6 GHz except at very low elevation angles.

A couple of other atmospheric effects that may sometimes need to be considered are radio wave ray bending due to refraction and radiowave scintillations. The angle deviations due to height variations of the refractive index of the atmosphere will generally be less than half of a degree. Ionospheric scintillations are most severe in the equatorial zone where fades of several dB can occur for several seconds or more. There are also some effects observed in the auroral zone, but in general, scintillation fading outside the equatorial zone is ignored.

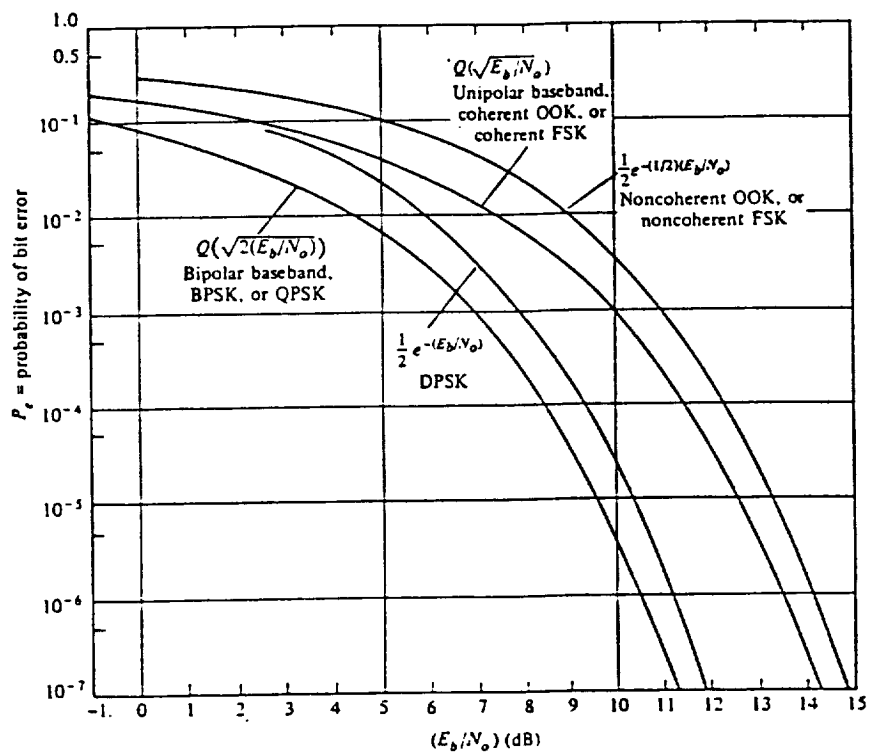


Figure 1. Comparison of probability of bit error for several optimum digital signalling methods.

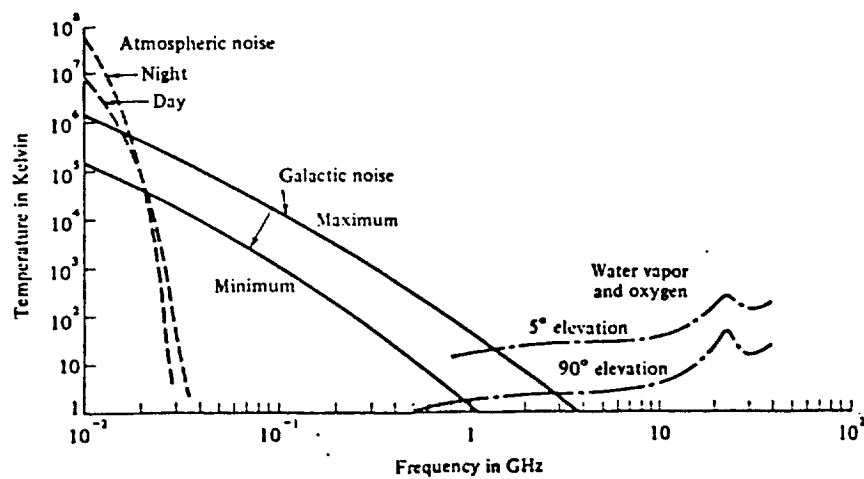
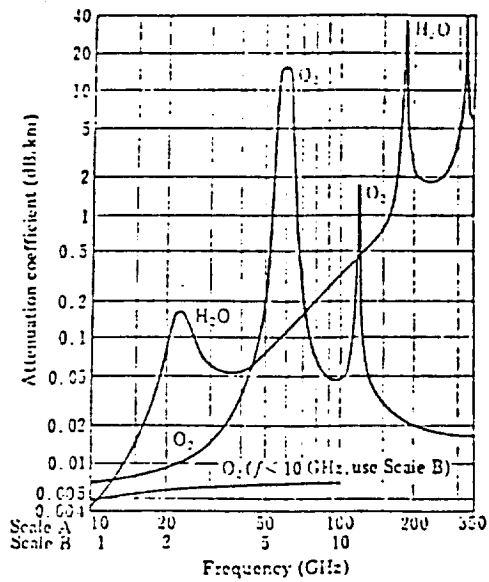
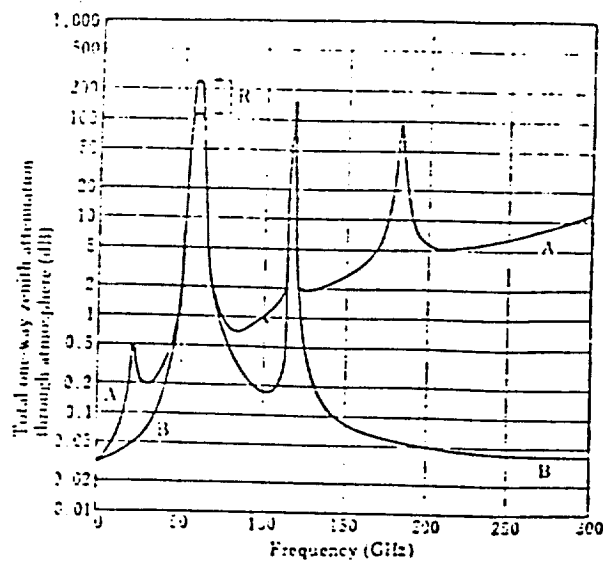


Figure 2. Average sky noise temperatures.



Surface pressure: 1 atm (1013.6 mb)
 Surface temperature: 20°C
 Surface water vapor density: 7.5 g/m³

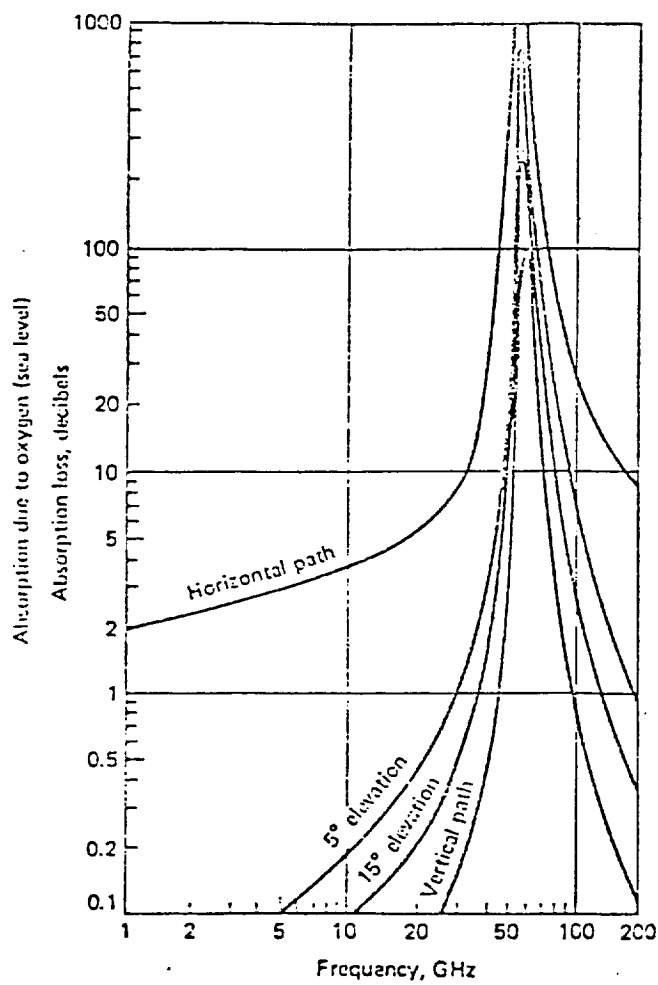
Figure 3. Specific attenuation by atmospheric O₂ and H₂O vapor.



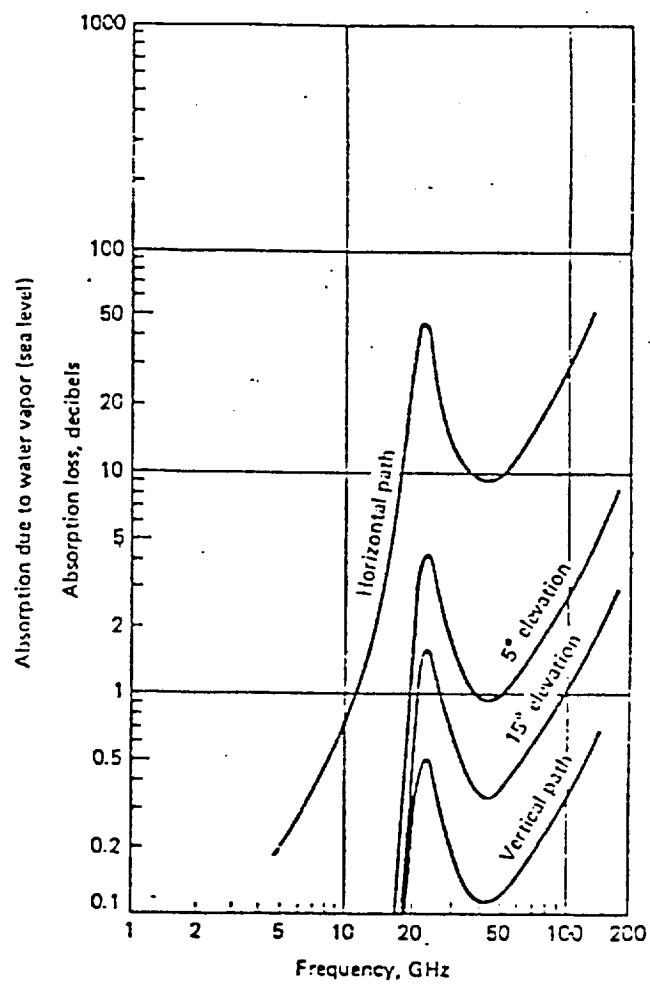
Surface water vapor density
 A: 7.5 g/m³
 B: 0 g/m³ (dry atmosphere)
 R is the range of variation due to fine structure

Figure 4. Total one-way zenith attenuation through the atmosphere.

ORIGINAL PAGE IS
 OF POOR QUALITY



(a)



(b)

Figure 5. Absorption of radiowaves in the atmosphere by molecular systems, (a) O_2 (b) H_2O .

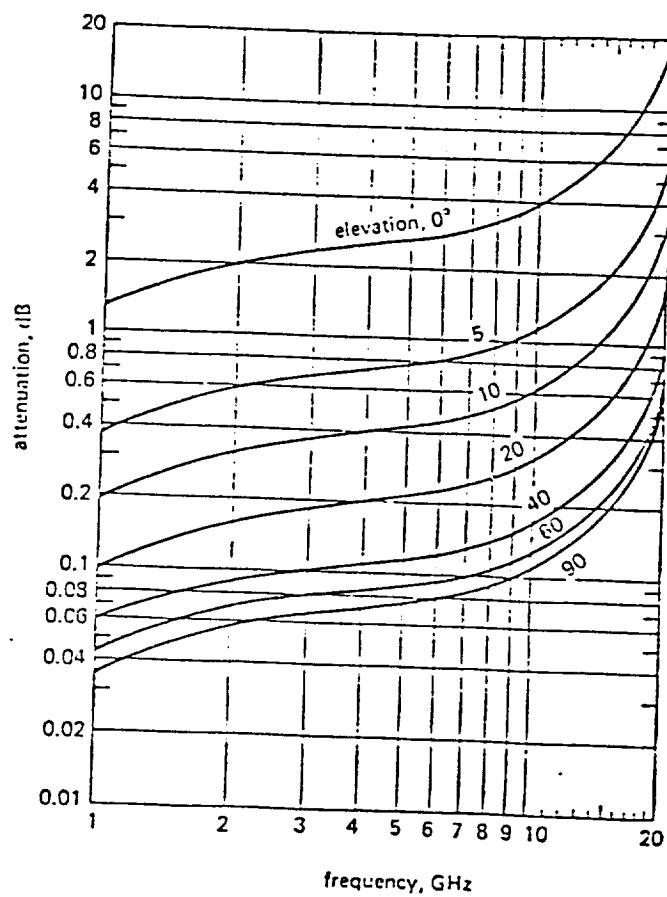


Figure 6. Atmospheric attenuation due to oxygen and water vapor.

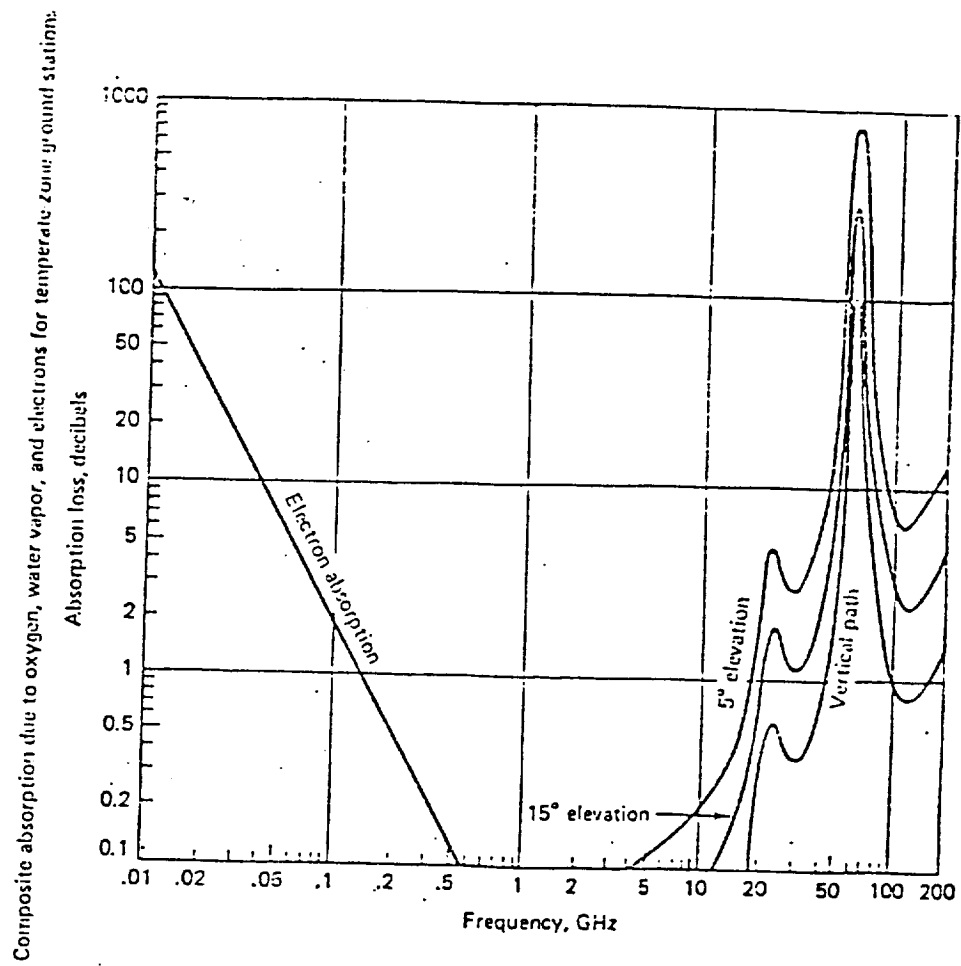


Figure 7. Absorption in the atmosphere caused by molecular species and electrons.

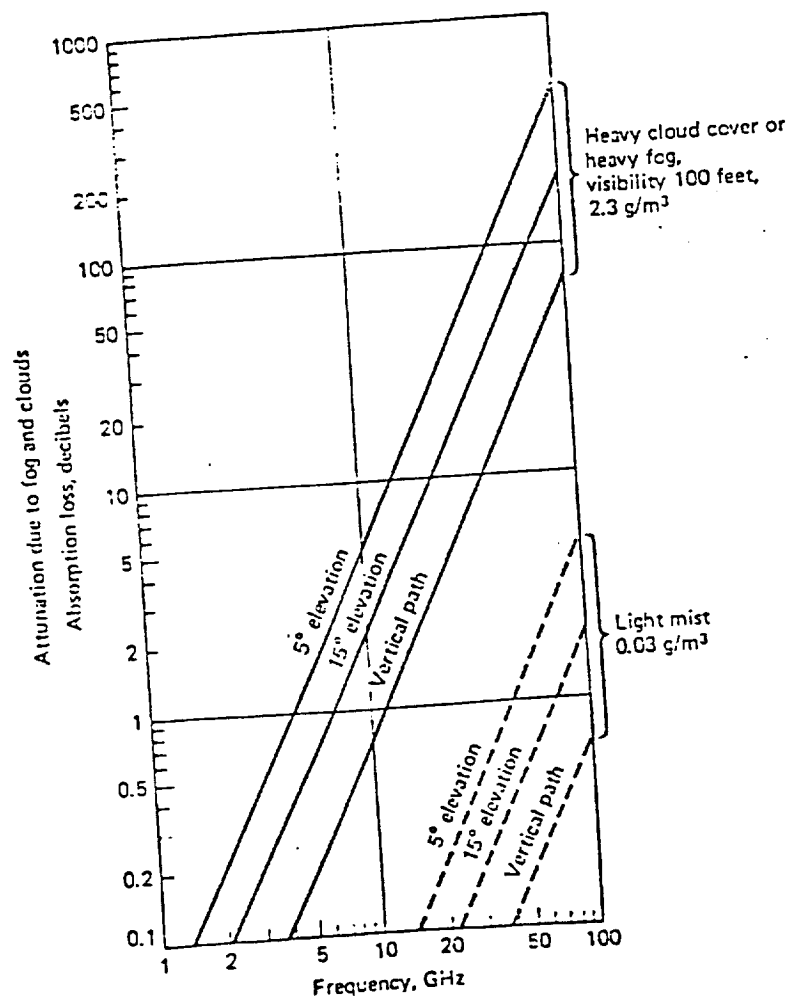


Figure 8. Typical absorption due to fog, mist and clouds.

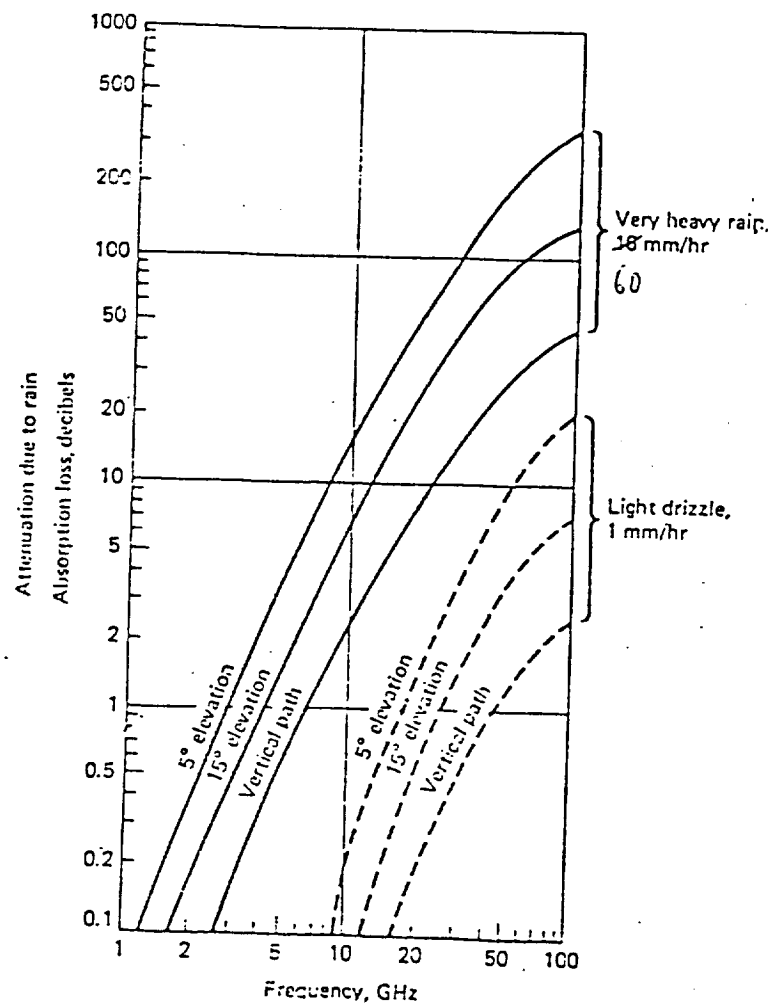


Figure 9. Typical absorption due to rain in the atmosphere.

APPENDIX G

ELF SATELLITE STRUCTURE AND CONFIGURATION

WEITZMANN CONSULTING, Inc.

AEROSPACE ENGINEERING

47 CASA WAY
SAN FRANCISCO, CALIFORNIA 94123-1206
TELEPHONE: (415) 922-4059

April 18, 1990

Space Dynamics Lab/USU
Engineering Building
Room L206B
Logan, Utah 84327-4140

Attn.: Mr. Scott Jamieson

Subject: E-Field Booms

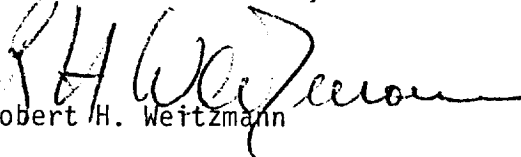
Dear Mr. Jamieson:

After our discussion on the on-axis boom, I thought the enclosed information on our type 87400 boom might be of interest to you for your on-axis application.

I think this 1.9-meter extension boom could be modified to suit your needs. We have built some 42 units for the Naval Research Lab, who is using the boom as a transmitting antenna on classified spacecrafts.

Sincerely,

WEITZMANN CONSULTING, INC.


Robert H. Weitzmann

enc.

WEITZMANN CONSULTING, Inc.

AEROSPACE ENGINEERING

SPECIFICATION NUMBER 87400, Revision C (June, 1989)

75 INCH STACER* ANTENNA

47 CASA WAY
SAN FRANCISCO, CALIFORNIA 94123
TELEPHONE: (415) 822-4059

1. DESCRIPTION

The STACER element is fabricated from beryllium copper spring material. The strip material is formed to a fixed coil diameter and helix angle, selected to provide significant overlap of adjacent coils. The spring energy of the stowed Stacer causes it to rapidly self extend when released. An important characteristic of the STACER is the observation that the element forms one coil at a time, such that a fully formed tubular element emerges from the housing. The extended Stacer element behaves like a continuous thin walled tube, exhibiting cantilever bending stiffness, and subject to failure by localized buckling.

In this application, the strip material will be coated on the outside with a organically bonded molybdenum disulfide film to reduce surface reflectivity, and to provide a lubricating film between coils. Stiffening clips will be included to provide cantilever stiffness from the canister end. A Deployment Assist Device, using coil springs, will also be included to reliably initiate the Stacer extension. Deployment will be initiated by a ICI Americas electro-explosive pin puller containing redundant bridge wires. A safety pin will be provided for safe pre-launch handling. The Stacer element and its housing will be isolated from ground.

SPECIFICATIONS

2. Dimensions

Refer to Interface Control Drawing Number 87400-MMC-ICD.

]C

3. Mass Properties

Total Mechanism Mass: approximately 1.88 pounds

]C

Stacer Element Mass Rate: approximately 0.1 pounds per foot

4. PERFORMANCE PARAMETERS

4.1 Deployed Length

The deployment stroke will be 72 inches \pm 2 inch under simulated zero G conditions. This condition will be accomplished by deploying the Stacer horizontally on a smooth sliding surface, so as to avoid cantilever bending forces on the Stacer element.

]C

4.2 Deployed Pointing Accuracy

The Stacer Tip shall fall within a 2 inch radius target measured from the nominal deployment centerline, as shown in the Interface Control Drawing. The simulated zero G environment for this measurement shall be established by pointing the Stacer element vertically upward to measure straightness.

4.3 Deployment Loads

The Stacer element may be safely deployed up, down, or horizontally in a one G environment, however the length and pointing accuracy requirements of section 4.2 may not be satisfied.

4.4 Deployment Velocity

The Stacer element will be free popped, causing it to extend very rapidly. The deployment speed or time will not be measured.

4.5 Deployment Initiation

Deployment is initiated by a dual bridge electro-explosive pin puller. The maximum no fire current is 100 milliamps for 5 minutes, the minimum all fire current is 550 milliamps for 10 milliseconds, and the bridge resistance is 4 to 5 ohms. Applying power to either or both of the E.E.D. filament wires will initiate deployment without hesitation. The filament wires might short together, or to ground after firing.

4.6 Deployment Confirmation

No devices will be included in the mechanism for deployment confirmation.

4.7 Extended Antenna Properties

4.7.1 Stacer Element Flexural Properties

Boom Element Average Flexural Stiffness:	$EI = 12,000 \text{ lb in}^2$
Spring Constant for Tip Applied Loads: This value includes the degree of fixity afforded by the Stacer stiffening clips.	$K_t = 0.09 \text{ lb/in }]B$
Critical Buckling Moment:	$M_b = 13 \text{ ft lb}$
Approximate Flexural Damping:	$\frac{dU}{dn} = 0.002 X^{2.35} + 0.05 (X - \frac{0.015}{K_t})$

This is the energy decrement in inch lbs per cycle, where X is the tip deflection in inches. The first term is hysteretic damping and the second term is friction damping (for $X > 0.015/K_t$).

4.8 Environment

4.8.1 On-Orbit, Non-Operational and Operational

The mechanism will survive the following environment without degradation of performance:

Configuration: Stowed, Extending, or Fully Extended

Temperature Limits: -45'C to 65'C

]B

Pressure: Atmospheric to Hard Vacuum

Acceleration: 10 G's DC, 3 axes (stowed)

Spin Rates: 45 RPM maximum (not during extension)

5. ELECTRICAL PROPERTIES

5.1 Electrical Interface

The Electro-Explosive Device (EED) connector will be a Cannon MS-3470 L10-6P. The pin assignments are as follows:

pin B: filament 1	pin E: filament 2	Pin A: not used
pin C: filament 1	pin F: filament 2	Pin D: not used

The signal connection is made via a customer provided filter box and pigtail lead, as shown in the Interface Control Drawing (87400-NRL-ICD).

]C
]C

5.2 Grounding

The Electro-Explosive Device (EED) body connector will be grounded by a wire attached to filter box body which has a ground lug, as shown in the ICD.

]C
]C

5.3 Insulation and Capacitance

The Stacer element and canister shall be insulated from spacecraft ground by at least 1 Mohm, both before and after deployment. Insulation from ground before deployment is for test purposes only, and not experiment critical. Insulation after deployment is experiment critical. The capacitive coupling to ground shall be 60 picofarads or less, including a circuit path through the grounded EED body (after deployment) not including the internal capacity of the filter box. The ground plane stops just forward of the mounting feet.

]B
]C
]C
]C

5.4 Conductivity

Resistance from the electrical attachment stud to the Stacer element shall be less than 0.1 ohms. End to end resistance of the stacer element shall be less than 0.1 ohms at room temperature.

5.5 Surface Conductivity

The exterior surface of the Stacer element will be coated with non-conductive Molybdenum Disulfide. The housing will have various non-conductive surfaces.

6. QUALITY CONTROL

6.1 Purchased Components

All purchased components will be procured with manufacturers certifications and 100% inspected for compliance to manufacturers specifications, upon receipt at WCI. Electro-explosive devices will be procured with 100% visual inspection, bridge resistance measurements, and X-ray examination.

6.2 Fabricated Components

All materials will be procured with certifications. Traceability from source through manufacturing processes and delivery will be provided. Machined components will be 100% inspected for compliance with drawing specifications.

6.3 Test and Inspection Equipment

All required test and measuring equipment will be kept in current calibration, traceable to the National Bureau of Standards.

6.4 Storage

All materials, fabricated parts, and purchased components will be kept in controlled storage by the WCI quality control engineer.

7. TESTING

All units will be tested at the point of manufacture. Because of the special nature of the Stacer element, expert restoring of the mechanism, after testing, is critical to proper functioning. Additional testing and restoring is, therefore, at the buyer's responsibility unless supervised or performed by our personnel.

7.1 TEST PROGRAM

Each delivered unit will be subjected to the following test sequence:

- Physical and Electrical Measurements
- Functional Test and Measurements
- Three Axis Random Vibration
- Post Vibration Functional Test

7.1.1 Physical Measurements

The physical dimensions and mass properties, as shown on the Interface Control Drawing, will be measured and mounting feet aligned by a fixture.

7.1.2 Electrical Measurements

The electrical properties, as stated in Section 5 of this document will be measured.

7.1.3 Functional Test

The deployment test will be initiated by applying power to one or both of the pin puller bridge wires. The Stacer will deploy horizontally on a smooth sliding surface, so as to avoid cantilever bending forces on the Stacer element. The stroke will be measured in the horizontal position, and then the mechanism will be rotated to a vertical position to measure total indicated runout. The mechanism will then be stowed in accordance with the established procedure, and the pin puller will be replaced.

7.1.4 Three Axis Random Vibration

A vibration fixture survey will be conducted. Each unit will be subjected to the random vibration spectrum provided by the customer, along three axes (one minute each axis). The fixture will allow for simultaneous testing of several units.

8. TRANSPORTATION AND STORAGE

For transportation and storage, the units will be mounted in controlled atmosphere aluminum containers in compliance with MIL-STD-108.

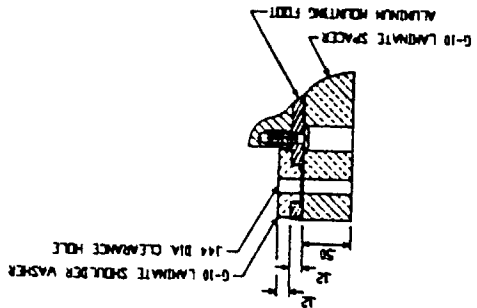
A shelf life of two years, after final restoring of the Stacer, and before flight deployment is recommended.

NOTICE: This design was originated by, and is the exclusive property of Weitzmann Consulting Inc., San Francisco, CA. It is disclosed in confidence with the understanding that no reproduction or other use of the information is authorized without the specific agreement by W.C.I.

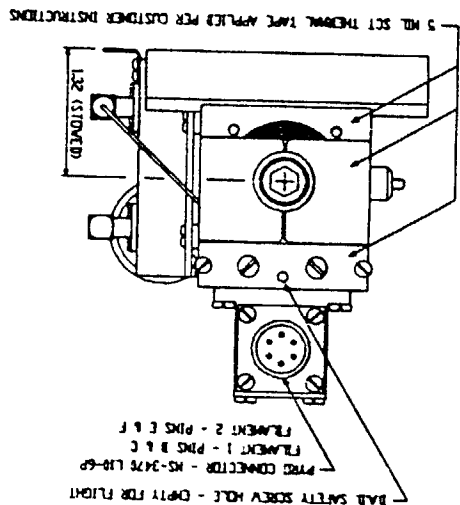
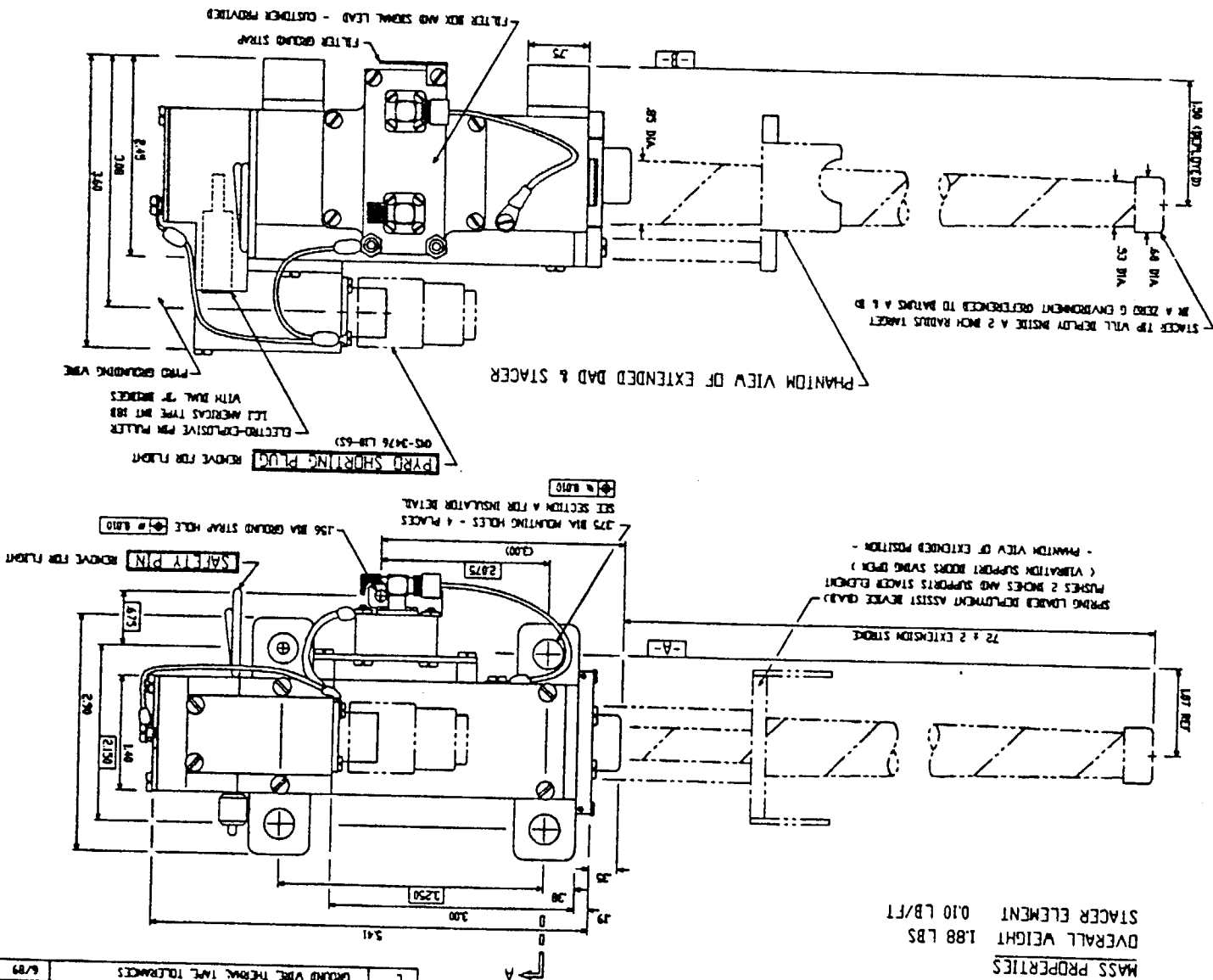
* Manufactured by Weitzmann Consulting Inc., San Francisco, CA, under license from Ametek, Inc.. The trademark STACER and U.S. Patent Numbers 3,467,329; 3,587,658; 3,680,802; 3,743,267; 3,822,874; and 3,863,405 are the property of Ametek, Inc.

DATE	DESCRIPTION	8	NEW DRAWING TO INCLUDE FILTER BOX	12/88
		C	GROUND WIRE, THERMAL TAP, TOLERANCES	6/89

MOUNTING FOOT DETAIL - SECTION A



MASS PROPERTIES
OVERALL WEIGHT 1.88 LBS
STACER ELEMENT 0.10 LB/FT



NOTE: SHOULDER WASHERS NOT SHOWN IN THESE VIEWS

APPROVALS	DATE	REMARKS	DATE	REMARKS
APPROVALS	12/08	75 INCH NPL STACED ANTENNA - INTERFAC CONTROL BRAYING	8/7/00 - 10/1/00	8/7/00 - 10/1/00

WEITZMANN CONSULTING INC.
47 CASH WAY, SAN FRANCISCO 94123
(415) 822 - 4069
AEROSPACE ENGINEERING

Sec	Typ	Mass	A	B	C	X	Y	Z	Rot
1	3	0.353	0.269	0.1020	0.0000	0.1165	0.0000	0.0300	3
2	3	0.353	0.269	0.1020	0.0000	-0.1165	0.0000	0.0300	3
3	3	0.154	0.131	0.0690	0.0000	0.0000	0.1000	0.0300	4
4	10	2.021	0.225	0.3530	0.0000	0.0000	0.0000	0.0000	1
5	10	0.125	0.038	0.1520	0.0000	0.1165	0.0000	0.0630	4
6	10	0.125	0.038	0.1520	0.0000	-0.1165	0.0000	0.0630	4
7	9	0.625	0.038	0.0000	0.0000	0.1165	-0.1525	0.0630	4
8	9	-0.563	0.036	0.0000	0.0000	0.1165	-0.1525	0.0630	4
9	9	0.625	0.038	0.0000	0.0000	-0.1165	-0.1525	0.0630	4
10	9	-0.563	0.036	0.0000	0.0000	-0.1165	-0.1525	0.0630	4
11	9	0.625	0.038	0.0000	0.0000	0.1165	0.1525	0.0630	4
12	9	-0.563	0.036	0.0000	0.0000	0.1165	0.1525	0.0630	4
13	9	0.625	0.038	0.0000	0.0000	-0.1165	0.1525	0.0630	4
14	9	-0.563	0.036	0.0000	0.0000	-0.1165	0.1525	0.0630	4
15	2	0.644	0.225	0.0000	0.0000	0.0000	0.0000	0.1890	4
16	2	0.644	0.225	0.0000	0.0000	0.0000	0.0000	-0.1640	4
17	2	2.727	0.225	0.0000	0.0000	0.0000	0.0000	-0.0070	4
18	4	0.400	0.065	0.1600	0.0000	0.0000	0.0000	0.1650	1
19	10	0.400	0.070	0.1890	0.0000	0.0000	0.0000	0.0950	1
20	7	0.312	0.060	0.0600	0.0800	-0.0905	-0.1850	0.0450	4
21	7	0.312	0.060	0.0600	0.0800	0.0905	-0.1850	0.0450	4
22	7	0.312	0.060	0.0600	0.0800	0.0905	0.1850	0.0450	4
23	7	0.312	0.060	0.0600	0.0800	-0.0905	0.1850	0.0450	4
24	7	0.312	0.110	0.0200	0.0800	0.0000	-0.0590	0.0450	4
25	7	0.300	0.058	0.1270	0.0380	0.0000	-0.1615	0.1100	4
26	7	6.364	3.940	3.9400	0.2900	0.0000	0.0000	-0.0820	4
27	7	0.132	0.058	0.0660	0.0510	0.0000	0.1800	0.1560	4
28	7	0.132	0.058	0.0660	0.0510	0.0000	0.1800	-0.1130	4
29	3	0.111	0.335	0.0254	0.0000	0.0000	0.1340	0.0120	1
30	3	0.089	0.025	0.2690	0.0000	-0.1675	0.0000	0.0120	2
31	3	0.089	0.025	0.2690	0.0000	0.1675	0.0000	0.0120	2
32	3	0.034	0.102	0.0254	0.0000	-0.1165	-0.1344	0.0120	1
33	3	0.034	0.102	0.0254	0.0000	0.1165	-0.1344	0.0120	1
34	3	0.066	0.025	0.2000	0.0000	-0.0650	-0.0350	0.0120	2
35	3	0.066	0.025	0.2000	0.0000	0.0650	-0.0350	0.0120	2
36	3	0.043	0.131	0.0254	0.0000	0.0000	0.0655	0.0120	1
37	1	1.200	1.500	0.0000	0.0000	0.0000	0.0000	0.8250	2

Total moment of inertia about the C of M
of the satellite system

Ixx	Iyx	Izx
Ixy	Iyy	Izy
Ixz	Iyz	Izz

9.606890 0.000000 0.000000

0.000000	9.564749	0.004632
0.000000	0.004632	16.785563

Distances from datum to C of M of system

Rx =	0.000000
Ry =	0.000005
Rz =	0.040281

Total Mass = 18.413820

Sec	Typ	Mass	A	B	C	X	Y	Z	Rot
1	3	0.353	0.269	0.1020	0.0000	0.1165	0.0000	0.0300	3
2	3	0.353	0.269	0.1020	0.0000	-0.1165	0.0000	0.0300	3
3	3	0.154	0.131	0.0690	0.0000	0.0000	0.1000	0.0300	4
4	10	2.021	0.225	0.3530	0.0000	0.0000	0.0000	0.0000	1
5	10	0.125	0.038	0.1520	0.0000	0.1165	0.0000	0.0630	4
6	10	0.125	0.038	0.1520	0.0000	-0.1165	0.0000	0.0630	4
7	9	0.625	0.038	0.0000	0.0000	0.1165	-0.1525	0.0630	4
8	9	-0.563	0.036	0.0000	0.0000	0.1165	-0.1525	0.0630	4
9	9	0.625	0.038	0.0000	0.0000	-0.1165	-0.1525	0.0630	4
10	9	-0.563	0.036	0.0000	0.0000	-0.1165	-0.1525	0.0630	4
11	9	0.625	0.038	0.0000	0.0000	0.1165	0.1525	0.0630	4
12	9	-0.563	0.036	0.0000	0.0000	0.1165	0.1525	0.0630	4
13	9	0.625	0.038	0.0000	0.0000	-0.1165	0.1525	0.0630	4
14	9	-0.563	0.036	0.0000	0.0000	-0.1165	0.1525	0.0630	4
15	2	0.644	0.225	0.0000	0.0000	0.0000	0.0000	0.1890	4
16	2	0.644	0.225	0.0000	0.0000	0.0000	0.0000	-0.1640	4
17	2	2.727	0.225	0.0000	0.0000	0.0000	0.0000	-0.0070	4
18	4	1.590	0.065	0.1600	0.0000	0.0000	0.0000	0.1650	1
19	10	0.400	0.070	0.1890	0.0000	0.0000	0.0000	0.0950	1
20	7	0.312	0.060	0.0600	0.0800	-0.0905	-0.1850	0.0450	4
21	7	0.312	0.060	0.0600	0.0800	0.0905	-0.1850	0.0450	4
22	7	0.312	0.060	0.0600	0.0800	0.0905	0.1850	0.0450	4
23	7	0.312	0.060	0.0600	0.0800	-0.0905	0.1850	0.0450	4
24	7	0.312	0.110	0.0200	0.0800	0.0000	-0.0590	0.0450	4
25	7	0.300	0.058	0.1270	0.0380	0.0000	-0.1615	0.1100	4
26	7	6.364	0.358	0.3580	0.2900	0.0000	0.0000	-0.0820	4
27	7	0.132	0.058	0.0660	0.0510	0.0000	0.1800	0.1560	4
28	7	0.132	0.058	0.0660	0.0510	0.0000	0.1800	-0.1130	4
29	3	0.111	0.335	0.0254	0.0000	0.0000	0.1340	0.0120	1
30	3	0.089	0.025	0.2690	0.0000	-0.1675	0.0000	0.0120	2
31	3	0.089	0.025	0.2690	0.0000	0.1675	0.0000	0.0120	2
32	3	0.034	0.102	0.0254	0.0000	-0.1165	-0.1344	0.0120	1
33	3	0.034	0.102	0.0254	0.0000	0.1165	-0.1344	0.0120	1
34	3	0.066	0.025	0.2000	0.0000	-0.0650	-0.0350	0.0120	2
35	3	0.066	0.025	0.2000	0.0000	0.0650	-0.0350	0.0120	2
36	3	0.043	0.131	0.0254	0.0000	0.0000	0.0655	0.0120	1

Total moment of inertia about the C of M
of the satellite system

Ixx	Iyx	Izx
Ixy	Iyy	Izy
Ixz	Iyz	Izz
0.466860	0.000000	0.000000
0.000000	0.424729	0.004626
0.000000	0.004626	0.459678

Distances from datum to C of M of system

Rx = 0.000000
Ry = 0.000005
Rz = -0.002822

Total Mass = 18.403820

APPENDIX H

THERMAL CONTROL SYSTEM

APPENDIX H1

Table H-1 List of nodes and a description of each for the SINDA 1987/ANSI computer model.

<u>Node #</u>	<u>Description</u>	<u>Node #</u>	<u>Description</u>
1	top plate	22	battery pack
2	top plate	23	battery pack
3	top plate	24	battery pack
4	top plate	25	electronic components
5	top plate	26	electronic components
6	bottom plate	27	electronic components
7	bottom plate	28	cold-gas tank
8	bottom plate	29	cold-gas tank
9	bottom plate	30	sun-sensor camera
10	bottom plate	31	sun-sensor camera
11	side panel	32	cold-gas nozzle
12	side panel	33	cold-gas nozzle
13	side panel	34	support structure tube
14	side panel	35	single boom
15	honeycomb plate	36	quadrapole housing
16	honeycomb plate	37	boom
17	honeycomb plate	38	boom
18	honeycomb plate	39	boom
19	honeycomb plate	40	boom
20	battery pack	41	horizon-sensor camera
21	battery pack	42	magnetometer
		43	magnetometer

APPENDIX H2

BCD 3THERMAL LPCS

END

BCD 3NODE DATA

1,290.0,118.16
2,290.0,118.16
3,290.0,118.16
4,290.0,118.16
5,290.0,118.16
6,290.0,118.16
7,290.0,118.16
8,290.0,118.16
9,290.0,118.16
10,290.0,118.16
11,290.0,459.63
12,290.0,459.63
13,290.0,459.63
14,290.0,459.63
15,290.0,1.71
16,290.0,1.71
17,290.0,1.71
18,290.0,1.71
19,290.0,1.71
20,290.0,253.48
21,290.0,253.48
22,290.0,253.48
23,290.0,253.48
24,290.0,253.48
25,290.0,674.1
26,290.0,1506.9
27,290.0,674.1
28,290.0,287.98
29,290.0,287.98
30,290.0,66.0
31,290.0,66.0
32,290.0,19.5
33,290.0,19.5
34,290.0,255.53
35,290.0,2210.0
36,290.0,325.0
37,290.0,2210.0
38,290.0,2210.0
39,290.0,2210.0
40,290.0,2210.0
41,290.0,586.95
-80,3.0,0.0
-90,290.0,0.0

END

BCD 3SOURCE DATA

20,0.25
21,0.25
22,0.25

23,0.25
24,0.25
25,3.333
26,3.333
27,3.333
1,18.984
2,18.984
3,18.984
4,18.984
5,18.984
11,12.67
12,12.67
13,12.67
14,12.67
32,7.203
33,7.203
35,7.7878
37,7.7878
38,7.7878
39,7.7878
40,7.7878

END

BCD 3CONDUCTOR DATA

12,1,2,0.1499
13,1,3,0.380
14,1,4,0.1499
112,1,12,0.511
23,2,3,0.380
25,2,5,0.1499
211,2,11,0.511
34,3,4,0.38
35,3,5,0.38
334,3,34,0.798
45,4,5,0.1499
413,4,13,0.511
514,5,14,0.511
67,6,7,0.1499
68,6,8,0.38
69,6,9,0.1499
612,6,12,0.511
78,7,8,0.38
710,7,10,0.1499
711,7,11,0.511
89,8,9,0.38
810,8,10,0.38
836,8,36,7.97
910,9,10,0.1499
913,9,13,0.511
1014,10,14,0.511
1115,11,15,0.309
1112,11,12,0.358
1114,11,14,0.358
1132,11,32,0.327
1213,12,13,0.358

1216,12,16,0.309
1314,13,14,0.358
1317,13,17,0.309
1333,13,33,0.327
1419,14,19,0.309
1516,15,16,1.87
1518,15,18,4.75
1519,15,19,1.87
1520,15,20,6.32
1521,15,21,6.32
1526,15,26,12.0
1617,16,17,1.87
1618,16,18,4.75
1627,16,27,12.0
1718,17,18,4.75
1719,17,19,1.87
1722,17,22,6.32
1723,17,23,6.32
1724,17,24,8.0
1819,18,19,4.75
1834,18,34,0.798
1836,18,36,7.97
1925,19,25,12.0
2529,25,29,0.077
2531,25,31,0.00454
2526,25,26,4.631
2533,25,33,0.057
2627,26,27,4.631
2641,26,41,0.00454
2728,27,28,0.077
2730,27,30,0.00454
2732,27,32,0.057
2832,28,32,0.011
2933,29,33,0.011
1835,18,35,0.0111
3637,36,37,0.0111
3638,36,38,0.0111
3639,36,39,0.0111
3640,36,40,0.011
-680,6,80,7.26E-11
-780,7,80,7.26E-11
-880,8,80,7.26E-11
-980,9,80,7.26E-11
-1080,10,80,7.26E-11
-1180,11,80,7.22E-11
-1280,12,80,7.22E-11
-1380,13,80,7.22E-11
-1480,14,80,7.22E-11
-3280,32,80,3.40E-11
-3380,33,80,3.40E-11
-3580,35,80,1.0E-10
-3780,37,80,1.0E-10
-3880,38,80,1.0E-10
-3980,39,80,1.0E-10

-4080,40,80,1.0E-10
-1190,11,90,2.06E-10
-1290,11,90,2.06E-10
-1390,13,90,2.06E-10
-1490,14,90,2.06E-10
-3290,32,90,1.13E-11
-3390,33,90,1.13E-11
-3590,35,90,3.33E-10
-3790,37,90,3.33E-10
-3890,38,90,3.33E-10
-3990,39,90,3.33E-10
-4090,40,90,3.33E-10

END

BCD 3CONSTANTS DATA
NDIM=2500

END

BCD 3ARRAY DATA

END

BCD 3EXECUTION
SNDSNR

END

BCD 3VARIABLES 1

END

BCD 3VARIABLES 2

END

BCD 3OUTPUT CALLS
TPRINT

END

BCD 3END OF DATA